

	<b>Vapor Cloud Explosion at Nil Wind</b>	03904-RP-006
	DOT-PHMSA	Rev A
	Final Report - Public	Page 1 of 213



**Vapor Cloud Explosion at Nil Wind**  
**DOT PHMSA Agreement #693JK32010004POTA**  
**Final Report**

Rev	Issue Purpose:	Date:	BY	CHK	APP
A	Final Report Issued to PHMSA	June 3, 2022	FG	BH	JW

	<b>Vapor Cloud Explosions at Nil Wind</b>	03904-RP-006
	PHMSA	Rev A
	Final Report	Page 2 of 213

## Acknowledgment

The research project team (Dr. Filippo Gavelli, Ms. Jenna Wilson and Mr. Bryant Hendrickson) expresses its sincere thanks to PHMSA and to PHMSA's Agreement Officer Representative, Mr. Robert Smith, and PHMSA's Technical Task Inspector, Ms. Katherine Roth, General Engineer. Ms. Roth's insights, input and comments throughout this project greatly supported this project and advanced PHMSA's objective to enhance safety.

The research project team also expresses its sincere thanks to all members of this project's Technical Advisory Panel (TAP), and the support of the organizations for which they work:

- Jay Jablonski – Hartford Steam Boiler
- Pat Convery – Cornerstone Energy Services
- Jeff Brightwell – Energy Transfer
- Seth Schreiber – Federal Energy Regulatory Commission
- Felix Azenwi-Fru – National Grid
- Tom Drube – Chart Industries
- Kevin Ritz – Baltimore Gas and Electric
- Roberto Vara – Freeport LNG

	<b>Vapor Cloud Explosions at Nil Wind</b>	03904-RP-006
	PHMSA	Rev A
	Final Report	Page 3 of 213

## Table of Contents

<b><u>Section</u></b>	<b><u>Page</u></b>
<b>EXECUTIVE SUMMARY</b> .....	<b>11</b>
<b>1 INTRODUCTION</b> .....	<b>15</b>
<b>2 DEFINITION OF NIL WIND</b> .....	<b>17</b>
2.1 Richardson Number .....	17
2.2 Gravity Slumping .....	18
2.3 Modeling Constraints.....	24
2.4 Proposed Nil Wind Definition.....	24
<b>3 WEATHER STATISTICS</b> .....	<b>25</b>
3.1 Wind Data Sources .....	25
3.2 Wind Analysis Results.....	26
3.3 Wind Speed Statistics Summary .....	40
<b>4 VAPOR CLOUD DEVELOPMENT IN NIL-WIND CONDITIONS</b> .....	<b>42</b>
4.1 Vapor Cloud Explosions .....	43
4.2 Review of Historical Incidents .....	49
<b>5 CONSEQUENCE MODELING IN NIL-WIND</b> .....	<b>58</b>
5.1 Generic LNG Facility Layout .....	58
5.2 Modeling Tool.....	63
5.3 Modeling Test Matrix.....	64
5.4 Ambient Conditions .....	65
5.5 Release Scenarios .....	66
5.6 Vapor Cloud Explosion Potential .....	70
5.7 FLACS Modeling Parameters .....	74
5.8 Modeling Results – ESC Volumes.....	75
5.9 Modeling Results – VCE Overpressures .....	94
5.10 Consequence Modeling Summary .....	101

	<b>Vapor Cloud Explosions at Nil Wind</b>	03904-RP-006
	PHMSA	Rev A
	Final Report	Page 4 of 213

<b>6</b>	<b>QUANTITATIVE RISK ASSESSMENT .....</b>	<b>103</b>
6.1	QRA Methodology .....	103
6.2	Risk Tolerance Criteria .....	103
6.3	System Description .....	104
6.4	Hazard Identification .....	105
6.5	Hazard Endpoints .....	106
6.6	Release Scenarios .....	107
6.7	Release Hole Sizes .....	109
6.8	Other Release Parameters .....	110
6.9	Parts Count .....	110
6.10	Failure Rates .....	110
6.11	Ignition Probabilities .....	112
6.12	Potential Explosion Sites .....	113
6.13	Ambient Conditions .....	113
6.14	Consequence Modeling Methodology .....	115
6.15	Consequence Modeling Results .....	117
6.16	Consequence Modeling Discussion .....	129
6.17	Risk Assessment Results .....	131
6.18	Risk Assessment Discussion .....	134
6.19	QRA Summary .....	139

	<b>Vapor Cloud Explosions at Nil Wind</b>	03904-RP-006
	PHMSA	Rev A
	Final Report	Page 5 of 213

<b>7</b>	<b>CONCLUSIONS AND SUMMARY RECOMMENDATIONS.....</b>	<b>140</b>
<b>8</b>	<b>IMPACT FROM THE RESEARCH RESULTS .....</b>	<b>143</b>
<b>9</b>	<b>FINAL FINANCIAL SECTION.....</b>	<b>144</b>
<b>10</b>	<b>ACRONYMS.....</b>	<b>145</b>
<b>11</b>	<b>BIBLIOGRAPHY .....</b>	<b>147</b>
	<b>APPENDIX A – FACILITY DESIGN DRAWINGS .....</b>	<b>150</b>
	<b>APPENDIX B – EQUIVALENT STOICHIOMETRIC CLOUD VOLUMES .....</b>	<b>159</b>
	<b>APPENDIX C – VAPOR CLOUD EXPLOSION RESULTS .....</b>	<b>184</b>

	<b>Vapor Cloud Explosions at Nil Wind</b>	03904-RP-006
	PHMSA	Rev A
	Final Report	Page 6 of 213

## List of Tables and Figures

<b><u>Table/Figure</u></b>	<b><u>Page</u></b>
Figure 2-1: Schematic of the parameters to quantify the Richardson number .....	18
Table 2-1: Critical Ri calculations for different dense vapor clouds .....	20
Figure 2-2: Upwind dispersion for a dense vapor cloud from an LNG spill .....	21
Figure 2-3: Upwind dispersion for a dense vapor cloud from a pre-mixed propane/air cloud at UFL .....	21
Figure 2-4: Q9 values for a dense vapor cloud from an LNG spill, at different wind speeds .....	23
Figure 2-5: Q9 values for a dense vapor cloud from a pre-mixed propane/air cloud at UFL, at different wind speeds .....	23
Figure 3-1: Weather stations across the United States .....	25
Figure 3-2: US Department of Commerce Segmentation of Regions .....	27
Figure 3-3: Average wind speed at 80 meters elevation .....	28
Figure 3-4: Wind speed percentiles for the Pacific Division .....	29
Figure 3-5: Wind speed percentiles for the Mountain Division .....	30
Figure 3-6: Wind speed percentiles for the West North Central Division .....	31
Figure 3-7: Wind speed percentiles for the East North Central Division .....	32
Figure 3-8: Wind speed percentiles for the Middle Atlantic Division .....	33
Figure 3-9: Wind speed percentiles for the New England Division .....	34
Figure 3-10: Wind speed percentiles for the West South Central Division .....	35
Figure 3-11: Wind speed percentiles for the East South Central Division .....	36
Figure 3-12: Wind speed percentiles for the South Atlantic Division .....	37

	<b>Vapor Cloud Explosions at Nil Wind</b>	03904-RP-006
	PHMSA	Rev A
	Final Report	Page 7 of 213

Figure 3-13: NOAA Weather Buoy near Freeport, Texas .....	39
Figure 3-14: NOAA Weather Buoy in Cove Point, Maryland .....	40
Figure 4-1. Flame propagation plot during episodic deflagration [1]. .....	45
Figure 4-2. Comparison of overpressure curves from detonation (blue) and episodic deflagration (red) [1]. .....	45
Figure 4-3. Numerical simulation showing the buoyancy of heated gases [13].....	46
Figure 4-4. Example of flame propagation tests [16].....	48
Table 4-1. Vapor cloud explosion incidents examined in RR1113.....	49
Figure 5-1. Plot plan for the generic LNG export facility. ....	60
Figure 5-2. 3D model of the generic LNG export facility.....	61
Table 5-1 Export facility documents created for this study.....	62
Table 5-3. SALS table for the generic LNG export facility. ....	66
Table 5-4. Release scenarios in the consequence modeling task. ....	68
Figure 5-3. Release locations and directions (star indicates liquid spill). ....	69
Figure 5-4. Potential Explosion Sites in the generic export facility.....	71
Figure 5-5. Footprint of a flammable vapor cloud: (top) 60 s into the release; (bottom) 150 s into the release. ....	72
Table 5-5. Test matrix for the FLACS flammable dispersion simulations.....	74
Table 5-6. Plant-wide peak ESC volumes for scenario 00. ....	76
Figure 5-6. Plant-wide ESV traces for scenario 00: FV (top), Q8 (middle), and Q9 (bottom). ....	77
Figure 5-7. Overall flammable cloud footprint for scenario 00 (winds at 0.0, 0.5, 1.0, and 2.0 m/s). ....	79

	<b>Vapor Cloud Explosions at Nil Wind</b>	03904-RP-006
	PHMSA	Rev A
	Final Report	Page 8 of 213

Figure 5-8. Plant-wide ESC traces for scenario 04, released to the West: FV (top), Q8 (middle), and Q9 (bottom).....80

Figure 5-9. Plant-wide ESC traces for scenario 04, released to the North: FV (top), Q8 (middle), and Q9 (bottom).....81

Table 5-7. Plant-wide peak ESC volumes for scenario 04. ....82

Table 5-8. Peak Q9 vs. release direction for scenario 04. ....83

Table 5-9. Peak Q9 vs. hole size for scenario 04.....83

Figure 5-10. Q9 traces in Train 2 for scenario 12, released to the North. ....85

Figure 5-11. Q9 traces in Train 2 for scenario 12, released to the West.....85

Table 5-10. Plant-wide peak Q9 volumes for scenario 12.....85

Figure 5-12. Plant-wide Q9 traces for scenario 18, released to the North.....87

Figure 5-13. Plant-wide Q9 traces for scenario 18, released to the East. ....87

Table 5-11. Plant-wide peak Q9 volumes for scenario 18.....88

Figure 5-14. Plant-wide Q9 traces for scenario 18 (3-inch release): to the North (top) and to the East (bottom).....89

Figure 5-15. Plant-wide Q9 traces for scenario 18 (2-inch release): to the North (top) and to the East (bottom).....90

Figure 5-16. Plant-wide Q9 traces for scenario 18 (1-inch release): to the North (top) and to the East (bottom).....91

Table 5-12. Sensitivity analysis of plant-wide peak Q9 vs. hole size for scenario 18. ....91

Figure 5-17. Plant-wide Q9 traces for scenario 22, released to the North.....93

Figure 5-18. Plant-wide Q9 traces for scenario 22, released to the East. ....93

Table 5-13. Plant-wide peak Q9 volumes for scenario 22.....94

Figure 5-19. ESC cloud placements and ignition locations for the VCE modeling. ....96

	<b>Vapor Cloud Explosions at Nil Wind</b>	03904-RP-006
	PHMSA	Rev A
	Final Report	Page 9 of 213

Figure 5-20. Overpressure hazard footprint for LNG Q9 at low wind.....	98
Figure 5-21. Overpressure hazard footprint for LNG Q9 at nil wind. ....	98
Figure 5-22. Overpressure hazard footprint for MR Q9 at low wind.....	99
Figure 5-23. Overpressure hazard footprint for MR Q9 at nil wind.....	99
Figure 5-24. Overpressure hazard footprint for MR Q8 at low wind.....	100
Figure 5-25. Overpressure hazard footprint for Propane Q9 at low wind.....	100
Table 6-1: Criteria for tolerability of individual risk (IR) of fatality.....	104
Figure 6-1: Event tree for a flammable release.....	106
Table 6-2: Inventory List.....	108
Table 6-3: Hole sizes for QRA.....	109
Table 6-4: Failure rate table for the facility's inventories.....	111
Figure 6-2: UKOAA model for ignition probabilities.....	113
Figure 6-3: Discretized wind rose for the generic LNG facility.....	114
Table 6-5: Dispersion modeling results – distance to LFL (nomalized w.r.t. F2).....	118
Table 6-6: Dispersion modeling results – ESC volume (nomalized w.r.t. F2).....	122
Figure 6-4: Dispersion modeling results – effect of nil-wind on distance to LFL.....	127
Figure 6-5: Dispersion modeling results – effect of nil-wind on Q9 volume.....	128
Figure 6-6: Dispersion modeling results – effect of nil-wind on Q8 volume.....	128
Figure 6-7: Side view of flammable cloud at maximum extent for inventory 10 (gas to BOG compressor), full rupture of 24-in line: X0 wind (top) vs. F2 wind (bottom).....	130
Figure 6-8: Plan view of flammable cloud at maximum extent for inventory 20 (propane makeup line), 2-in release: X0 wind (top) vs. F2 wind (bottom).....	130

	<b>Vapor Cloud Explosions at Nil Wind</b>	03904-RP-006
	PHMSA	Rev A
	Final Report	Page 10 of 213

Figure 6-9: Plan view of flammable cloud at maximum extent for inventory 20 (propane makeup line), full rupture of 8-in line: X0 wind (top) vs. F2 wind (bottom). .....131

Figure 6-10: Individual risk contours for the 'Traditional' QRA.....132

Figure 6-11: Individual risk contours for the 'Nil-wind' QRA. ....133

Figure 6-12: Comparison of individual risk contours: Traditional QRA (grey) vs. Nil-Wind QRA (yellow).....134

Figure 6-13: Comparison of individual risk contours from flash fire scenarios: Traditional QRA (left) vs. Nil-Wind QRA (right).....135

Figure 6-14: Comparison of individual risk contours from jet fire scenarios: Traditional QRA (left) vs. Nil-Wind QRA (right).....136

Figure 6-15: Comparison of individual risk contours from pool fire scenarios: Traditional QRA (left) vs. Nil-Wind QRA (right).....137

Figure 6-16: Comparison of individual risk contours from VCE scenarios: Traditional QRA (left) vs. Nil-Wind QRA (right). ....138

	<b>Vapor Cloud Explosions at Nil Wind</b>	03904-RP-006
	PHMSA	Rev A
	Final Report	Page 11 of 213

## Executive Summary

Federal safety regulations for siting, design, construction, operation and maintenance of LNG facilities are codified in 49 CFR Part 193. Siting requirements are given in Subpart B, with ambient conditions for flammable vapor dispersion specified in section 193.2059(b)(2), which reads:

*Dispersion conditions are a combination of those which result in longer predicted downwind dispersion distances than other weather conditions at the site at least 90 percent of the time, based on figures maintained by National Weather Service of the U.S. Department of Commerce, or as an alternative where the model used gives longer distances at lower wind speeds, Atmospheric Stability (Pasquill Class) F, wind speed = 4.5 miles per hour (2.01 meters/sec) at reference height of 10 meters, relative humidity = 50.0 percent, and atmospheric temperature = average in the region.*

Based on these specifications, most LNG facility siting studies consider worst-case wind speeds of 1 or 2 m/s, depending on site-specific wind data.

In 2017, the Health and Safety Executive (HSE) issued a report entitled “Review of Vapour Cloud Explosion Incidents” (RR1113) [1] which reviewed several large vapor cloud explosion accidents that occurred in industrial facilities around the world. The report found that “a high proportion of vapor cloud incidents occurred in nil/low wind conditions”. Even though vapor cloud explosions (VCEs) are not explicitly addressed in the current edition of 49 CFR 193, VCE hazards must be evaluated during facility siting as “other factors that have a bearing on safety”, as specified in NFPA 59A (paragraph 2.1.1(d), 2001 edition) [2] which is incorporated by reference in the federal safety regulations. Therefore, the publication of RR1113 raised concerns on whether the range of weather conditions currently specified for LNG facility siting should be expanded to include lower wind speeds.

In September 2020, the U.S. Department of Transportation's Pipeline and Hazardous Materials Safety Administration (PHMSA) awarded Blue Engineering and Consulting (BLUE) a research project titled “Vapor Cloud Explosions at Nil Wind”. The scope of the project was to evaluate how “nil wind” conditions may affect vapor cloud explosion hazards in LNG facilities and to present the findings so that PHMSA staff can make an informed decision regarding possible changes to regulatory requirements. The findings of the research project are presented in this report and summarized below.

The first task in the study was to provide a definition for “nil wind” conditions to properly distinguish them from “low wind” or other conditions; the following definitions were therefore proposed, based on the lower bound of wind speeds that can be used by integral models:

	<b>Vapor Cloud Explosions at Nil Wind</b>	03904-RP-006
	PHMSA	Rev A
	Final Report	Page 12 of 213

- Nil wind = wind speed less than 1 m/s, measured at a height of 10 m above grade.
- Low wind = wind speed equal to or greater than 1 m/s and less than or equal to 2 m/s, measured at a height of 10 m above grade.

Based on these definitions, a statistical analysis of wind speeds across the United States found nil winds to occur approximately 20.1% of the time and low winds approximately 11.4% of the time. However, these figures were found to be affected by how wind speeds below 1.5 m/s are measured and reported, therefore they likely overestimate the frequency of occurrence of “nil wind” conditions. Ultimately, for accuracy, any siting study would have to be based on data from the nearest (or most relevant) weather station.

A critical review of RR1113 was also performed as part of this study, leading to the following observations:

- The majority of the accidents reviewed in RR1113 occurred at night or during the early morning hours, which is when nil/low wind conditions tend to be prevalent. However, that is also when staffing is reduced, and darkness affects the operators' ability to detect a release. These factors cannot be discounted when assessing the relative frequency of accidents and appear more reasonable than the unsubstantiated allegation that “a wider range of smaller losses of containment (with much higher frequency) have the potential to cause a large cloud in [nil/low wind] conditions”.
- The concept of episodic deflagration, which RR1113 claims to be responsible for several large vapor cloud explosion accidents, has been sharply criticized and rebuked by several groups of explosion experts, both on the physical basis of the phenomenon and on the evaluation of forensic evidence. Based on the review of available literature on the topic, the current understanding of VCEs appears adequate to explain those accidents, and the hypothesis that episodic deflagration led to those events cannot be supported.
- Only one of the 24 accidents reviewed occurred at an LNG facility (Skikda) and the severe consequences of that accident are attributable to the confined area in which ignition occurred and the high congestion present outside, therefore, wind conditions likely played a minimal role in the accident. In all other cases, the HSE report discussed the causes but did not address the different regulatory requirements between those facilities and PHMSA-jurisdictional LNG facilities, nor their effect on the likelihood of similar accidents occurring at LNG facilities.

Finally, the effect of nil wind conditions on flammable releases was evaluated quantitatively by performing extensive modeling on a broad range of realistic scenarios, using a Computational Fluid Dynamics (CFD) tool – FLACS – which has been validated and approved by PHMSA for LNG dispersion modeling.

	<b>Vapor Cloud Explosions at Nil Wind</b>	03904-RP-006
	PHMSA	Rev A
	Final Report	Page 13 of 213

The effect of nil wind on flammable hazards was evaluated on a prescriptive basis, following current PHMSA requirements for LNG facility siting and on a risk basis, according to the quantitative risk assessment procedure outlined in NFPA 59A, 2019 edition. In both cases, a generic LNG export facility was specified, at early-design stage, for the purpose of defining realistic scenarios to be evaluated.

For the prescriptive case study, modeling considered a total of 15 release scenarios, each under four different wind conditions (no wind; 0.5 m/s; 1 m/s; and 2 m/s) and three wind directions. The modeling results showed that:

- Equivalent stoichiometric cloud (ESC) volumes tend to be higher in low winds than nil winds, for pressurized releases (without rainout). In these cases, the wind direction (relative to the direction of the release) has a stronger effect on ESC volumes than wind speed; the effect of wind direction is reduced for clouds that enter congested areas.
- ESC volumes tend to be higher in nil winds for evaporating liquid spills. This behavior is consistent with a highly stratified cloud, which is progressively diluted at the air/cloud interface by wind-induced turbulence and molecular diffusion.
- It should be noted that liquid spill scenarios, or pressurized jet releases scenarios with rainout, are typically not the bounding cases for LNG facility siting due to the liquid being collected and conveyed into an impoundment to minimize its vaporization rate.

For the risk-based case study, over 120 different release scenarios were evaluated, each modeled under four wind conditions (nil wind, low wind, and two higher wind speeds); FLACS was used to determine flammable dispersion distances and ESC volumes. The individual risk was then calculated under two sets of assumptions:

1. The “traditional” approach, where nil-wind conditions are combined with low-wind conditions, so that the frequencies are added together and the consequences are calculated at the representative, low wind speed.
2. The “nil-wind” approach, where nil-wind is considered as its own wind category and the consequences are calculated in zero wind.

The overall risk from a QRA performed while explicitly accounting for nil-wind conditions was found to be slightly smaller than from a “traditional” QRA, meaning that QRAs conducted according to the “traditional” approach tend to be slightly conservative. This outcome was explained by observing that nil wind conditions tend to increase hazards for large-bore releases (particularly with rainout), which are less frequent, but they tend to reduce the same hazards for small-bore and high-pressure releases, which are more frequent.

	<b>Vapor Cloud Explosions at Nil Wind</b>	03904-RP-006
	PHMSA	Rev A
	Final Report	Page 14 of 213

The project team therefore does not recommend any changes to the regulatory requirements regarding wind speeds to be included in an LNG facility siting study, as currently specified in 49 CFR 193.2059.

	<b>Vapor Cloud Explosions at Nil Wind</b>	03904-RP-006
	PHMSA	Rev A
	Final Report	Page 15 of 213

## 1 Introduction

Federal safety regulations for siting, design, construction, operation and maintenance of LNG facilities are codified in 49 CFR Part 193. Siting requirements are given in Subpart B, with ambient conditions for flammable vapor dispersion specified in section 193.2059(b)(2), which reads:

*Dispersion conditions are a combination of those which result in longer predicted downwind dispersion distances than other weather conditions at the site at least 90 percent of the time, based on figures maintained by National Weather Service of the U.S. Department of Commerce, or as an alternative where the model used gives longer distances at lower wind speeds, Atmospheric Stability (Pasquill Class) F, wind speed = 4.5 miles per hour (2.01 meters/sec) at reference height of 10 meters, relative humidity = 50.0 percent, and atmospheric temperature = average in the region.*

Since the publication of 49 CFR Part 193, there have been questions on the wind speeds specified by code and whether lower wind speeds should be included in siting studies. Typically, the bounding cases in most LNG facility siting studies are based on wind speeds of 1 or 2 m/s, depending on the wind data for each site. Since the consequences of vapor dispersion scenarios tend to become worse as the wind speed decreases, it follows that a worst-case study should consider wind speeds down to zero. The 90<sup>th</sup> percentile threshold in 193.2059(b)(2) is intended to prevent safety designs from having to protect against conditions occurring infrequently.

In 2017, the Health and Safety Executive (HSE) issued a report entitled “Review of Vapour Cloud Explosion Incidents” (RR1113) [1] which reviewed several large vapor cloud explosion accidents that occurred in industrial facilities around the world. The report found that “a high proportion of vapor cloud incidents occurred in nil/low wind conditions”. Even though vapor cloud explosions (VCEs) are not explicitly addressed in the current edition of 49 CFR 193, VCE hazards must be evaluated during facility siting as “other factors that have a bearing on safety”, as specified in NFPA 59A (paragraph 2.1.1(d), 2001 edition) [2] which is incorporated by reference in the federal regulations. Therefore, the publication of RR1113 raised concerns on whether the range of weather conditions currently specified for LNG facility siting should be expanded to include lower wind speeds.

In September 2020, the U.S. Department of Transportation's Pipeline and Hazardous Materials Safety Administration (PHMSA) awarded Blue Engineering and Consulting (BLUE) a research project titled “Vapor Cloud Explosions at Nil Wind”. The scope of the project is to evaluate how “nil wind” conditions may affect vapor cloud explosion hazards in LNG facilities and to present the findings so that PHMSA staff can make an informed decision regarding possible changes to regulatory requirements.

	<b>Vapor Cloud Explosions at Nil Wind</b>	03904-RP-006
	PHMSA	Rev A
	Final Report	Page 16 of 213

This report summarizes the work performed during this project. Section 2 provides a definition of “nil wind” conditions, including a rationale for the definition. Section 3 performs a statistical analysis of historical weather data across the United States, to quantify the frequency of occurrence of nil and low-wind conditions. Section 4 addresses RR1113, focusing particularly on the topic of episodic deflagration and the differences in regulations and safety measures present in PHMSA-regulated LNG facilities versus the facilities where the historical accidents occurred (i.e., primarily fuel storage depots or pipelines). Section 5 summarizes the results of flammable vapor dispersion modeling performed to evaluate the effect of wind speed on the potential for vapor cloud explosion hazards (i.e., equivalent stoichiometric cloud volumes). Section 6 compares the results for a quantitative risk assessment (QRA) on a generic LNG export facility, performed by explicitly considering nil-wind conditions (and their impact on hazard distances) in the calculations, relative to a QRA performed in the ‘traditional’ manner. Section 7 provides final recommendations to PHMSA staff based on the results of this study.

	<b>Vapor Cloud Explosions at Nil Wind</b>	03904-RP-006
	PHMSA	Rev A
	Final Report	Page 17 of 213

## 2 Definition of Nil Wind

RR1113 found that “a high proportion of vapor cloud incidents occurred in nil/low wind conditions”. Later in the same report, nil wind is defined as “a wind that was so weak close to the ground that it did not significantly affect the gravity driven transport of released vapor”. Therefore, “[r]ather than moving downwind, the vapor in these cases spread out in all directions and or followed any downward slopes around the source”.

Since the above definition is too vague to be used for regulatory purposes, the first task of this research study was to provide a clear definition that could be included in 49 CFR 193, should PHMSA decide to include nil-wind conditions as a requirement for LNG facility siting.

### 2.1 Richardson Number

The VCE accidents reviewed by the HSE originated with the release of heavy hydrocarbons, resulting in large, dense vapor clouds at ground level. Due to the low wind speeds and stable atmosphere, the dense clouds were able to linger with limited dilution by ambient air, until ignition occurred. The interaction between a dense vapor cloud and ambient air is driven by two counteracting effects:

- The shear caused by the wind, which tends to push the cloud downwind as well as to create turbulence and therefore mix air into the cloud, progressively diluting its concentration; and
- The slumping of the heavier vapors caused by gravity, which tends to spread the cloud against the ambient air as well as to smother the shear-induced turbulence.

The relative strength of gravity vs. shear is frequently quantified via the Richardson number:

$$Ri = \frac{\text{gravity}}{\text{shear}} = \frac{g \Delta\rho H}{\rho_0 U^2} = \frac{g' H}{U^2} \quad (1)$$

where, as depicted in Figure 2-1:

- $g$  is the acceleration due to gravity
- $\rho_0$  is the density of ambient air
- $\Delta\rho$  is the density difference between the vapor cloud and ambient air
- $H$  is a characteristic (vertical) dimension
- $U$  is a characteristic velocity

	<b>Vapor Cloud Explosions at Nil Wind</b>	03904-RP-006
	PHMSA	Rev A
	Final Report	Page 18 of 213

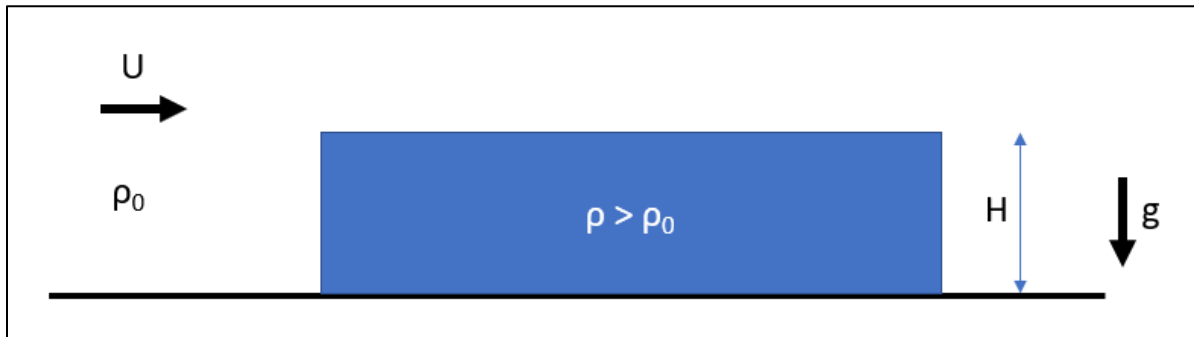


Figure 2-1: Schematic of the parameters to quantify the Richardson number

As Equation 1 shows, higher values of  $Ri$  correspond to heavier, less turbulent clouds that tend to mix more slowly with ambient air; conversely, lower values of  $Ri$  correspond to lighter clouds subject to more intense mixing at the cloud/air interface. A generally accepted threshold for the “laminarization” of a cloud/air interface is  $Ri = 0.25$ , which is defined as the critical Richardson number, or  $Ri_c$ .

## 2.2 Gravity Slumping

RR1113 attempted to define “nil/low-wind” by recognizing that such conditions “develop in stably stratified atmospheric conditions and are easily recognised. The density gradient near the ground is sufficient to suppress turbulent mixing in the lowest part of the atmosphere. This occurs when the Richardson number is greater than about 0.25” as demonstrated by Grachev et al. [3] and generally agreed upon by most researchers.

The report proceeded to quantify the range of wind speeds corresponding to the critical  $Ri$  by incorporating the analysis by Briggs et al. [4] on detrainment of heavy gases from a dense cloud filling a depression. The report concluded that wind speeds less than approximately 1.35-1.95 m/s (measured at the typical height of 10 m above grade) would result in a typical dense cloud remaining 75% undiluted.

Upon review of the calculations presented in RR1113, some of the assumptions appear questionable, including:

- The relevance of the Briggs methodology is debatable, since it applies to a stationary dense cloud confined within a depression, whereas most dense clouds would be free to expand throughout an LNG facility; further, the HSE analysis considered clouds larger than 150 acres.
- A direct consequence of the Briggs methodology is that the characteristic height was defined as the thickness of the mixing layer, which was assumed to be 25% of the cloud height. For an unconfined dense cloud, the characteristic height should instead be given by the “effective height” as defined by Witlox in the Unified Dispersion Model Theory report [5]:

	<b>Vapor Cloud Explosions at Nil Wind</b>	03904-RP-006
	PHMSA	Rev A
	Final Report	Page 19 of 213

$$H_{eff} = \frac{1}{c_0} \int_0^{\infty} c(x, y, z) dz \quad (2)$$

where:

- $H_{eff}$  is the effective height (thickness) of the cloud
- $c(x,y,z)$  is the gas concentration within the cloud
- $c_0$  is the reference gas concentration (e.g., the concentration at ground level)

For a uniform concentration cloud, the effective height would be equal to the actual cloud thickness. Comparing the example provided by the HSE to typical conditions at LNG facilities, the characteristic height would be 4 times larger than assumed, resulting in a threshold wind speed twice as high than calculated.

- The characteristic velocity was calculated from equation (1) and appropriately defined as the wind speed at the top surface of the cloud (i.e., 2 m height in the HSE example). However, a ratio of approximately 1.5 was applied to estimate the wind speed at 10 m height based on the calculated value at 2 m, which corresponds to a power law coefficient of approximately 0.25. Under stable conditions, as postulated to be required for nil/low-wind conditions to develop, the power law coefficient should be in the range of 0.4-0.5 [6], resulting in a wind speed ratio of 1.9 or greater.
- The "typical" range for density differences in a vapor cloud was specified as 0.05 to 0.1 (5-10%). This appears inexplicable, at least when applied to accidental releases in LNG facilities, since vapors from liquefied hydrocarbon releases can be much heavier than ambient air, as demonstrated below.

A revised analysis was therefore performed to calculate the range of wind speeds corresponding to the critical  $Ri$ , under the following assumptions:

- Critical  $Ri = 0.25$
- Ambient temperature = 10 C
- Ambient air density = 1.25 kg/m<sup>3</sup>
- Uniform concentration vapor cloud
- Characteristic height = 2 m (full cloud thickness)
- Wind power law coefficient = 0.4 (if  $U(10\text{ m}) < 4\text{ m/s}$ ) or 0.17 (otherwise)

Several different vapor clouds were evaluated, for liquid releases of LNG, propane and isopentane; for each fluid, a pure vapor cloud, a cloud mixed with air to the Upper Flammable Limit (UFL) and a cloud mixed with air to the Lower Flammable Limit (LFL) were considered. The pure vapor clouds were assumed to be at the normal boiling temperature for the released fluid, as would occur from an evaporating liquid spill; the

temperature of the mixed vapor/air clouds was calculated assuming adiabatic mixing between the boiling vapors and ambient air. The results are listed in Table 2-1.

Table 2-1: Critical Ri calculations for different dense vapor clouds

	LNG @ LFL	LNG @ UFL	LNG, pure	Propane @ LFL	Propane @ UFL	Propane, pure	Pentane @ LFL	Pentane @ UFL	Pentane, pure
Cloud temperature [C]	-0.4	-20.4	-161.5	7.7	-0.2	-42.1	11.5	17.0	36.1
Cloud density [kg/m <sup>3</sup> ]	1.28	1.33	1.82	1.27	1.36	2.32	1.27	1.4	3.0
Relative density difference ratio	2%	6%	46%	2%	9%	86%	2%	10%	138%
"Critical" wind speed at cloud height [m/s]	1.4	2.2	6.0	1.1	2.6	8.2	1.1	2.9	10.4
"Critical" wind speed at 10 m [m/s]	2.6	2.9	7.8	2.1	3.4	10.7	2.1	3.7	13.5

The results in Table 2-1 show that  $Ri_c$ , which represents the threshold for the "laminarization" of a cloud/air interface, is generally reached or exceeded at wind speeds already included in regulatory requirements for vapor dispersion. Therefore, wind speeds below the current regulatory requirement are not expected to result in a different type of interaction between the dispersing dense cloud and the wind.

Even though gravity begins to smother the wind-induced turbulent mixing at relatively high wind speeds, that does not mean that wind speed has no effect on dense cloud dispersion. Figure 2-2 and Figure 2-3 show the upwind portion of vapor clouds, respectively, from an evaporating LNG pool and a premixed propane/air cloud at UFL, spreading against wind at different speeds (all measured at 10 m elevation); each figure shows a snapshot of four CFD simulations, taken at the same time from the start of the cloud dispersion.

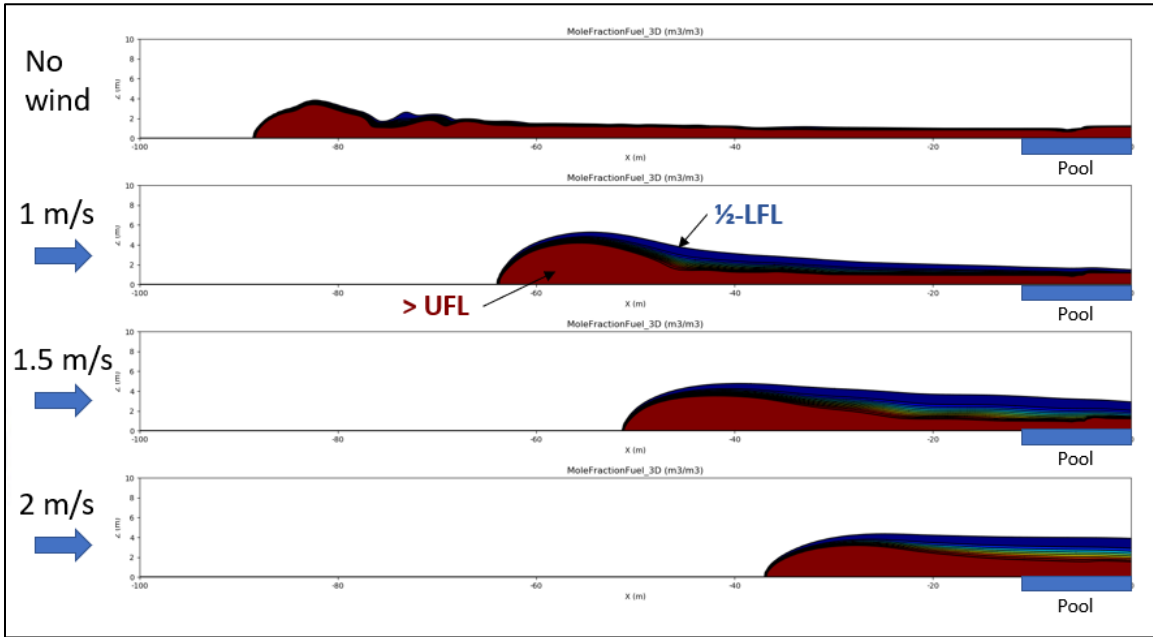


Figure 2-2: Upwind dispersion for a dense vapor cloud from an LNG spill

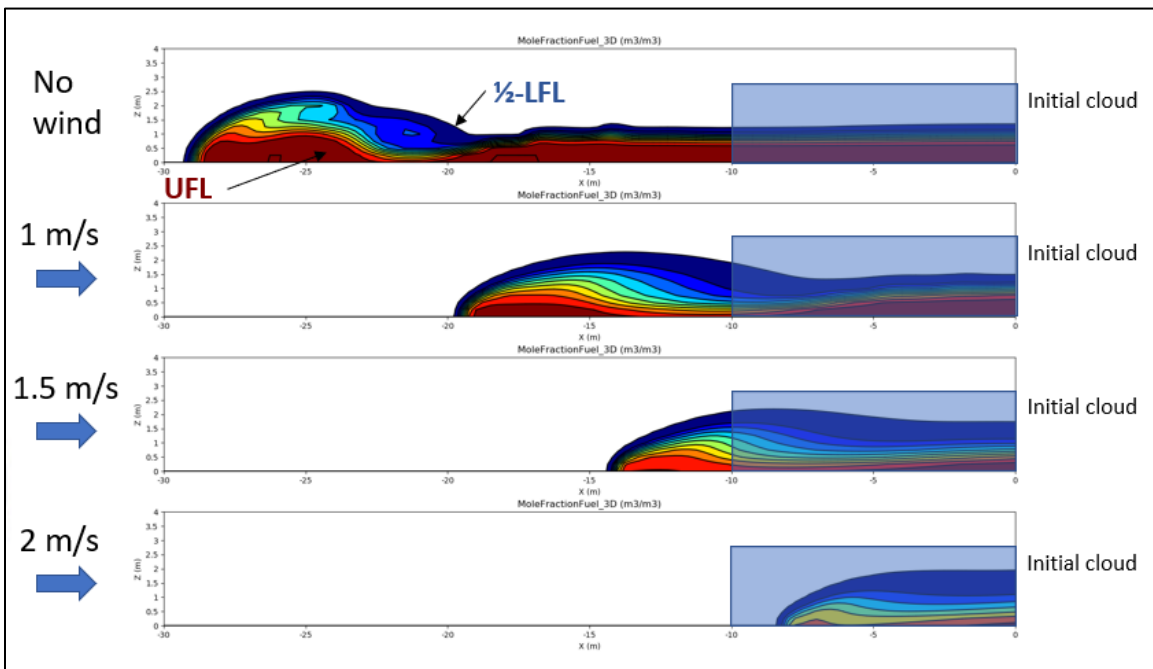


Figure 2-3: Upwind dispersion for a dense vapor cloud from a pre-mixed propane/air cloud at UFL

	<b>Vapor Cloud Explosions at Nil Wind</b>	03904-RP-006
	PHMSA	Rev A
	Final Report	Page 22 of 213

The plots show how the dense clouds push farther upwind as the wind decreases from 2 to 0 m/s, as expected. However, the concern raised in RR1113 about nil wind conditions is not relative to the dispersion distance of flammable clouds, but to the potential for increased vapor cloud explosion hazards due to the slower mixing and dilution of these clouds. Figure 2-2 and Figure 2-3 show qualitatively how the flammable portion of the cloud is relatively similar across the four wind speeds; if anything, the thickness of the flammable region appears larger for wind speeds above zero.

A quantitative comparison of the vapor cloud explosion potential is shown in Figure 2-4 and Figure 2-5, respectively, for the evaporating LNG pool and premixed propane/air cloud at UFL shown above. The plots show the equivalent stoichiometric volume ( $Q_9$ )<sup>1</sup> calculated over the entire computational domain (upwind and downwind of the release), for each simulation. The modeling results show that, in the case of the evaporating pool, the lower wind speeds (0 and 1 m/s) result in a  $Q_9$  volume that continues to grow after the end of the release, whereas the higher wind speeds (1.5 and 2 m/s) rapidly reduce the cloud volume once the release stops. For the pressurized propane release, the  $Q_9$  values are less affected by wind speed and the maximum  $Q_9$  values for nil wind simulations are comparable to those with low wind.

It should be noted that these scenarios were defined and simulated for demonstration purposes; a broader set of release scenarios will be defined and modeled in a later task of this research project.

---

<sup>1</sup> A detailed discussion of equivalent stoichiometric cloud and the definition of  $Q_9$  and other parameters are provided in section 5.6.2.

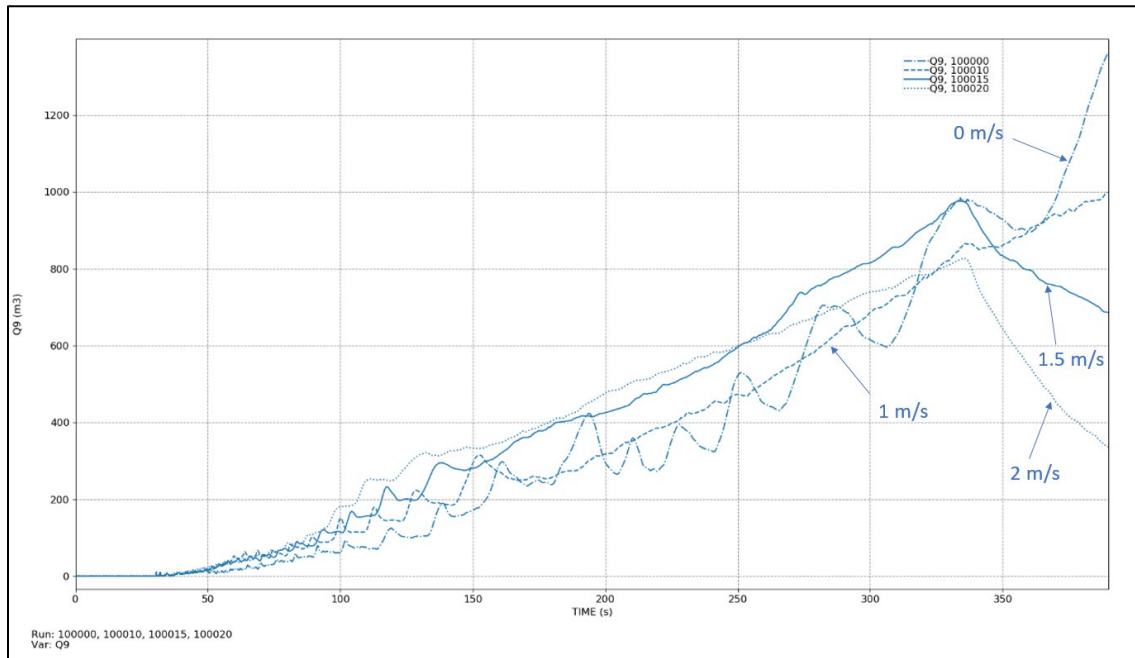


Figure 2-4: Q9 values for a dense vapor cloud from an LNG spill, at different wind speeds

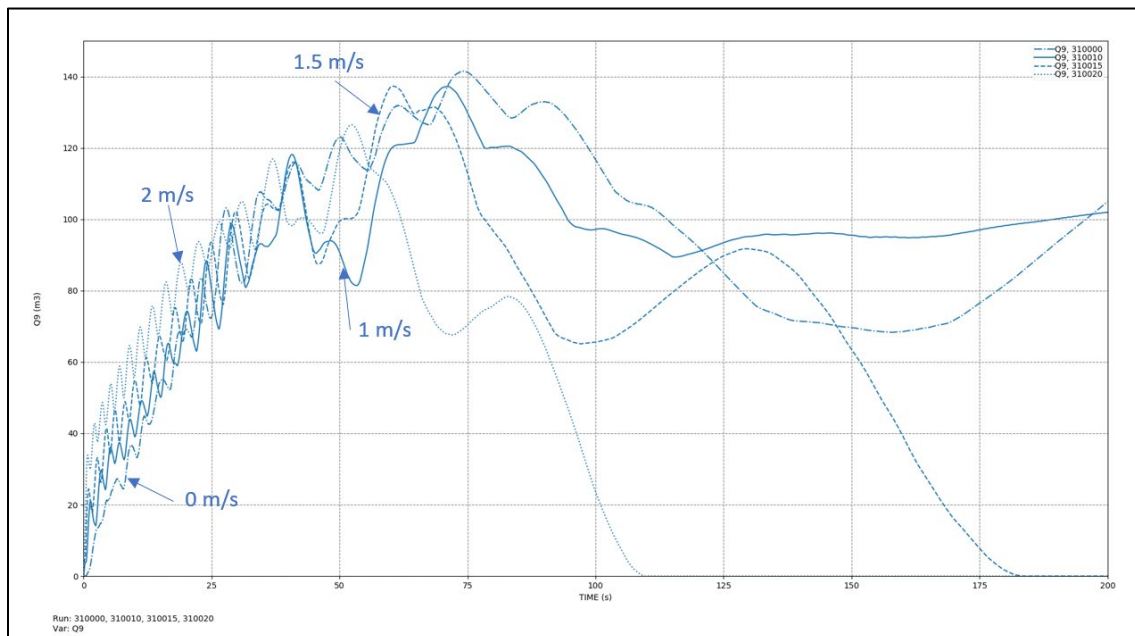


Figure 2-5: Q9 values for a dense vapor cloud from a pre-mixed propane/air cloud at UFL, at different wind speeds

	<b>Vapor Cloud Explosions at Nil Wind</b>	03904-RP-006
	PHMSA	Rev A
	Final Report	Page 24 of 213

### 2.3 Modeling Constraints

Even though the analysis presented in the previous sections did not identify any substantial physical differences in the behavior of a dense vapor cloud in wind speeds below 2 m/s, a critical difference arises when modeling tools are considered. In fact, integral models such as Phast (currently approved by PHMSA for LNG vapor cloud dispersion) have a lower wind speed limit, below which the equations they apply cannot be used: the lower bound on wind speed is generally 1.0 m/s. CFD models are not affected by such limitation and can model dispersion in wind speeds down to zero.

Therefore, a distinction between wind speeds higher and lower than 1 m/s may be warranted, due to the limitations of a widely used category of dispersion models.

### 2.4 Proposed Nil Wind Definition

The previous subsections of this report demonstrated that:

- Current LNG facility siting regulations require cloud dispersion to be modeled for 2 m/s wind speed; lower wind speeds (typically 1 m/s) need to be modeled in some cases if warranted based on site-specific weather data.
- The transition to a gravity-dominated spread tends to occur within the range of wind speeds already modeled in LNG facility siting scenarios. Therefore, defining nil wind based on the Richardson number as detailed above does not introduce 'new' weather conditions to LNG facility siting studies and another derivation is required to include winds below what is currently evaluated.
- A practical distinction should be made for wind speeds above and below 1 m/s, to take into account the limitations of integral dispersion models.

Based on these facts, the following definitions are proposed:

- Nil wind is defined as a wind speed less than 1 m/s, measured at a height of 10 m above grade.
- Low wind is defined as a wind speed equal to or greater than 1 m/s and less than or equal to 2 m/s, measured at a height of 10 m above grade.

It should be pointed out that providing a definition for nil wind does not imply that nil wind conditions should be included in regulatory requirements for LNG facility siting. A recommendation on that matter will follow at the end of this report.

	<b>Vapor Cloud Explosions at Nil Wind</b>	03904-RP-006
	PHMSA	Rev A
	Final Report	Page 25 of 213

### 3 Weather Statistics

Nil- and low-wind conditions are generally considered to be infrequent. According to RR1113, such conditions tend to occur at night, in the presence of high-pressure weather systems; therefore, they are estimated to occur approximately 5% of the time across the United Kingdom.

Current regulations recognize the burden that may be imposed on project developers to design against rarely occurring weather conditions, therefore, the frequency of occurrence of nil-wind conditions needs to be factored in when deciding whether the range of ambient conditions to be modeled should be expanded. Task 3 of this research project thus set out to quantify the frequency of occurrence of nil-wind conditions.

#### 3.1 Wind Data Sources

Data for this analysis was provided by the National Centers for Environmental Information (NCEI), a division of the National Oceanic and Atmospheric Administration (NOAA) within the Department of Commerce. This task considered 2,874 US weather stations for the 50 states but excluded US territories such as Guam and Puerto Rico; the location of these weather stations is shown in Figure 3-1.



Figure 3-1: Weather stations across the United States.

	<b>Vapor Cloud Explosions at Nil Wind</b>	03904-RP-006
	PHMSA	Rev A
	Final Report	Page 26 of 213

The NCEI data is provided to the public at the following link:

<https://www.ncei.noaa.gov/data/global-hourly/access/>

This site includes hourly data starting in 1901, at which time only five US stations were reporting. The number of available weather stations has grown tremendously, and the website includes international locations as well. This analysis considered data from the most recent ten full years (2010 to 2019).

Data from each weather station is provided in individual files (one per year of operation) for download. The data sets include information on the station number, latitude, longitude, station name, visibility, temperature, dew points, wind direction, and wind speed. Each parameter includes quality status checks to ensure that the recorded values are not suspect or erroneous. The weather station data, however, do not include information on the height above grade of the anemometer or other instruments; in most cases, these can be found by looking up the weather station on the website.

Most weather stations record at intervals shorter than one hour, some as frequent as 5 minutes, others every 20 minutes. The analysis considered the first wind speed from each hour for stations that report at intervals less than 60 minutes.

### **3.2 Wind Analysis Results**

The statistical analysis presented below was aimed at estimating the wind speed distribution across the United States; it considered each station within the 50 states and then divided into regions and sub-regions. The divisions and regions used in this task follow the segmentation developed by the US Department of Commerce, US Census Bureau, as illustrated in Figure 3-2.

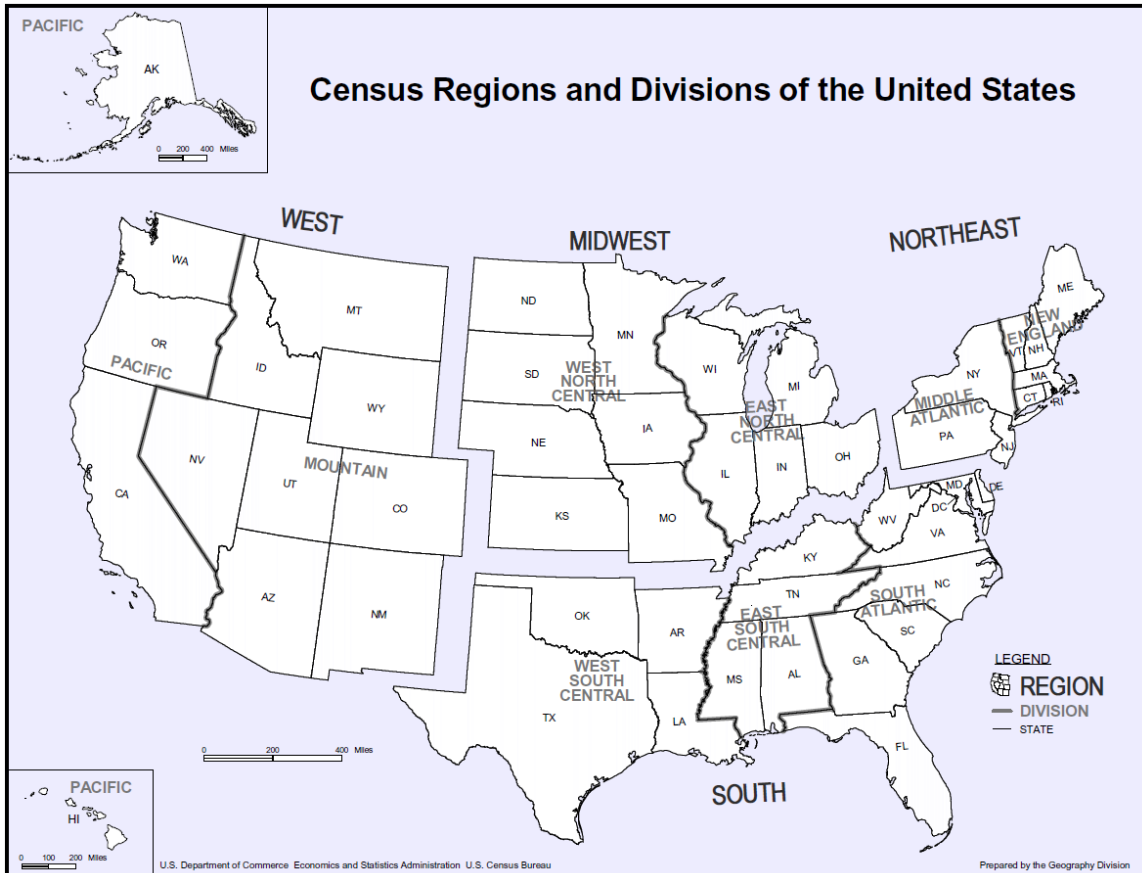


Figure 3-2: US Department of Commerce Segmentation of Regions

### 3.2.1 Overall Results

An overall wind analysis was performed for the entire set of weather stations. Average wind speeds across the country have been evaluated at great length for the wind power industry, but most of that analysis is provided at greater elevations, typically 80 meters, where a wind turbine may be located. For reference, Figure 3-3, presents the Annual Average Wind Speeds, developed by AWS Truepower, LLC for the National Renewable Energy Laboratory.

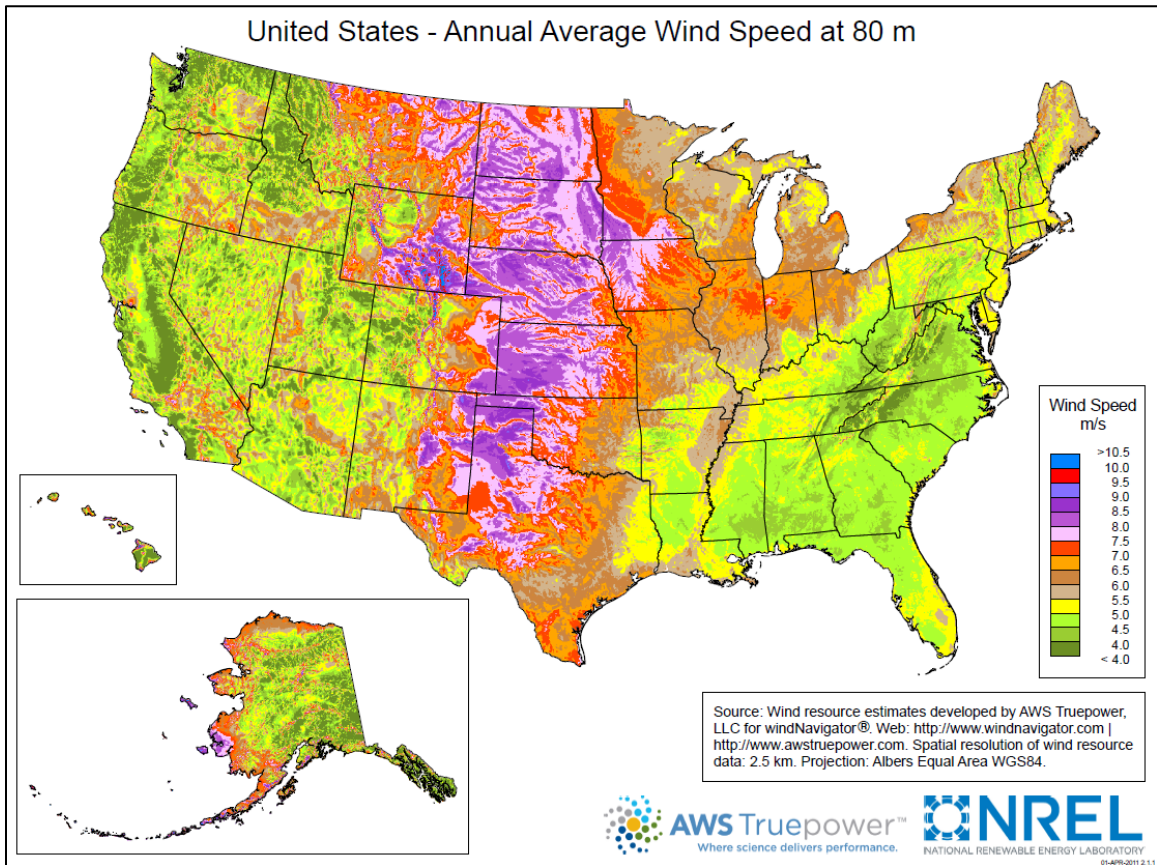


Figure 3-3: Average wind speed at 80 meters elevation

For the current analysis, which considered over 180 million hourly weather data points recorded between 2010 and 2019, nil-wind conditions (speed < 1 m/s) were found to occur approximately 20.7% of the time. Low wind conditions (speed between 1 and 2 m/s) occurred approximately 10.8% of the time. It should be noted how these values are significantly larger than the rough estimate provided by HSE for the United Kingdom.

The following subsections will evaluate the wind speed distribution for the different US Census Divisions, for the purpose of providing more locally refined data. Several other approaches are possible to partition the data set, such as separating coastal stations from inland ones, but extend beyond the purpose of this task.

### 3.2.2 Divisional Results

#### 3.2.2.1 Pacific Division

The Pacific Division is in the West Region, made up of Alaska, Hawaii, Washington, Oregon and California. The analysis for this division included 522 stations and approximately 30.7 million hourly weather data points. The frequency of occurrence of nil-wind conditions is approximately 23.8%, while low winds occur approximately 12.6% of the time. The cumulative wind speed distribution is shown in Figure 3-4.

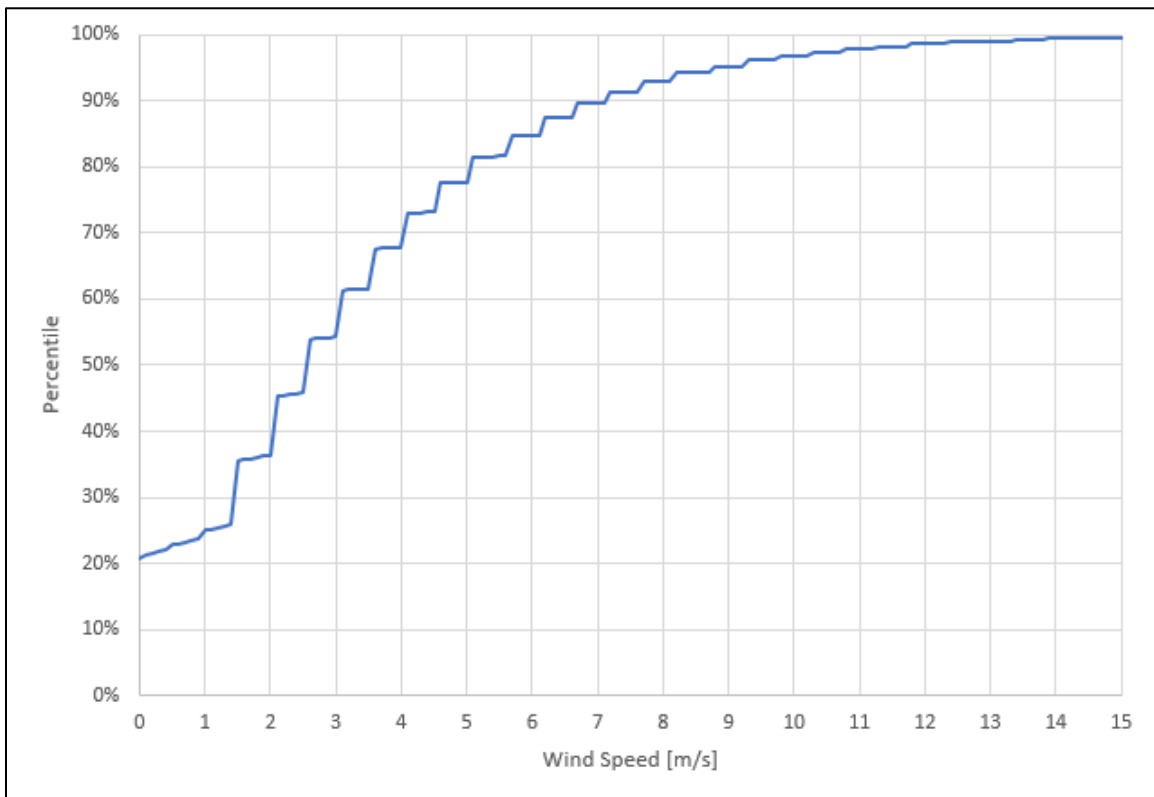


Figure 3-4: Wind speed percentiles for the Pacific Division

### 3.2.2.2 Mountain Division

The Mountain Division is the second group in the West Region. This large section consists of Montana, Idaho, Nevada, Wyoming, Utah, Colorado, Arizona and New Mexico. The analysis for this division included 312 stations and approximately 20.2 million hourly weather data points. The frequency of occurrence of nil-wind conditions is approximately 17.8%, while low winds occur approximately 12.8% of the time. The cumulative wind speed distribution is shown in Figure 3-5.

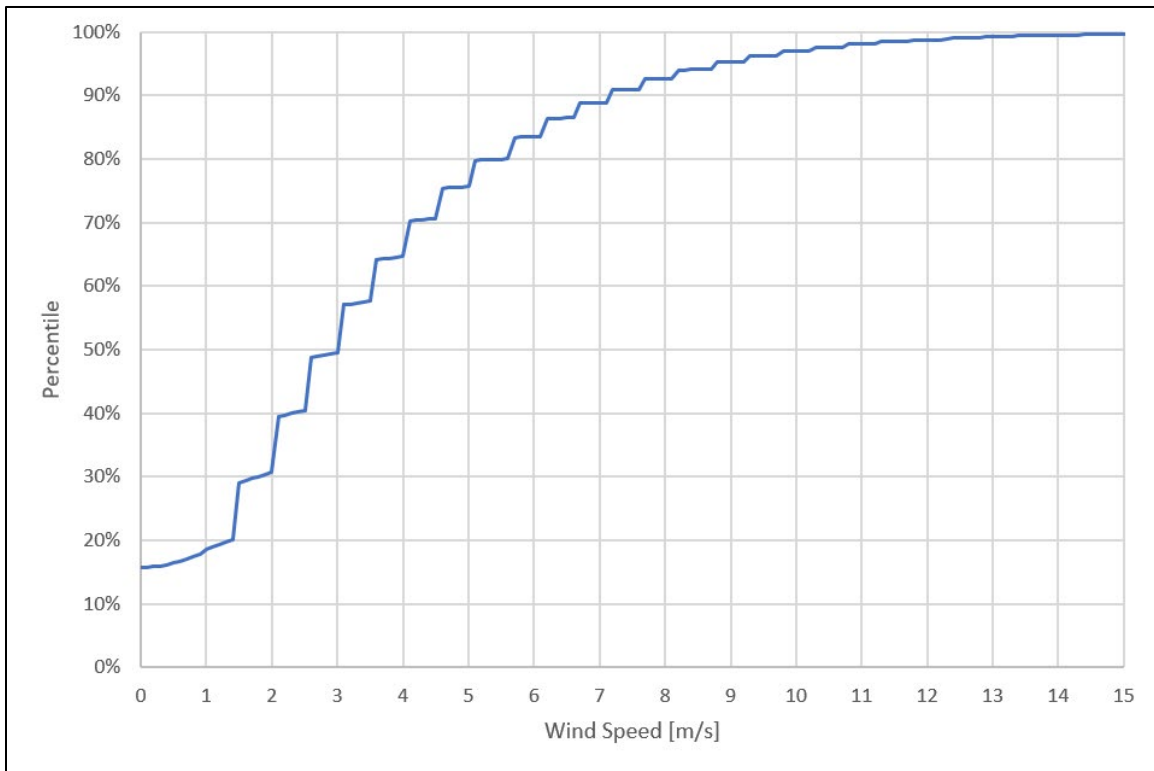


Figure 3-5: Wind speed percentiles for the Mountain Division

### 3.2.2.3 West North Central Division

The West North Central grouping lies in the Midwest and consists of North and South Dakota, Nebraska, Kansas, Minnesota, Iowa and Missouri. The analysis for this division included 389 stations and approximately 26.8 million hourly weather data points. The frequency of occurrence of nil-wind conditions is approximately 13.3%, while low winds occur approximately 8.1% of the time. The cumulative wind speed distribution is shown in Figure 3-6.

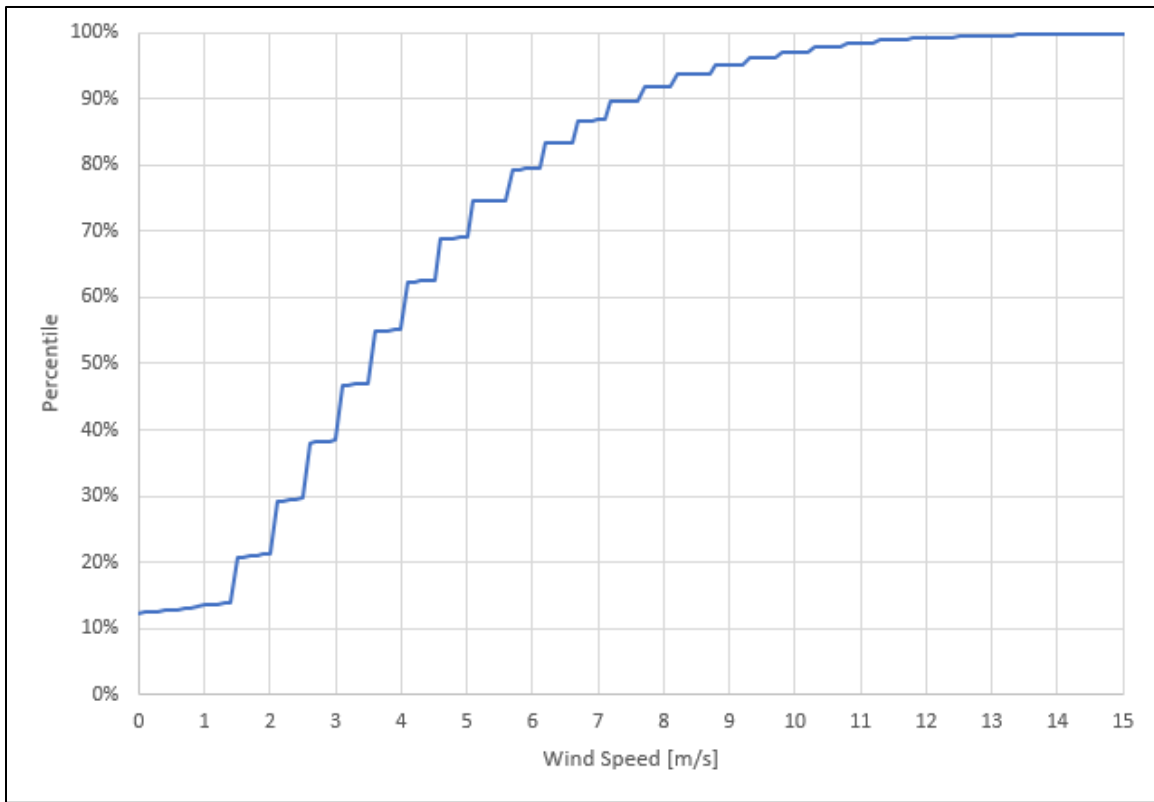


Figure 3-6: Wind speed percentiles for the West North Central Division

**3.2.2.4 East North Central Division**

The East North Central Division is located in the Midwest and includes Wisconsin, Illinois, Indiana, Michigan and Ohio. The analysis for this division included 343 stations and approximately 22.2 million hourly weather data points. The frequency of occurrence of nil-wind conditions is approximately 17.0%, while low winds occur approximately 9.6% of the time. The cumulative wind speed distribution is shown in Figure 3-7.

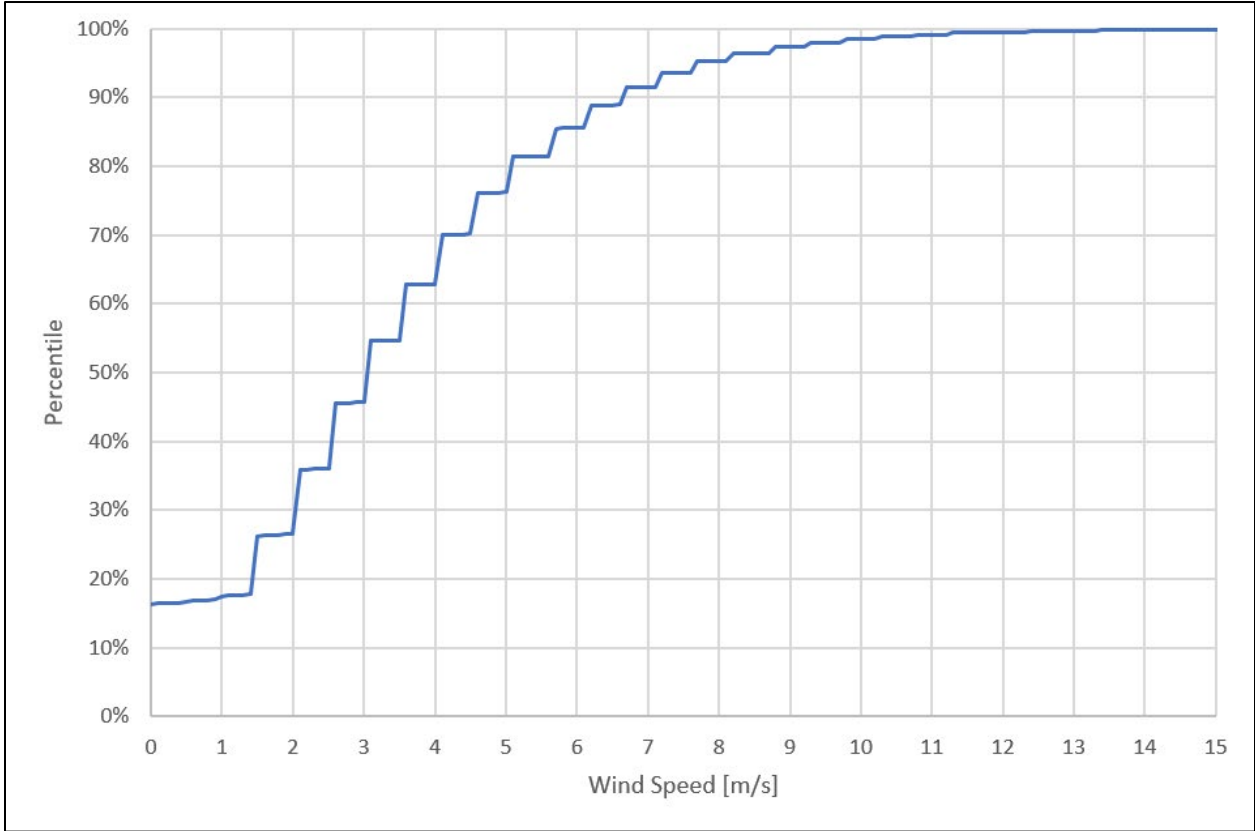


Figure 3-7: Wind speed percentiles for the East North Central Division

### 3.2.2.5 Middle Atlantic Division

The Middle Atlantic Division is the western portion of the Northeast, consisting of New York, Pennsylvania, and New Jersey. The analysis for this division included 123 stations and approximately 7.6 million hourly weather data points. The frequency of occurrence of nil-wind conditions is approximately 23.0%, while low winds occur approximately 10.5% of the time. The cumulative wind speed distribution is shown in Figure 3-8.

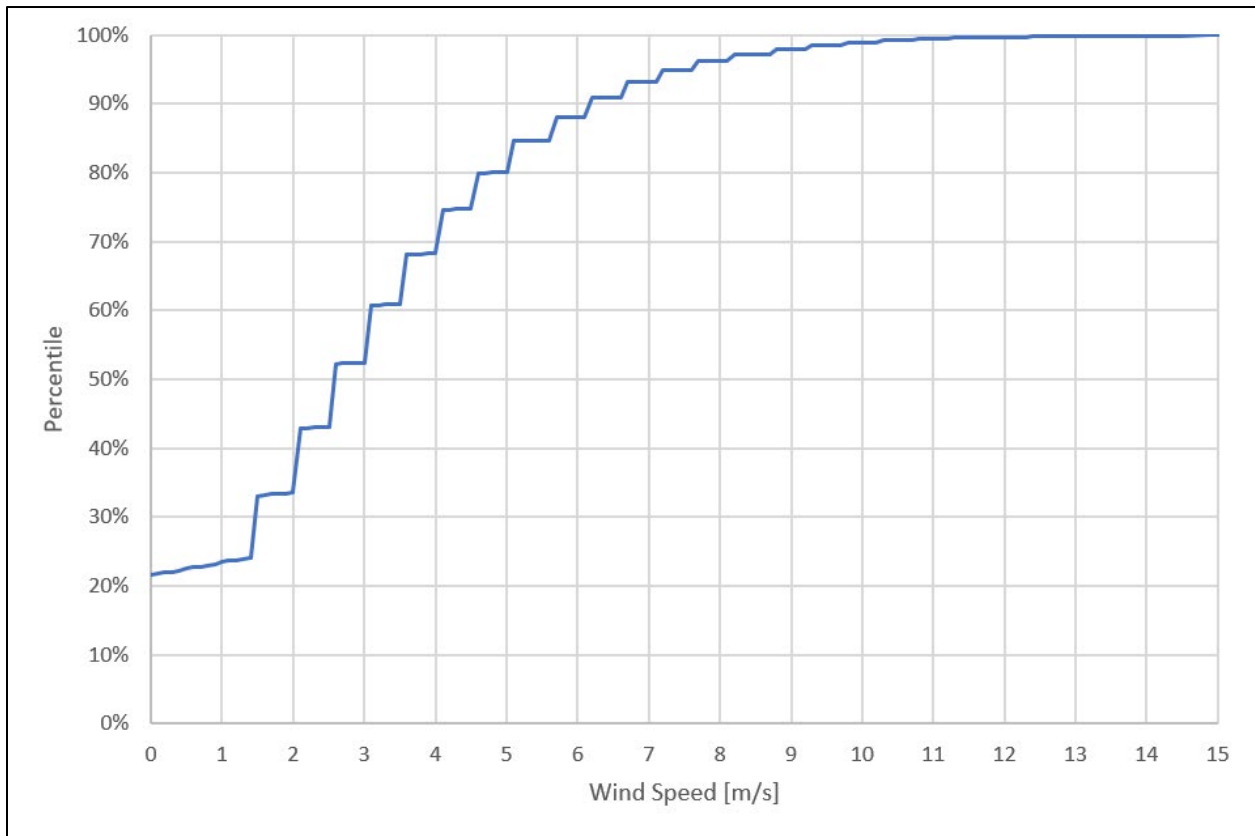


Figure 3-8: Wind speed percentiles for the Middle Atlantic Division

### 3.2.2.6 New England Division

The New England Division of the Northeast Region includes Maine, New Hampshire, Vermont, Massachusetts, Connecticut, and Rhode Island. The analysis for this division included 115 stations and approximately 7.2 million hourly weather data points. The frequency of occurrence of nil-wind conditions is approximately 23.3%, while low winds occur approximately 11.6% of the time. The cumulative wind speed distribution is shown in Figure 3-9.

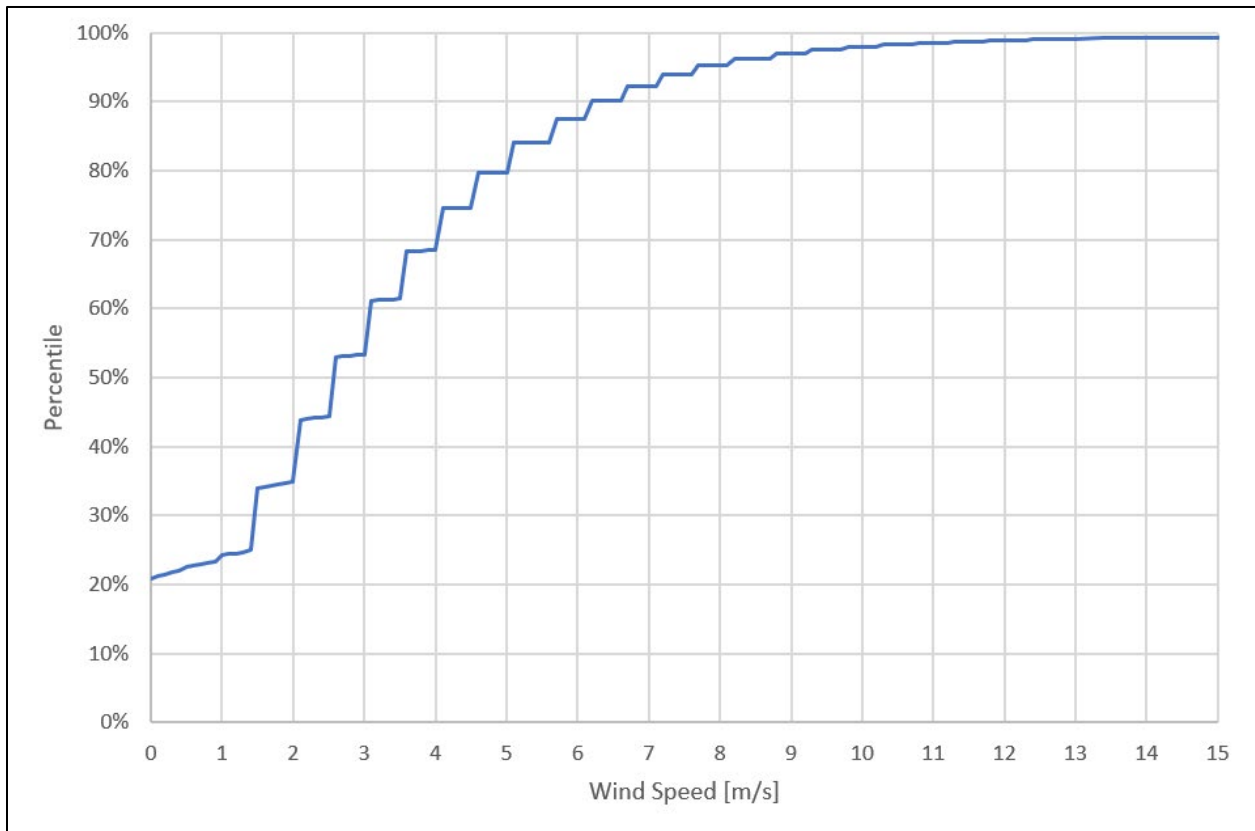


Figure 3-9: Wind speed percentiles for the New England Division

### 3.2.2.7 West South Central Division

The West South Central Division of the Southern Region consists of Oklahoma, Texas, Arkansas, and Louisiana. The analysis for this division included 388 stations and approximately 25.5 million hourly weather data points. The frequency of occurrence of nil-wind conditions is approximately 16.8%, while low winds occur approximately 9.1% of the time. The cumulative wind speed distribution is shown in Figure 3-10.

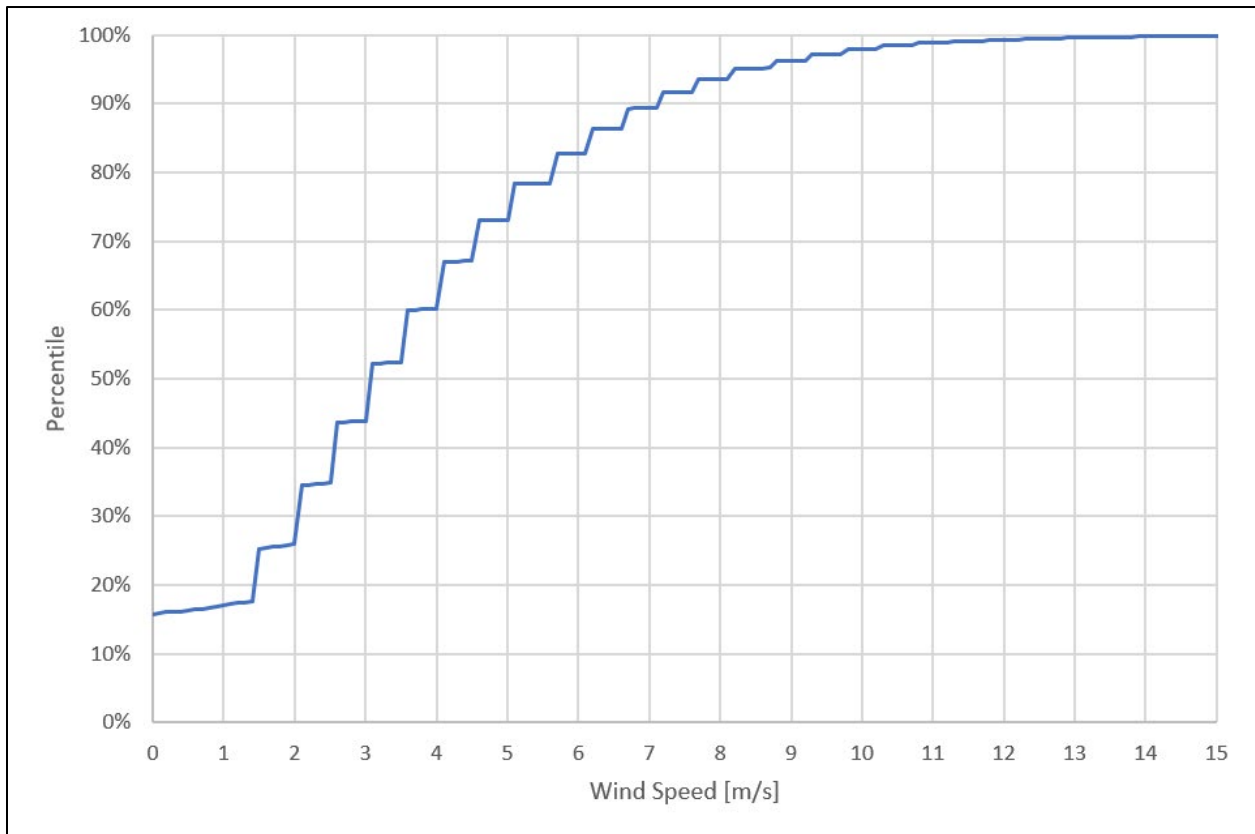


Figure 3-10: Wind speed percentiles for the West South Central Division

### 3.2.2.8 East South Central Division

The East South Central Division of the Southern Region includes Kentucky, Tennessee, Mississippi, and Alabama. The analysis for this division included 168 stations and approximately 9.6 million hourly weather data points. The frequency of occurrence of nil-wind conditions is approximately 29.3%, while low winds occur approximately 13.9% of the time. The cumulative wind speed distribution is shown in Figure 3-11.

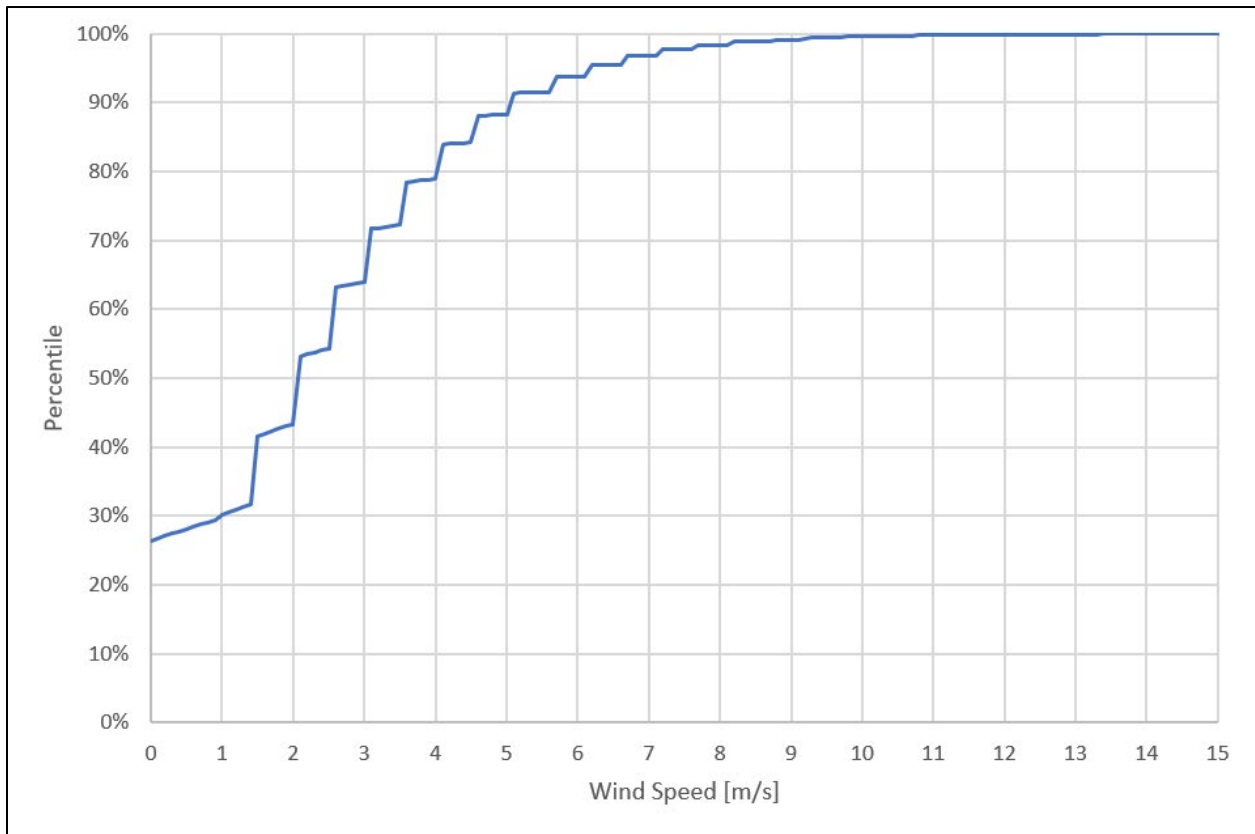


Figure 3-11: Wind speed percentiles for the East South Central Division

### 3.2.2.9 South Atlantic Division

The South Atlantic Division of the southern Region includes West Virginia, Maryland, Delaware, Virginia, North Carolina, South Carolina, Georgia, and Florida. The analysis for this division included 501 stations and approximately 29.9 million hourly weather data points. The frequency of occurrence of nil-wind conditions is approximately 28.1%, while low winds occur approximately 12.3% of the time. The cumulative wind speed distribution is shown in Figure 3-12.

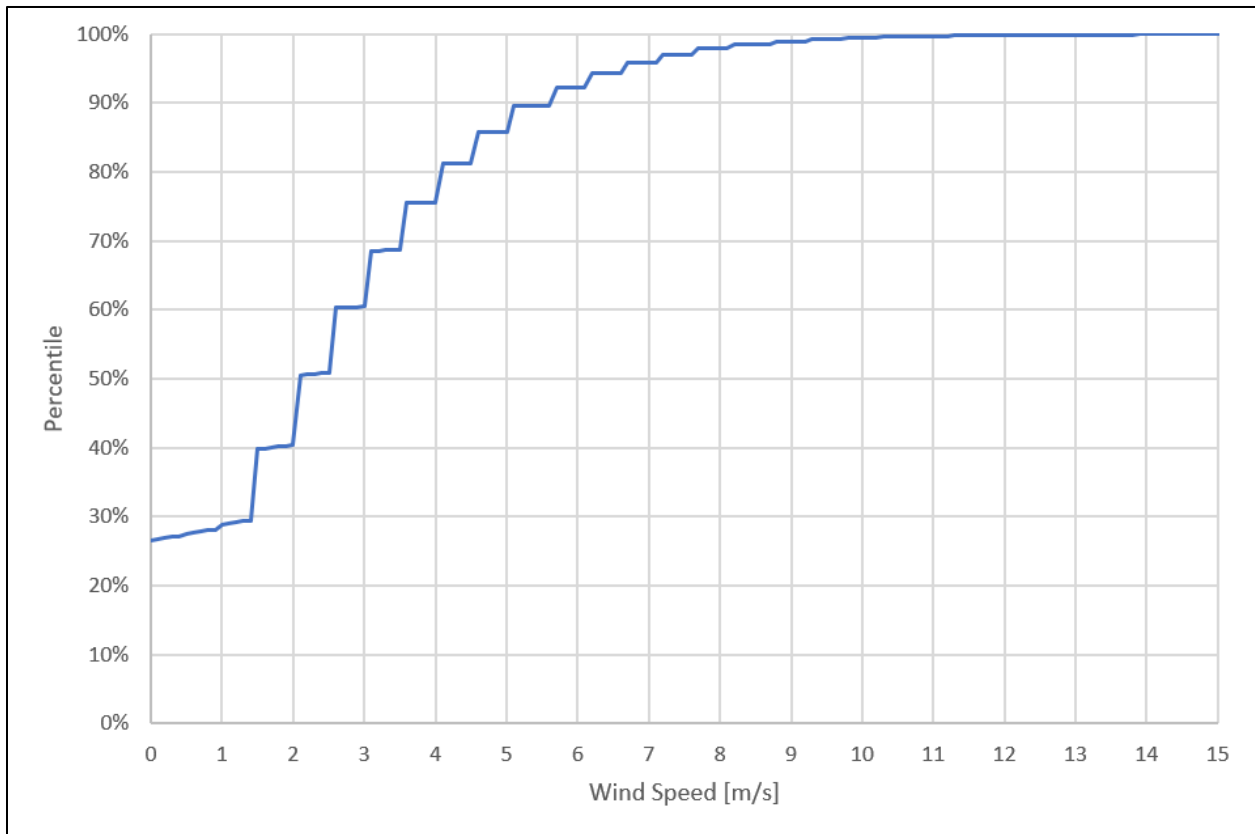


Figure 3-12: Wind speed percentiles for the South Atlantic Division

	<b>Vapor Cloud Explosions at Nil Wind</b>	03904-RP-006
	PHMSA	Rev A
	Final Report	Page 38 of 213

### 3.2.3 Wind Speed Analysis Observations

The wind speed percentile curves in the previous subsection have a pronounced stepped profile, which is due to an inconsistent reporting of wind speeds among weather stations. In fact, approximately 82% of weather stations do not report wind speeds below 1.5 m/s, listing any measurement below this threshold as “calm” wind (0 m/s wind speed); additionally, they report higher wind speeds at intervals of approximately 0.5 m/s. The remaining 18% of weather stations, instead, report wind speed measurements down to 0.1 m/s, with a resolution of 0.1 m/s. NOAA staff were contacted about this inconsistency and provided data sheets for instrumentation, which indicated that wind speeds should be recorded from 0 m/s up to at least 65 m/s. A station-by-station review of the instrumentation, maintenance and calibration was not possible within the scope of this task.

Another concern with broad averaging of weather data is that not all weather stations have anemometers located at the standard elevation of 10 m above grade. Since the instrumentation height is not included in the weather data files, a station-by-station review and power-law adjustment of reported wind speeds would not be practical. Additionally, the focus of this study is on nil-wind speeds, which were defined as wind speeds less than 1 m/s and therefore are marginally affected by power-law adjustments; therefore, no modifications were made to the reported wind speed data.

While considering average data across the country, or portions of the country, is important in order to establish the overall relevance of certain conditions, local data overrides any national or regional averages when evaluating a specific site. This will be further discussed in the next subsection.

As pointed out by the technical advisory panel, wind direction is also an important parameter when evaluating the consequences of a hazardous release, particularly within the context of a risk analysis. Coastal facilities are more likely to experience winds to/from the water and, therefore, are affected by wind direction differently than inland facilities, which tend to see a more uniform distribution of wind directions, particularly at low wind speeds. Another factor that may be considered in a risk assessment is that industrial incidents tend to occur with a higher frequency during nighttime hours, which often coincide with a higher frequency of nil/low wind conditions.

### 3.2.4 Site-Specific Results

A site-specific wind speed analysis is provided here for two existing US-based LNG facilities. The purpose of this analysis is to demonstrate the criticality of analyzing local data for each project, as it may be significantly different from the respective regional or divisional averages.

### 3.2.4.1 Freeport LNG, Quintana Island, Texas

Freeport LNG falls within the West South Central Division of the Southern Region. It is located on Quintana Island on the edge of the Gulf of Mexico. Adjacent to the site is a NOAA Weather Buoy, FPST2, which collects data at 6-minute intervals. The location of the buoy is illustrated in Figure 3-13.

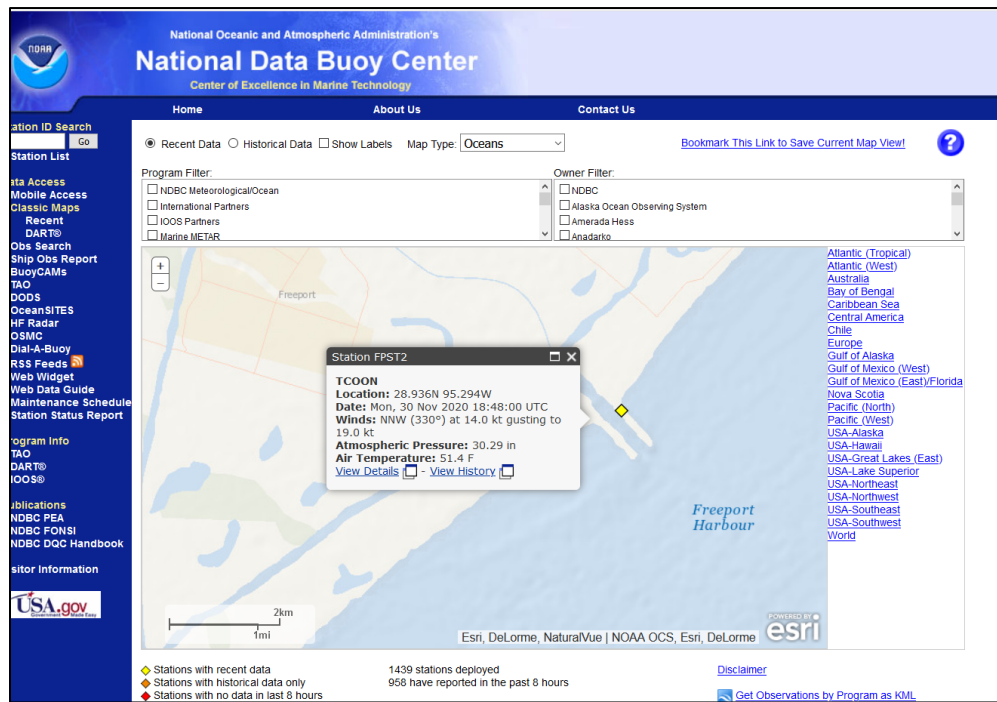


Figure 3-13: NOAA Weather Buoy near Freeport, Texas

Data from this weather buoy was analyzed and compared with the corresponding divisional data. The buoy provided 121,885 hourly weather data points from 2018 and 2019. As the buoy anemometer is located at 15 m above mean sea level, the power law was applied to estimate the wind speed at the nominal 10 m elevation. The percentage of nil wind conditions at the buoy was calculated as approximately 3.0%, while low wind was found to occur 4.9% of the time, a reduction of 13.8% and 4.2%, respectively, from the West South Central Division average results.

	<b>Vapor Cloud Explosions at Nil Wind</b>	03904-RP-006
	PHMSA	Rev A
	Final Report	Page 40 of 213

### 3.2.4.2 Cove Point LNG, Lusby, Maryland

Cove Point LNG is in Maryland and therefore falls within the South Atlantic Division of the Southern Region. It is located on the Chesapeake Bay in Southern Maryland. Adjacent to the site is NOAA Weather Buoy COVM2. This buoy collects data at 6-minute intervals. The location of the buoy is illustrated by the diamond with associated label information in Figure 3-14.

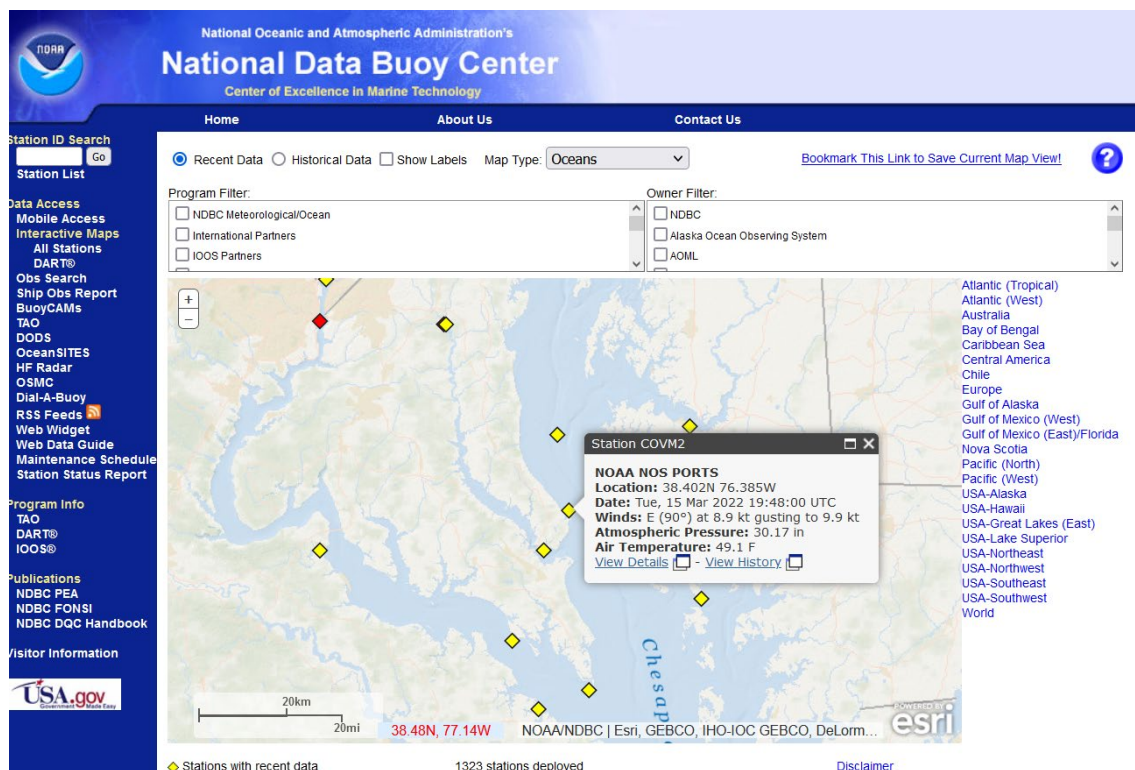


Figure 3-14: NOAA Weather Buoy in Cove Point, Maryland

Data from this weather buoy was analyzed and compared with the corresponding divisional data. The buoy provided 405,873 hourly weather data points from 2015 to 2019. As in the previous case, the power law has been used to adjust the wind speed to 10 m height. The percentage of nil wind was found to be 1.4%, with low wind at 3.0%, a reduction of 26.7% and 9.3%, respectively, from the South Atlantic Division results.

### 3.3 Wind Speed Statistics Summary

The statistical analysis of wind speed data resulted in the following observations:

- The average frequency of occurrence of nil-wind conditions (wind speed < 1 m/s at 10 m elevation) across the United States, as well as within several of the US

	<b>Vapor Cloud Explosions at Nil Wind</b>	03904-RP-006
	PHMSA	Rev A
	Final Report	Page 41 of 213

Census Bureau divisions, exceeds 20%, which is significantly higher than expected based on the wind speed ranges considered in most LNG facility siting studies.

- Over 80% of weather stations report no wind speed values between 0 and 1.5 m/s, meaning that any wind speed below 1.5 m/s is reported as 0 m/s; therefore, the available data overestimates the occurrence of “nil wind” and does not provide a reliable indication of the actual frequency of these conditions.
- Site-specific data can be significantly different from national or even divisional averages, particularly for coastal facilities, where a buoy may be the most representative source of data.
- While national averages may be used to inform regulatory decision making, site-specific data should always be applied to individual siting studies.

	<b>Vapor Cloud Explosions at Nil Wind</b>	03904-RP-006
	PHMSA	Rev A
	Final Report	Page 42 of 213

#### 4 Vapor Cloud Development in Nil-Wind Conditions

The HSE's review of large vapor cloud incidents found that “[i]n many of cases examined, 50% (12/24), there is clear evidence from the well-documented transport of vapor in all directions and/or meteorological records that the vapor cloud formed in nil/low-wind conditions. In a further 21% (5/24), the pattern of vapor transport suggests nil/low-wind conditions but there is insufficient data available to be sure”. The authors noted how this frequency is much higher than the overall frequency of nil/low-wind conditions, which they estimated at approximately 5%; consequently, they hypothesized that “[t]he likely explanation for this finding is that a wider range of smaller losses of containment (with much higher frequency) have the potential to cause a large cloud in these conditions, if the releases are not stopped and the vapor is allowed to accumulate around the source”.

Before addressing the technical aspects of vapor dispersion, it is worth observing that the majority of the incidents reviewed in RR1113 occurred at night or in the early morning, which is when nil/low-wind conditions are more likely to occur but also when plant personnel numbers are typically reduced in many industrial facilities. This is consistent with statistical data on industrial fires, which indicate that a majority of large-loss events occurs during the night shifts [7].

It is also important to note that, for LNG facilities, the “smaller losses of containment” typically consist of small-bore releases from pressurized piping or vessels. Vapor dispersion modeling shows that these scenarios tend to reach a steady state very rapidly and result in limited hazard areas; furthermore, given the high momentum due to the pressurized release, these scenarios are not strongly affected by low wind conditions.

The trend of lower wind speeds resulting in longer dispersion distances, particularly when accompanied by stable atmospheric conditions, is generally recognized and attributed to the lower degree of turbulent mixing at the interface between the cloud and ambient air. However, whether this trend continues as wind speeds approach zero is not as well established. For example, a zero-momentum release (e.g., a liquid spill) on flat, unobstructed terrain would result in a circular cloud, which would slowly mix with ambient air by molecular diffusion; this could result in a large footprint due to the slow mixing process, however, the distance traveled from the source will be shorter than a cloud pushed by a non-zero wind. Similarly, the effect of the release's own momentum and turbulence on the mixing of the vapor cloud, as the wind speed decreases, should not be dismissed. Finally, there is no direct correlation between the footprint of a flammable cloud and its vapor cloud explosion hazard potential, as the VCE potential is associated with the flammable portion of the cloud: therefore, it is certainly possible for a highly-stratified, poorly mixed cloud to extend farther than a turbulent, well-mixed one, yet have a smaller VCE hazard potential because a large portion of the cloud is too rich to burn.

	<b>Vapor Cloud Explosions at Nil Wind</b>	03904-RP-006
	PHMSA	Rev A
	Final Report	Page 43 of 213

RR1113 introduced a single example to support their argument: they evaluated a 2" release from a propane storage tank, under 5 m/s, 2 m/s and nil/low-wind conditions (the actual wind speed was not provided). The modeling was performed using the HSE's own integral dispersion model, DRIFT [8]. The single example is insufficiently described to allow for proper verification; it is also insufficient to illustrate "why nil/low-wind conditions dominate records of major vapor cloud incidents even though the weather frequency is low". In order to evaluate the effect of nil/low wind conditions on the potential hazards of flammable releases, the BLUE project team performed a broader analysis including several scenarios typical of LNG facility siting studies, modeled using the PHMSA-approved CFD tool FLACS<sup>2</sup>. The details and results of the analysis are discussed in Sections 5 and 6.

#### 4.1 Vapor Cloud Explosions

The scope of this section is to revisit RR1113 within the context of PHMSA-regulated LNG facilities and to clarify the phenomena associated with VCEs according to the current leading point of view within the scientific community.

RR1113 provides some background information on vapor cloud explosions, briefly discussing concepts such as the effects of confinement and congestion on the propagation of the flame front through a flammable mixture. The report then discusses three types of severe events: high-order (supersonic) deflagrations; episodic deflagrations; and detonations. While the concepts of supersonic deflagrations and detonations represent well-defined and generally agreed-upon stages of certain vapor cloud explosions, the concept of episodic deflagration is more recent ([8]–[10]) and far from accepted by the scientific community.

The concept of episodic deflagration is described by Atkinson and Cusco within the context of the Buncefield accident [9] as a situation which might occur for very large clouds in the open (i.e., with relatively low congestion) as a result of natural flame instability. In this event, they argue that "a target ahead of the flame would experience a series of separate blasts that increased in strength as the flame approached" and postulate that "[o]ne possible mechanism that might allow such a burning pattern is the effect of preheating of unburned gas ahead of a flame by thermal radiation". A characteristic of episodic deflagrations is that they would be unlikely to transition to detonation, "because fast burning would be confined to finite volumes of gas preheated by radiation" and "[w]hen such preheated material was consumed there would be a pause until thermal radiation had regenerated the conditions necessary for fast burning".

---

<sup>2</sup> The FLACS CFD tool is described in section 5.2.

	<b>Vapor Cloud Explosions at Nil Wind</b>	03904-RP-006
	PHMSA	Rev A
	Final Report	Page 44 of 213

Therefore, deflagration-to-detonation-transition (DDT) and episodic deflagrations are mutually exclusive events.

RR1113 argues that episodic deflagrations, rather than detonations, occurred in several of the large vapor cloud explosion accidents they reviewed: for example, they indicate that accidents such as Buncefield, Jaipur, Amuay and San Juan did not show evidence of detonation. The basis for introducing a new phenomenon is that detonation is currently “the only established theory that allows sufficiently rapid burning to be sustained in open areas”, however, “there are serious discrepancies between the effects of experimental detonation on a variety of objects and what has been observed at most VCE incidents”; as a result, they conclude that there must be a different phenomenon which can cause the propagation of high-speed flame fronts through uncongested portions of a flammable cloud. The kingpin of the episodic deflagration mechanism, as explained in RR1113, is the role of radiation in pre-heating gases ahead of the flame front and producing localized explosions.

However, to date, the concept of episodic deflagration has not been generally accepted by the scientific community. In fact, several authors have presented counter-arguments that highlight flaws in the episodic deflagration theory.

For example, forensic evidence from the Buncefield accident is used in RR1113 to suggest that the high pressures observed over a large, uncongested area could only be explained in terms of a new mechanism (i.e., episodic deflagration). However, the authors ignored an alternative plausible explanation: the trees and dense shrubbery along the roads bounding the Buncefield facility provided congestion and such congestion was sufficient to accelerate the flame front to a DDT with associated high overpressures. The accident investigation found that DDT overpressures were consistent with the damage observed in and around the site. Additionally, a large experimental and modeling campaign was conducted, which demonstrated that congestion introduced by vegetation can indeed lead to flame acceleration in a similar manner to what piping and structural elements would do, and that current VCE modeling tools are capable of accurately predicting these effects [11], [12].

The concept of episodic deflagration was rejected by Abdel-jawad and Gavelli [13], who concluded that it should not be considered a realistic explanation for any real industrial accident due to the numerous non-physical assumptions. They focused their critique on the non-physical assumptions made by Atkison et al. in the description of the mechanism. For example, the diagram used in RR1113 to explain the behavior of the flame front during an episodic deflagration event (Figure 4-1) shows a stair-stepped curve, which suggests that the flame front would advance for a period of time, then suddenly stop (presumably as it waits for the gases ahead to warm up and ignite), then it suddenly resumes advancing, and then repeats the cycle. This is clearly a non-physical behavior, as the flame front cannot remain still within a flammable vapor cloud: it must either burn through the flammable mixture or be quenched. Furthermore, as the flame

front is still, any overpressures accumulated during the advancing phase would rapidly dissipate. It should further be noted that the curve in Figure 4-1 is inconsistent with the HSE's own explanation of building damage (Figure 4-2), where they assume a linear pressure increase over time which, in turn, can only be achieved by a flame front advancing at a slowly increasing speed.

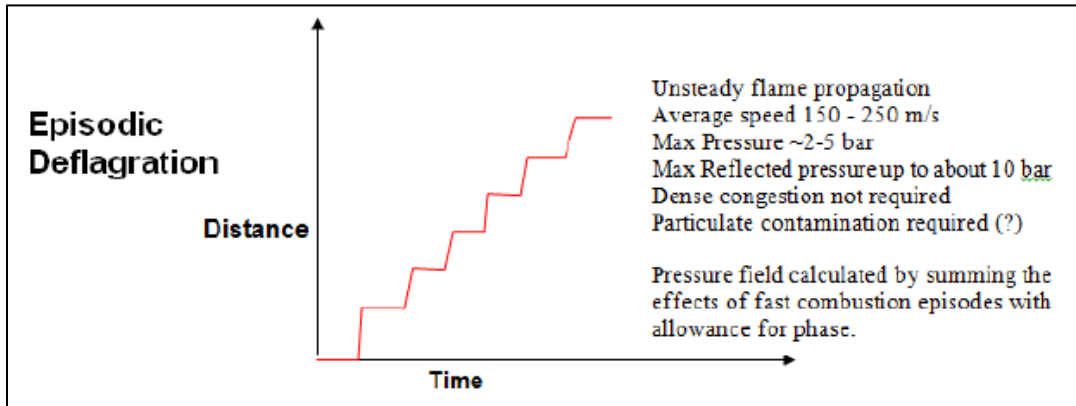


Figure 4-1. Flame propagation plot during episodic deflagration [1].

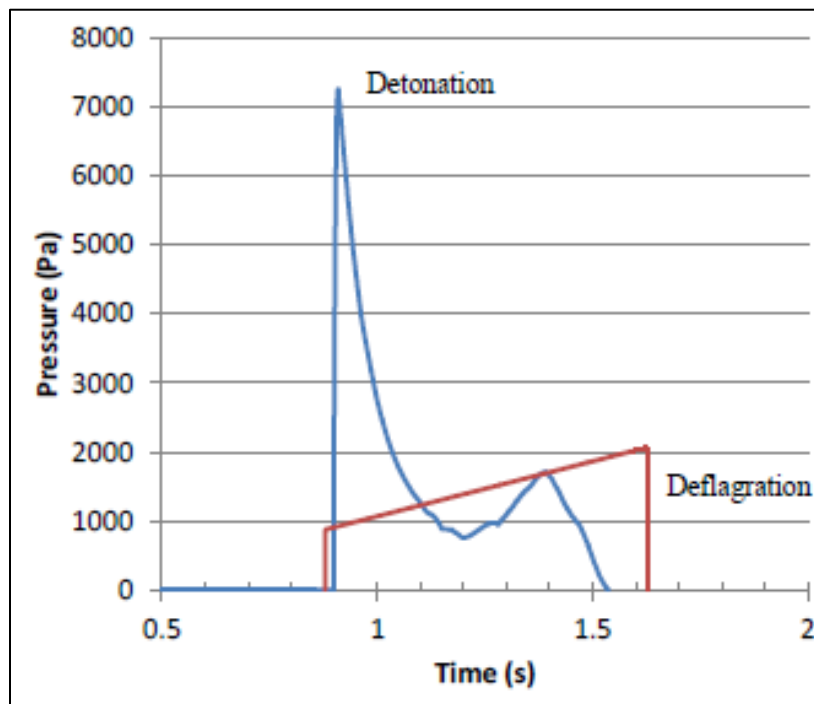


Figure 4-2. Comparison of overpressure curves from detonation (blue) and episodic deflagration (red) [1].

	<b>Vapor Cloud Explosions at Nil Wind</b>	03904-RP-006
	PHMSA	Rev A
	Final Report	Page 46 of 213

RR1113 estimates that temperature rise on the order of 200-400 °C are possible under certain conditions; however, as the flammable gases ahead of the flame front are heated up, they would become lighter than the surrounding, colder cloud and begin to rise. The density of a gas heated 400 °C above ambient temperature is approximately 40% of the density of the surrounding ambient (assuming ideal gas conditions, for simplicity). As shown by Abdel-jawad and Gavelli (see Figure 4-3), this degree of buoyancy would result in strong upward currents lifting the heated gases and removing them from the path of the flame front, halting the flame propagation.

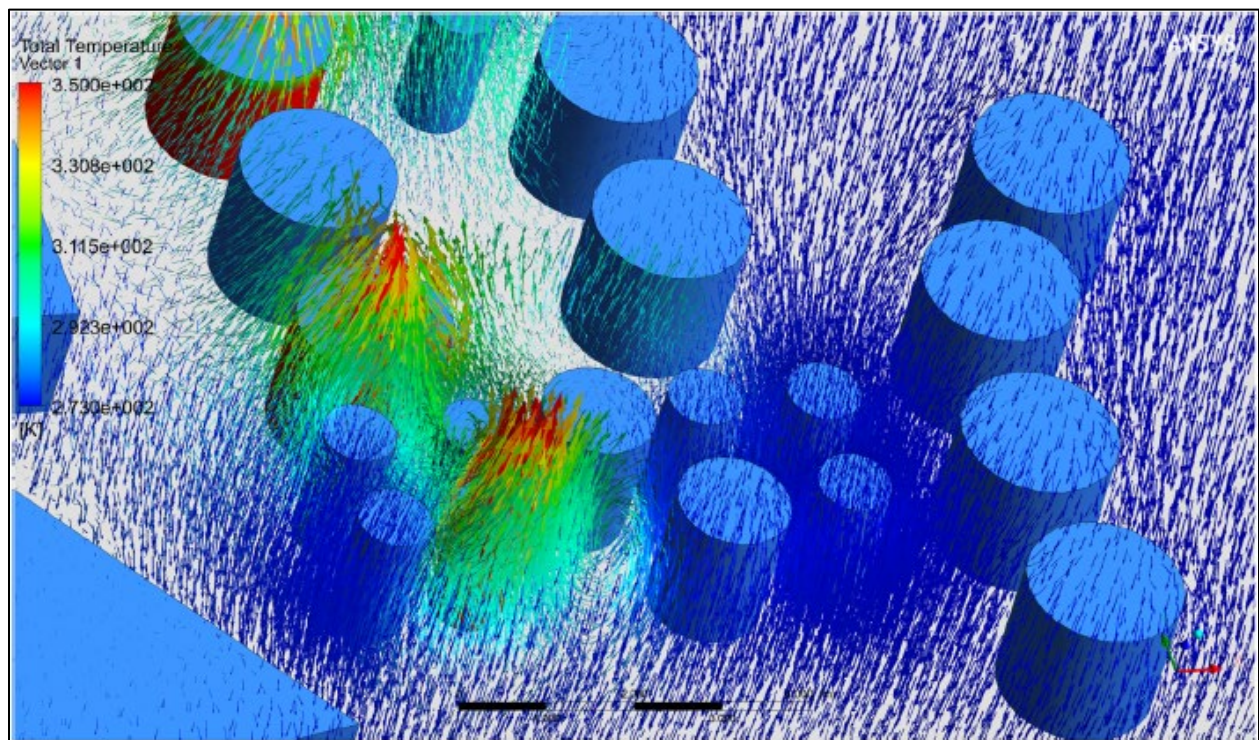


Figure 4-3. Numerical simulation showing the buoyancy of heated gases [13].

Johnson and Tam [14] also rejected episodic deflagration as a possible explanation for Buncefield. Instead, based on the evidence from the accident and the results of a joint industry research project into the explosion mechanism [8], they concluded that the flame accelerated in the line of trees and bushes and quickly underwent a DDT at the north end of the site. Johnson and Tam drew the similar conclusions after reviewing the accidents in Jaipur, Port Hudson, and Ufa: in each case, minimal pipework congestion was present, however, the flammable cloud extended over vegetation; additionally, each case presented the same pattern of directional indicators pointing “inwards”

	<b>Vapor Cloud Explosions at Nil Wind</b>	03904-RP-006
	PHMSA	Rev A
	Final Report	Page 47 of 213

towards the source of the explosion due to the expansion of the hot combustion products behind the flame front. The paper also includes a discussion of physical testing on oil drums and other objects, which further supports the occurrence of DDT in those accidents. The same conclusions regarding DDT were drawn by Chamberlain et al. [15], who reviewed several of the large VCE accidents also included in RR1113.

Davis et al. [16] rejected the explanation of these large vapor cloud explosions as examples of episodic deflagrations. The authors explained how experiments – ranging from laboratory to large scale, and under conditions much more favorable to the postulated mechanism than any realistic scenario – conducted to demonstrate episodic deflagrations failed to produce the forward thermal radiation that supposedly drives this phenomenon and did not result in increased overpressures. An example is provided in Figure 4-4, which shows two images used in RR1113 as alleged evidence of the effect of fine particulate on the flame front propagation: as Davis et al. explained, there was no evidence in these tests of ignition ahead of the flame front or of increased overpressures; the only difference was a brighter flame due to radiation from the particulate.

The same group also reviewed and critiqued the HSE's analysis of the forensic evidence from several large vapor cloud explosion accidents; their conclusion is that the HSE's arguments were based on partial evidence and focused on examples that favor their argument while disregarding other available evidence that disproves it. The authors also introduced newly acquired results from an extensive set of explosion tests which further support the well-established theory of DDT over the unproven episodic deflagration hypothesis.

Another factor that was neglected in RR1113 is the ignition location. In several cases, the flammable cloud is known to have ignited within a confined space – for example, inside the boiler chamber at Skikda, or inside the pump house at Buncefield. A VCE originating in a confined space is likely to receive a boost to the flame speed and emerge from the confined space as a stronger explosion than a VCE originating in an unconfined area. This observation is important for the purpose of facility siting studies, particularly when a facility may not include the ability to detect flammable gas ingress into buildings or enclosed spaces with non-explosion proof equipment and to initiate appropriate executive actions.

	<b>Vapor Cloud Explosions at Nil Wind</b>	03904-RP-006
	PHMSA	Rev A
	Final Report	Page 48 of 213



**Figure 246: Flame propagating through clean pipe array**

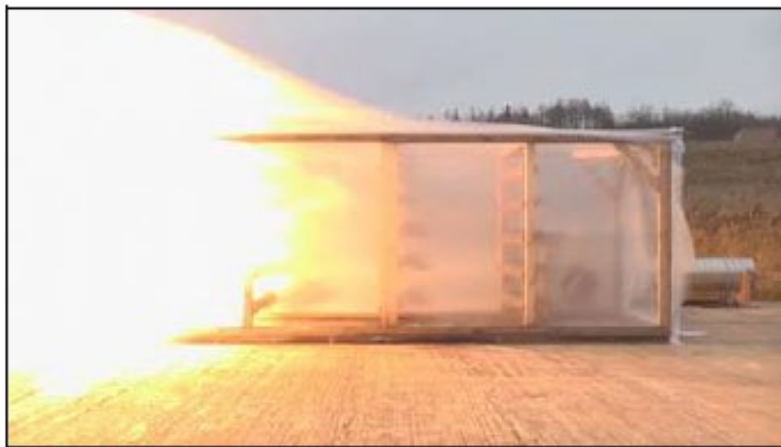


**Figure 247: Flame propagating through pipes contaminated with soot at 500 mg/m<sup>2</sup>**

Figure 4-4. Example of flame propagation tests [16].

Based on the review of available literature on the topic, the project team agrees with the prevailing opinion, that the observed vapor cloud explosion consequences in accidents such as Buncefield are consistent with DDT and that the flame acceleration required to achieve those conditions was caused by interaction of the flame front with congestion due to vegetation. Therefore, the concept of episodic deflagration is not relevant to these scenarios. Furthermore, as demonstrated by Bakke et al. [11], existing VCE modeling tools are able to accurately predict that interaction; therefore, there is no evidence that “our fundamental understanding of the mechanisms that operate in large VCEs is incomplete” nor that there are gaps in the ability to perform accurate safety analyses of vapor cloud explosions.

## 4.2 Review of Historical Incidents

RR1113 reviewed and examined a total of 24 vapor cloud explosion incidents, as listed in Table 4-1.

Table 4-1. Vapor cloud explosion incidents examined in RR1113.

Location	Date	Type of Facility	Release Notes
Geismer, LA	2013	Petrochemical plant	Heat exchanger explosion
Amuay, Venezuela	2012	Refinery tank farm	Light hydrocarbon spray
San Juan, Puerto Rico	2009	Fuel storage depot	Gasoline overfill
Jaipur, India	2009	Fuel storage depot	Gasoline spray
Big Spring, TX	2008	Refinery	Propylene spray
Buncefield, United Kingdom	2005	Fuel storage depot	Gasoline overfill
Skikda, Algeria	2004	LNG facility	Refrigerant leak
Lively, TX	1996	LPG pipeline	Pipeline leak
Naples, Italy	1995	Fuel depot	Gasoline overfill
Brenham, TX	1992	LPG storage cavern	Spray release
La Mede, France	1992	Refinery	Light hydrocarbon release
St. Herblain, France	1991	Fuel depot	Gasoline spray
North Blenheim, NY	1990	LPG pipeline	Pipeline leak
Ufa, Russia	1989	LPG pipeline	Pipeline leak
Baton Rouge, LA	1989	Refinery	Hydrocarbon spray
Pasadena, TX	1989	HDPE unit	Ethylene/isobutane release
Norco, LA	1988	Refinery	Propane release
Newark, NJ	1983	Fuel depot	Gasoline overfill
Donnellson, IA	1978	LPG pipeline	Pipeline leak
Ruff Creek, PA	1977	LPG pipeline	Pipeline leak
Devers, TX	1975	LPG pipeline	Pipeline leak
Flixborough, United Kingdom	1974	Process plant	Cyclohexane release
Austin, TX	1973	LPG pipeline	Pipeline leak
Port Hudson, MO	1970	LPG pipeline	Pipeline leak

	<b>Vapor Cloud Explosions at Nil Wind</b>	03904-RP-006
	PHMSA	Rev A
	Final Report	Page 50 of 213

The primary objective of RR1113 “was to improve understanding of vapor cloud development and explosion in order to examine the potential for these hazards to exist or develop at LNG export plants [...]”. Even though the HSE study was co-sponsored by PHMSA and the project was specifically focused on VCE hazards in LNG facilities, only one of the 24 accidents included in their study occurred at an LNG facility (the 2004 explosion at the Sonatrach liquefaction plant in Skikda, Algeria); all other accidents occurred in facilities or pipelines that are not subject to PHMSA’s LNG regulatory requirements. RR1113 did not discuss any of the differences in design, safety measures and regulations between the accident plants and PHMSA-regulated LNG facilities, nor how these differences might affect the likelihood of certain accidents occurring or their magnitude. Since the current research project is funded by PHMSA and is specifically aimed at informing potential future regulatory changes, it is important to review these accidents in the context of LNG facilities designed and built to current PHMSA requirements.

It is also important to note that any reference in this report to PHMSA regulations refers to currently applicable requirements, not to proposed regulatory changes nor to earlier editions. This is important because LNG facilities in operation would be considered “grandfathered” with respect to any regulatory changes and therefore not required to update their facility siting study.

The following subsections briefly discuss the common precipitating events leading to the accidents reviewed in RR1113, framing them within the context of PHMSA’s regulatory environment. Unless otherwise noted, the source of information on each accident described below is RR1113 itself.

#### **4.2.1 Tank Overfills**

Several of the accidents in Table 4-1 consisted of large releases due to the overflow of atmospheric storage tanks. For example:

- Buncefield: the site consisted of a gasoline, diesel, and jet fuel storage terminal for Hertfordshire Oil Storage Ltd in Buncefield, UK. The overflow was initiated due to the malfunction of the tank process level indicator and automatic high level shutoff system. The overflowing continued for 23 minutes at 550 m<sup>3</sup>/hr – 900 m<sup>3</sup>/hr, until the vapor cloud eventually reached the tanker loading gantry where a driver reported the vapor cloud. The site emergency system was activated, starting a fire pump, which reportedly ignited the vapor cloud.
- Naples: the Agip gasoline storage facility in Naples, Italy included a gasoline tank that overflowed leading to a vapor cloud and subsequent explosion. The cause leading to the overflow is not known in detail; however, the overflowing is estimated to have continued for approximately 90 minutes.
- Newark: the Texaco fuel storage site in Newark, New Jersey was filling the incident tank at a rate of 5,000 gpm. During their regular rounds, operators discovered that

	<b>Vapor Cloud Explosions at Nil Wind</b>	03904-RP-006
	PHMSA	Rev A
	Final Report	Page 51 of 213

the tank was overflowing, followed by an explosion minutes later. The duration of the overfill is unknown.

- San Juan: the Caribbean Petroleum Corporation facility in San Juan, Puerto Rico consisted of a gasoline tank farm and import operation. One of the storage tanks overfilled for an estimated 26 minutes developing a large vapor cloud, which eventually ignited. The cause was determined to be a combination of a malfunctioning tank level gauge and a change in the gasoline fill rate; RR1113 also suggested a potential failure in the tank's floating roof.
- Brenham: the facility owned by MAPCO Natural Liquids consisted of an LPG underground storage cavern. That cavern was overfilled resulting in the development of a large vapor cloud, which ignited. The cause of the overfill was that the capacity of the storage cavern was not accurately known, and operators did not effectively track inventory changes. Additionally, the well-head safety system was inoperative and was not fail-safe.

LNG facilities can contain several storage tanks designed to store liquid hydrocarbons, including LNG storage tanks, refrigerant make-up vessels and heavy condensate storage tanks.

Unlike the gasoline storage tanks involved in most of the accidents listed above, LNG storage tanks at LNG facilities are required by 49 CFR 193 (via NFPA 59A-2001, §7.1.1.1) to be equipped with two independent liquid level gauging systems that alarm operators with sufficient time to shut off flow to the tank before overfilling. In addition, regulations require an independent high liquid switch to be installed that would automatically cut off flow to the tank on a high liquid level reading (NFPA 59A-2001, §7.1.1.2 and §7.1.2.1). Therefore, a minimum of three independent systems would have to fail at the same time, in order for an LNG tank overfill scenario to occur.

Non-LNG storage containers currently have similar, albeit slightly less stringent, requirements: each storage tank for refrigerants of flammable process fluids must have one liquid level gauging device and, if it is possible to overfill the tank, a high-liquid-level alarm is required, that would notify operators with sufficient time to shut off flow to the tank before overfilling (NFPA 59A-2001, §7.1.2.1); flammable refrigerant storage containers also require a high-liquid-level flow cutoff device (NFPA 59A-2001, §7.1.2.2). It should also be noted that the number of independent liquid level gauging devices for refrigerant of flammable process fluid containers was increased to two in NFPA 59A-2019, to make the requirement consistent with LNG containers.

In contrast to the requirements at LNG facilities, API RP 2350 "Overfill Protection for Storage Tanks in Petroleum Facilities" [17] does not require level detection for tanks at attended facilities. However, in the absence of level detectors, written procedures for product receipt, shutdown and diversion are required to be developed by the facility operator. These procedures require tanks receiving product to be checked by personnel, including verification of functioning gauging equipment, as well as periodic

	<b>Vapor Cloud Explosions at Nil Wind</b>	03904-RP-006
	PHMSA	Rev A
	Final Report	Page 52 of 213

checks during the filling operation. If performed properly, these procedures would identify malfunctioning gauging equipment and manually track tank fill levels to reduce the risk of an overflow.

PHMSA-regulated LNG facilities are also required to have a gas detection system to alarm operators when flammable vapors are detected (49 CFR 193.2507 and 193.2801); the same requirement does not apply to fuel storage depots. It should be noted that current PHMSA regulations do not specify minimum criteria (performance or other) for gas detector layouts; in fact, a parallel research effort (PHMSA R&D project #852, "Develop a Risk-Based Approach and Criteria for Hazard Detection Layout") was conducted by BLUE to evaluate performance criteria for hazard detection systems. Nonetheless, with any reasonable detector layout it is highly unlikely that the vapor cloud from a tank overflow would go undetected for as long as the incident cases listed above (e.g., more than 20 minutes at full flow). Additionally, LNG storage tanks are equipped with sensors to detect low temperatures and/or high pressures in the gap between inner and outer tank, which provides another layer of protection to stop operations if overflowing has occurred.

It is also worth noting that flat-bottom LNG storage tanks are often commonly designed, as "full-containment". The full containment tanks include a secondary container, sized to contain 110 percent of the maximum liquid capacity of the inner container. This secondary container would therefore hold overflow of LNG in the event that all the instrumentation layers of protection fail and the inner tank is filled past its operating limit.

As discussed further in section 4.2.3, LNG facilities are subject to maintenance and inspection requirements for all in-service equipment. Maximum maintenance and testing intervals are specified in order to minimize the likelihood of a problem. While mechanical failures and malfunctions cannot be completely prevented by maintenance alone, a properly conducted program (especially when combined with redundancy of critical components) can minimize the likelihood of accidents due to instrument or control malfunction, as occurred in several of the reviewed accidents.

It should also be noted that the volumes of heavy hydrocarbons (i.e., alkanes heavier than methane) present in LNG export plants for use in the liquefaction process or as a by-product from the liquefaction are often much smaller than those present in fuel depots, refineries or other facilities where these large VCEs occurred. Additionally, the liquid transfer rates associated with refrigerant storage or heavy condensate tanks in an LNG facility are typically much smaller (one to two orders of magnitude) than those in fuel depots. While these differences do not preclude the possibility that a large flammable vapor cloud may develop within an LNG facility, they do reduce the likelihood that a Buncefield-type event may occur and should therefore be recognized within the purpose of this study.

As discussed in section 4.1, some of these vapor cloud explosions were triggered by the ignition of the flammable cloud inside a confined space (e.g., the pump house at

	<b>Vapor Cloud Explosions at Nil Wind</b>	03904-RP-006
	PHMSA	Rev A
	Final Report	Page 53 of 213

Buncefield); this ignition scenario contributed to the initial acceleration of the flame front and may have led to worse consequences than a different ignition location. It is therefore important to note that LNG facilities under the jurisdiction of the Federal Energy Regulatory Commission are subject to additional requirements such as the installation of gas detection at each air intake to occupied buildings and other enclosed areas where non-explosion proof equipment is installed; while the same requirement is not currently in PHMSA regulations, it is included in the 2019 edition of NFPA 59A (NFPA 59A-2019, §16.4.1) [18]. This requirement is intended specifically to avoid the occurrence of strong initiating events, which could exacerbate the consequences of a vapor cloud explosion.

#### 4.2.2 Other Tank Spills

Two of the 24 accidents in Table 4-1 consisted of large liquid spills from atmospheric storage tanks, from causes other than overfills:

- Jaipur: The site consisted of a gasoline storage terminal for the Indian Oil Company that was entirely surrounded by an 8-ft tall wall. The incident was caused by a gasoline spill, which occurred due to mal-operation of a valve at the foot of a full storage tank: an operator opened the valve without noticing that the line included an open blind flange. The gasoline flow was driven by the head of liquid in the tank, and an attempt to shut down the leak failed due to a remote shut-off valve having been out of service for several years. The site did not have gas detection (although the leak was detected by operators, who tried unsuccessfully to control it).
- St. Herblain: A gasoline depot which included several storage tanks. A large leak developed in a union fitting at the foot of one tank, leading to the release of gasoline for approximately 20 minutes. The resulting vapor cloud reached an ignition source, leading to an explosion.

Both accidents listed above resulted in long-release gasoline spills because the storage tanks had a bottom withdrawal line, which allowed the head of liquid in the tank to continue pushing fuel through the leak. When reviewing these accidents within the context of PHMSA-regulated LNG facilities, it should be recognized that tanks with penetrations below the liquid level are present in many cases, and their installation in new facilities (which could be subject to any regulatory changes resulting from this research project) is currently allowed. However, atmospheric LNG tanks with penetrations below the liquid level have not been installed in the U.S. for over 20 years, and a provision was introduced in NFPA 59A-2019 prohibiting pipe penetrations below the liquid level in double, full, and membrane containment tank systems (§8.4.2.2); therefore, it is unlikely that new, large-volume LNG storage tanks with penetrations below the liquid level will be proposed to be installed.

However, pressurized LNG storage vessels, as well as flammable refrigerants and other flammable process fluids storage vessels for new LNG facilities typically include bottom

	<b>Vapor Cloud Explosions at Nil Wind</b>	03904-RP-006
	PHMSA	Rev A
	Final Report	Page 54 of 213

withdrawal lines. Therefore, tank emptying scenarios can occur in LNG facilities; in fact, such scenarios are frequently examined when performing LNG facility siting studies. The effect of nil wind conditions on these scenarios are evaluated and discussed in Sections 5 and 6.

#### 4.2.3 Maintenance Failure

Several of the accidents in Table 4-1 can be attributed to failure to perform proper maintenance. For example:

- Amuay: the Amuay refinery for the Paraguana Refinery Complex contained an olefin tank with an associated pump. Two different reports were produced following the accident, with somewhat inconsistent conclusions about the size and duration of the leak. However, the reports concur that the cause of the leak was corrosion in a pipe.
- Jaipur: One of the contributing factors to the magnitude of the Jaipur accident was the operators' failure to stop the leak due to a remote shut-off valve being taken out of service several years earlier and never restored.
- La Mede: the La Mede refinery for Total had an accident in the absorber stripper column cooler. A 25 cm<sup>2</sup> hole in the 8" piping resulted in a 10-minute release of LPG and light naphtha, before the vapor cloud found an ignition source resulting in an explosion. The root cause of the piping failure was determined to be internal corrosion and poor inspection and maintenance of the line.
- Norco: the Shell oil refinery in Norco, Louisiana experienced a leak in the vapor line out of the depropanizer. The release lasted approximately 30 seconds before the vapor cloud found an ignition source, resulting in an explosion. The root cause of the leak was determined to be corrosion of the pipe.
- Port Hudson: an LPG pipeline owned by the Phillips 66 Company experienced a failure downstream of the Port Hudson pumping station, releasing a spray of LPG into the air for 20 minutes. Prior to this incident, the same pipeline had 12 previous releases of similar magnitude; however, in this instance, the LPG vapor cloud reached an ignition source and caused an explosion.
- St. Herblain: the root cause for the gasoline release was the failure of a union fitting equipped with a seal unsuitable for the material being stored. Since the facility had been in operation for a long time, the failure is attributable to poor maintenance.

LNG facilities may not be immune from maintenance-related accidents. However, NFPA 59A and 49 CFR 193 specify maintenance and inspection requirements for all in-service equipment at LNG facilities. Maximum maintenance and testing intervals are specified in order to minimize the likelihood of a problem, such as incipient corrosion, growing to the point of causing a loss of containment. Therefore, it is probable that the material degradation that caused some of these accidents would have been identified prior to the incident, had proper maintenance and inspection been performed. This is even

	<b>Vapor Cloud Explosions at Nil Wind</b>	03904-RP-006
	PHMSA	Rev A
	Final Report	Page 55 of 213

more likely when considering that most of the process lines in an LNG facility operate with non-corrosive (LNG) or lightly corrosive (propane, butane, etc.) fluids unlike gasoline and naphtha.

Maintenance and inspection requirements under PHMSA regulations would have been particularly critical in the Port Hudson case, due to the numerous previous failures: mandatory reporting requirements would have triggered a shutdown of the facility after the first incident and required extensive testing before resuming operation.

#### 4.2.4 Testing or Installation Failure

In several of the accidents in Table 4-1, the loss of containment was likely due to improper welding and lack of pre-service inspections. For example:

- Big Springs: the Alon Israel Oil Refinery in Big Springs, TX had a propylene release due to a faulty weld on a pump casing within the propylene splitter unit; the resulting vapor cloud reached an ignition source resulting in an explosion.
- Flixborough: the Flixborough site of NYPRO produced Carolactam, a component of Nylon 6. A reactor had been taken out of service and a bypass had been installed that was not subject to a structural analysis or pressure test. The 20" bypass failed leading to 40 tons of cyclohexane being released; ignition of the vapor cloud occurred approximately 45 seconds later.
- UFA: the Trans-Siberian pipeline consists of a 700 mm-diameter buried pipeline, operating at approximately 550 psig. The pipeline suffered a catastrophic rupture; the root cause was never fully determined, but the most likely cause was reported as an installation fault, possibly from improper welding.
- Geismar: the Williams Geismar plant suffered the rupture of a heat exchanger. While RR1113 listed the accident sequence as a rupture leading to the release of hydrocarbons and eventually to a vapor cloud explosion, the Chemical Safety Board's investigation later concluded that the explosion was due to an overpressure within the heat exchanger itself, not to a vapor cloud explosion. Therefore, this accident should be removed from further consideration when evaluating the potential for VCEs.

PHMSA-regulated LNG facilities are required to do non-destructive examination (NDE) testing as well as structural calculations on all piping and welds to ensure their integrity under all foreseeable structural and thermal cycling loads. LNG facilities also minimize the use of buried pipelines within the plant's boundaries, which allows for regular inspection and maintenance of all lines within the plant.

PHMSA regulations also require all bypass lines, even temporary ones, to be tested and inspected as if they were permanent process piping. Therefore, the rupture of a large bypass line (as in the Flixborough accident) is considered a very low probability event:

	<b>Vapor Cloud Explosions at Nil Wind</b>	03904-RP-006
	PHMSA	Rev A
	Final Report	Page 56 of 213

for example, the failure rate database in NFPA 59A-2019 lists the probability of catastrophic rupture for a 20-inch diameter line as 2.E-8 /m/yr.

#### 4.2.5 Operator Error

Operator error was a factor in several of the accidents in Table 4-1:

- Jaipur: one of the contributing factors to this accident was that the operator opened the valve without noticing that the line included an open blind flange.
- Brenham: one of the contributing factors to this accident was that the operators lost track of the net amount of fuel that had been pumped into the cavern.
- Pasadena: the Phillips Petroleum Chemical Complex experienced a hydrocarbon release (it is unclear whether ethylene or butane, or both, were released). The release occurred from an un-blanked process line being opened by an operator during maintenance. The resulting vapor cloud found an ignition source, resulting in an explosion.
- Tank overfills (see section 4.2.1): operators failed to properly monitor tank liquid level and liquid flow into the tanks.

LNG facilities are not immune from operator error; however, 49 CFR 193 requires procedures and records to be maintained and followed at site. For example, maintenance procedures in place at the Pasadena facility had been modified without official sign-off, which led to improper isolation of the line. Operator training requirements are also in place for LNG facilities, which further decrease the likelihood of procedural errors.

#### 4.2.6 Design Flaws

In two of the accidents in Table 4-1, design choices played a significant role in the sequence of events:

- Baton Rouge: the Exxon Corporation refinery lost primary power to the site, leading to all valves going into their fail-safe position. This resulted in the entrapment of propane and lighter hydrocarbons within a blocked piping section, without pressure relief. The thermal expansion of the trapped liquids caused overpressurization and eventually failure of the line. This led to a large release of hydrocarbons for approximately 2.5 minutes; the vapor cloud then reached an ignition source resulting in an explosion.
- Skikda: the Sonatrach LNG plant suffered a refrigerant release, whose cause remains unknown, in one of the liquefaction trains. The vapor cloud entered the nearby boiler's firebox through an air intake located near ground level, resulting in overpressurization and explosion within the boiler.

	<b>Vapor Cloud Explosions at Nil Wind</b>	03904-RP-006
	PHMSA	Rev A
	Final Report	Page 57 of 213

The cause of the Baton Rouge accident case appears attributable to a design flaw, which allowed a piping section carrying pressurized liquids to be blocked off, without appropriate pressure relief. It is unclear whether any of the piping codes applicable to the Baton Rouge facility required the evaluation of thermal expansion under shutdown conditions and, if so, why this flaw was not discovered. Regardless, the design of PHMSA-regulated LNG facilities is required to protect against thermal expansion-related failures, given the prevalence of pressurized liquid lines; therefore, the likelihood of this accident scenario may be reduced to negligible levels.

The Skikda accident represents the only case among the 24 large vapor cloud explosions reviewed by the HSE to have occurred at an LNG facility. The explosion occurred once flammable vapors, from an undetermined refrigerant leak, entered the boiler chamber through the air intakes. It must be noted that the boiler was located adjacent to the liquefaction train where the leak occurred and that the air intakes were placed near the ground: both factors contributed directly to the accident, by providing a strong ignition source within a confined space and in close proximity to the source of flammable vapors. The placement of combustion equipment or non-explosion proof electrical equipment in relative proximity to potential sources of flammable mixtures is not prohibited by current PHMSA regulations; however, the lessons learned from the Skikda accident have been driving facility design towards increased separation of strong ignition sources and/or the use of gas detection at air intakes. Given the purpose of the current project, it is also important to note that, given the short distance between the process area where the initial leak occurred and the boiler air intakes, the calm wind conditions likely had a minimal effect on the magnitude of the accident: in fact, the strength of the explosion was clearly driven by the bang-box effect due to ignition within the boiler chamber and by the congested process area outside the boiler.

#### **4.2.7 Pipelines**

One third of the vapor cloud explosion accidents considered in the HSE review consisted of liquefied petroleum gas (LPG) pipeline incidents. RR1113 stated that "Only 2 of these incidents caused vapor cloud explosions whilst 6 were consistent with flash fires. This contrasts with gasoline overfill incidents where all of the recorded incidents that caused very large clouds (cloud radius > 200m) have resulted in explosions. Part of the reason for this difference may be the potential for very rich clouds to be formed in low wind speed conditions for an LPG release. [...] Overall, the incident history suggests that large clouds are generally associated with very light or zero winds. If such a cloud develops the risk of a VCE is probably less than 50%. It may be that there is a significant probability that, even if a large LPG cloud accumulates in very light or nil wind conditions, it will be too rich to undergo transition to a VCE." However, no supporting evidence was provided for this statement. Additionally, the discussion neglected to include a potential alternative explanation for the difference between pipeline incidents and storage tank overfills: the lack of sufficient congestion in proximity of the pipelines to cause the flame acceleration necessary to produce damaging overpressures. In fact, given the typically high pressures

	<b>Vapor Cloud Explosions at Nil Wind</b>	03904-RP-006
	PHMSA	Rev A
	Final Report	Page 58 of 213

associated with pipelines, the suggestion that a release from a pipeline would be unable to mix with air, whereas a large spill from a storage tank would mix to near stoichiometric, is highly questionable.

## 5 Consequence Modeling in Nil-Wind

As discussed earlier in this report, the consequences of vapor dispersion scenarios are generally expected to become worse as the wind speed decreases, as the lower wind speed reduces the turbulent mixing at the air/cloud interface; vapor cloud explosions generally follow a similar trend, as lower wind speeds generally result in larger flammable cloud volumes, which in turn lead to higher overpressures. However, it is unclear whether the trend continues as wind speeds tend to zero, especially for high-momentum releases. Therefore, modeling is required in order to quantify the change in vapor dispersion and vapor cloud explosion hazards as wind speed is reduced below the current regulatory requirements.

The consequence modeling task consisted of:

- Developing the layout for a generic LNG facility, including a process flow diagram and other information typical of an early design;
- Defining a set of release scenarios for the LNG facility, consistent with PHMSA regulations (49 CFR 193) and regulatory guidance as provided in PHMSA's LNG Plant Requirements: Frequently Asked Questions (FAQs)<sup>3</sup>;
- Performing flammable vapor dispersion modeling, under different wind conditions, in order to evaluate the effect of wind speed on the potential for vapor cloud explosion hazards;
- Performing vapor cloud explosion modeling based on the results of the flammable dispersion simulations.

### 5.1 Generic LNG Facility Layout

When selecting the facility design upon which to base the consequence modeling task, the project team evaluated whether both a large-scale (e.g., liquefaction/export) facility and a small-scale (e.g., peakshaver) facility should be included in the study. The main reason for considering both facility types was to evaluate the effect of nil-wind conditions on facilities with congested regions of very different dimensions as well as using different types of refrigerants (e.g., mixed refrigerants for larger liquefiers and methane or nitrogen for smaller ones). The experience of the project team with LNG facility siting studies, however, is that the severity of VCE hazards for smaller LNG facilities is generally limited and rarely the bounding case for siting purposes, due to the small, congested areas and

---

<sup>3</sup> <https://www.phmsa.dot.gov/pipeline/liquified-natural-gas/lng-plant-requirements-frequently-asked-questions>

	<b>Vapor Cloud Explosions at Nil Wind</b>	03904-RP-006
	PHMSA	Rev A
	Final Report	Page 59 of 213

the limited (or missing) inventory of heavier hydrocarbons. Therefore, the small-scale facility was not included in the consequence modeling task and the computational efforts were redirected towards evaluating additional sensitivity cases for the large-scale LNG export facility, as discussed in the following sections.

The plot plan and process data for the generic large-scale LNG export facility were based on previous PHMSA R&D projects such as: “Comparison of Exclusion Zone Calculations and Vapor Dispersion Modeling Tools” (PHMSA project #640), “Develop a Risk-Based Approach and Criteria for Hazard Detection Layout” (PHMSA project #852) and “Consistency Review of Methodologies for Quantitative Risk Assessment” (PHMSA project #731).

The documents necessary to conduct a siting study for LNG facilities under PHMSA jurisdiction are specified in the Design Spill Package requirements in PHMSA’s FAQs and include:

- Plot plans
- Process Flow Diagrams (PFD)
- Piping and Instrument Drawings (P&ID)
- Heat and Material Balance Sheets (H&MB)
- Process Datasheets
- Site specific weather data

For the purpose of this study, the generic LNG facility was assumed to be at early design stage, therefore the documents developed include a plot plan, PFDs, and H&MBs. All documents are included in Appendix A.

### 5.1.1 LNG Export Facility

The LNG export facility was designed to have three (3) pretreatment and three (3) liquefaction trains, each capable of liquefying 5 million tons per annum (MTPA) of natural gas from the pipeline utilizing a closed mixed refrigerant loop, for a total LNG liquefaction capacity of 15 MTPA. It was assumed that feed gas would be supplied at the appropriate pressure required for liquefaction, therefore, booster compression was not included in the design.

LNG is stored in two (2) 160,000 m<sup>3</sup> atmospheric full containment tanks and pumped to an LNG carrier via four (4) in-tank pumps. Three (3) boil-off gas (BOG) compressors are used to compress vapor from the tanks or ships and transfer it to the inlet of the facility. The vapor return line from the carrier ties into the BOG system.

The liquefaction process was assumed to use a pre-cooled mixed refrigerant (MR) stream, composed of nitrogen, methane, ethylene, propane, and butane. The refrigerants were assumed to be stored in pressure vessels (bullets) located onsite.

	<b>Vapor Cloud Explosions at Nil Wind</b>	03904-RP-006
	PHMSA	Rev A
	Final Report	Page 60 of 213

The facility plot plan is shown in Figure 5-1 and the 3D model used for the consequence modeling (as discussed below) is shown in Figure 5-2.

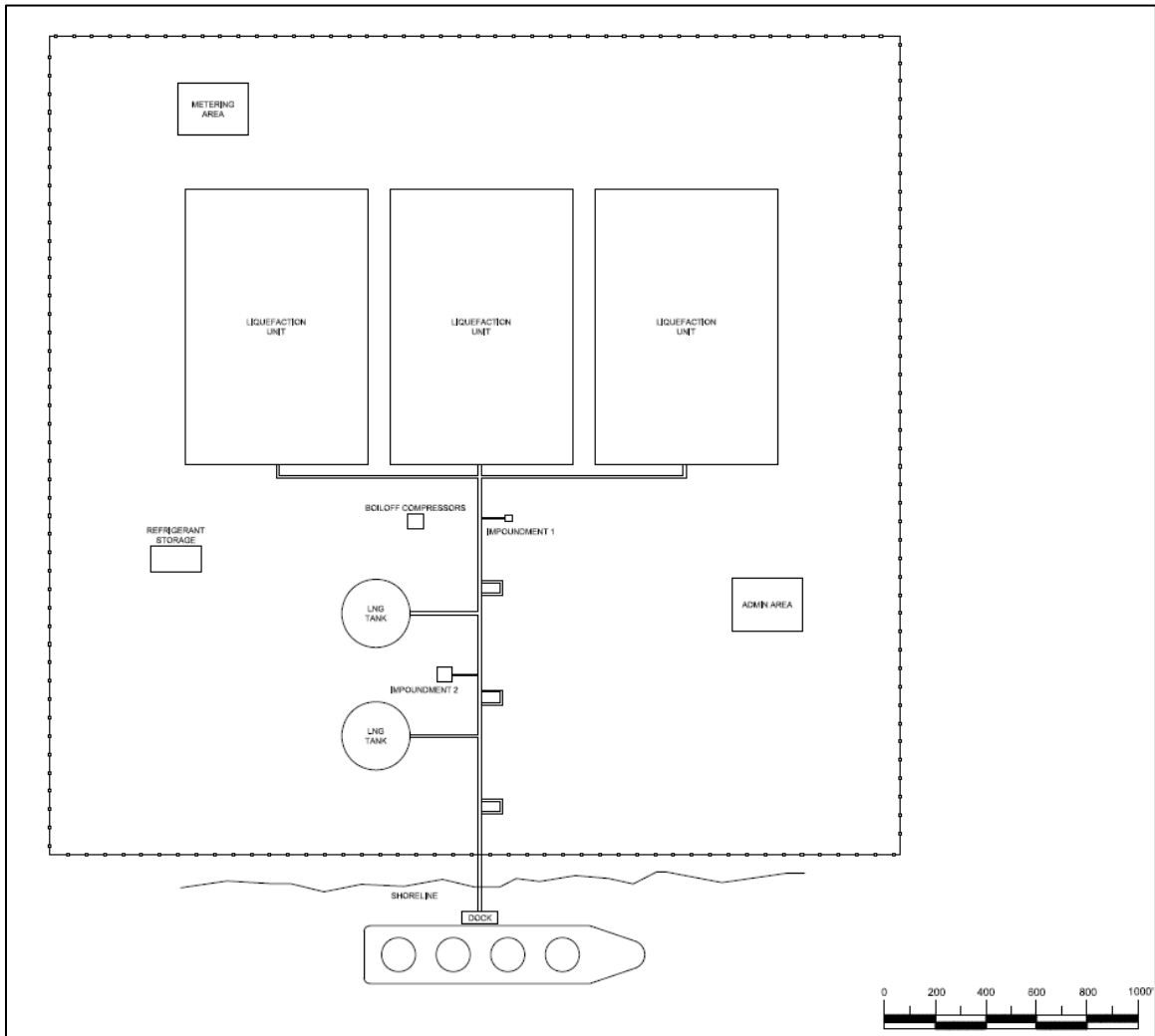


Figure 5-1. Plot plan for the generic LNG export facility.

	<b>Vapor Cloud Explosions at Nil Wind</b>	03904-RP-006
	PHMSA	Rev A
	Final Report	Page 61 of 213

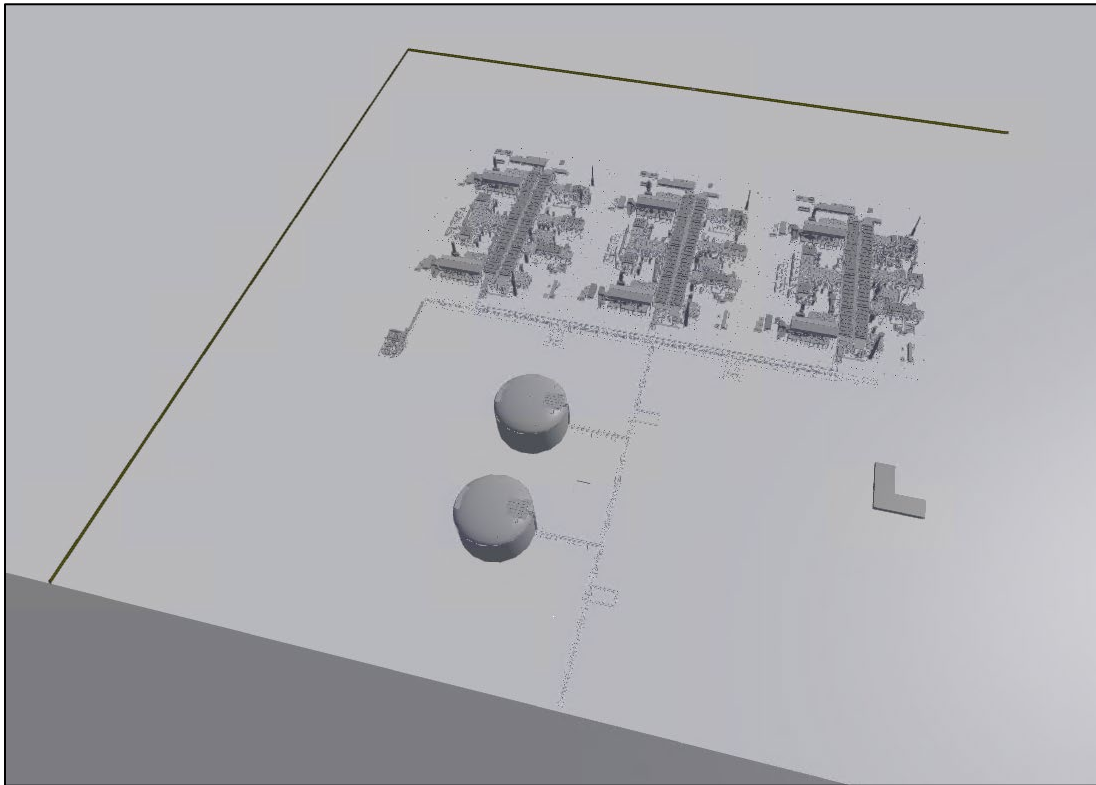


Figure 5-2. 3D model of the generic LNG export facility.

Figure 5-2 shows that 20 ft tall vapor barriers (walls) were placed along the western and northern boundaries of the facility. Vapor barriers are commonly installed in LNG facilities to limit the dispersion of the flammable clouds from accidental releases; however, as discussed by Gavelli and Davis [19], the flammable vapor holdup caused by the barriers may result in a larger flammable cloud volume within the plant and possibly inside congested areas. Therefore, vapor barriers were added to the generic LNG facility in this study to account for vapor holdup.

	<b>Vapor Cloud Explosions at Nil Wind</b>	03904-RP-006
	PHMSA	Rev A
	Final Report	Page 62 of 213

The design parameters for the export facility are specified in the following subsections and serve as the basis for the Plot Plan, PFDs, and HMB documents listed in Table 5-1.

Table 5-1 Export facility documents created for this study.

Document Name	Document Number
<b>Plot Plan</b>	03904-DG-001
<b>Process Flow Diagram – Inlet Gas</b>	03904-PF-111
<b>Process Flow Diagram – Pretreatment</b>	03904-PF-112
<b>Process Flow Diagram – Liquefaction</b>	03904-PF-211
<b>Process Flow Diagram – Balance of Plant</b>	03904-PF-212
<b>Process Flow Diagram – Mixed Refrigerant</b>	03904-PF-213
<b>Process Flow Diagram – Refrigerant Storage</b>	03904-PF-811
<b>Heat and Material Balance</b>	03904-PF-001

#### 5.1.1.1 Feed Gas

The inlet feed gas parameters are listed below:

- Flowrate: 17.11 MTPA (2,443 MMscfd)
- Pressure: 1,000 psig (68.9 barg)
- Temperature: 90°F (32 °C)

#### 5.1.1.2 Liquefaction

The parameters for the gas, downstream of pretreatment, that is sent to liquefaction (per train) are listed below:

- Flowrate: 5 MTPA (714 MMscfd)
- Pressure: 850 psig (58.6 barg)
- Temperature: 85 °F (29 °C)

#### 5.1.1.3 LNG Storage Tank

The parameters for each LNG storage tank are listed below:

- Capacity: 160,000 m<sup>3</sup> (3.3 bcf)
- Pressure: 0.5 psig (0.03 barg)
- Temperature: -260 °F (-162 °C)

	<b>Vapor Cloud Explosions at Nil Wind</b>	03904-RP-006
	PHMSA	Rev A
	Final Report	Page 63 of 213

#### 5.1.1.4 LNG Loading

The parameters for the LNG sent to the LNG carrier are listed below:

- Flowrate: 52,834 gpm (12,000 m<sup>3</sup>/hr)
- Pressure: 40 psig (2.8 barg)
- Temperature: -260 °F (-162 °C)

#### 5.1.1.5 Refrigerant Storage

The parameters for the refrigerant storage system are listed below:

- Propane:
  - Storage capacity: 20,000 gal (151.4 m<sup>3</sup>)
  - Pressure: 120 psig (8.3 barg)
  - Temperature: 75 °F (23.9 °C)
- Butane:
  - Storage capacity: 25,000 gal (94.6 m<sup>3</sup>)
  - Pressure: 20 psig (1.4 barg)
  - Temperature: 75 °F (23.9 °C)
- Ethylene:
  - Storage capacity: 4,000 gal (15.1 m<sup>3</sup>)
  - Pressure: 93 psig (6.4 barg)
  - Temperature: -77 °F (-60.5 °C)

## 5.2 Modeling Tool

As discussed in Section 2.3, integral models have a lower wind speed limit, below which the equations they apply cannot be used. The lower bound on wind speed is generally 1.0 m/s, which makes integral models not suitable for modeling vapor dispersion under nil-wind conditions. CFD models are not affected by such limitation and can model dispersion in wind speeds down to zero. Therefore, all consequence modeling for this task was performed using FLACS.

### 5.2.1 FLACS

FLACS is a CFD tool capable of modeling gas and aerosol releases, dispersion of vapors, ventilation in structures, and ignition of flammable fuel-air mixtures to evaluate the flame front progression and overpressures due to vapor cloud explosions; all these physical phenomena are simulated in a full three-dimensional domain and take into account the interaction between the fluid flow and obstacles, obstructions and topography.

	<b>Vapor Cloud Explosions at Nil Wind</b>	03904-RP-006
	PHMSA	Rev A
	Final Report	Page 64 of 213

FLACS solves the compressible conservation equations (mass, momentum, enthalpy, and species) on a 3D Cartesian grid using a finite volume method. A porosity concept is implemented to model details not resolved on the numerical grid. Buoyancy effects for atmospheric gas dispersion are taken into account in the turbulent equations. The atmospheric boundary layer is modeled by specifying vertical profiles of wind speed and direction, temperature, turbulent kinetic energy and eddy dissipation rate at inflow boundaries. Both explosion and vapor dispersion modeling capabilities of FLACS have been validated against several field experiment series. FLACS is currently the only CFD model currently approved by PHMSA for LNG vapor dispersion [20].

### 5.3 Modeling Test Matrix

The focus of this task is on the effect of wind speed on vapor cloud explosion hazards, for a set of scenarios typical of LNG facility siting studies. Therefore, the workflow consisted of the following steps:

- Identify release scenarios;
- Perform flammable vapor dispersion simulations to quantify their respective VCE potential;
- Perform VCE modeling to quantify the overpressure hazards.

The results of an LNG facility siting study are project-specific, therefore, the results of consequence modeling on a generic LNG facility should not be considered applicable to every facility. However, by selecting an adequate set of scenarios and modeling parameters, and analyzing the results, useful observations can be made that can inform regulatory decisions. The test matrix for the consequence modeling task was developed with the intent of evaluating scenarios and conditions commonly encountered in LNG facility siting studies, to assess the effects of nil-wind conditions on public hazards from VCE.

The test matrix for the dispersion scenarios (which were used to determine the flammable cloud volumes) was set up to include combinations of:

- Fluid density:
  - Lighter-than-air at ambient temperature (i.e., LNG)
  - Heavier-than-air at ambient temperature (e.g., propane, mixed refrigerant)
- Release type:
  - Momentum-driven (flashing and jetting)
  - No-momentum (liquid spill)
- Release direction (for momentum-driven releases):
  - Towards the liquefaction area (most congested region)
  - Towards the center of the facility
- Release location:
  - Within a congested area

	<b>Vapor Cloud Explosions at Nil Wind</b>	03904-RP-006
	PHMSA	Rev A
	Final Report	Page 65 of 213

- Outside of congested areas
- Wind speed:
  - Low wind (1-2 m/s)
  - Nil wind (< 1 m/s)
- Wind direction (for momentum-driven releases):
  - Along the release
  - Opposite the release
  - Across the release (perpendicular)

The test matrix for the VCE scenarios, which would be based on the flammable cloud volumes calculated during the dispersion simulations, was set up to include combinations of:

- Cloud shape:
  - Square
  - Elongated in the North-South direction
  - Elongated in the East-West direction
- Cloud location:
  - Various locations, primarily around the perimeter of the congested region, to project overpressure towards property boundaries
- Ignition location:
  - Various locations, primarily around the perimeter of the cloud, to project overpressure towards property boundaries

Additional details on the dispersion and overpressure modeling are provided in sections 0 and 5.6, respectively.

#### **5.4 Ambient Conditions**

The ambient conditions to be used in the modeling were specified consistent with regulatory requirements (49 CFR 193.2059), with the exception of wind speed, which was parameterized as discussed in Section 3. Table 5-2 summarizes the ambient conditions selected for this task.

Table 5-2. Ambient conditions for the dispersion modeling.

Parameter	Value
<b>Ambient Temperature [°F]</b>	71
<b>Relative Humidity</b>	N/A <sup>4</sup>
<b>Wind Speed [m/s]</b>	0.0; 0.5; 1.0; 2.0
<b>Atmospheric Stability [Pasquill-Gifford class]</b>	F
<b>Ground Roughness [m]</b>	0.03

## 5.5 Release Scenarios

The Single Accidental Leakage Sources (SALS) methodology described in the PHMSA FAQs was applied to the LNG facility design, resulting in the SALS shown in Table 5-3. It should be noted that the capacity of the propane storage vessel was doubled (to 40,000 gal) from the design value in order to model a release longer than 10 minutes.

Table 5-3. SALS table for the generic LNG export facility.

Scenario No.	Description	Fluid	Release Elevation [ft]	SALS [in]	Nominal Pressure [psig]	Nominal Temp. [F]
<b>NG-03</b>	Gas from Pretreatment to Cold Box	NG	3	2	850	85.0
<b>LNG-04</b>	LNG Rundown from Coldbox to Tank	LNG	3	2	160	-260.0
<b>LNG-06</b>	BOG from tank to compressor	LNG	20	2	0.5	-260.0
<b>HC-08</b>	Heavies removal	HEA	3	2	450	-126.5
<b>MR-09</b>	MR compressor inlet	MR1	10	2	65	50.0
<b>MR-10</b>	MR compressor 1st stage	MR1	10	2	50	-40.0
<b>MR-11</b>	MR compressor 2nd stage	MR1	10	2	480	80.0
<b>MR-12</b>	HP MR Liquid	MR3	10	2	880	-30.0
<b>MR-13</b>	HP MR Vapor	MR2	10	2	880	-30.0
<b>LNG-14</b>	LNG from tank to ship loading	LNG	20	4	40	-260.0
<b>PRO-16</b>	Propane truck unloading	PRO	3	3	120	75.0
<b>PRO-18</b>	Propane tank (40,000 gal)	PRO	3	3	120	75.0
<b>PRO-19</b>	Propane makeup	PRO	20	2	120	75.0

<sup>4</sup> While 49 CFR 193.2059 specifies a relative humidity of 50%, FLACS does not take relative humidity into account, therefore, no relative humidity was used in the modeling.

	<b>Vapor Cloud Explosions at Nil Wind</b>	03904-RP-006
	PHMSA	Rev A
	Final Report	Page 67 of 213

Scenario No.	Description	Fluid	Release Elevation [ft]	SALS [in]	Nominal Pressure [psig]	Nominal Temp. [F]
<b>BUT-20</b>	Butane truck unloading	BUT	3	3	20	75.0
<b>BUT-22</b>	Butane tank (25,000 gal)	BUT	3	3	20	75.0
<b>BUT-23</b>	Butane makeup	BUT	20	2	20	75.0
<b>ETH-24</b>	Ethylene truck unloading	ETH	2	2	93	-77
<b>ETH-26</b>	Ethylene storage (4,000 gal)	ETH	3	3	93	-77
<b>ETH-27</b>	Ethylene makeup	ETH	20	2	92	-75.0
<b>NG-28</b>	LNG carrier vapor return	NG	2	2	7	-150.0
<b>LNG-30</b>	LNG Rundown at Tank Top	LNG	120	2	160	-260.0
<b>LNG-00</b>	LNG sendout, full guillotine	LNG	spill	-	-	-258.7

Based on the SALS table and the criteria listed in section 5.3, the following scenarios were selected for the dispersion modeling test matrix:

- LNG-04 (LNG rundown line), which represents a flashing and jetting release of LNG (lighter-than-air fluid) in proximity of the liquefaction train (a congested area).
- MR-12 (High Pressure MR Liquid line), which represents a flashing and jetting release of MR (heavier-than-air fluid) within the liquefaction train.
- PRO-18 (Propane storage vessel withdrawal line), which represents a flashing and jetting release of propane (heavier-than-air fluid) remote from the liquefaction area.
- BUT-22 (Butane storage vessel withdrawal line), which represents a flashing and jetting release of butane (heavier-than-air fluid) remote from the liquefaction area. Note that the butane release results in approximately 23% liquid rainout.
- LNG-00 (LNG sendout line), which represents a liquid spill of LNG. Note that the spill was assumed to occur directly into the LNG impoundment sump.

For two of the scenarios listed above (LNG-04 and PRO-18), additional simulations were added to evaluate the sensitivity of the results to the release hole diameter. This sensitivity analysis was performed to evaluate the accuracy of the statement in RR1113 that "a wider range of smaller losses of containment (with much higher frequency) have the potential to cause a large cloud in [nil/low wind] conditions". The complete set of flammable dispersion scenarios included in the consequence modeling task is shown in Table 5-4.

Table 5-4. Release scenarios in the consequence modeling task.

Scenario No.	Description	Fluid	Release Elev. [ft]	SALS [in]	Nominal Pressure [psig]	Nominal Temp. [F]	Release Rate [lbm/hr]	Duration [s]
<b>LNG-04</b>	LNG Rundown from Coldbox to Tank	LNG	3	2	160	-260.0	295,500	600
				3			664,900	600
<b>MR-12</b>	HP MR Liquid	MR3	10	2	880	-30.0	656,400	600
<b>PRO-18</b>	Propane tank (40,000 gal)	PRO	3	3	120	75.0	649,200	1,080
	Propane tank (20,000 gal)			2			288,500	1,210
	Propane tank (20,000 gal)			1			72,100	4,840
<b>BUT-22</b>	Butane tank (25,000 gal)	BUT	3	3	20	75.0	284,000	1,670
<b>LNG-00</b>	LNG sendout, full guillotine	LNG	0	-	-	-258.7	11,220,000	600

	<b>Vapor Cloud Explosions at Nil Wind</b>	03904-RP-006
	PHMSA	Rev A
	Final Report	Page 69 of 213

Figure 5-3 shows the approximate release locations (at the base of the arrows for the flashing and jetting releases; at the center of the star for the liquid spill) and directions for the scenarios in Table 5-4.

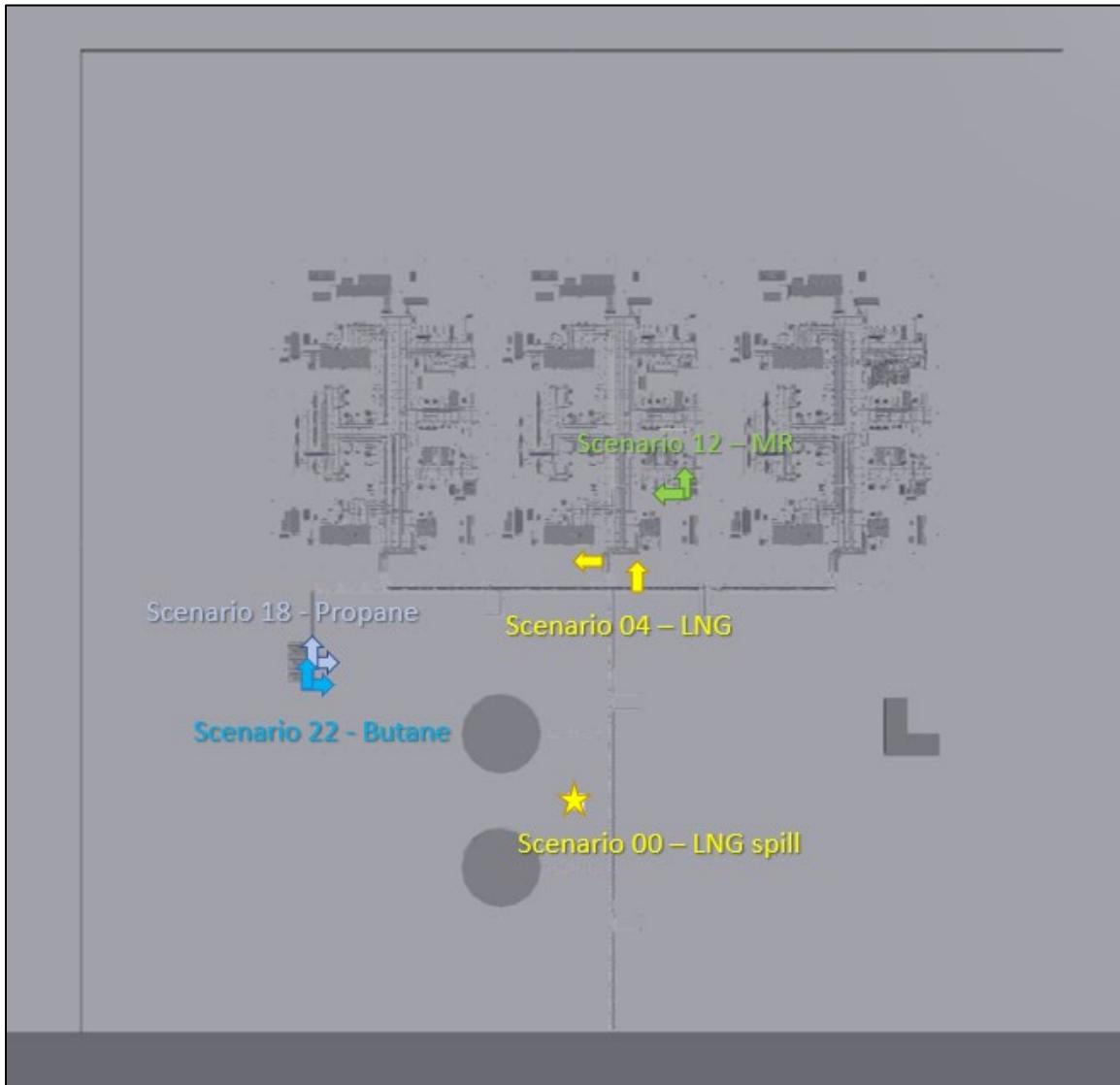


Figure 5-3. Release locations and directions (star indicates liquid spill).

Based on the test matrix criteria (e.g., release direction) listed in section 5.3 and the wind speeds listed in Table 5-2, a total of 19 simulations were performed for each of the eight release scenarios in Table 5-4. A discussion of the quantities tracked during each simulation, as well as the modeling results, is provided in the next subsection.

	<b>Vapor Cloud Explosions at Nil Wind</b>	03904-RP-006
	PHMSA	Rev A
	Final Report	Page 70 of 213

## 5.6 Vapor Cloud Explosion Potential

The focus of this research project is on the effect of nil-wind conditions on the potential hazards from vapor cloud explosions. Therefore, the purpose of the flammable vapor dispersion simulations described above was to quantify the volume of the flammable clouds that can form for different release scenarios and under different wind conditions.

### 5.6.1 Congested Areas

It is well established [21] that several conditions need to be satisfied in order for a flammable cloud ignition to result in a vapor cloud explosion with damaging overpressures:

- The vapor cloud must reach a sufficiently large volume prior to ignition.
- The vapor cloud must mix with air to produce a sufficiently large flammable mixture volume.
- The flame front must accelerate within the flammable cloud, to velocities sufficient to create high overpressures.

Experimental data and empirical evidence demonstrate that flame acceleration is driven largely by turbulent stretching of the flame front, which occurs as the flame front is pushed by the expanding combustion gases and interacts with obstacles and obstructions along its path. As turbulence increases, stretching the flame front, the fuel burning rate also increases; in turn, this increases the expansion rate of the combustion gases, which further increases turbulence and stretches the flame front, in a positive-feedback loop. The feedback loop is interrupted only when the flame front reaches the edge of the flammable cloud or exits the region occupied by turbulence-inducing obstacles (in the latter case, unless the flame front has reached the conditions for deflagration-to-detonation transition – DDT – which are outside the scope of this study).

Therefore, a necessary step to quantify the potential VCE overpressure hazards for a facility is to identify the congested regions (or potential explosion sites, PES) within the facility boundaries. The criteria provided by Pitblado et al. [22] were followed to identify and define the PES boundaries. As shown in Figure 5-4, four distinct PESs are present in the generic LNG export facility used for this study:

- Each of the three liquefaction trains (identified respectively as Train 1, Train 2, and Train 3). The footprint of each train measures approximately 700 ft by 890 ft (210 m by 270 m);
- The Refrigerant Storage area. The footprint of the refrigerant storage area measures approximately 100 ft by 150 ft (30 m by 45 m).

In addition to tracking the flammable cloud volumes in each PES, every simulation tracked the flammable cloud within the entire plant area, which measures

	<b>Vapor Cloud Explosions at Nil Wind</b>	03904-RP-006
	PHMSA	Rev A
	Final Report	Page 71 of 213

approximately 3400 ft by 3250 ft (1030 m by 990 m) and is identified by the red box in Figure 5-4). Note that each PES (as well as the entire plant area) was limited in height to 25 ft (7.5 m) for the purpose of tracking flammable cloud volumes, in accordance with established facility siting practices [23].

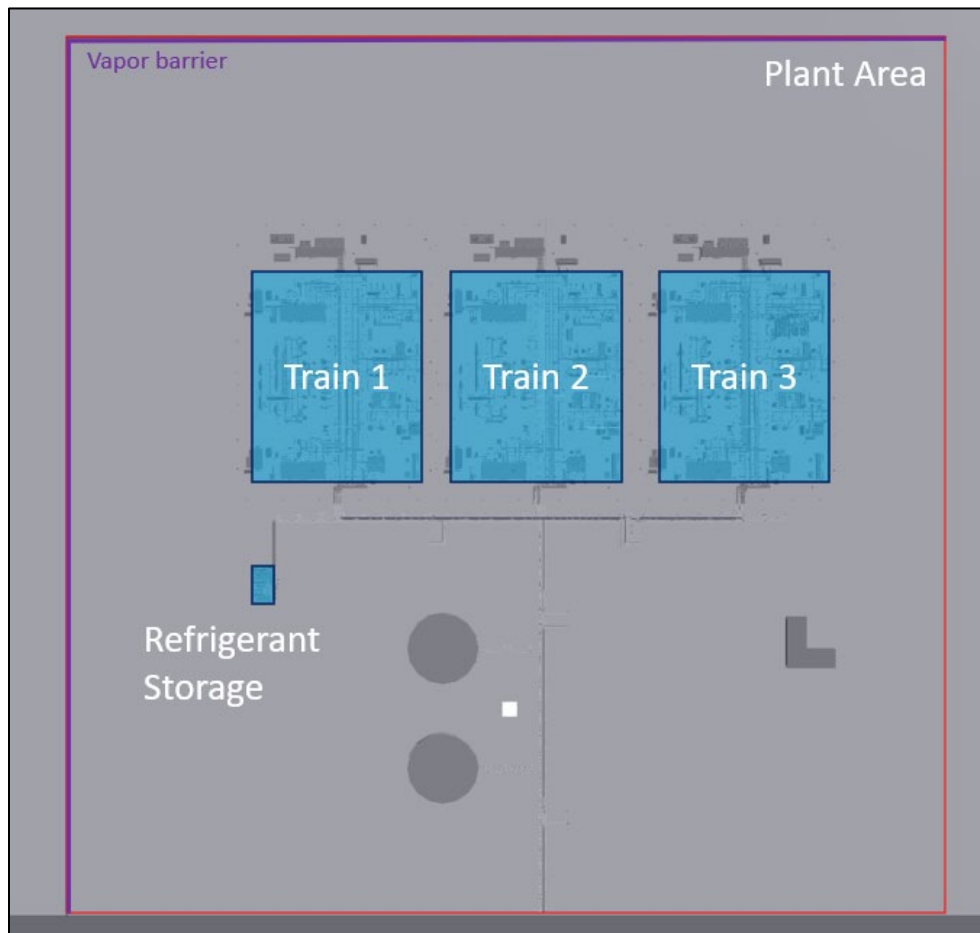


Figure 5-4. Potential Explosion Sites in the generic export facility.

### 5.6.2 Equivalent Stoichiometric Clouds

Figure 5-5 shows the footprints of a flammable vapor cloud from one of the simulations included in this study, at two separate instants during the release. The clouds are color-coded according to the maximum fuel concentration at any given horizontal location, ranging from dark blue at the LFL to dark red at or above the UFL. Both figures show a complex footprint (i.e., not a circle or a tear shape) and a non-homogeneous cloud concentration; a comparison between the two images also shows how the cloud changes shape, size, and concentration profile over time.

	Vapor Cloud Explosions at Nil Wind	03904-RP-006
	PHMSA	Rev A
	Final Report	Page 72 of 213

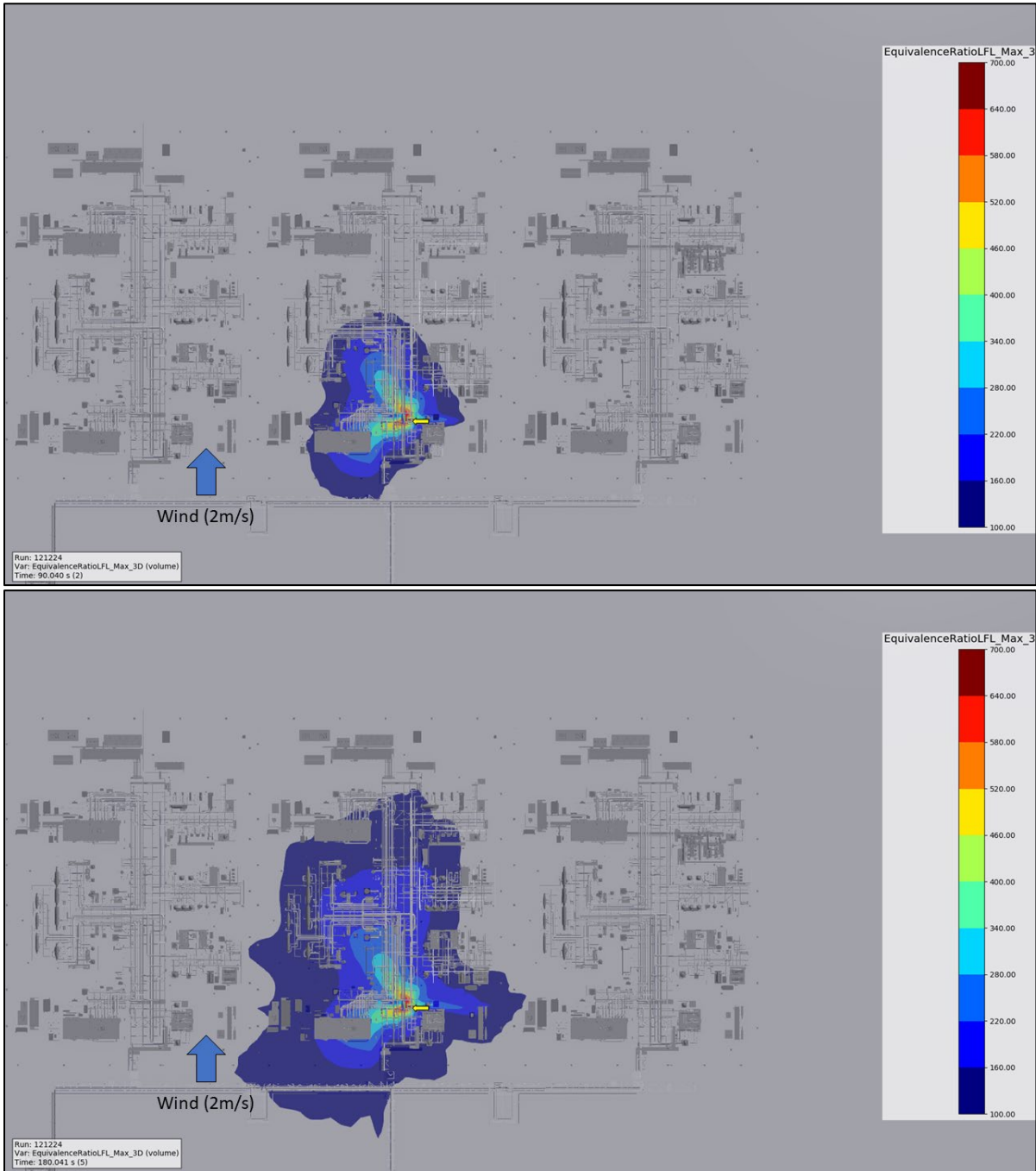


Figure 5-5. Footprint of a flammable vapor cloud: (top) 60 s into the release; (bottom) 150 s into the release.

	<b>Vapor Cloud Explosions at Nil Wind</b>	03904-RP-006
	PHMSA	Rev A
	Final Report	Page 73 of 213

Critical questions that need to be answered when performing a hazard analysis include how to determine the potential VCE consequences associated with a developing vapor cloud, and how to compare the potential VCE consequences of different clouds. In order to answer these questions, the concept of Equivalent Stoichiometric Clouds (ESC) was developed in the 1990s and has been widely used since: the concept is to convert a non-homogeneous gas cloud to an equivalent stoichiometric cloud which, if ignited within the same congested region, would yield comparable explosion consequences. Since a flammable mixture tends to be most reactive near its stoichiometric concentration and least reactive near its flammability limits, the volume of an ESC is generally smaller than the volume of the non-homogeneous cloud it represents. The goal is for the ESC to yield VCE consequences that are equal, or slightly conservative, relative to those from the actual non-homogeneous cloud.

Different 'types' of ESCs have been proposed and tested over the years; each type is based on a semi-empirical correlation that converts each unit volume of the non-homogeneous cloud into an equivalent volume of a stoichiometric cloud by applying scaling factors tied to the behavior of the flammable cloud when ignited; the total ESC volume is then obtained by adding together each equivalent volume across the cloud. The ESC definitions that are currently used most frequently are:

- Flammable Volume (FV): each unit volume,  $V$ , of the non-homogeneous cloud translates to the same volume of stoichiometric mixture:

$$FV = \sum_{Flamm.Cloud} V$$

- Q8: each unit volume,  $V$ , of the non-homogeneous cloud is multiplied by the normalized gas expansion ratio,  $E$ :

$$Q8 = \sum_{Flamm.Cloud} V \frac{E}{E_{max}}$$

- Q9: each unit volume,  $V$ , of the non-homogeneous cloud is multiplied by a normalization factor that combines the laminar burning velocity,  $S$ , and the gas expansion ratio,  $E$ :

$$Q9 = \sum_{Flamm.Cloud} V \frac{SE}{(SE)_{max}}$$

Even though the ratios between these three ESC definitions vary for every scenario, in nearly every case FV will be larger than Q8, which will be larger than Q9 (rough estimates for the relative volumes of these ESCs are FV:Q8:Q9 = 3:2:1). Testing of the ESCs [24] indicates that, for onshore facilities with adequate ventilation (i.e., without large enclosed areas), the Q9 tends to yield the closest, conservative comparison to experimental data, while the other ESCs tend to be overly conservative. However, the Q9 can yield non-

conservative results for releases in enclosed or poorly ventilated areas [25], or if very fast flame speeds (e.g., approaching DDT) are achieved; in such situations, the expansion ratio is a more critical parameter than the burning velocity, therefore, the Q8 ESC is considered more representative of the actual conditions. The FV ESC is more rarely used as it is generally considered overly conservative.

Since the purpose of the Consequence Modeling task is to provide PHMSA with quantitative data on the VCE potential of scenarios typical of LNG facility siting studies, the FLACS modeling tracked each of the three ESCs; the results are presented in the next section.

### 5.7 FLACS Modeling Parameters

As previously discussed, a large number of flammable dispersion simulations were performed using FLACS to determine the effect of wind speed on the potential VCE hazards for several different release scenarios. Table 5-5 summarizes the parameters that define the simulation test matrix.

Table 5-5. Test matrix for the FLACS flammable dispersion simulations.

Scenario No.	Material	Release Size	Release Direction	Wind Speed [m/s]	Wind Direction <sup>5</sup>	ESCs	Gas Monitor Regions <sup>6</sup>
<b>00</b>	LNG	Spill	-	0.0; 0.5; 1.0; 2.0	From N; From E; From W	FV; Q8; Q9	Train 1; Train 2; Train 3; Ref. Storage; Whole Plant
<b>04</b>	LNG	2"; 3"	To N; To W		Along; Opposite; Across		
<b>12</b>	MR	2"	To N; To W				
<b>18</b>	Propane	1"; 2"; 3"	To N; To E				
<b>22</b>	Butane	3"	To N; To E				

<sup>5</sup> Directions are specified relative to the release direction, except for the LNG spill.

<sup>6</sup> "Gas Monitor Region" is the label used in FLACS to specify volumes within which ESCs are tracked

	<b>Vapor Cloud Explosions at Nil Wind</b>	03904-RP-006
	PHMSA	Rev A
	Final Report	Page 75 of 213

The computational grid extended horizontally approximately 150 m beyond the plant boundaries and the shoreline, and vertically up to 100 m above ground; the base grid size, prior to any leak refinement, was set to 10 m horizontally and 1 m vertically. Leak refinement and grid stretching were applied in accordance with FLACS modeling guidelines. For each scenario, the release was initiated after allowing the wind profile to stabilize for 30 seconds; the simulations were allowed to continue for up to 1 hour, however, they were periodically checked and terminated if, following the end of the release, the Q9 volume within the entire plant fell below 25% of the peak value.

## 5.8 Modeling Results – ESC Volumes

The purpose of the simulations test matrix shown in Table 5-5 is to evaluate quantitatively the effect of wind speed on the VCE hazard potential of different release scenarios. As discussed in section 5.6.2, the VCE hazard potential of different non-homogeneous clouds within the same congested area (i.e., PES) can be compared in terms of ESCs: given the same material reactivity and congested region, larger ESCs will be expected to result in larger overpressures if ignited.

This section discusses the results from a subset of simulations; Appendix B includes ESC plots for all simulations and gas monitor regions, excluding those for which the maximum Q9 did not reach at least 1,000 m<sup>3</sup> (i.e., the equivalent of a cube with 10 m sides).

It should be noted that, for most scenarios, the discussion will be based on the ESC volumes calculated over the entire plant footprint (up to 25 ft above grade). The main reason for this choice is that the results are largely independent of the relative position of the release location to any PES; in addition, the ESC volumes are also conservative (i.e., larger than the respective values within a single PES).

### 5.8.1 LNG Spill

Scenario 00 was specified in Table 5-3 as a spill from the guillotine failure of the LNG sendout line, which would result in a 11,220,000 lb/hr (12,000 m<sup>3</sup>/hr) spill with a duration of 10 minutes. This typically represents the largest LNG spill encountered in a facility siting study. In order to minimize any plant-specific effects, the spill was assumed to occur directly into the LNG impoundment sump, which measures 66 ft by 66 ft, with a depth of 16 ft. The impoundment sump was assumed to be lined with regular concrete.

Vapor dispersion from the LNG spill was modeled for wind speeds of 0.5, 1.0, and 2.0 m/s (all with atmospheric stability class F), as well as for no wind (wind speed = 0 m/s). Since the spill has no momentum, wind direction was specified relative to the plant axes rather than the release direction: winds from the South, East and West were considered; wind from the North was not included in the modeling since it would push the cloud towards the water and away from any congested areas.

Figure 5-6 shows, from top to bottom, the traces for FV, Q8, and Q9 for the entire plant gas monitor region. The peak ESC values across the entire plant area are listed in Table 5-6.

Table 5-6. Plant-wide peak ESC volumes for scenario 00.

ESC	2 m/s	1 m/s	0.5 m/s	0 m/s
<b>FV</b>	1,300	1,700	18,100	32,100
<b>Q8</b>	1,100	1,500	14,600	26,000
<b>Q9</b>	650	1,000	7,800	12,100

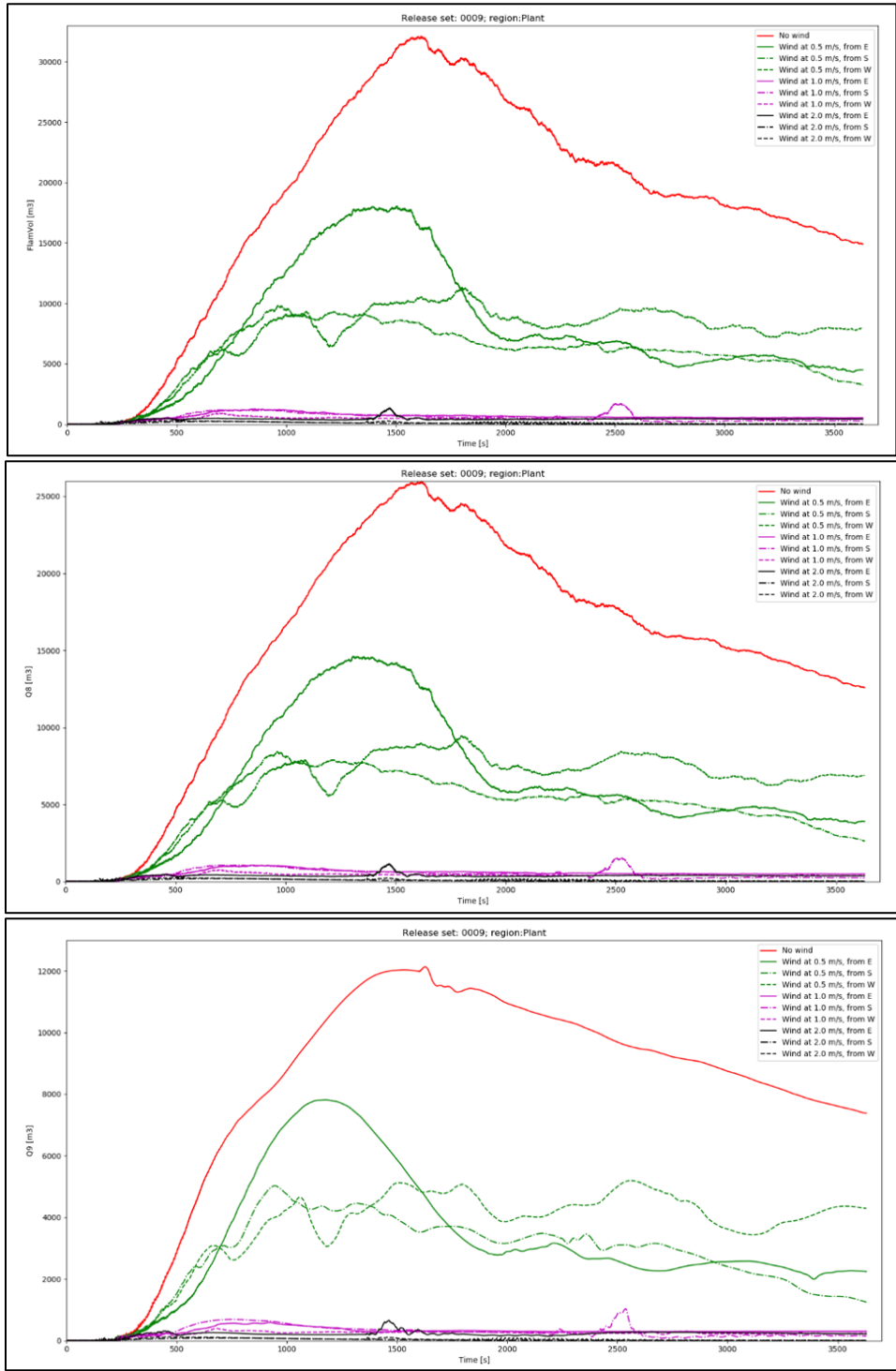


Figure 5-6. Plant-wide ESV traces for scenario 00: FV (top), Q8 (middle), and Q9 (bottom).

	<b>Vapor Cloud Explosions at Nil Wind</b>	03904-RP-006
	PHMSA	Rev A
	Final Report	Page 78 of 213

A review of these results leads to the following observations:

- The FV, Q8 and Q9 curves for each simulation (i.e., same wind speed and direction) look very similar in both shape and relative values. This trend, which holds with very few exceptions across all simulations performed for this study, is important because it allows any other observations to be made irrespective of the ESC being considered.
- The ESC volumes become progressively larger as the wind speed decreases. Using the 2 m/s values as reference, the increase is limited to less than a factor of 2 within the low wind range (i.e., as the wind is decreased from 2 to 1 m/s) but grows by over a factor of 10 under nil wind conditions.
- The ESC volumes continue to grow even after the end of the spill, due to the presence of liquid in the sump that continues evaporating. The time to peak ESC tends to grow with lower wind speeds, and the following decay is progressively slower. This behavior is consistent with a highly stratified cloud, which is progressively diluted at the air/cloud interface by wind-induced turbulence and molecular diffusion.

It should be noted that this spill scenario involves LNG, which is composed primarily of methane (in fact, the typical modeling assumption is to consider LNG as 100% methane) and therefore is a low reactivity fuel; thus, even large ESC volumes may not result in VCE hazards of concern to the public. Additionally, while it is reasonable to expect a similar trend for vapor clouds from spills of heavier hydrocarbons, those fluids have a higher boiling temperature, therefore, liquid spills will evaporate more slowly, which is likely to result in smaller ESC volumes than LNG, for a given pool surface.

Finally, it is important to note that the results shown above represent the ESC volumes within the entire plant, however, most of that area is open and not congested; therefore, only a fraction of these ESC volumes would actually contribute to generate VCE overpressures. In fact, given the location of the impoundment sump relative to the congested areas in the example facility, the largest ESC volume (FV) calculated within a PES during the scenario 00 simulations was approximately 10 m<sup>3</sup>. Figure 5-7 shows how the maximum footprint of the flammable cloud for this scenario only reaches the southern edge of the Train 2 PES.

	<b>Vapor Cloud Explosions at Nil Wind</b>	03904-RP-006
	PHMSA	Rev A
	Final Report	Page 79 of 213

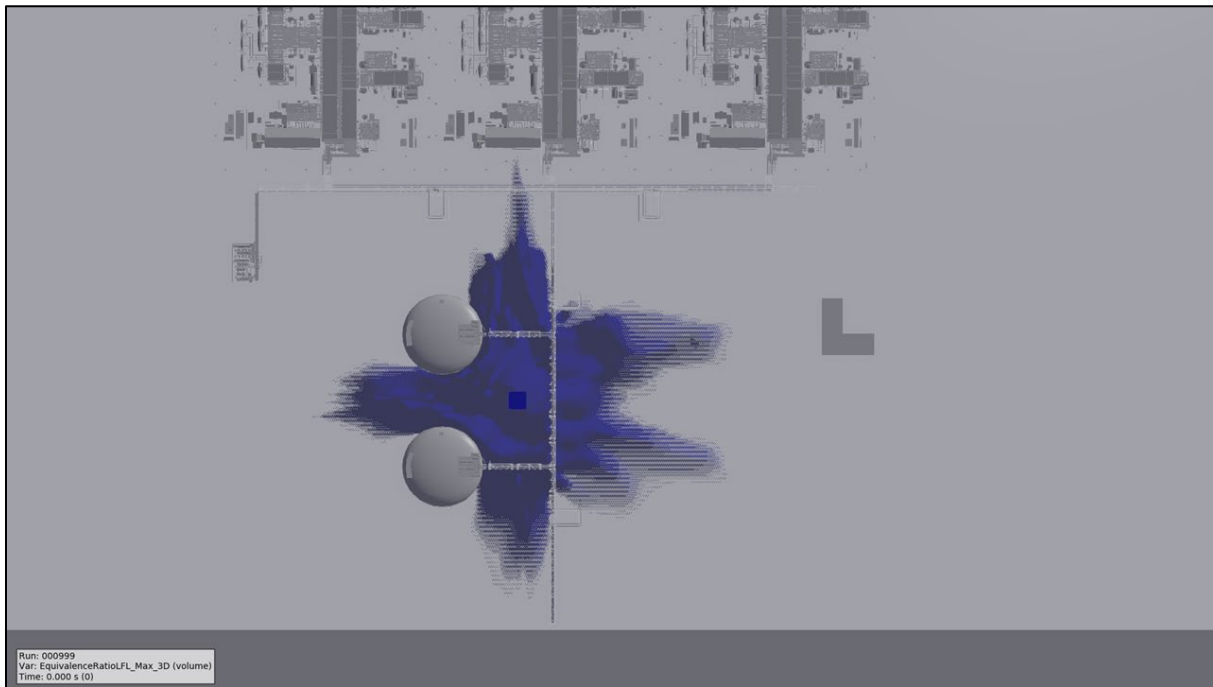


Figure 5-7. Overall flammable cloud footprint for scenario 00 (winds at 0.0, 0.5, 1.0, and 2.0 m/s).

### 5.8.2 LNG Flashing and Jetting

Scenario 04 was specified in Table 5-3 as a pressurized liquid release (a.k.a. flashing and jetting) from the LNG rundown line; in the generic facility design, the rundown line has a diameter of 14 inches, therefore the SALS is a 2-inch diameter hole, which would result in a 295,500 lb/hr release with a duration of 10 minutes, conservatively assuming the line to remain at full pressure for the entire release duration. Screening of the release behavior, performed using Phast at the minimum allowable wind speed (1 m/s), shows that the flashing jet vaporizes before touching the ground, with no liquid rainout.

Vapor dispersion from the LNG spill was modeled for wind speeds of 0.5, 1, and 2 m/s (all with atmospheric stability class F), as well as for no wind (wind speed = 0 m/s). Two release directions were considered: to the North (i.e., towards the liquefaction train) and to the West (i.e., parallel to the rundown line piperack). The wind direction was specified relative to the release direction: for each release direction, winds along and directly opposite the release were considered, as well as perpendicular to (i.e., across) the release.

Figure 5-8 and Figure 5-9 show the traces for FV, Q8, and Q9 over the entire plant footprint for the two release directions (respectively, to the West and to the North). The peak ESC values across the entire plant area are listed in Table 5-7.

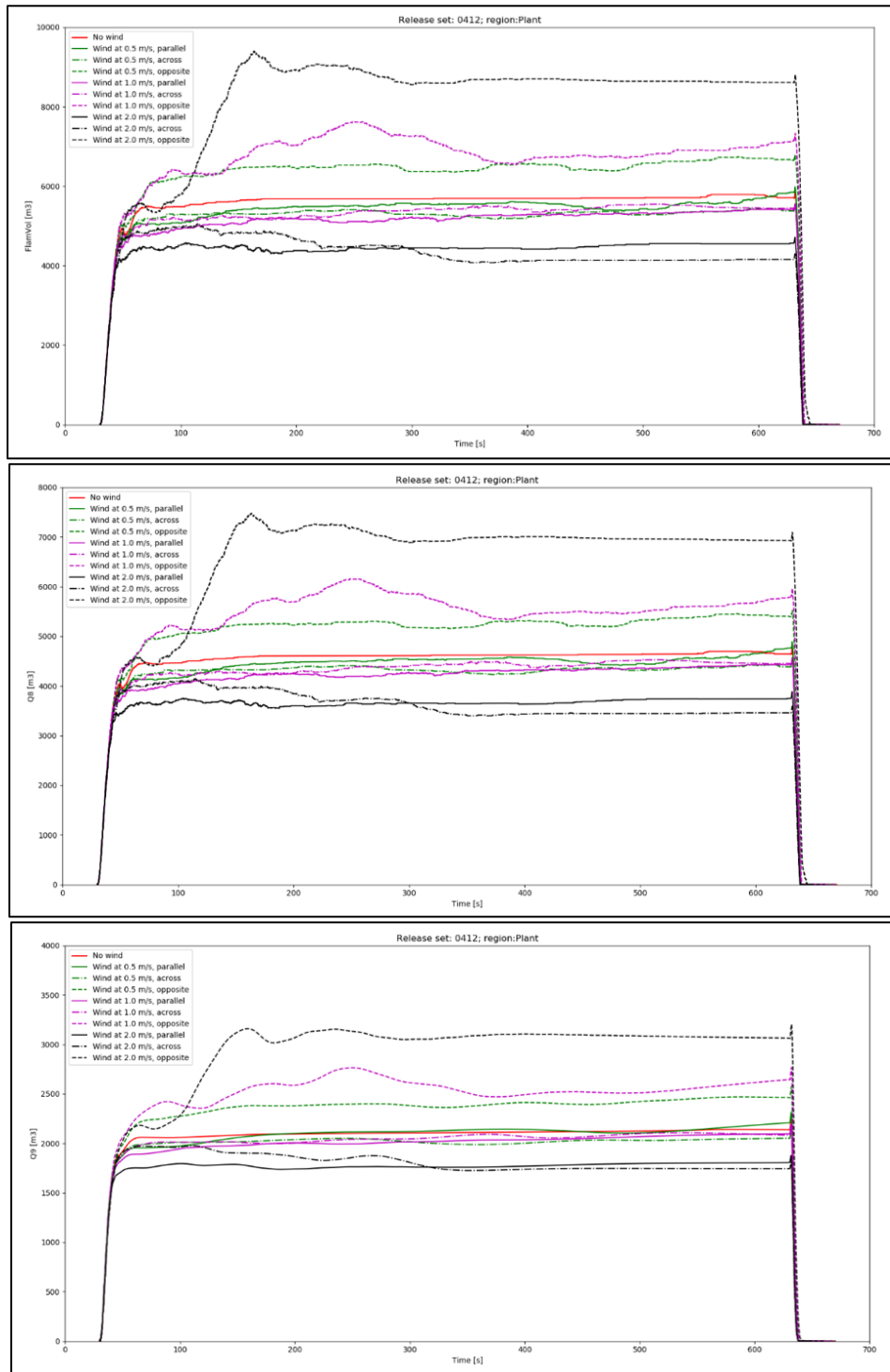


Figure 5-8. Plant-wide ESC traces for scenario 04, released to the West: FV (top), Q8 (middle), and Q9 (bottom).

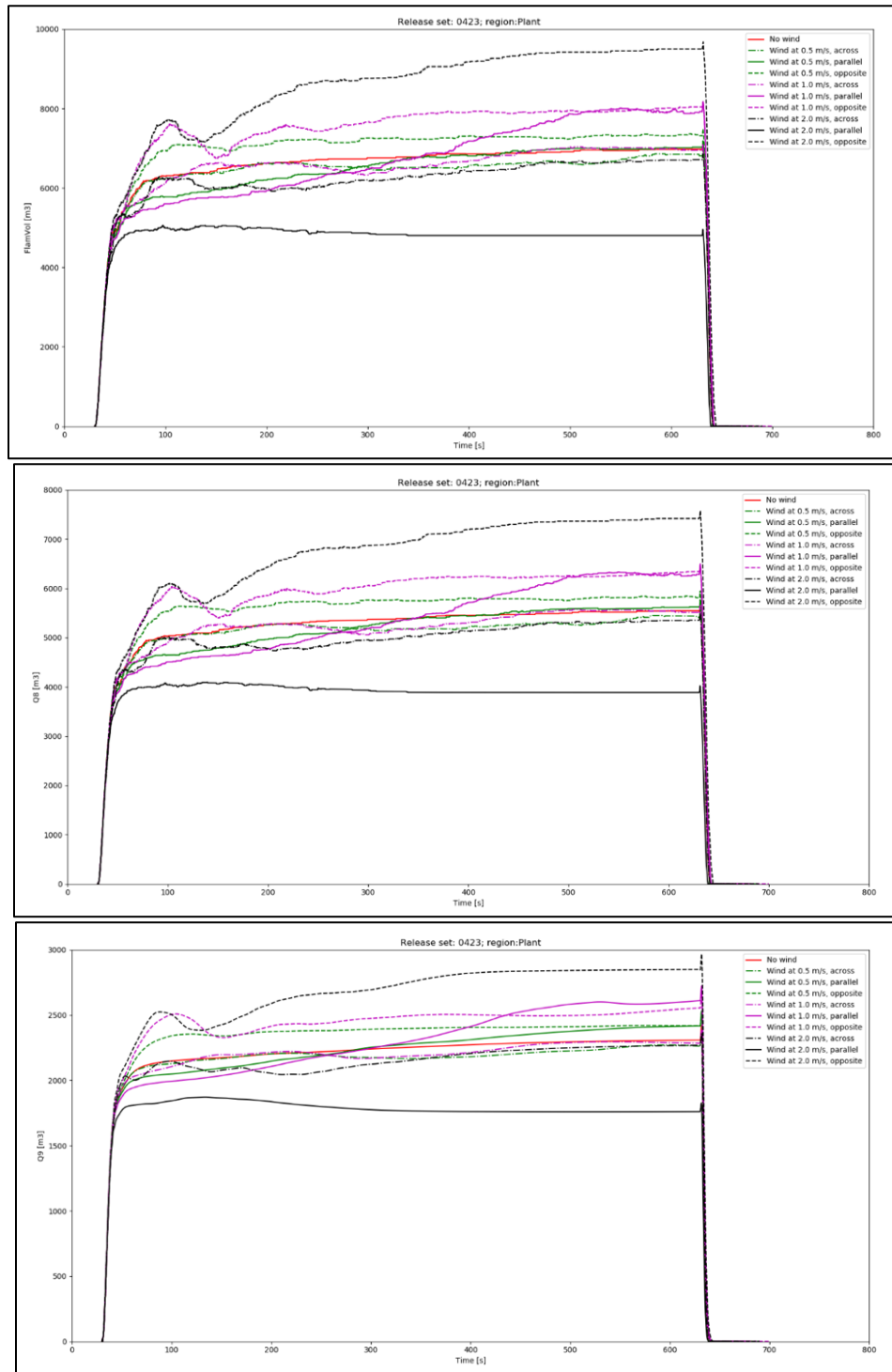


Figure 5-9. Plant-wide ESC traces for scenario 04, released to the North: FV (top), Q8 (middle), and Q9 (bottom).

Table 5-7. Plant-wide peak ESC volumes for scenario 04.

ESC	Release Direction	2.0 m/s	1.0 m/s	0.5 m/s	0.0 m/s
FV	N	9,700	8,200	7,500	7,100
	W	9,400	7,600	6,800	5,800
Q8	N	7,600	6,500	6,000	5,700
	W	7,500	6,200	5,500	4,800
Q9	N	3,000	2,700	2,500	2,400
	W	3,200	2,800	2,600	2,200

A review of these results leads to the following observations:

- The FV, Q8 and Q9 curves for each simulation (i.e., same wind speed and direction) look very similar in both shape and relative values, as for the LNG spill.
- Unlike the LNG spill scenario, for this flashing and jetting release, decreasing the wind speed does not result in an increase in ESC volumes: in fact, the largest ESC occurs at the highest wind speed included in the study (2 m/s).
- The effect of wind direction (relative to the release direction) is stronger than the effect of wind speed. In particular, releases into the wind (i.e., the wind direction is parallel but opposite to the direction of the release) consistently result in larger ESCs than releases with wind alongside or across the release and the difference increases with higher wind speeds. This suggests that the wind pushing against the momentum of the cloud can result in a thicker and increasingly mixed cloud.
- For releases into the wind, larger wind speeds result in larger ESC volumes, which is consistent with the previous observations.
- A 'blip' in the ESC values is observed shortly after the end of the release, followed by a rapid decrease in the ESC volumes. The increase in the ESC volume at the end of the release is frequently observed in these types of scenarios and is due to mixing occurring at the tail end of the cloud, once the continuous supply of rich fuel is interrupted. The rapid decrease in the ESC volumes is consistent with the behavior of a momentum-driven turbulent cloud, as opposed to the no-momentum, highly stratified cloud from an evaporating pool.

The modeling results and above observations suggest that turbulence from the flashing jet release is controlling the cloud mixing, rather than shear-induced turbulence at the air/cloud interface.

The plant-wide ESC volumes shown above are only slightly dependent on the release direction, since the release and most of the resulting cloud are within the gas monitor region. However, Table 5-8 shows that the release direction has a significant effect on

the ESC values (for brevity, only Q9 is shown) within any of the individual PES: this is expected since the release is outside the PES and the path of resulting cloud will depend on the direction of the release and of the wind. It is also worth noting that the flammable cloud only reaches the Train 2 PES, however, that is due to the release locations selected for modeling; if the same release location were selected relative to Train 1, for example, similar ESC values would be expected to occur in that train.

Table 5-8. Peak Q9 vs. release direction for scenario 04.

PES	Release Direction	2.0 m/s	1.0 m/s	0.5 m/s	0.0 m/s
<b>Train 1</b>	N	0	0	0	0
	W	0	0	0	0
<b>Train 2</b>	N	2,900	2,700	2,500	2,400
	W	1,500	1,300	1,100	840
<b>Train 3</b>	N	0	0	0	0
	W	0	0	0	0
<b>Refr. Storage</b>	N	0	0	0	0
	W	0	0	0	0

The hole size for scenario 04 was set to 2 inches based on current SALS criteria. However, for the sole purpose of evaluating the sensitivity of VCE potential to the release hole size, the same scenario was also evaluated assuming a 3-inch hole size. Table 5-9 shows a comparison of the peak Q9 values between 2- and 3-inch releases.

Table 5-9. Peak Q9 vs. hole size for scenario 04.

PES	Hole Size	2.0 m/s	1.0 m/s	0.5 m/s	0.0 m/s
<b>Plant</b>	2"	3,200	2,800	2,600	2,400
	3"	26,100	20,700	19,300	18,900
<b>Train 2</b>	2"	2,900	2,700	2,500	2,400
	3"	25,200	20,500	19,200	18,700

The modeling results show an 8- to 10-fold increase in the Q9 values for the larger hole size. For reference, it is worth noting that the release rate for a 3-inch hole is only approximately 2.25 times larger than for a 2-inch hole. Therefore, the modeling shows a high sensitivity of VCE potential to the release size, with larger releases yielding larger explosion potentials. However, Q9 values still decrease with decreasing wind speed.

	<b>Vapor Cloud Explosions at Nil Wind</b>	03904-RP-006
	PHMSA	Rev A
	Final Report	Page 84 of 213

### 5.8.3 MR Flashing and Jetting

Scenario 12 was specified in Table 5-3 as a pressurized liquid release (a.k.a. flashing and jetting) from the high-pressure mixed refrigerant liquid line; in the generic facility design, this line has a diameter of 2 inches, therefore the SALS is a guillotine failure, which would result in a 656,400 lb/hr release with a duration of 10 minutes, conservatively assuming the line to remain at full pressure for the entire release duration. Phast modeling of the release shows that the flashing jet vaporizes before touching the ground, with no liquid rainout.

Vapor dispersion from the MR spill was modeled for wind speeds of 0.5, 1, and 2 m/s (all with atmospheric stability class F), as well as for no wind (wind speed = 0 m/s). Two release directions were considered: to the North and to the West; note that the release location is inside the liquefaction train, and the release was located within Train 2 so that dispersion to the East or to the West would end up in another PES. The wind direction was specified relative to the release direction: for each release direction, winds along and directly opposite the release were considered, as well as perpendicular to (i.e., across) the release.

Since the MR release occurs within a train, and therefore the relative position of the release to the PES is less relevant, the results shown in this section are relative to the train within which the release occurs, which is the PES with the largest ESCs. Figure 5-10 and Figure 5-11 show the Q9 traces<sup>7</sup> within the Train 2 PES for the two release directions (respectively, to the North and to the West). The peak Q9 values across the entire plant area are listed in Table 5-10.

---

<sup>7</sup> The previous sections already established that FV, Q8, and Q9 follow similar trends. Therefore, for brevity, only Q9 results are shown in the remainder of this report. FV and Q8 traces for each scenario are included in Appendix B.

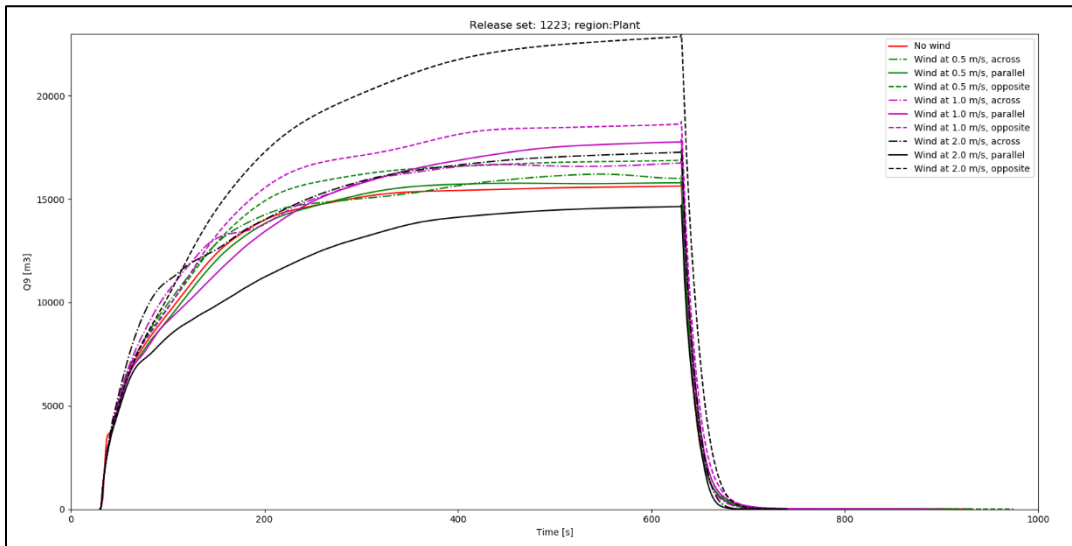


Figure 5-10. Q9 traces in Train 2 for scenario 12, released to the North.

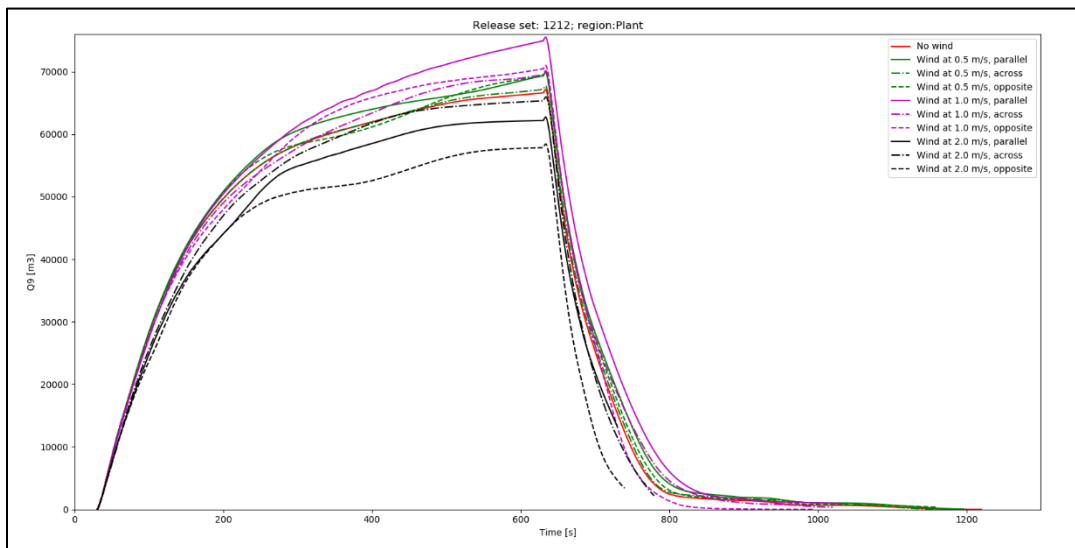


Figure 5-11. Q9 traces in Train 2 for scenario 12, released to the West.

Table 5-10. Plant-wide peak Q9 volumes for scenario 12.

ESC	Release Direction	2.0 m/s	1.0 m/s	0.5 m/s	0.0 m/s
Q9	N	22,500	18,300	16,800	15,600
	W	61,800	54,200	50,100	47,900

	<b>Vapor Cloud Explosions at Nil Wind</b>	03904-RP-006
	PHMSA	Rev A
	Final Report	Page 86 of 213

A review of these results leads to the following observations:

- Similar to the LNG flashing and jetting scenario decreasing the wind speed does not result in an increase in ESC volumes: in fact, the largest ESC occurs at the highest wind speed included in the study (2 m/s). However, the results are much more dependent on the release direction, due to the complex geometry surrounding the release. In fact, the Q9 values for releases to the West (i.e., into the train) are nearly 3 times larger than those for release to the North (i.e., between adjacent trains), as shown in Table 5-10.
- The effect of wind direction (relative to the release direction) is still noticeable, at least in the release to the North; however, it is much less pronounced than for scenario 04. The likely explanation is that MR is released and disperses primarily in an area with many obstacles and obstructions, which disrupt the wind profile and create turbulence and recirculation.
- Following the end of the release, the ESCs show the same 'blip' and rapid decrease observed in the LNG flashing and jetting case, consistent with the behavior of a momentum-driven turbulent cloud.

The modeling results and above observations suggest that turbulence from the flashing jet release is controlling the cloud mixing, rather than shear-induced turbulence at the air/cloud interface.

### 5.8.3.1 Propane Vessel Release

Scenario 18 was specified in Table 5-3 as a pressurized liquid release (a.k.a. flashing and jetting) from the withdrawal line at the bottom of the propane storage vessel; in the generic facility design, this line has a diameter of 3 inches, therefore the SALS is a guillotine failure, which would result in a 649,200 lb/hr release, driven by the pressure in the vessel and lasting until the vessel is empty. The facility design assumed the vessel to have a 20,000 gallon capacity; at the calculated release rate, the vessel would empty in approximately 540 seconds (i.e., 9 minutes). The HSL report argued that vessel-emptying scenarios were likely to result in large flammable vapor clouds under nil wind conditions, because of the large volumes released and the long duration of the release; in order to evaluate that argument quantitatively, the propane vessel was conservatively assumed to have double the capacity (40,000 gal) so that the 3-inch release would last longer than 10 minutes. Phast modeling of the release shows that the flashing jet vaporizes before touching the ground, with no liquid rainout.

Vapor dispersion from the propane release was modeled for wind speeds of 0.5, 1, and 2 m/s (all with atmospheric stability class F), as well as for no wind (wind speed = 0 m/s). Two release directions were considered: to the North and to the East (the refrigerant storage area is near the west end of the liquefaction area, therefore a release to the West would have been away from any PES). The wind direction was specified relative to

the release direction: for each release direction, winds along and directly opposite the release were considered, as well as perpendicular to (i.e., across) the release.

Figure 5-12 and Figure 5-13 show the Q9 traces over the entire plant footprint for the two release directions (respectively, to the North and to the East). The peak Q9 values across the entire plant area are listed in Table 5-11.

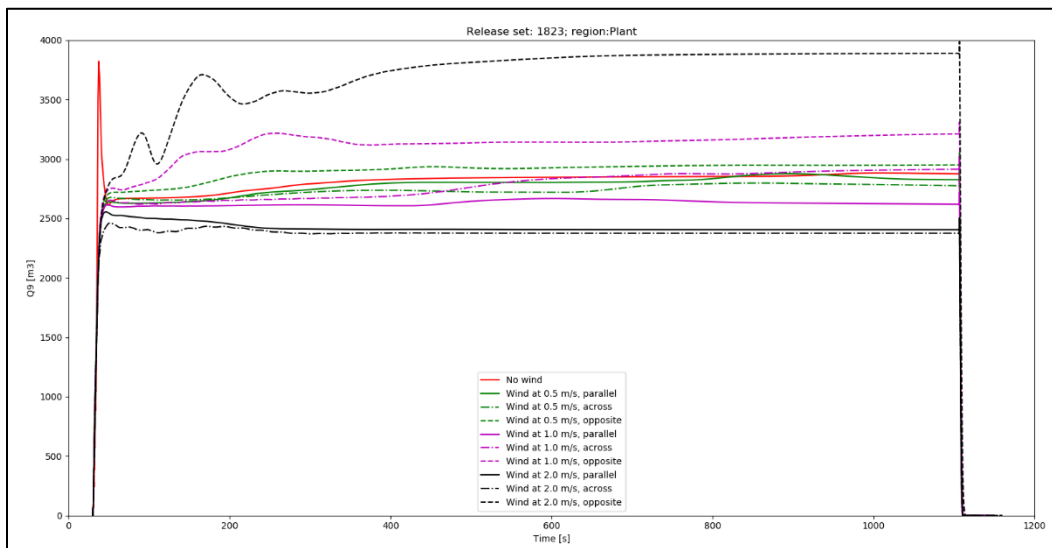


Figure 5-12. Plant-wide Q9 traces for scenario 18, released to the North.

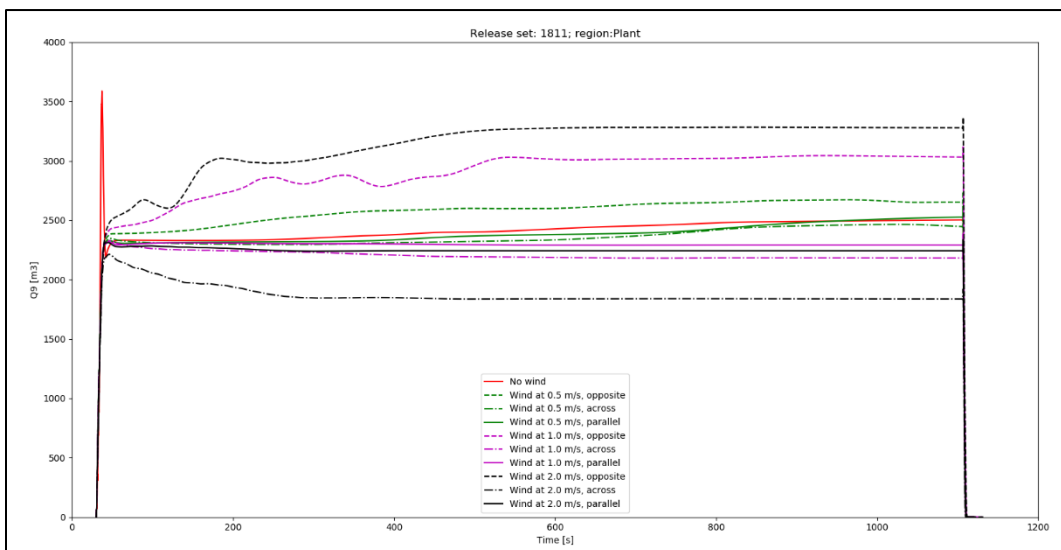


Figure 5-13. Plant-wide Q9 traces for scenario 18, released to the East.

Table 5-11. Plant-wide peak Q9 volumes for scenario 18.

ESC	Release Direction	2.0 m/s	1.0 m/s	0.5 m/s	0.0 m/s
Q9	N	4,000	3,300	3,100	3,800
	E	3,400	3,100	2,700	3,600

A review of these results leads to the following observations:

- Similar to the LNG and MR flashing and jetting scenario, there is no effect of decreasing wind speed leading to larger ESC volumes. The 2 m/s ESCs for different wind directions bracket all lower wind speed scenarios.
- There is, however, an interesting effect that occurs at the beginning of the release (within approximately the first 30 seconds) under zero wind conditions: the ESC volume grows and peaks rapidly, then decreases to a lower near-steady value. For this scenario, the peak zero-wind ESC remains smaller than the peak ESC under low wind conditions; however, it deviates from the trend described above and in the previous flashing and jetting scenarios. The likely explanation is that the initial jet from the release undergoes stronger mixing as it begins to displace the still ambient air, resulting in a larger fraction of the cloud being in the flammable range.
- As the release continues, the same trends and behaviors described for the LNG and MR flashing and jetting scenarios are observed for propane, as well: opposite wind direction results in larger ESCs, and a 'blip' occurs right after the end of the release, followed by a rapid decrease in ESC volumes.

The modeling results and above observations suggest that turbulence from the flashing jet release is controlling the cloud mixing, rather than shear-induced turbulence at the air/cloud interface.

The hole size for scenario 18 was specified as 3 inches (i.e., a guillotine failure of the 3-inch line) based on current SALS criteria. Since the HSL report [1] suggested that "*a wider range of smaller losses of containment (with much higher frequency) have the potential to cause a large cloud in these conditions, if the releases are not stopped and the vapor is allowed to accumulate around the source*", a sensitivity analysis was performed on this release scenario, to evaluate how the VCE potential changes with the release hole size. The propane release was therefore also modeled assuming a 2-inch and a 1-inch diameter hole. Note that, given the smaller leak rates, the 2- and 1-inch release scenarios used the 'design' vessel inventory of 20,000 gal (rather than the double volume assumed for the 3-inch release) to limit the duration of the modeling. Figure 5-14 through Figure 5-16 show the plant-wide Q9 traces, respectively, for the 3-inch, 2-inch, and 1-inch hole sizes; Table 5-12 summarizes the peak Q9 values for each hole size and wind speed. Note

that the ESC traces reached an equilibrium value long before the end of the release, therefore the different vessel inventory did not affect the results.

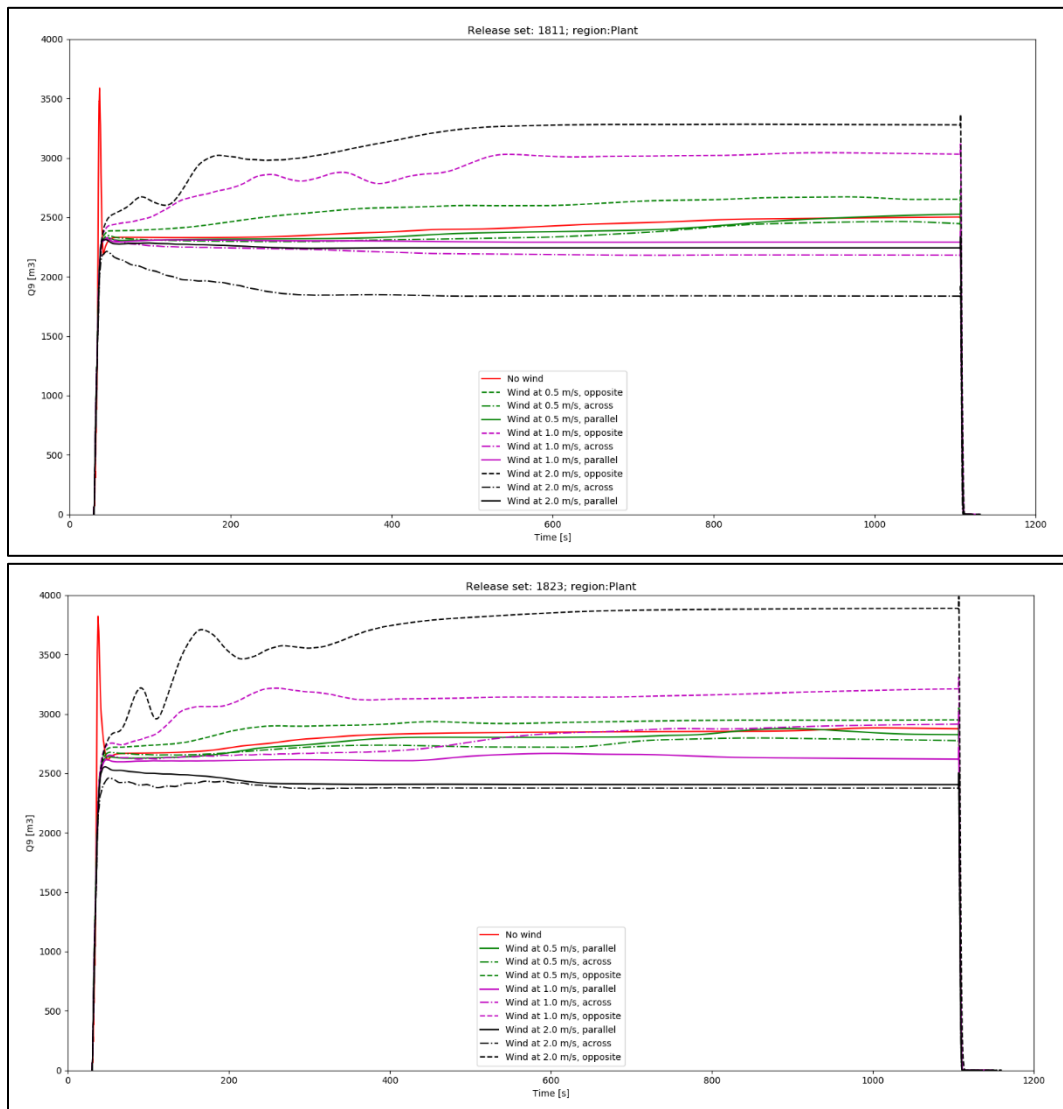


Figure 5-14. Plant-wide Q9 traces for scenario 18 (3-inch release): to the North (top) and to the East (bottom).

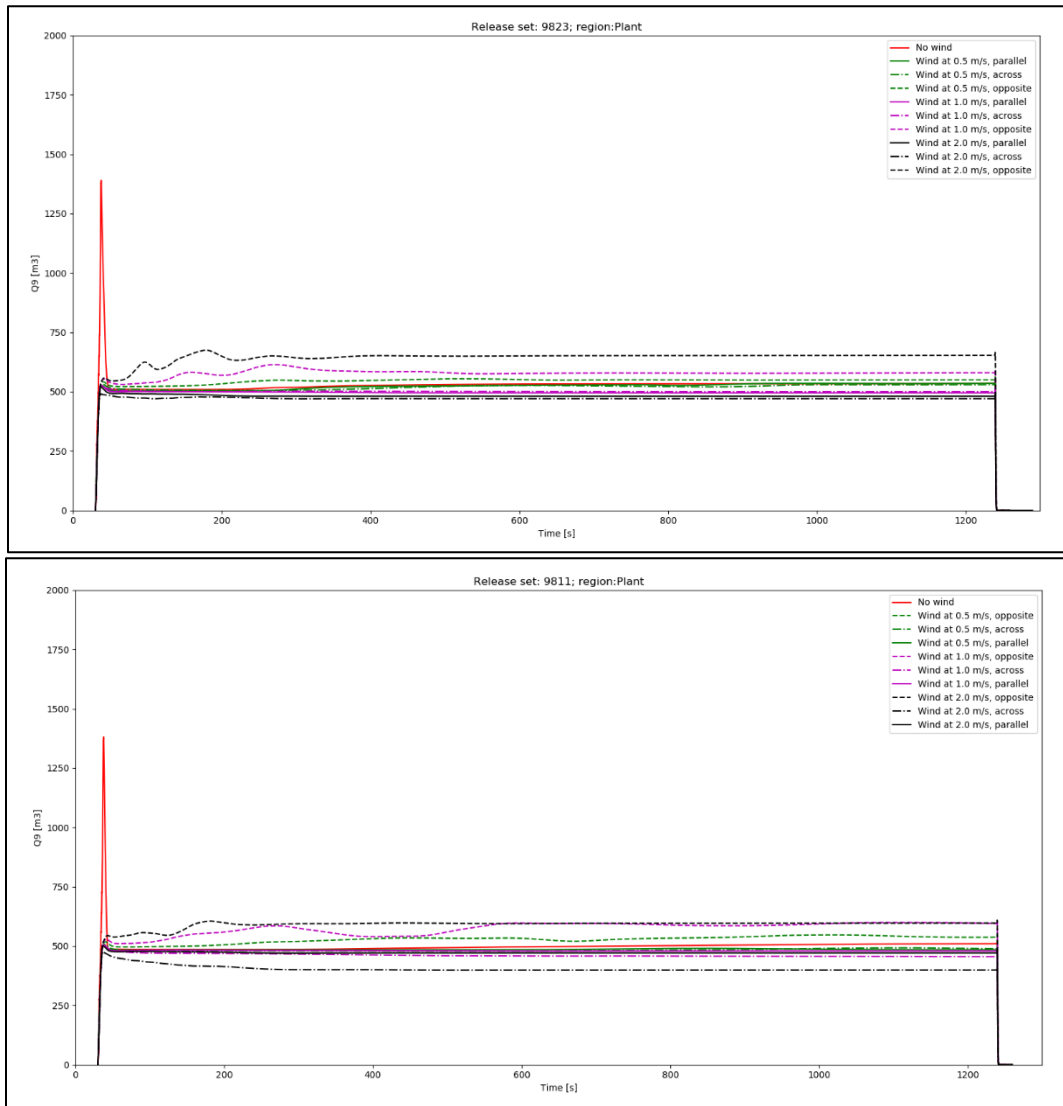


Figure 5-15. Plant-wide Q9 traces for scenario 18 (2-inch release): to the North (top) and to the East (bottom).

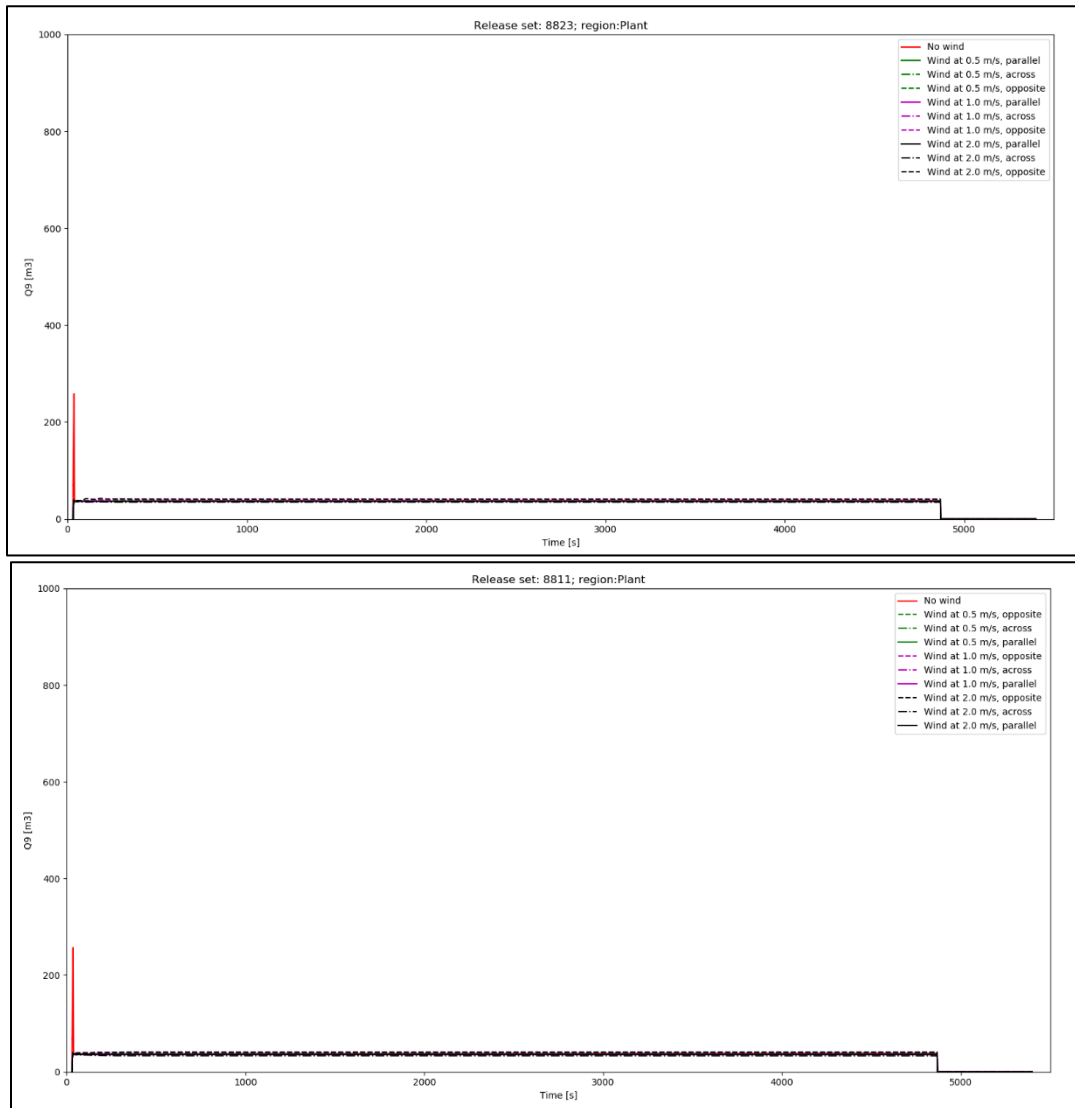


Figure 5-16. Plant-wide Q9 traces for scenario 18 (1-inch release): to the North (top) and to the East (bottom).

Table 5-12. Sensitivity analysis of plant-wide peak Q9 vs. hole size for scenario 18.

Hole Size	2.0 m/s	1.0 m/s	0.5 m/s	0.0 m/s
3"	4,000	3,300	3,100	3,800
2"	670	610	560	1,400
1"	40	40	40	260

	<b>Vapor Cloud Explosions at Nil Wind</b>	03904-RP-006
	PHMSA	Rev A
	Final Report	Page 92 of 213

The following observations can be made from the results of the hole size sensitivity analysis:

- Smaller flashing and jetting releases result in smaller ESC volumes, contradicting the HSL's suggestion that smaller, more frequent releases may contribute to increasing a facility's risk from VCEs. This result is consistent with the comparison of 2- and 3-inch releases for the LNG flashing and jetting scenario discussed in section 5.8.2.
- The ESC volumes decrease more rapidly than the release flow rate, as the hole size is reduced. In this case, the release flow rates scale as 9:4:1 whereas the ratio of ESCs is approximately 80:15:1 (decreasing to 15:5:1 for zero wind, due to the initial cloud expansion effect previously described). This result is also consistent with observations for the LNG flashing and jetting scenario.
- The initial cloud expansion effect at zero wind becomes more pronounced for smaller release rates, causing the nil-wind results to be bounding for the smaller hole sizes. However, due to the smaller release rates, the nil-wind ESC volumes are notably less than the 2 m/s peak Q9 for the 3" hole, and which itself is over an order of magnitude smaller than the ESCs obtained from other releases (e.g., MR scenario 12) and therefore not likely to result in increased VCE hazards for a facility.

### 5.8.3.2 Butane Vessel Release

Scenario 22 was specified in Table 5-3 as a pressurized liquid release (a.k.a. flashing and jetting) from the withdrawal line at the bottom of the butane storage vessel; in the generic facility design, this line has a diameter of 3 inches, therefore the SALS is a guillotine failure, which would result in a 284,000 lb/hr release, driven by the pressure in the vessel and lasting until the vessel is empty. The facility design assumed the vessel to have a 25,000-gallon capacity; at the calculated release rate, the vessel would empty in approximately 1,670 seconds (i.e., nearly 18 minutes).

Phast modeling of the release shows that most of the flashing jet vaporizes before touching the ground, however, approximately 23% of the release rains out to form a liquid pool on the ground. The refrigerant storage area was assumed to be bounded by a curb, which would contain any liquid spills and prevent them from spreading beyond its perimeter.

Vapor dispersion from the butane release was modeled for wind speeds of 0.5, 1, and 2 m/s (all with atmospheric stability class F), as well as for no wind (wind speed = 0 m/s). Two release directions were considered: to the North and to the East (the refrigerant storage area is near the west end of the liquefaction area, therefore a release to the West would have been away from any PES). The wind direction was specified relative to the release direction: for each release direction, winds along and directly opposite the release were considered, as well as perpendicular to (i.e., across) the release.

Figure 5-17 and Figure 5-18 show the Q9 traces over the entire plant footprint for the two release directions (respectively, to the North and to the East). The peak Q9 values across the entire plant area are listed in Table 5-13.

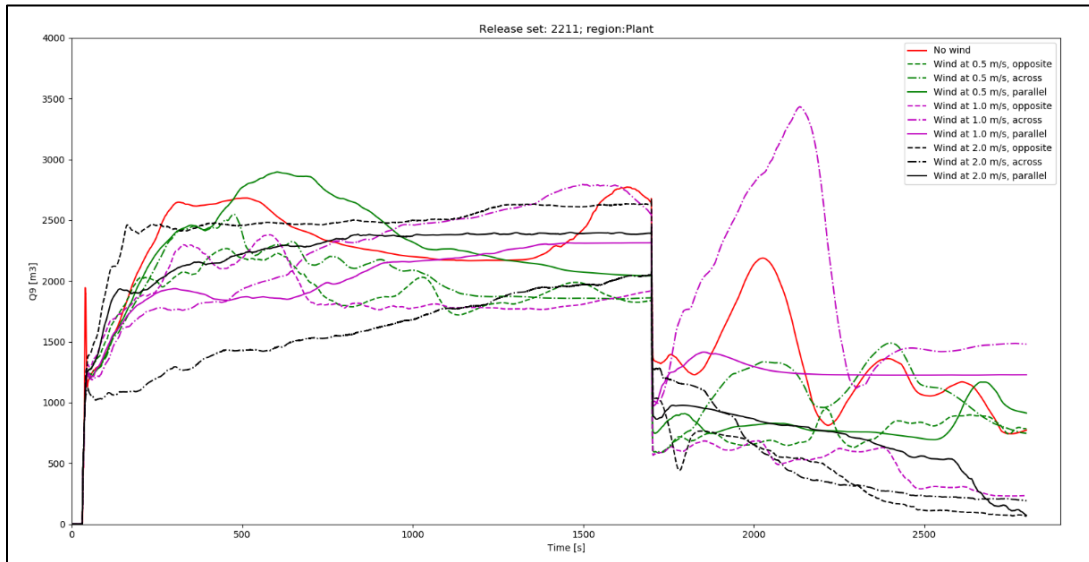


Figure 5-17. Plant-wide Q9 traces for scenario 22, released to the North.

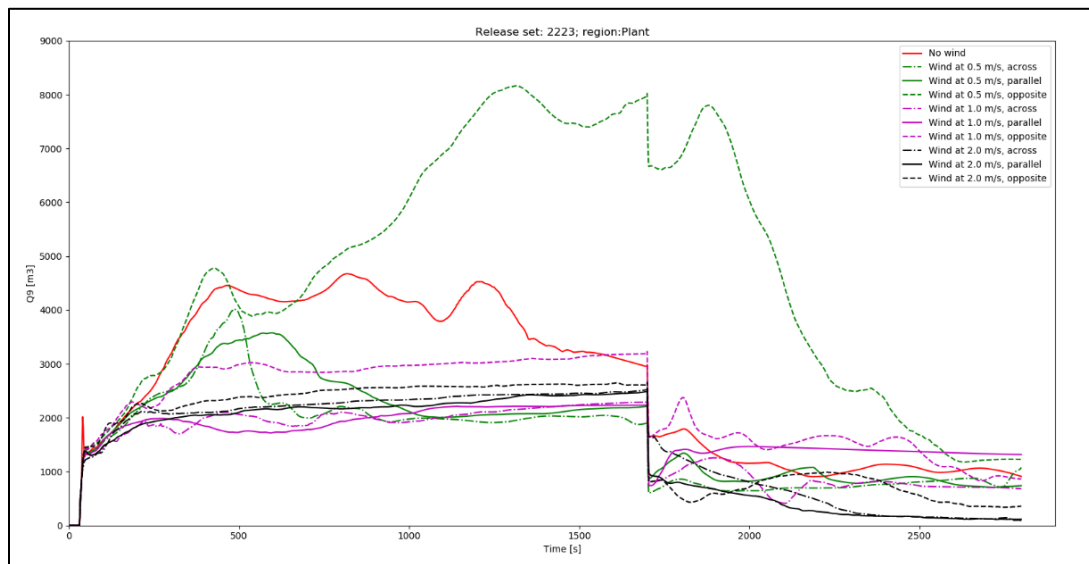


Figure 5-18. Plant-wide Q9 traces for scenario 22, released to the East.

Table 5-13. Plant-wide peak Q9 volumes for scenario 22.

Release Direction	2.0 m/s	1.0 m/s	0.5 m/s	0.0 m/s
<b>N</b>	2,700	3,200	8,200	4,700
<b>E</b>	2,700	3,400	2,900	2,800

A review of these results leads to the following observations:

- Unlike the other scenarios, which consisted of a pure spill or a flashing and jetting release, the ESC traces for this scenario do not show any clear trends. This is most likely attributable to the presence of a flashing jet as well as an evaporating pool, due to the liquid rainout.
- All ESC traces show a sharp drop shortly after the end of the release. This is due to the rapid dissipation of the flashing jet; however, unlike the previous flashing and jetting cases, the liquid pool formed by rainout continues to evaporate and therefore sustains a flammable vapor cloud for a longer period of time.
- Even though, in some cases (i.e., combination of release and wind direction), nil-wind conditions resulted in larger ESCs than low winds, the maximum ESCs are still smaller than obtained from other releases (e.g., MR scenario 12) and therefore not likely to result in increased VCE hazards for a facility, especially when PES-based ESCs are considered rather than plant-wide ones.

## 5.9 Modeling Results – VCE Overpressures

The flammable dispersion simulations discussed in section 5.8 provided quantitative data to determine, for each release scenario included in this study, which wind speeds produce the largest equivalent stoichiometric clouds as well as the volume of these ESCs. Since it is well established that, for a given fuel and congested area, a larger ESC will yield larger overpressures, a review of the flammable dispersion simulation results provided insight into whether and under which circumstances nil wind conditions may lead to increased VCE hazards.

In this section, FLACS was used to perform VCE simulations based on the ESCs obtained from the dispersion modeling. The purpose of the VCE modeling was to compare quantitatively the overpressure hazard areas for ESC volumes obtained under different wind conditions.

The VCE modeling used the Train 2 PES as the congested area in which the ESCs were placed and ignited. Each ESC volume was arranged in clouds of different shapes, placed at various locations within the PES, and ignited at various locations. In order to obtain the VCE hazard footprint around Train 2, the clouds were placed preferentially around the perimeter of the PES and the ignition locations were selected to project the

	<b>Vapor Cloud Explosions at Nil Wind</b>	03904-RP-006
	PHMSA	Rev A
	Final Report	Page 95 of 213

blast wave outward. The following criteria were set to define the VCE modeling test matrix:

- The cloud height was set to 25 ft (7.5 m), consistent with the height of the gas monitor regions
- The base of the cloud was set at grade
- Cloud footprints were specified as:
  - Square
  - Elongated in the North-South direction (Y length / X length = 2)
  - Elongated in the East-West direction (Y length / X length = 1/2)
- Cloud locations were selected among 9 possible positions:
  - Four corners of the PES
  - Middle of the four PES sides
  - Center of the PES
- Ignition locations were selected among 9 possible positions:
  - Four corners of the cloud
  - Middle of the four cloud sides
  - Center of the cloud
- All ignition locations were set near grade

A total of 18 VCE simulations were selected for each ESC, as a compromise to provide sufficient data to compare various scenarios with a manageable computational effort; the different cloud shapes and placements (red boxes), and the respective ignition locations (stars) are shown in Figure 5-19. Note that this set of simulations was selected for the purpose of this study and should not be used as basis for any project-specific siting study.

	<b>Vapor Cloud Explosions at Nil Wind</b>	03904-RP-006
	PHMSA	Rev A
	Final Report	Page 96 of 213

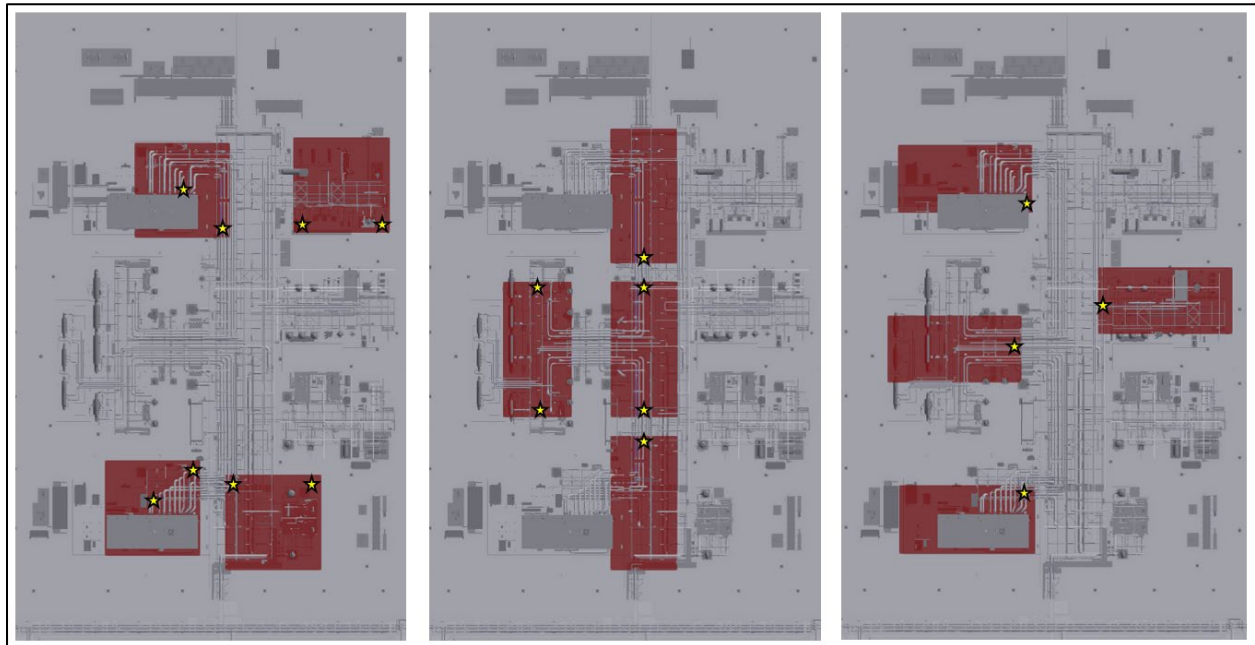


Figure 5-19. ESC cloud placements and ignition locations for the VCE modeling.

The computational grid was set to cubical cells of 0.75 m size throughout the PES as well as the region where the blast wave could propagate; stretching was performed, consistent with FLACS guidelines, outside of that region to the edges of computational domain. A total of approximately 13.6 million grid cells were used.

Given the computational effort required to perform VCE modeling at these scales, only the following scenarios were modeled:

- LNG
  - Maximum plant-wide Q9 at low wind (1,000 m<sup>3</sup>) and nil wind (12,100 m<sup>3</sup>) conditions. The plant-wide values were selected, instead of the PES-based values, to provide a conservative worst-case for this facility, independent of the distance between the impoundment sump and the liquefaction area.
- MR:
  - Maximum plant-wide Q9 at low wind (61,800 m<sup>3</sup>) and nil wind (48,000 m<sup>3</sup>) conditions. The plant-wide values were again selected to provide a conservative worst-case. Also, even though the nil-wind Q9 is smaller than the low-wind value, both were evaluated to provide a quantitative comparison between the VCE hazard areas, since the MR release has the largest VCE potential among all scenarios modeled in this study.
  - Maximum plant-wide Q8 (96,500 m<sup>3</sup>, which occurred at low wind). This case was included to provide a quantitative comparison between Q9 and Q8. Note that this should not be considered as an endorsement or requirement to use the Q8 ESC for land-based, well-ventilated LNG facilities.

	<b>Vapor Cloud Explosions at Nil Wind</b>	03904-RP-006
	PHMSA	Rev A
	Final Report	Page 97 of 213

- Propane:
  - Maximum plant-wide Q9 (4,000 m<sup>3</sup>, which occurs at low wind). The plant-wide values were again selected to provide a conservative worst-case.

The VCE modeling results are summarized in Figure 5-20 through Figure 5-25. Each figure shows the maximum overpressure footprint as a composite between the 18 simulations performed for each scenario described above; the color coding ranges from 1 psig (dark blue) to 10 psig or above (dark red). Overpressure footprints for each individual simulation, excluding those which did not reach the 1 psig threshold, are shown in Appendix C.

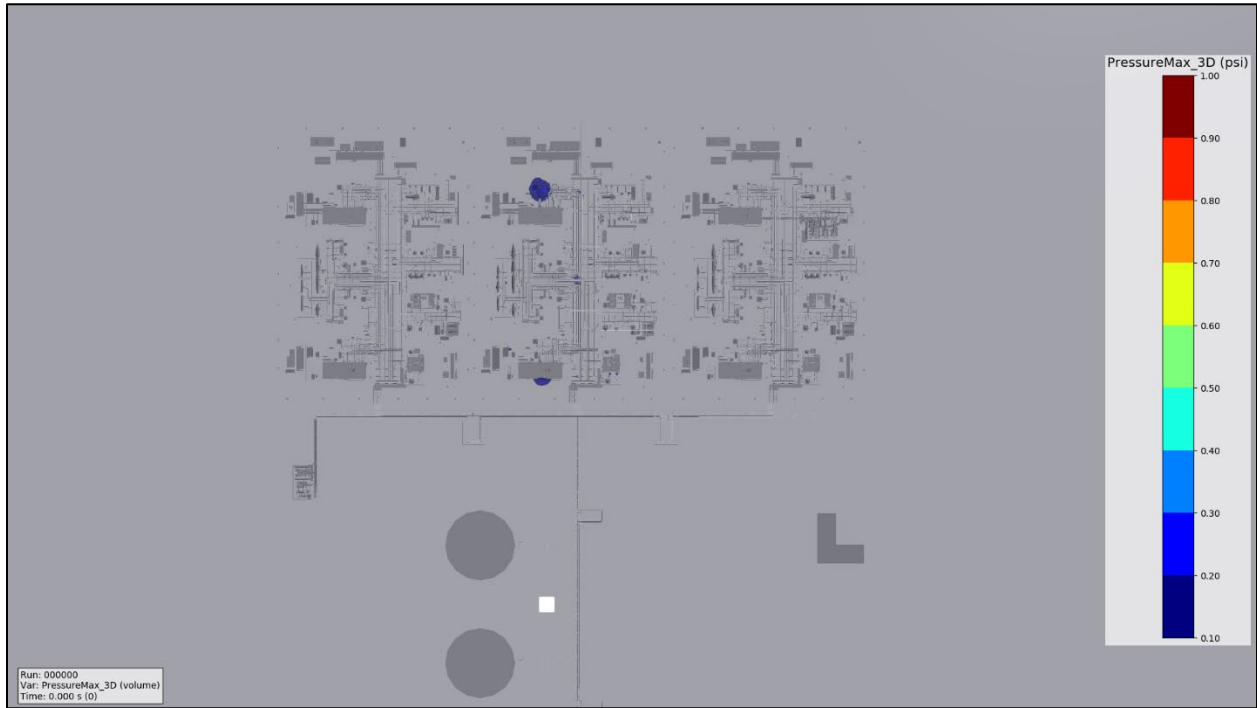


Figure 5-20. Overpressure hazard footprint for LNG Q9 at low wind.

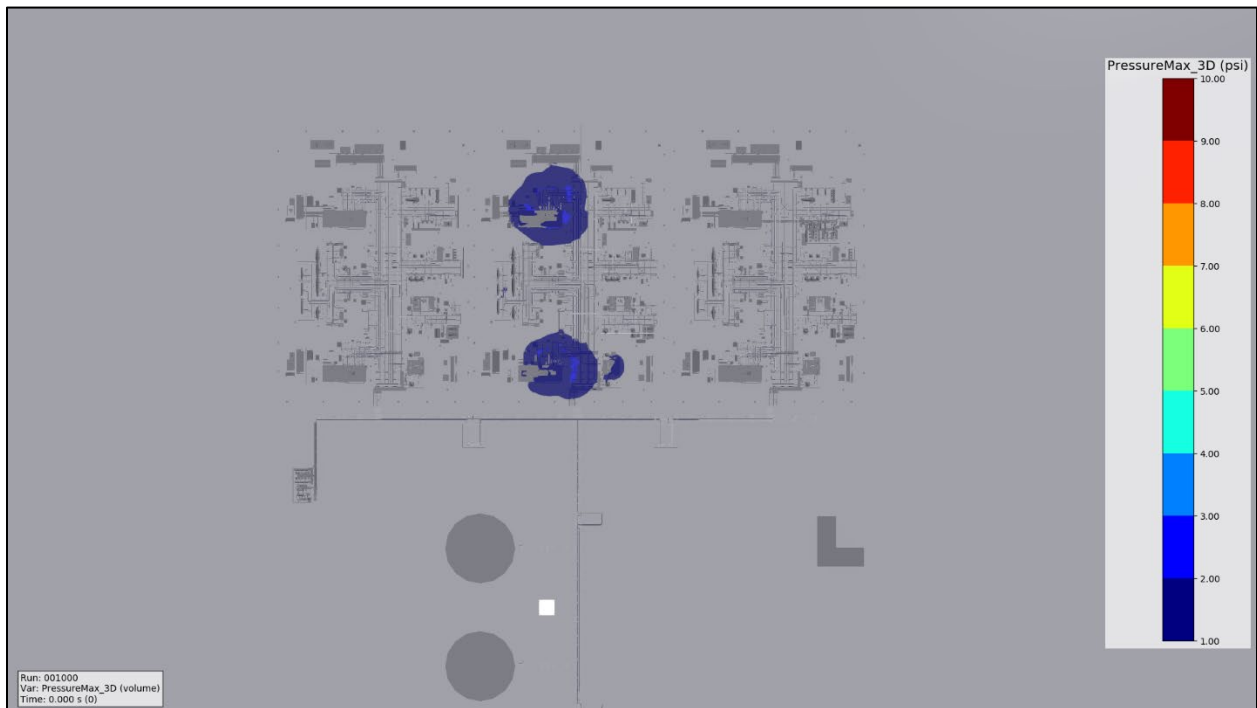


Figure 5-21. Overpressure hazard footprint for LNG Q9 at nil wind.

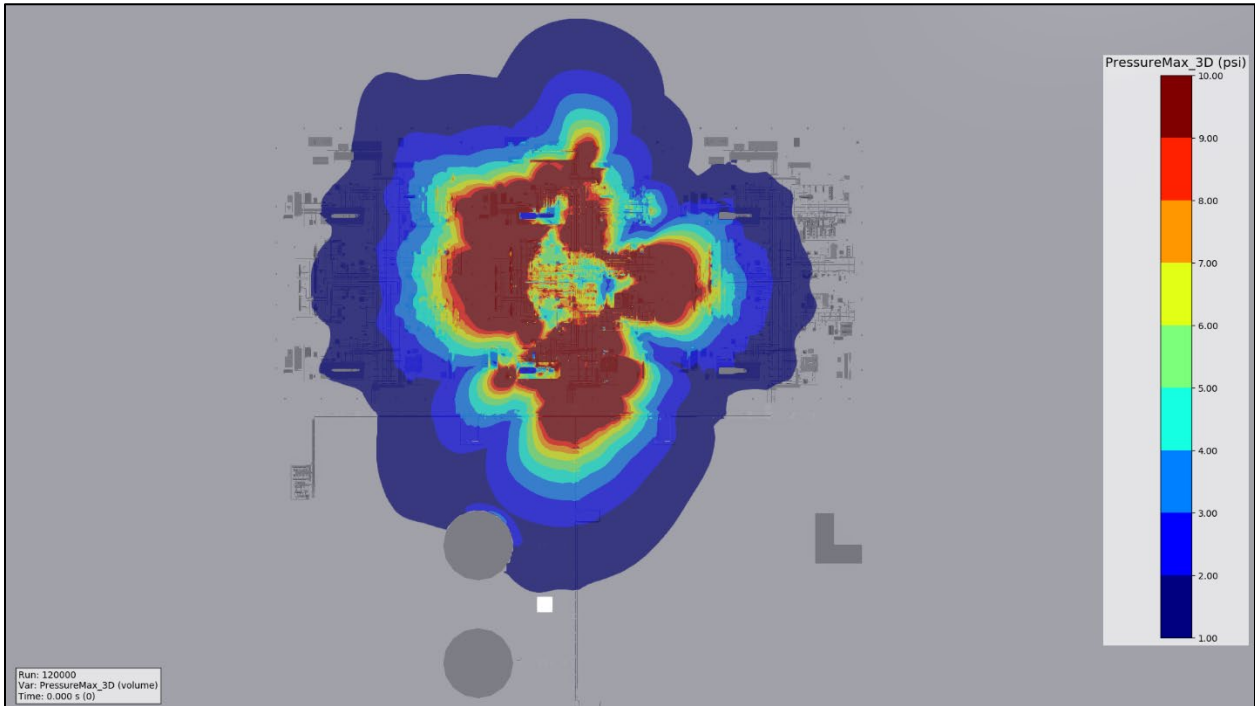


Figure 5-22. Overpressure hazard footprint for MR Q9 at low wind.

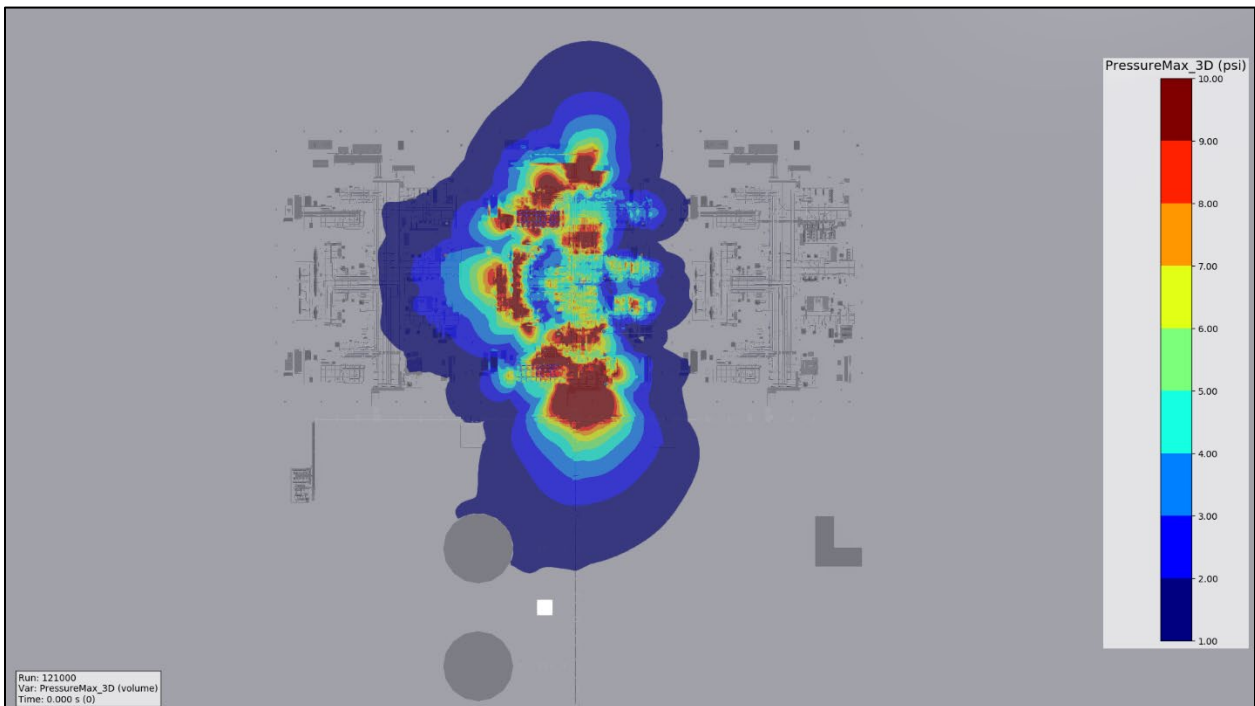


Figure 5-23. Overpressure hazard footprint for MR Q9 at nil wind.

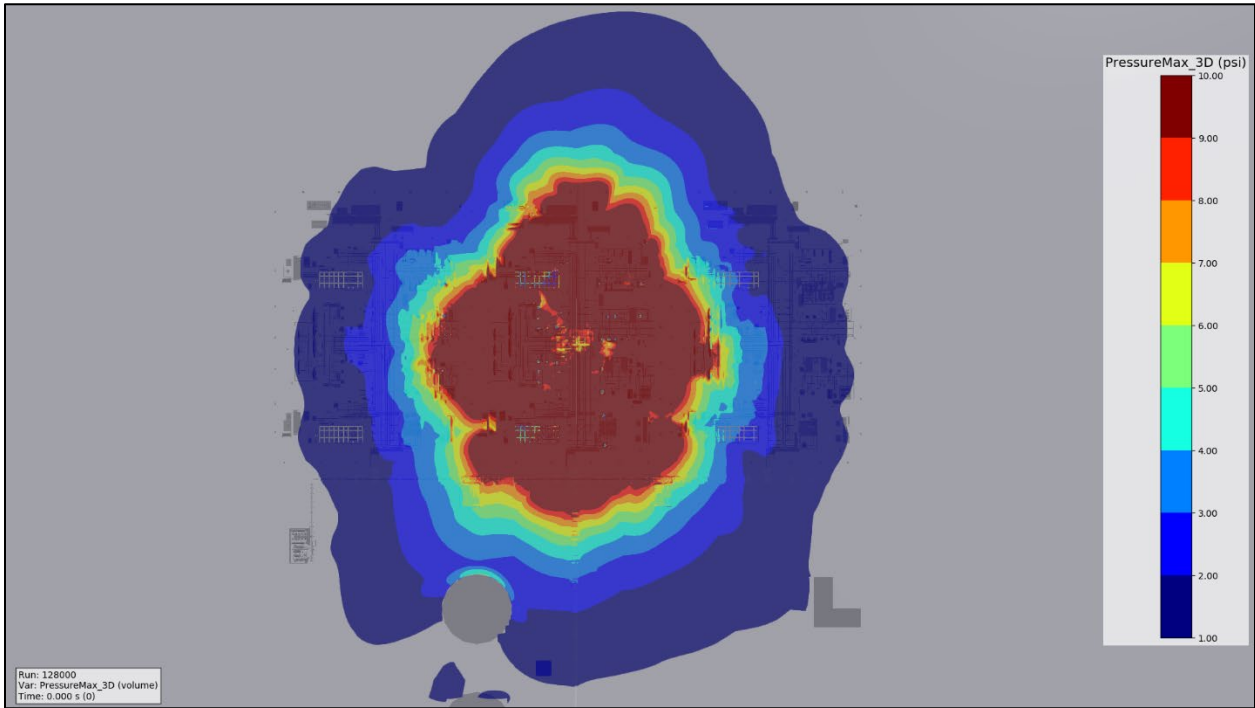


Figure 5-24. Overpressure hazard footprint for MR Q8 at low wind.

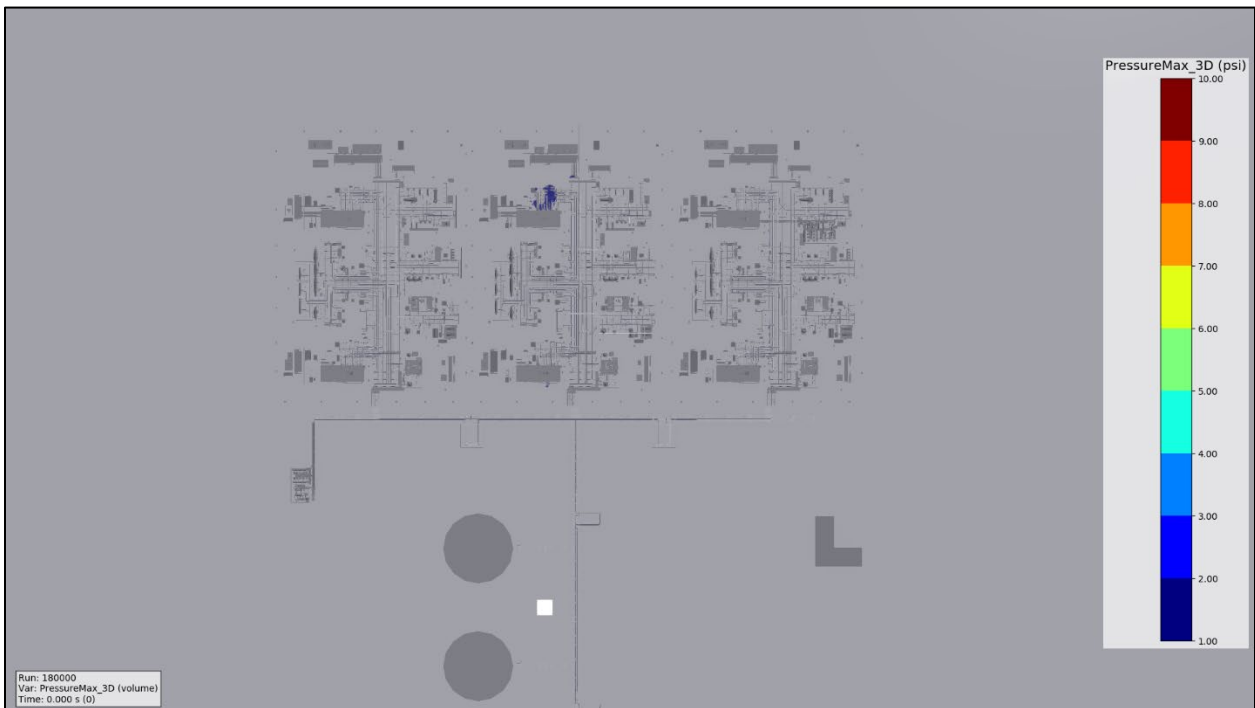


Figure 5-25. Overpressure hazard footprint for Propane Q9 at low wind.

	<b>Vapor Cloud Explosions at Nil Wind</b>	03904-RP-006
	PHMSA	Rev A
	Final Report	Page 101 of 213

The following observations can be made from the overpressure plots shown above:

- The largest VCE overpressure hazard footprints were obtained from the ignition of MR clouds. This was expected, since MR releases resulted in the largest ESC volumes, and the MR stream is considered a medium reactivity fuel.
- Among the three MR VCE scenarios modeled (respectively, Q9 at low wind conditions, Q9 at nil wind conditions, and Q8 at low wind conditions), the overpressure hazard footprints ranked in size according to the respective ESC volume, that is, the largest ESC volume (Q8 at low wind) yielded the largest hazard area, followed by the second highest ESC (Q9 at low wind) and then by the smallest (Q9 at nil wind).
- Since the largest MR ESCs occurred under low wind, for this facility design the inclusion of nil wind conditions in the siting study would not result in an increased overpressure hazard footprint.
- Unlike MR, the VCEs hazards from the LNG spill scenario increased at nil wind relative to low wind; this is consistent with the earlier observation that the ESC volumes increased at lower wind speeds. However, even for the larger VCE scenarios, the overpressure hazard footprint remained limited in size and the peak overpressure only reached approximately 4 psig; this is consistent with LNG (modeled as pure methane, as typically done in LNG facility siting studies) being a low reactivity fuel.
- The propane overpressure hazard footprint (based on Q9 at low wind) was also limited in size, and the peak overpressure only reached approximately 2 psig; this is due to the small ESC volume (4,000 m<sup>3</sup>) obtained during the dispersion simulations.

### 5.10 Consequence Modeling Summary

The results of modeling flammable dispersion and VCE using the PHMSA-approved CFD tool FLACS showed that:

- ESC volumes for flashing jets (without rainout) are affected more by wind direction (relative to the direction of the release) than wind speed: for releases 'with' the wind, higher wind speeds yield smaller ESCs, however, for releases 'into' the wind, higher wind speeds yield larger ESCs. Overall, the largest ESCs occurred under low wind (1-2 m/s) conditions.
- For flashing jets, the effect of wind direction tends to be reduced when the cloud is dispersing in large, congested areas (e.g., a liquefaction train). Overall, however, the largest ESCs still occurred under low wind (1-2 m/s) conditions.
- Evaporating liquid spills tend to yield increasing ESC volumes as wind speed decreases. This behavior is expected from highly stratified clouds, for which mixing occurs at the air/cloud interface and is driven by wind-induced turbulence and molecular diffusion.

	<b>Vapor Cloud Explosions at Nil Wind</b>	03904-RP-006
	PHMSA	Rev A
	Final Report	Page 102 of 213

- For an LNG facility, the largest spills are likely to be from LNG piping. Given the low reactivity of methane, even large ESC volumes are unlikely to result in overpressure footprints exceeding those of typical refrigerant releases.
- Spills of refrigerant are likely to be smaller in volume and are also likely to be contained within small areas (either by curbing or by conveyance to impoundments), therefore resulting in smaller ESCs.
- A scenario not included in this study and that should be considered, when relevant, is a spill of ethylene, which is a high reactivity fuel.
- The spills presented in this study evaluated the peak ESC within the entire plant, rather than within a PES. This is a very conservative because it neglects the inherent mitigation provided by placing impoundment areas remote from congested areas.
- The VCE potential for flashing jet release with rainout is difficult to predict, as the flashing jet and liquid pool ESCs trend in opposite directions.
  - The outcome will ultimately depend on the rainout fraction as well as the size of the liquid containment area (a larger area would lead to more evaporation and therefore a larger stratified cloud).

Overall, the results of the consequence modeling indicate that inclusion of nil wind conditions in an LNG facility siting study under current PHMSA regulations and guidance is not warranted.

	<b>Vapor Cloud Explosions at Nil Wind</b>	03904-RP-006
	PHMSA	Rev A
	Final Report	Page 103 of 213

## 6 Quantitative Risk Assessment

The last task in this study consisted of performing a quantitative risk assessment (QRA) on a generic LNG export facility, to evaluate how the explicit inclusion of nil-wind conditions (and their impact on hazard distances) in the calculations affects the overall risk associated with the facility.

### 6.1 QRA Methodology

A QRA is a formal and systematic approach to obtain a quantitative estimate of the risk to people from a given activity – in this case, the operation of an LNG facility. The approach to performing a QRA varies to some extent, depending on the type of operation being addressed as well as the entity performing the study. However, as described in a recent PHMSA-sponsored study [26], the key elements of a QRA methodology typically include:

- System description
- Hazard identification
- Frequency and consequence estimation
- Risk estimation
- Risk evaluation
- Risk mitigation (as necessary)

The following sections will review and discuss the various steps followed as part of this study, to evaluate the risk associated with a generic LNG facility with and without the explicit inclusion of nil-wind conditions.

### 6.2 Risk Tolerance Criteria

The first step in a QRA is to define how risk will be calculated and what risk levels are considered tolerable. Risk can be described in different ways, but the two most common measures are individual risk and societal risk. Individual risk is defined as the annual probability of harm (note that in this study 'harm' corresponds to 'fatality') at a particular location, assuming an individual is continuously present at that location. By performing this calculation at several locations, risk contours can be produced that can be overlaid upon a map of the area surrounding the site to determine compliance with the risk tolerance criteria. Societal risk factors in the possibility of multiple people being harmed and is defined as the relationship between the probability of an accident and the number of resulting casualties. Societal risk is typically presented as a curve in a log-log plot of cumulative frequency of occurrence versus number of fatalities.

Individual risk was identified as the best choice for this study, as risk contours can easily be compared and evaluated. The overall risk to an individual is calculated by adding together the risks of each individual event, each of which is given by combining the

consequences of the event with its probability of occurrence. The individual risk tolerability criteria for fatality used in this QRA were adopted from NFPA 59A-2019, Table 19.10.1(a) and are listed in Table 6-1.

Table 6-1: Criteria for tolerability of individual risk (IR) of fatality.

Tolerable Individual Risk (IR) [1/yr]		Permitted Developments
<b>Zone 1</b>	$IR > 5.0E-5$	All land uses under the control of the plant operator or subject to an approved legal agreement
<b>Zone 2</b>	$3.0E-7 \leq IR \leq 5.0E-5$	General public areas, excluding sensitive establishments (defined as institutional facilities that might be difficult to evacuate, such as schools, daycare facilities, hospitals, jails, etc.)
<b>Zone 3</b>	$IR < 3.0E-7$	No restrictions

### 6.3 System Description

Since the scope of this task is to inform PHMSA staff on the effect of including nil-wind conditions in a QRA, the object of the risk assessment was intentionally specified at a low level of detail so that the focus of the work would be on understanding the effect of nil-wind conditions rather than defining the minute details of a facility's design. Therefore, this study is based on what is typically defined as a "preliminary-design" QRA: the facility design information is limited to high-level schematics and material balances. The primary purpose of a preliminary-design QRA is to support site selection, with the expectation that the QRA will be revised at later stages of the design process.

The documents required to conduct this analysis include:

- Plot plan
- Process Flow Diagrams (PFDs)
- Heat and Material Balance Sheets (H&MBs)
- Site-specific weather data

Preparation of detailed engineering documents, such as detailed P&IDs and process datasheets, is outside the scope of the current project, therefore parts counts and process inventory volumes are estimated based on the experience of the project team.

#### 6.3.1 Facility Design

The generic large-scale LNG export facility selected for this study is the same previously described in Section 5.1.1 and used for the "Consequence Modeling" task.

	<b>Vapor Cloud Explosions at Nil Wind</b>	03904-RP-006
	PHMSA	Rev A
	Final Report	Page 105 of 213

#### 6.4 Hazard Identification

The typical hazard scenarios associated with LNG facilities include:

- Ignition of flammable gases, vapors or liquids, which may result in flash fires, jet fires, pool fires, or vapor cloud explosions.
- Exposure to toxic or asphyxiating gas or vapor clouds.
- Catastrophic rupture of pressure vessels, resulting in pressure vessel bursts (PVBs) or boiling liquid expanding vapor explosions (BLEVEs).

Following a loss of containment, different events may occur depending on what happens to the release, and each event has its own hazard footprint and probability of occurrence. In this study, only the following hazards were considered:

- Flash fires
- Jet fires
- Pool fires
- Vapor cloud explosions (VCEs)

Toxic and asphyxiation hazards were not included in the study, as the effects of nil-wind conditions on the dispersion of these clouds are the same as on the dispersion of flammable clouds and, therefore, are addressed through flash fires and VCEs. BLEVEs and PVBs were also not included in this study because their hazards are effectively independent of wind conditions, as will be discussed later regarding VCEs. The event tree for the flammable releases considered in this study is shown in Figure 6-1.

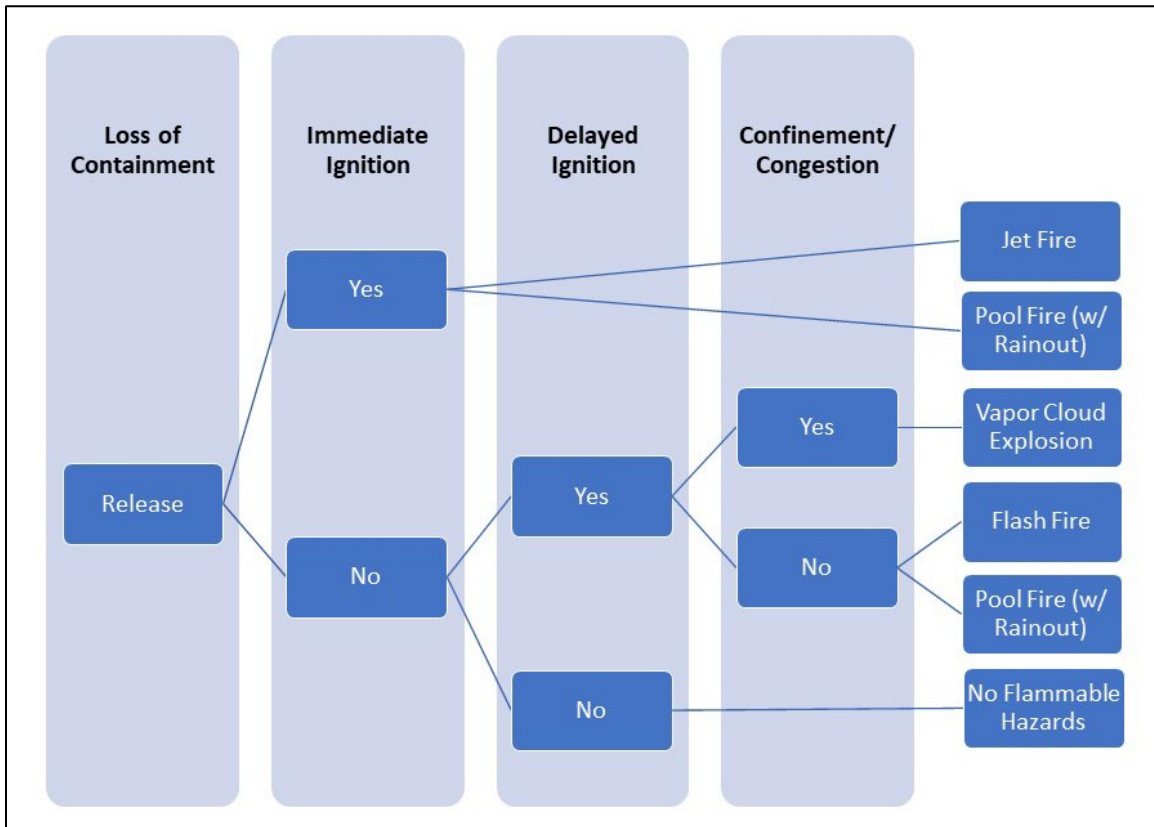


Figure 6-1: Event tree for a flammable release.

## 6.5 Hazard Endpoints

The QRA performed in this study evaluated the risk of an individual person sustaining a fatal injury; the hazard endpoints for fatality were selected consistent with section 19.8 of NFPA 59A-2019, as discussed in the following sections.

As common practice when evaluating individual risk contours, exposed persons were assumed to be outdoors.

### 6.5.1 Flammable Dispersion (Flash Fire)

Fatality of persons within an ignited flammable gas or vapor cloud may occur at fuel concentrations in air higher than or equal to the LFL for the stream being considered. Since a flammable cloud can be ignited instantaneously, it was assumed that any person located within the flammable cloud envelope at any time following a loss of containment event would be a fatality.

	<b>Vapor Cloud Explosions at Nil Wind</b>	03904-RP-006
	PHMSA	Rev A
	Final Report	Page 107 of 213

### 6.5.2 Jet Fires and Pool Fires

Individuals exposed to a fire outdoors were conservatively assumed to wear no personal protective equipment. Therefore, fatalities were assumed to occur for exposure to a radiant heat flux greater than or equal to 3,000 BTU/hr-ft<sup>2</sup> (9 kW/m<sup>2</sup>).

It should be noted that the selection of a radiant heat flux threshold rather than a thermal dose threshold implicitly assumes that the duration of exposure is sufficient to cause the specified damage. This is a reasonable assumption for outdoor exposure, since all releases considered in this study lasted over 60 seconds.

### 6.5.3 Vapor Cloud Explosions

Fatality due to VCEs for persons outdoor were assumed to occur when the peak overpressure at the person's location reached or exceeded 3 psig (0.207 barg).

### 6.5.4 Model Validation Factors

Model predictions of the consequences of hazardous events are generally affected by uncertainties, whether due to approximations made in defining the event or the environmental conditions, or due to the model's own capabilities. Therefore, model validation is a critical step in building confidence in the results of a hazard analysis; in fact, efforts to develop model validation databases and evaluation protocols for the different hazards associated with LNG facilities are ongoing (see PHMSA research project #798, "Develop an Evaluation Protocol for Non-LNG Release Hazards – Modeling" performed by BLUE, and a parallel effort by Sandia National Laboratories on pool and jet fire modeling). Completion of these model validation and evaluation efforts may result, as already occurred for flammable dispersion models, in the recognition that model validation factors (a.k.a. safety factors) should be applied to model outputs in order to more accurately predict hazard areas. However, any such efforts (beyond flammable dispersion) are still incomplete.

For this study, the application of validation factors would change the overall risk calculations (in general, a higher factor would result in longer hazard distances and therefore larger risk contours); however, it would not change the effect of nil-wind conditions: if nil-wind increases the hazard distance to LFL, it would also increase the hazard distance to ½-LFL, and vice versa. Therefore, to avoid speculation on which validation factors may be appropriate for different hazards, the consequence modeling performed for this study did not include any model validation factors.

## 6.6 Release Scenarios

The first step in identifying release scenarios is to define isolatable inventories. The boundaries of individual inventories were selected based on automatic or remotely-

controlled isolation valves, such that when the system is shut down following the detection of a loss of containment, the associated inventory of that section will be shut-in. Thus, when the ESD activates, the inventory available for release from a leak in that section is limited to the volume of fluid contained between the isolation valves. Each isolatable inventory was marked on the facility's PFDs. A list of the inventories is given in Table 6-2.

Table 6-2: Inventory List.

Inv #	Description	Stream	Phase
1	Feed Gas	NG	Vapor
2	Pipeline to pretreatment	NG	Vapor
3	Pretreatment	NG	Vapor
4	HHC	Heavies	Liquid
5	LNG Outlet	LNG	Liquid
6	LNG Rundown Header	LNG	Liquid
7	LNG Tank Fill	LNG	Liquid
8	Pump outlet	LNG	Liquid
9	BOG at the Tank	NG	Vapor
10	BOG to compressor	NG	Vapor
11	BOG compression	NG	Vapor
12	BOG to fuel gas	NG	Vapor
13	MR Compressor inlet	MR-1	Vapor
14	MR 1st Stage Outlet	MR-1	Vapor
15	MR compressor 2nd stage outlet	MR-1	Liquid
16	MR Liquid	MR-3	Liquid
17	MR vapor	MR-2	Vapor
18	Propane truck	Propane	Liquid
19	Propane tank outlet	Propane	Liquid
20	Propane to liquefier	Propane	Liquid
21	Butane truck	Butane	Liquid
22	Butane tank outlet	Butane	Liquid
23	Butane to liquefier	Butane	Liquid

Inv #	Description	Stream	Phase
24	Ethylene truck connection	Ethylene	Liquid
25	Ethylene liquid outlet	Ethylene	Liquid
26	Ethylene vapor	Ethylene	Vapor

## 6.7 Release Hole Sizes

For each inventory, different consequences are possible depending on the size and location of the release. Since larger releases generally yield worse consequences but are less likely to occur than smaller ones, it is important to consider release scenarios across the full range of potential hole sizes, while also factoring in their respective probabilities of occurrence. The typical approach consists of subdividing the range of potential hole sizes into a discrete set of ranges for the purpose of estimating leak frequencies.

For each component within an inventory, the probability  $f_{d1-d2}$  of a release hole size within each of the discrete ranges is calculated from the total failure rate for that component, based on a log-normal distribution (as discussed in OGP report 434-01 [27]):

$$P(d) = C D^m + B$$

$$f_{d1-d2} = P(d2) - P(d1)$$

This QRA was conducted in accordance with the approach most frequently followed in the industry, which considers five (5) hole size ranges, as shown in Table 6-3. For each range, the maximum line diameter within the inventory was selected as the representative hole size. This approach is the most conservative possible (for reference, the most common approach among risk practitioners is to use the geometric mean diameter, as recommended by OGP 434-01) but it was chosen because it increases the number of scenarios likely to be affected by nil-wind conditions.

Table 6-3: Hole sizes for QRA.

Category	Hole Size Range	Representative Hole Size
<b>Pinhole (P)</b>	0.04 – 0.12 in. (1 – 3 mm)	0.12 in. (3 mm)
<b>Small (S)</b>	0.12 – 0.4 in. (3 – 10 mm)	0.4 in. (10 mm)
<b>Medium (M)</b>	0.4 – 2 in. (10 – 50 mm)	2 in. (50 mm)
<b>Large (L)</b>	2 – 6 in. (50 – 150 mm)	6 in. (150 mm)
<b>Rupture (R)</b>	> 6 in. (> 150 mm)	Max. diameter

	<b>Vapor Cloud Explosions at Nil Wind</b>	03904-RP-006
	PHMSA	Rev A
	Final Report	Page 110 of 213

## 6.8 Other Release Parameters

Other release parameters specified for this study include:

- All releases were modeled as horizontal and non-impacted.
- The release elevation was selected based on the 3D model of the facility.
- All releases were allowed to continue for 10 minutes at a constant flow (unless the available inventory was depleted before 10 minutes).

## 6.9 Parts Count

As indicated in section 6.3.1 and shown in Appendix A, the generic LNG facility's design is limited to a plot plan, PFDs, and H&MBs. Therefore, the parts count for each inventory is an early design estimate; if the QRA were performed for the siting of an actual facility, it would have to be revised and updated as the design develops to include P&IDs and more detailed process and layout information.

The early design estimates are considered adequate for the purpose of this study, as they result in failure rate distributions consistent with those observed in more advanced design QRAs.

## 6.10 Failure Rates

Several different databases are available that contain failure rate data for piping, fittings and equipment (e.g., NFPA 59A, OGP 434-01, HSE FRED). To date, no single database has emerged as the consensus reference for LNG facility QRAs. The failure rate data in OGP 434-01, 2019 edition, was used in this study due to the flexibility afforded by the use of a log-normal failure rate distribution. The OGP database was developed primarily from offshore oil and gas incidents and is therefore considered generally conservative when applied to LNG facilities, with the possible exception of components such as flange gaskets, which are underestimated relative to observed LNG facility frequencies (as compared, for example, to the total gasket failure rate in Table 19.6.1 of NFPA 59A-2019); however, general consensus among risk practitioners is that the underestimation in OGP 434-01 applies to the smaller hole size ranges (i.e., pinholes to medium holes, according to the discretization provided in Table 6-3). The effect of increasing the frequency of smaller holes, relative to large holes or full ruptures, would further confirm the findings of this study, as discussed in section 6.19.

For each inventory and hole size range defined in the previous sections, the probability of failure was calculated by applying to the inventory's parts count the individual failure rate values published in OGP 434-01. The failure frequencies are listed in Table 6-4.

Table 6-4: Failure rate table for the facility's inventories.

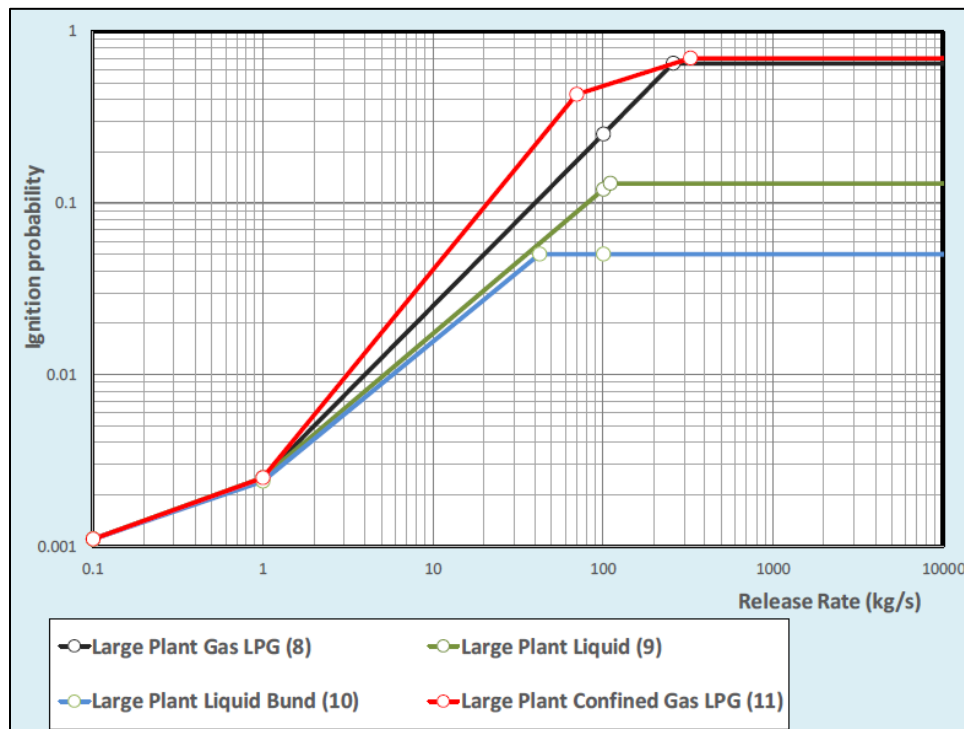
Inventory #	P	S	M	L	R
1	1.00E-02	3.47E-03	1.19E-03	1.89E-04	1.20E-04
2	1.84E-02	5.99E-03	1.92E-03	2.88E-04	1.28E-04
3	5.66E-02	1.95E-02	6.85E-03	1.16E-03	6.95E-04
4	3.53E-03	1.16E-03	3.65E-04	5.58E-05	3.03E-05
5	1.46E-02	4.40E-03	1.33E-03	1.69E-04	9.17E-05
6	2.60E-02	8.44E-03	2.72E-03	4.04E-04	1.84E-04
7	4.34E-03	1.38E-03	4.34E-04	4.28E-05	7.78E-05
8	5.50E-04	1.92E-04	6.80E-05	7.85E-06	7.83E-06
9	1.29E-03	4.18E-04	1.37E-04	2.12E-05	1.34E-05
10	1.19E-02	3.83E-03	1.24E-03	1.86E-04	8.27E-05
11	2.98E-02	1.01E-02	3.40E-03	5.54E-04	5.83E-04
12	6.31E-03	2.09E-03	6.59E-04	1.02E-04	4.66E-05
13	5.90E-03	1.97E-03	6.70E-04	1.08E-04	6.88E-05
14	1.19E-02	3.68E-03	1.22E-03	2.01E-04	1.29E-04
15	1.12E-02	3.37E-03	1.09E-03	1.73E-04	1.01E-04
16	4.07E-03	1.42E-03	4.83E-04	8.15E-05	5.31E-05
17	3.69E-03	1.19E-03	3.87E-04	5.42E-05	2.88E-05
18	1.44E-05	4.66E-06	2.08E-03	2.08E-04	0.00E+00
19	7.07E-04	3.04E-04	1.33E-04	5.83E-05	0.00E+00
20	8.81E-03	2.87E-03	8.96E-04	1.44E-04	5.55E-05
21	1.44E-05	4.66E-06	2.08E-03	2.08E-04	0.00E+00
22	1.15E-03	4.36E-04	1.71E-04	7.55E-05	0.00E+00
23	8.81E-03	2.87E-03	8.96E-04	1.44E-04	5.55E-05
24	1.66E-05	5.32E-06	2.08E-03	2.08E-04	0.00E+00
25	1.19E-03	4.49E-04	1.75E-04	7.64E-05	0.00E+00

Inventory #	P	S	M	L	R
<b>26</b>	9.37E-03	3.32E-03	1.20E-03	3.48E-04	5.65E-05

### 6.11 Ignition Probabilities

Once a flammable stream is released, different hazards are possible depending on whether the release is ignited or not. In order to quantify the risk associated with ignited and unignited releases, it is necessary to estimate the likelihood of ignition. A flammable release can be ignited immediately (i.e., upon release or near the release location) or after some delay (i.e., after the resulting flammable cloud had a chance to travel away from the release location).

The probability of ignition of a flammable release was calculated using the UKOOA model, as summarized in OGP report 434-06, "Ignition Probabilities" [28], which provides a set of 'look-up' correlations for representative facilities that allow to estimate the ignition probability of a scenario based on its release rate. Figure 6-2 provides a graphical representation of the ignition probability correlations for a few facility types, including the one identified as representative of the facility (Scenario No. 9, "Large Plant Liquid").



	<b>Vapor Cloud Explosions at Nil Wind</b>	03904-RP-006
	PHMSA	Rev A
	Final Report	Page 113 of 213

Figure 6-2: UKOAA model for ignition probabilities.

The total probability of ignition was then subdivided into a 30% probability of immediate ignition (jet fire or pool fire) and 70% probability of delayed ignition (flash fire or VCE), consistent with common practice and published work [5]. It should be noted that different ignition probability models or assumptions could be applied to this study without invalidating the results.

### 6.12 Potential Explosion Sites

VCE overpressures may only occur if a flammable cloud reaches and is ignited within a region with sufficient congestion (i.e., repeated obstacles) and/or confinement (i.e., walls, roofs or barriers) to affect the flame propagation. Regions that can generate damaging VCE overpressures are defined as potential explosion sites (PES). The QRA study used the same PESs previously identified in Section 5.6.1:

- Each of the three liquefaction trains; and
- The refrigerant storage area.

Each PES is characterized by the following parameters:

- Volume of the PES
- Obstacle density – i.e., congestion level (this can be low/medium/high)
- Flame expansion – describes the number of directions in which the flame can expand (the value can be between 1 and 3, with lower numbers corresponding to higher confinement and, therefore, higher overpressures)

Additionally, for each VCE scenario, the following parameters characterize the flammable cloud that is ignited:

- Fuel composition
- Fuel reactivity
- Flammable mass within the PES (note: the fuel/air mixture in VCE modeling is often assumed to be at stoichiometric conditions, whereas ‘real’ clouds are heterogeneous, therefore an Equivalent Stoichiometric Cloud mass – or volume – needs to be calculated)

### 6.13 Ambient Conditions

Risk calculations require ambient conditions to be defined, since the hazard footprint from each release scenario depends to some extent on the wind speed and direction and, to a lesser extent, on the ambient temperature. The task is even more critical in this study, which is aimed at evaluating the effect of ambient conditions on overall risk. Weather data from an unspecified location was used for the calculations in this report;

	<b>Vapor Cloud Explosions at Nil Wind</b>	03904-RP-006
	PHMSA	Rev A
	Final Report	Page 114 of 213

the ambient temperature was set to an annual average of 70°F, relative humidity was set to 50%, and the distribution of wind speed and direction was based on hourly data.

Hourly wind speed data was discretized into four (4) bins, as follows:

- High wind speeds ( $U \geq 7$  m/s) were represented by “D8” conditions (8 m/s wind speed and D stability)
- Medium wind speeds ( $3 \text{ m/s} \leq U < 7$  m/s) were represented by “E4” conditions (4 m/s wind speed and E stability)
- Low wind speeds ( $1 \text{ m/s} \leq U < 3$  m/s) were represented by “F2” conditions (2 m/s wind speed and F stability)
- Nil-wind speeds ( $U < 1$  m/s) were represented by the no-wind “X0” condition (0 m/s wind speed)

The wind rose for the four discretized wind categories is shown in Figure 6-3.

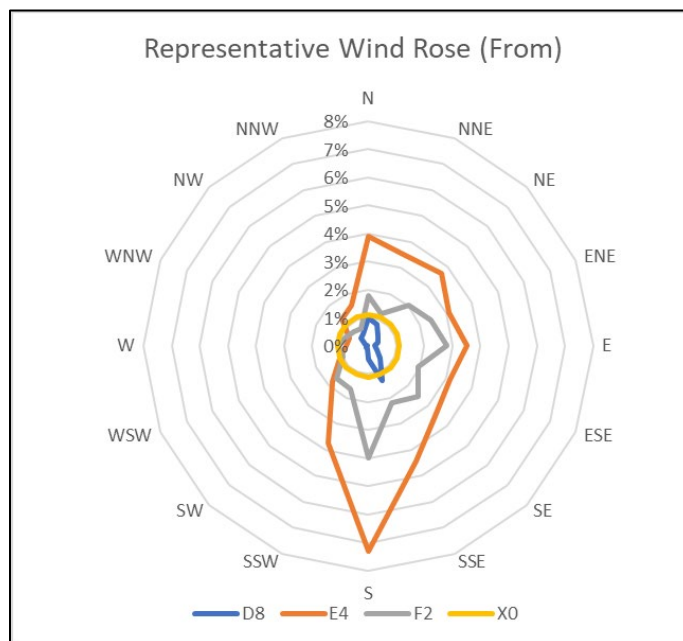


Figure 6-3: Discretized wind rose for the generic LNG facility.

As will be described later, the “traditional” QRA calculations will combine the X0 and F2 categories by adding their respective frequencies and assuming the consequences calculated under F2 conditions to be representative of both low- and nil-wind conditions, whereas the “nil-wind” QRA will calculate hazards and risk under nil-wind conditions separately.

	<b>Vapor Cloud Explosions at Nil Wind</b>	03904-RP-006
	PHMSA	Rev A
	Final Report	Page 115 of 213

## 6.14 Consequence Modeling Methodology

As previously discussed, integral models have a lower wind speed limit below which the equations they apply cannot be used. The lower bound on wind speed is generally 1.0 m/s, which makes integral models not suitable for modeling vapor dispersion under nil-wind conditions. CFD models, instead, are not affected by such limitation and can model dispersion in wind speeds down to zero. Therefore, hazard consequences for the X0 category can only be calculated using CFD tools, whereas other wind categories (e.g., F2, E4, etc.) can be calculated using either CFD or integral models.

This limitation posed the question of how the consequence modeling for the LNG facility QRAs in this study should be performed: given the large number of scenarios to be modeled, expediency would dictate the use of integral models for categories F2 and higher, and CFD models for category X0; however, the use of different models for would introduce a variability in the results which could mask, at least partially, the effect of wind speed. Therefore, the only reasonable option to minimize uncertainty in the comparison of results is to use the same model across all wind categories; additionally, all modeling parameters (inputs, boundary conditions, discretization, etc.) with the exception of wind speed and stability should be kept uniform across each scenario.

The following subsections discuss the model chosen to calculate each type of hazard.

### 6.14.1 Dispersion

Based on the results of Task 5, "Consequence Modeling", nil-wind conditions are known to have an impact on the dispersion hazard distances of flammable releases, at least for a subset of possible scenarios. Therefore, it is important for dispersion hazards to be quantified under nil-wind conditions and that, as discussed above, requires CFD modeling.

The results of a dispersion simulation using CFD are affected by several parameters besides wind speed, such as the location and direction of the release, the presence and characteristics of obstacles and obstructions, and the wind direction relative to the release. Taking all these parameters into consideration would rapidly render the modeling effort unmanageable within the timeframe of this project. Therefore, the decision was made to utilize the CFD model (FLACS)<sup>8</sup> as a surrogate of the integral model (Phast) which is frequently used in QRAs, which led to the following simplifications:

- Only releases in the direction of the wind were modeled;

---

<sup>8</sup> Currently, FLACS is the only CFD model and Phast the only integral model approved by PHMSA for LNG vapor dispersion.

	<b>Vapor Cloud Explosions at Nil Wind</b>	03904-RP-006
	PHMSA	Rev A
	Final Report	Page 116 of 213

- No obstacles or obstructions were included in the 3D model geometry.

#### 6.14.2 Jet Fires

Due to the high momentum and turbulence of ignited jet releases, the thermal radiation hazard distances from jet fires are generally only lightly affected by wind speed (at least when the wind speed is aligned with the jet release). Therefore, modeling jet fire hazards under nil-wind conditions is not considered necessary, as the results under low wind conditions provide a good approximation. Hence, in this study the nil-wind hazards from jet fires were calculated using the integral model (Phast) at the lowest allowable wind speed (i.e., 1 m/s).

#### 6.14.3 Pool Fires

Thermal radiation hazards from pool fires are also marginally dependent on wind speed, in the low- to nil- wind speed range, due to the minimal flame tilt that occurs at those speeds. Therefore, modeling pool fire hazards under nil-wind conditions is not considered necessary, as the results under low wind conditions provide a good approximation. Hence, in this study the nil-wind hazards from pool fires were calculated using the integral model (Phast)<sup>9</sup> at the lowest allowable wind speed (i.e., 1 m/s).

#### 6.14.4 Vapor Cloud Explosions

Overpressure hazards from vapor cloud explosions are effectively independent of wind speed, given the much higher propagation velocity of a blast wave. However, the size and distribution of the flammable cloud which may originate a VCE is likely to be affected by wind speed (as discussed in Section 6.14.1). Therefore, nil-wind VCE scenarios were treated as follows:

- The flammable vapor cloud dispersion was modeled at nil-wind using FLACS, same as other dispersion scenarios, to determine the flammable cloud volume within a PES. Note that the flammable cloud volume was calculated using the “Q9” method discussed in Task 5, to obtain an equivalent stoichiometric cloud (ESC).

---

<sup>9</sup> Phast is not currently approved by PHMSA as a model for pool fire hazards, but it is widely used in the oil and gas industry (as well as on LNG projects, for non-siting related matters). The PHMSA-approved LNGFIRE3 model could be used in this case, and it allows calculation under nil-wind conditions, however it also has important limitations such as only being applicable to LNG fires. This study used Phast primarily for consistency of handling inputs and outputs within the QRA; as described in this section, the effect of nil-wind on pool fires is largely negligible, therefore the choice of tool is not critical.

	<b>Vapor Cloud Explosions at Nil Wind</b>	03904-RP-006
	PHMSA	Rev A
	Final Report	Page 117 of 213

- The overpressure hazard distances from a PES, for the ESC volume obtained using CFD, were calculated using Phast (more specifically, the Baker-Strehlow-Tang explosion model) at the lowest allowable wind speed.

### 6.15 Consequence Modeling Results

The combination of inventories (26), hole sizes (up to 5), and wind speed categories (4) yielded a total of 496 distinct cases to be modeled for each type of hazard. As discussed in the previous section, jet and pool fire hazards are only marginally affected by wind speed (in the low- to nil-wind range), therefore, the review of modeling results in this section focuses on flammable dispersion and discusses both hazard distances as well as flammable cloud volumes (which affect overpressure hazards).

All dispersion simulations were performed using FLACS v.21.0<sup>10</sup> and all modeling assumptions (computational domain, grid refinement and stretching, CFL numbers, etc.) were specified in accordance with FLACS modeling guidelines and maintained uniform across all wind speeds wherever possible. Each release was assumed to continue for 10 minutes at the initial flow rate (capped by the pump runout flow, where applicable), unless the available inventory was depleted in less than 10 minutes. The flammable clouds were allowed to disperse until reaching the maximum dimensions and clearly beginning to recede, except in cases where a steady state was achieved before the end of the release therefore the simulation was stopped.

As previously discussed in Section 6.5.1, the hazard endpoint for the flammable dispersion simulations was set to the LFL for each released stream. No model validation factor was applied, for the sole purpose of limiting the computational domains and the computational time required for the modeling. Since the scope of this study was to compare QRA results with and without nil-wind conditions, the results of the study are considered independent of the actual endpoint chosen.

A summary of the flammable dispersion modeling results is given in Table 6-5 and Table 6-6, respectively, for the maximum distances to LFL and the maximum ESC volumes. The ESC volumes are presented, instead of the hazard distances to the overpressure endpoint, because they are not dependent on the size of the PES and, therefore, can provide a more general comparison. For example, if a hypothetical scenario yields a 10,000 m<sup>3</sup> ESC under low wind conditions and a 12,000 m<sup>3</sup> ESC under nil wind, but the PES

---

<sup>10</sup> The version of FLACS currently approved by PHMSA is 9.1; however, this single-processor version was considered inadequate to perform the large number of simulations included in this study within the project timeframe, therefore, the current version of FLACS was used. Since the same version was used for all simulations, any model uncertainties would have affected both nil-wind and low- or higher-wind cases, thus canceling out during the comparison of results.

volume is only 6,000 m<sup>3</sup>, the two conditions would result in the same hazard footprints and the 'extra' flammable volume outside the PES would be irrelevant; however, if a larger PES (e.g., 15,000 m<sup>3</sup>) is considered, nil wind conditions would result in a larger hazard footprint. Since, for a given PES, the overpressure hazard footprint increases with the volume of the cloud being ignited, a larger ESC volume inside a PES corresponds to a larger overpressure hazard footprint.

Note that all values in the tables were normalized with respect to the F2 results for each scenario, as presenting actual data might distract the reader from the real purpose of the tables, which is to establish how many, and which scenarios yield increased hazards when nil-wind conditions are taken into account. Also, any cases for which the hazard distance was less than 10 m (approximately 30 ft) or the ESC volume was less than 28 m<sup>3</sup> (approximately 1,000 ft<sup>3</sup>) were discarded (shown as "-" in the tables) because of their negligible consequences. Finally, Table 6-6 includes two sets of values in each cell: the first value represents the normalized ESC volumes based on the Q9 parameter, while the second value (in parentheses) represents the normalized volume based on Q8; consistent with the discussion in the Task 5 report, the Q9 parameter is considered more appropriate for onshore facilities with adequate ventilation, while the Q8 results are provided as a sensitivity case.

Table 6-5: Dispersion modeling results – distance to LFL (normalized w.r.t. F2).

Inventory	Hole Size [mm]	X0	E4	D8
1	3	-	-	-
1	10	-	-	-
1	50	100%	100%	103%
1	150	101%	101%	101%
1	1219	105%	104%	102%
2	3	-	-	-
2	10	-	-	-
2	50	107%	100%	103%
2	150	102%	100%	99%
2	711	103%	100%	99%
3	3	-	-	-
3	10	-	-	-
3	50	105%	100%	100%
3	150	104%	101%	100%
3	711	103%	100%	106%

Inventory	Hole Size [mm]	X0	E4	D8
4	3	-	-	-
4	10	-	-	-
4	50	97%	105%	106%
4	150	100%	105%	111%
4	203	93%	108%	112%
5	3	-	-	-
5	10	-	-	-
5	50	101%	103%	108%
5	150	58%	142%	101%
5	355	101%	81%	67%
6	3	-	-	-
6	10	-	-	-
6	50	117%	106%	114%
6	150	86%	111%	112%
6	609	99%	90%	84%
7	3	-	-	-
7	10	-	-	-
7	50	81%	115%	95%
7	150	101%	106%	107%
7	609	53%	134%	122%
8	3	-	-	-
8	10	-	-	-
8	50	83%	109%	97%
8	150	99%	108%	108%
8	914	81%	123%	117%
9	3	-	-	-
9	10	-	-	-
9	50	40%	36%	31%
9	150	49%	63%	58%
9	609	65%	125%	114%

Inventory	Hole Size [mm]	X0	E4	D8
10	3	-	-	-
10	10	-	-	-
10	50	-	-	-
10	150	100%	100%	100%
10	609	102%	100%	97%
11	3	-	-	-
11	10	-	-	-
11	50	-	-	-
11	150	107%	100%	100%
11	609	100%	101%	101%
12	3	-	-	-
12	10	-	-	-
12	50	108%	100%	100%
12	150	103%	97%	100%
12	254	82%	78%	78%
13	3	-	-	-
13	10	-	-	-
13	50	-	-	-
13	150	107%	97%	100%
13	1828	100%	101%	107%
14	3	-	-	-
14	10	-	-	-
14	50	104%	100%	104%
14	150	104%	101%	107%
14	1727	112%	102%	108%
15	3	-	-	-
15	10	108%	100%	100%
15	50	101%	101%	106%
15	150	70%	83%	95%
15	914	116%	83%	94%

Inventory	Hole Size [mm]	X0	E4	D8
16	3	-	-	-
16	10	-	-	-
16	50	-	-	-
16	150	109%	104%	108%
16	914	90%	113%	108%
17	3	-	-	-
17	10	-	-	-
17	50	100%	100%	100%
17	150	103%	97%	100%
17	609	102%	100%	105%
18	3	-	-	-
18	10	-	-	-
18	50	116%	100%	102%
18	76	106%	104%	112%
19	3	-	-	-
19	10	-	-	-
19	50	116%	100%	102%
19	76	106%	104%	112%
20	3	-	-	-
20	10	107%	100%	86%
20	50	92%	100%	67%
20	150	65%	105%	83%
20	203	53%	115%	86%
21	3	-	-	-
21	10	100%	93%	86%
21	50	95%	108%	104%
21	76	102%	110%	119%
22	3	-	-	-
22	10	100%	93%	86%
22	50	87%	98%	94%

Inventory	Hole Size [mm]	X0	E4	D8
22	76	102%	109%	119%
23	3	-	-	-
23	10	108%	100%	100%
23	50	103%	109%	99%
23	150	71%	123%	96%
23	203	48%	115%	95%
24	3	-	-	-
24	10	100%	100%	94%
24	50	101%	105%	113%
24	76	102%	106%	117%
25	3	-	-	-
25	10	100%	100%	94%
25	50	101%	105%	113%
25	76	104%	106%	115%
26	3	-	-	-
26	10	-	-	-
26	50	-	-	-
26	150	104%	104%	100%
26	203	100%	100%	100%

Table 6-6: Dispersion modeling results – ESC volume (nomalized w.r.t. F2).

Inventory	Hole Size [mm]	X0	E4	D8
1	3	-	-	-
1	10	-	-	-
1	50	103%	97%	85%
1	150	108%	93%	78%
1	1219	113%	96%	78%
2	3	-	-	-
2	10	-	-	-
2	50	104%	94%	82%



Inventory	Hole Size [mm]	X0	E4	D8
2	150	112%	91%	72%
2	711	108%	91%	73%
3	3	-	-	-
3	10	-	-	-
3	50	103%	97%	83%
3	150	108%	94%	78%
3	711	105%	94%	94%
4	3	-	-	-
4	10	-	-	-
4	50	105%	99%	91%
4	150	108%	94%	81%
4	203	109%	94%	82%
5	3	-	-	-
5	10	-	-	-
5	50	108%	95%	76%
5	150	131%	87%	29%
5	355	987%	34%	11%
6	3	-	-	-
6	10	-	-	-
6	50	178%	90%	53%
6	150	117%	89%	61%
6	609	922%	41%	25%
7	3	-	-	-
7	10	-	-	-
7	50	111%	89%	49%
7	150	108%	81%	45%
7	609	374%	89%	68%
8	3	-	-	-
8	10	-	-	-
8	50	116%	89%	51%

Inventory	Hole Size [mm]	X0	E4	D8
8	150	108%	81%	47%
8	914	523%	95%	69%
9	3	-	-	-
9	10	-	-	-
9	50	492%	17%	11%
9	150	524%	61%	19%
9	609	1110%	92%	64%
10	3	-	-	-
10	10	-	-	-
10	50	-	-	-
10	150	103%	94%	75%
10	609	116%	87%	63%
11	3	-	-	-
11	10	-	-	-
11	50	-	-	-
11	150	104%	96%	78%
11	609	111%	92%	73%
12	3	-	-	-
12	10	-	-	-
12	50	-	-	-
12	150	104%	96%	84%
12	254	87%	77%	67%
13	3	-	-	-
13	10	-	-	-
13	50	-	-	-
13	150	108%	91%	83%
13	1828	111%	92%	90%
14	3	-	-	-
14	10	-	-	-
14	50	110%	94%	92%

Inventory	Hole Size [mm]	X0	E4	D8
14	150	109%	93%	90%
14	1727	110%	92%	88%
15	3	-	-	-
15	10	-	-	-
15	50	101%	98%	97%
15	150	140%	91%	75%
15	914	924%	48%	41%
16	3	-	-	-
16	10	-	-	-
16	50	125%	89%	73%
16	150	111%	92%	77%
16	914	120%	89%	82%
17	3	-	-	-
17	10	-	-	-
17	50	-	-	-
17	150	105%	98%	92%
17	609	103%	96%	97%
18	3	-	-	-
18	10	-	-	-
18	50	139%	98%	91%
18	76	103%	96%	85%
19	3	-	-	-
19	10	-	-	-
19	50	139%	98%	91%
19	76	103%	96%	85%
20	3	-	-	-
20	10	-	-	-
20	50	128%	70%	15%
20	150	306%	80%	43%
20	203	309%	90%	49%

Inventory	Hole Size [mm]	X0	E4	D8
21	3	-	-	-
21	10	-	-	-
21	50	91%	97%	65%
21	76	99%	92%	71%
22	3	-	-	-
22	10	-	-	-
22	50	56%	59%	40%
22	76	99%	92%	71%
23	3	-	-	-
23	10	-	-	-
23	50	113%	69%	38%
23	150	128%	92%	45%
23	203	96%	92%	48%
24	3	-	-	-
24	10	-	-	-
24	50	103%	97%	84%
24	76	104%	97%	83%
25	3	-	-	-
25	10	-	-	-
25	50	103%	97%	84%
25	76	108%	96%	82%
26	3	-	-	-
26	10	-	-	-
26	50	-	-	-
26	150	112%	94%	76%
26	203	109%	91%	72%

Figure 6-4 through Figure 6-6 summarize the tabulated data as histogram plots showing the frequency of cases grouped by the percent worsening of the respective consequences.

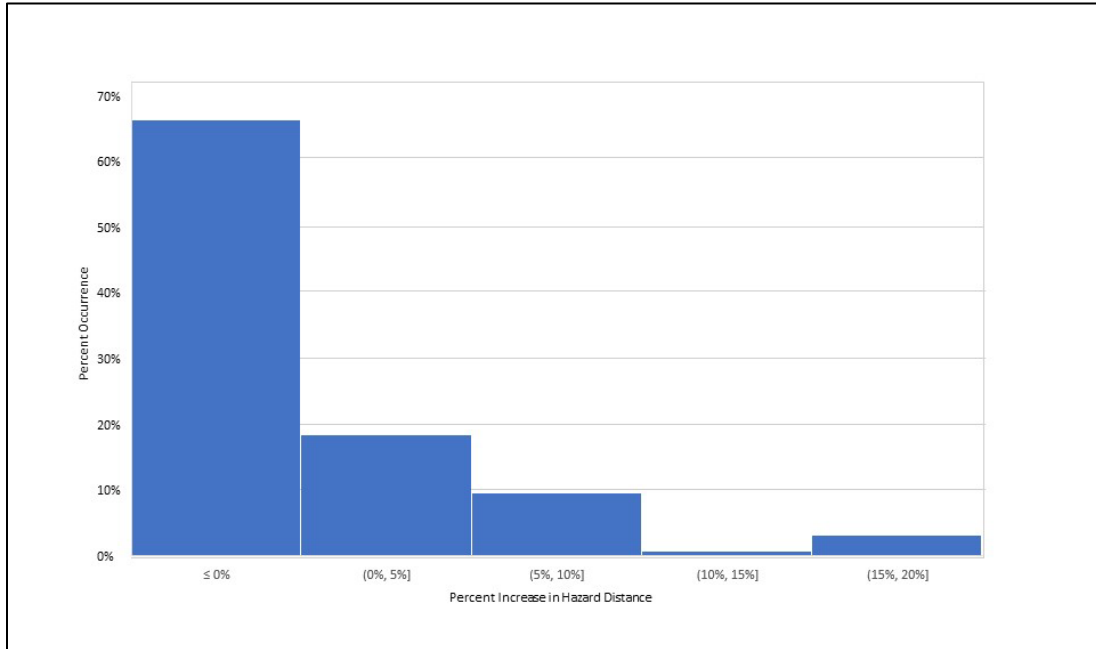


Figure 6-4: Dispersion modeling results – effect of nil-wind on distance to LFL.

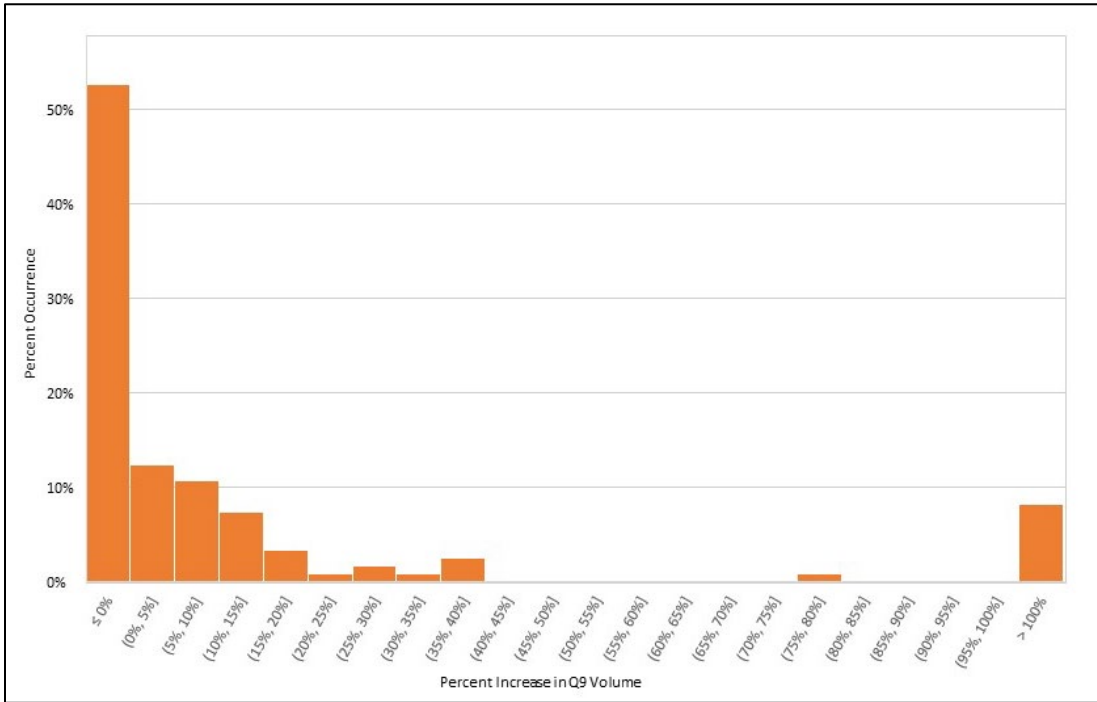


Figure 6-5: Dispersion modeling results – effect of nil-wind on Q9 volume.

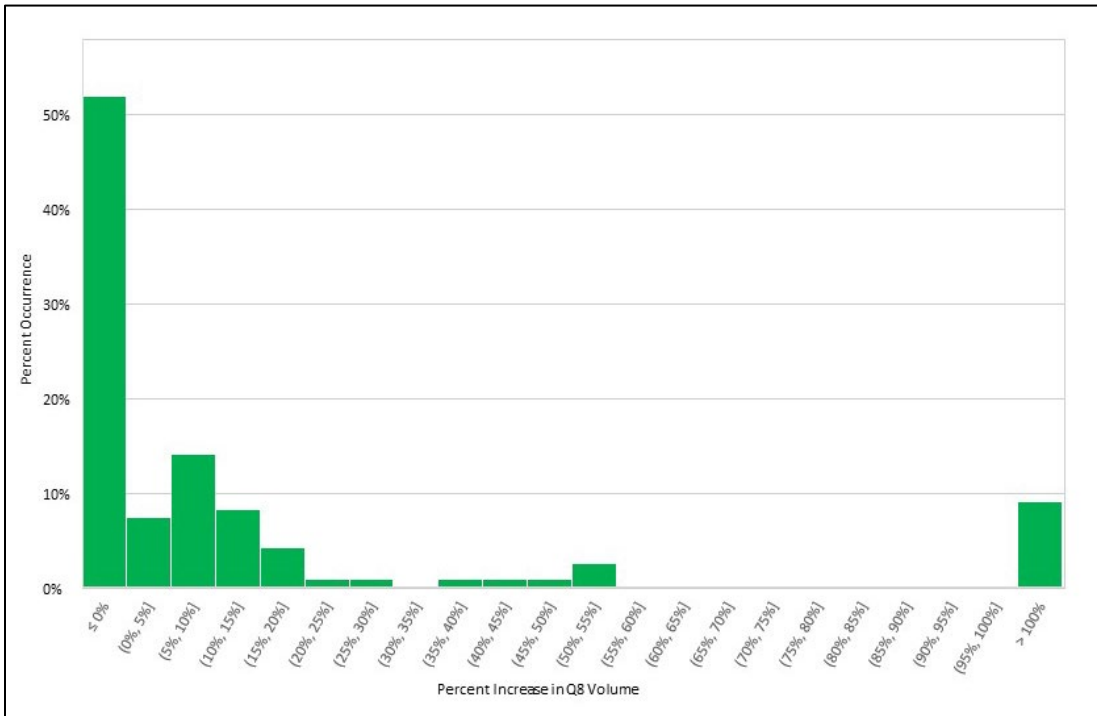


Figure 6-6: Dispersion modeling results – effect of nil-wind on Q8 volume.

	<b>Vapor Cloud Explosions at Nil Wind</b>	03904-RP-006
	PHMSA	Rev A
	Final Report	Page 129 of 213

## 6.16 Consequence Modeling Discussion

The plots in Figure 6-4 through Figure 6-6 show a prevalence of cases – approximately 66% and 52%, respectively, for distance to LFL and ESC volume – in which hazards under nil-wind are equal to or less than under low-wind conditions, while approximately 4% and 25% of cases resulted in the respective outcomes being worsened by more than 10%. The ESC volume trends vary only slightly if Q8 is considered instead of Q9.

As shown in Table 6-5 and Table 6-6, the scenarios resulting in the largest hazard increases consist primarily of large-bore releases (6" diameter hole or full line rupture), involving heavy streams (e.g., propane or mixed refrigerant) or low equilibrium pressures (due to flow-limited conditions); several of these scenarios include liquid rainout and pool formation. Pool spreading and vaporization from liquid rainout was conservatively modeled as unconfined by curbs or impoundments, thereby resulting in the largest possible low-momentum vapor clouds. Conversely, the scenarios resulting in the smallest hazard increases (or even in reduction of the hazards) consist primarily of high-pressure releases of lighter streams (LNG or natural gas), where the momentum and turbulence of the release drive the mixing and dilution of the flammable cloud. It should also be noted that the smaller scenarios (i.e., 'pinholes' and 'small' releases as well as, in some instances, 'medium' releases) were found to have negligible consequences from a facility siting standpoint (i.e., the distance to LFL was less than approximately 30 ft and/or the maximum ESC volume was less than approximately 1,000 ft<sup>3</sup>), therefore, the effect of nil-wind conditions on these scenarios was considered irrelevant.

Table 6-6 shows that a few scenarios resulted in greater than 100% increases in the ESC volume. These scenarios corresponded to large hole diameters or full-bore ruptures of large diameter lines, with liquid streams (LNG in most cases) pumped through; therefore, in each case, a low equilibrium pressure was achieved, and the release resulted in significant liquid rainout. As discussed earlier in this project, the heavy, low-momentum clouds produced by the vaporization of liquid pools require atmospheric turbulence to mix and dissipate, therefore, it is reasonable to expect longer dispersion distances and larger flammable volumes under nil-wind conditions.

To exemplify the effect of nil-wind conditions on different types of releases, Figure 6-7 through Figure 6-9 compare the flammable cloud contours (between LFL and 3\*LFL) for three different releases:

- A release of natural gas from a line rupture (24-in hole), at low pressure (1 psig).
- A release of liquefied propane from a medium diameter hole (2-in), at high pressure (120 psig).
- A release of liquefied propane from a line rupture (8-in hole), depressurized due to flow-limited conditions.

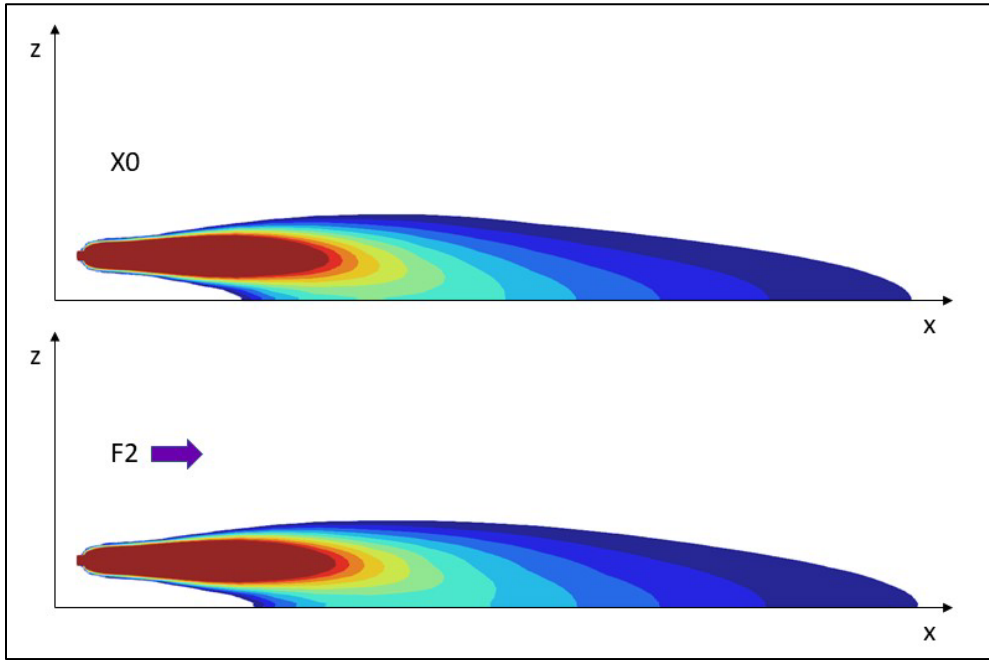


Figure 6-7: Side view of flammable cloud at maximum extent for inventory 10 (gas to BOG compressor), full rupture of 24-in line: X0 wind (top) vs. F2 wind (bottom).

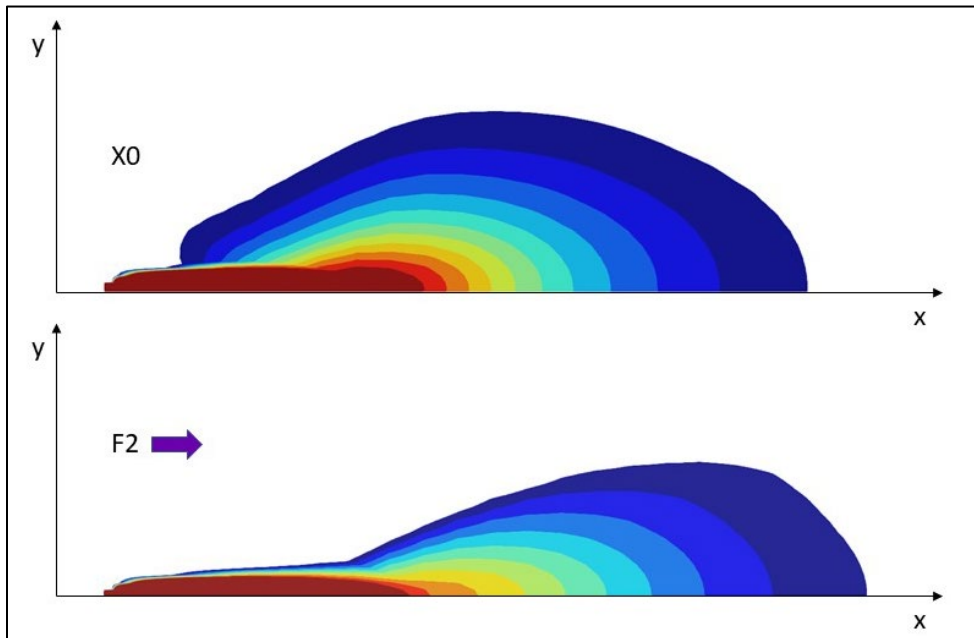


Figure 6-8: Plan view of flammable cloud at maximum extent for inventory 20 (propane makeup line), 2-in release: X0 wind (top) vs. F2 wind (bottom).

	<b>Vapor Cloud Explosions at Nil Wind</b>	03904-RP-006
	PHMSA	Rev A
	Final Report	Page 131 of 213

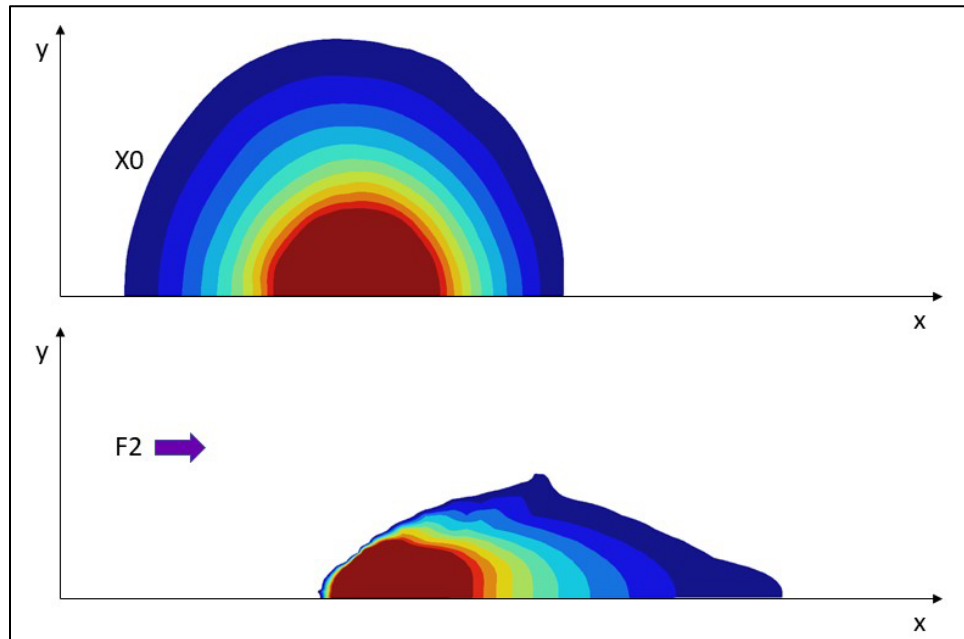


Figure 6-9: Plan view of flammable cloud at maximum extent for inventory 20 (propane makeup line), full rupture of 8-in line: X0 wind (top) vs. F2 wind (bottom).

As stated earlier, the mixing of lighter jet releases is driven primarily by the turbulence of the jet itself and by the momentum-driven entrainment of ambient air; therefore, the effect of wind speed (in the low- to nil-wind range) is minimal. Heavier or low-momentum releases, particularly those with rainout, result in heavier clouds with less turbulence. In these cases, the effect of nil-wind conditions is much more noticeable and results in: more lateral spread of the cloud against lower wind speeds, as there is no wind pressure to push against the gravity spreading; and less mixing due to the very limited ambient turbulence.

### 6.17 Risk Assessment Results

Risk estimation consists of calculating individual risk, which was previously defined as the annual chance of fatality for a hypothetical individual present at a fixed location 100% of the time. Individual risk due to all hazard scenarios is represented by equal probability of fatality (or iso-risk) contours around the source of risk (i.e., the LNG facility).

	<b>Vapor Cloud Explosions at Nil Wind</b>	03904-RP-006
	PHMSA	Rev A
	Final Report	Page 132 of 213

### 6.17.1 Traditional QRA

The individual risk contours for the generic LNG facility, calculated using the 'Traditional' approach (i.e., combining nil-wind conditions into the low-wind category) are shown in Figure 6-10.



Figure 6-10: Individual risk contours for the 'Traditional' QRA.

The red box indicates the facility property line. The risk contours are concentrated around the liquefaction units, which include the Pretreatment (north end) and Liquefaction (south end) areas, as well as the refrigerant storage area and the LNG rundown header and rundown line to the northern tank. Risk decreases progressively away from this central area.

	<b>Vapor Cloud Explosions at Nil Wind</b>	03904-RP-006
	PHMSA	Rev A
	Final Report	Page 133 of 213

### 6.17.2 Nil-Wind QRA

The individual risk contours for the generic LNG facility, calculated using the 'Nil-wind' approach (i.e., calculating nil-wind consequences and risk contribution separately from low-wind) are shown in Figure 6-11.



Figure 6-11: Individual risk contours for the 'Nil-wind' QRA.

A first look at the 'Nil-wind' risk contours suggests that they are very similar to those calculated using the 'Traditional' approach. In fact, the contours appear virtually identical around the liquefaction trains, while some small differences can be spotted around the tanks and towards the marine transfer area. A more detailed review of the results and comparison between the two approaches is given in the following section.

	<b>Vapor Cloud Explosions at Nil Wind</b>	03904-RP-006
	PHMSA	Rev A
	Final Report	Page 134 of 213

## 6.18 Risk Assessment Discussion

The individual risk contours for the generic LNG facility, with and without nil-wind calculated separately, were overlaid for a more direct comparison as shown in Figure 6-12.



Figure 6-12: Comparison of individual risk contours: Traditional QRA (grey) vs. Nil-Wind QRA (yellow).

As previously observed, the nil-wind risk contours are virtually indistinguishable from the 'Traditional' contours over much of the facility, especially at the 1E-4 level; where the two outcomes deviate, the 'Nil-wind' contours appear consistently inside the 'Traditional' ones, indicating a reduction in the overall risk in those areas.

The QRA comparison performed for this generic LNG facility therefore suggests that the 'Traditional' QRA approach may be conservative, and that explicitly taking into consideration on a risk basis the effects of nil-wind conditions on hazardous releases may actually reduce the calculated risk. Even though these results are based on a single, generic case study, the effect can be considered broadly applicable: in fact, the consequence modeling results in Section 6.15 showed that nil-wind conditions can

	<b>Vapor Cloud Explosions at Nil Wind</b>	03904-RP-006
	PHMSA	Rev A
	Final Report	Page 135 of 213

increase the hazard distance primarily for large-bore releases with rainout, whereas they can decrease the hazard distance for smaller bore, high-pressure releases; therefore, considering that small-bore releases are more likely to occur than large-bore ones, it is not surprising that the net effect of considering nil-wind, on a risk basis, may be a reduction rather than an increase of the overall risk.

The following subsections drill down deeper into the comparison between 'Traditional' and 'Nil-wind' QRA results, by looking at the risk from each type of hazard.

### 6.18.1 Flash Fires

Figure 6-13 offers a side-by-side comparison of the individual risk contours due solely to flash fire scenarios.

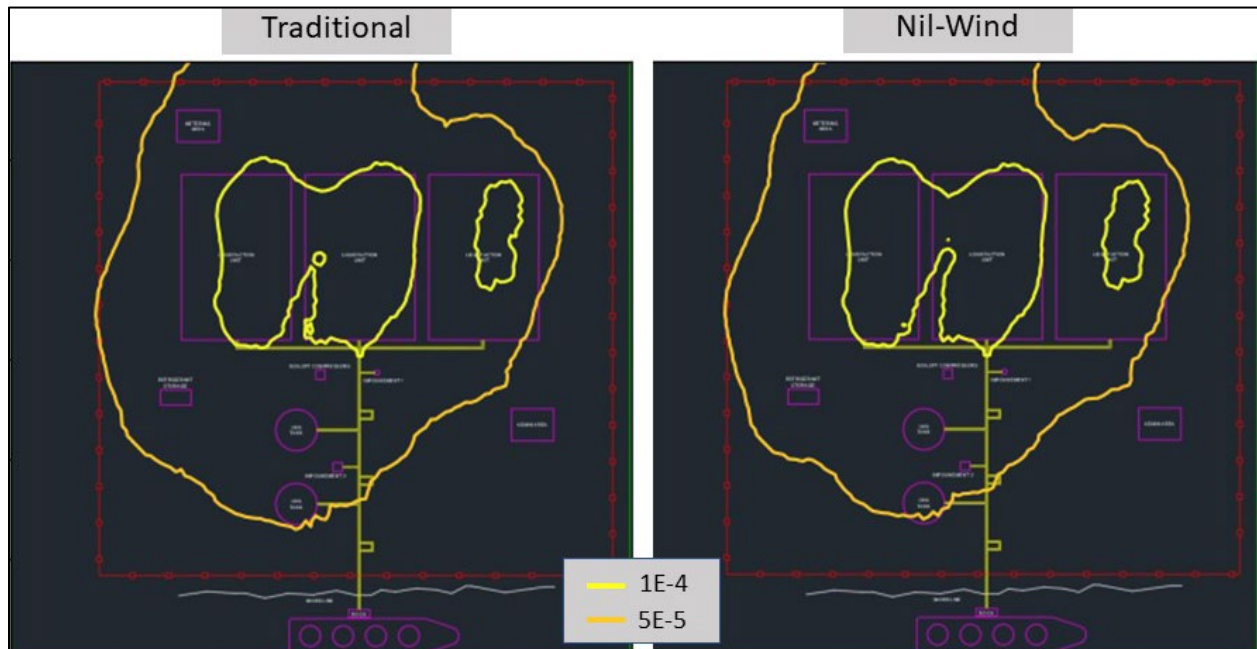


Figure 6-13: Comparison of individual risk contours from flash fire scenarios: Traditional QRA (left) vs. Nil-Wind QRA (right).

The comparison shows, as in the case of the overall risk results discussed above, that the two approaches yield similar results, and the nil-wind contours are slightly smaller than the Traditional ones.

	<b>Vapor Cloud Explosions at Nil Wind</b>	03904-RP-006
	PHMSA	Rev A
	Final Report	Page 136 of 213

### 6.18.2 Jet Fires

Figure 6-14 offers a side-by-side comparison of the individual risk contours due solely to jet fire scenarios.

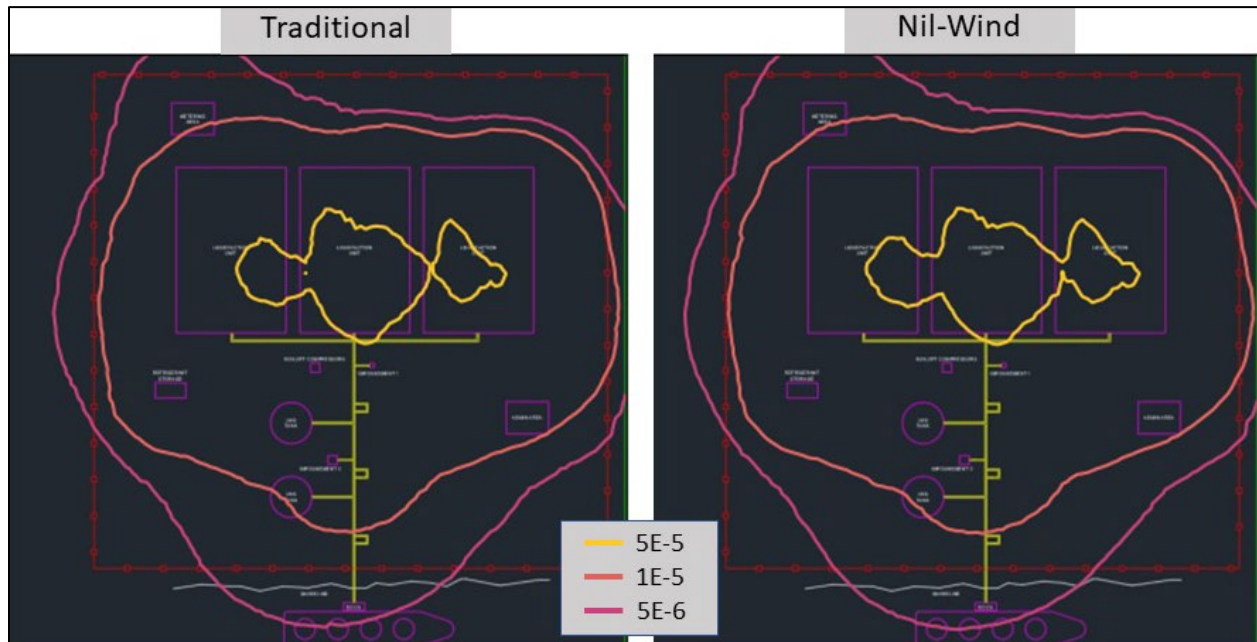


Figure 6-14: Comparison of individual risk contours from jet fire scenarios: Traditional QRA (left) vs. Nil-Wind QRA (right).

The comparison shows nearly identical risk contours, consistent with the earlier discussion about the minimal effect of wind speed on jet fire hazards. As a reminder, jet fire hazards in nil-wind were approximated by using Phast and the F1 wind category (1 m/s wind speed and F stability).

	<b>Vapor Cloud Explosions at Nil Wind</b>	03904-RP-006
	PHMSA	Rev A
	Final Report	Page 137 of 213

### 6.18.3 Pool Fires

Figure 6-15 offers a side-by-side comparison of the individual risk contours due solely to pool fire scenarios.

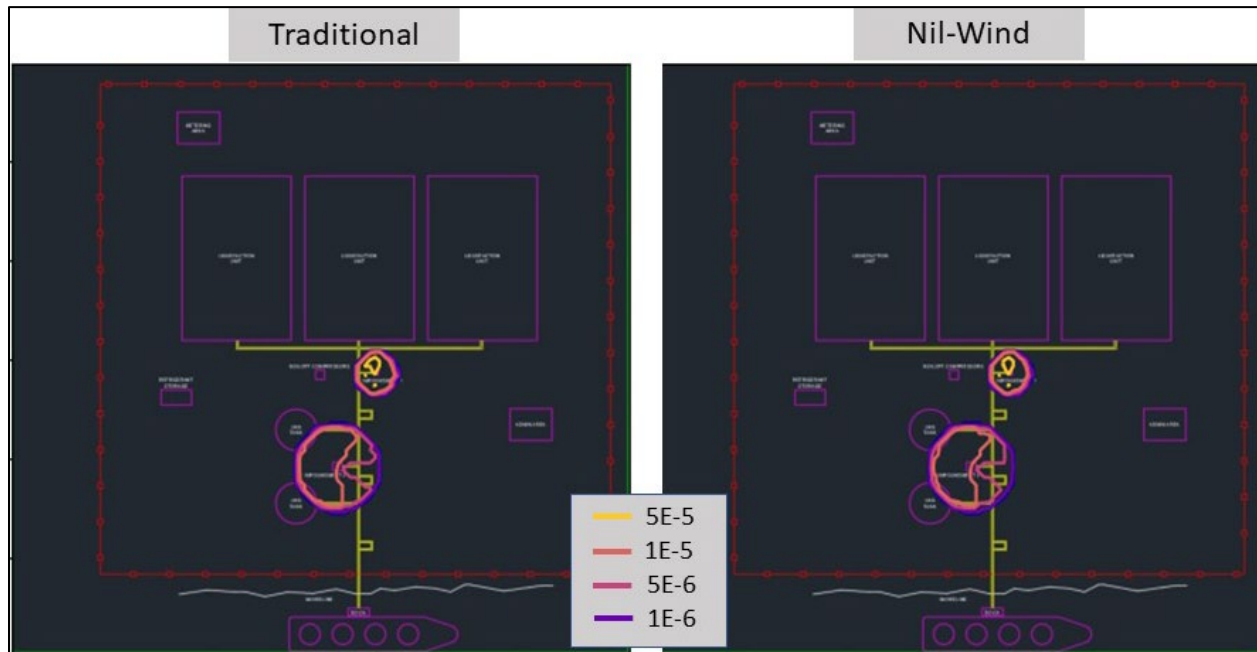


Figure 6-15: Comparison of individual risk contours from pool fire scenarios: Traditional QRA (left) vs. Nil-Wind QRA (right).

The comparison shows nearly identical risk contours, consistent with the earlier discussion about the minimal effect of wind speed on pool fire hazards. As a reminder, pool fire hazards in nil-wind were approximated by using Phast and the F1 wind category (1 m/s wind speed and F stability).

	<b>Vapor Cloud Explosions at Nil Wind</b>	03904-RP-006
	PHMSA	Rev A
	Final Report	Page 138 of 213

#### 6.18.4 Vapor Cloud Explosions

Figure 6-16 offers a side-by-side comparison of the individual risk contours due solely to overpressure hazards from vapor cloud explosion scenarios.

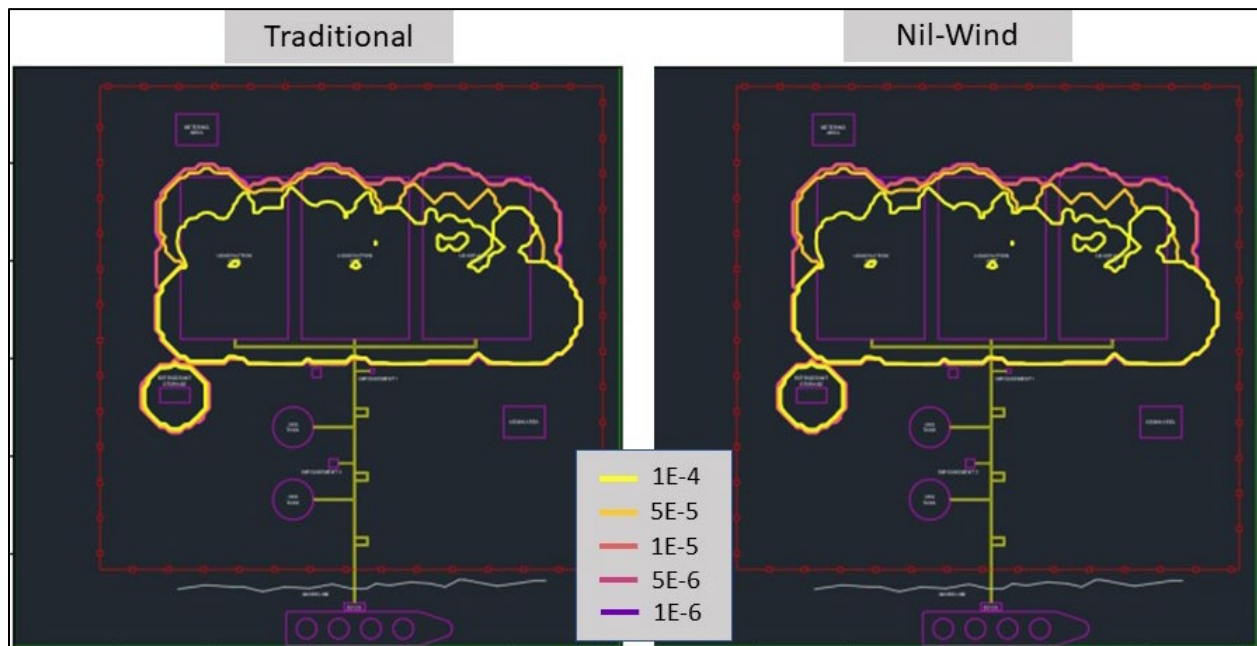


Figure 6-16: Comparison of individual risk contours from VCE scenarios: Traditional QRA (left) vs. Nil-Wind QRA (right).

The comparison shows nearly identical risk contours, consistent with the earlier discussion about the independence of VCE hazards on wind speed. While the size of the flammable cloud does depend on wind speed, in a typical LNG facility a large number of releases occur within, or in proximity of, the main PES's (e.g., the liquefaction trains), therefore wind speed has a limited effect on the cloud volume within the congested region.

	<b>Vapor Cloud Explosions at Nil Wind</b>	03904-RP-006
	PHMSA	Rev A
	Final Report	Page 139 of 213

### 6.19 QRA Summary

A generic LNG facility layout was used as the test case to evaluate individual risk under two sets of assumptions:

1. The “traditional” approach, where nil-wind conditions are combined with low-wind conditions, so that the frequencies are added together and the consequences are calculated at the representative, low wind speed (e.g., F2).
2. The “nil-wind” approach, where nil-wind is considered as its own wind category and the consequences are calculated in zero wind (X0).

The study evaluated over 120 different release scenarios, each modeled under four wind conditions (X0 and F2, as well as higher wind speeds). The consequence modeling, performed using a PHMSA-approved CFD model, showed that nil-wind conditions tend to increase flash fire and vapor cloud explosion hazards for large-bore releases with rainout; however, nil-wind conditions tend to reduce those hazards for small-bore and high-pressure releases.

The overall risk from a QRA performed while explicitly accounting for nil-wind conditions was found to be slightly smaller than from a “traditional” QRA. This can be explained based on the above observation regarding the effect of nil-wind on hazard consequences, as well as the facts that small-bore releases are more likely to occur than large-bore releases and that most streams in an LNG facility are under pressure.

	<b>Vapor Cloud Explosions at Nil Wind</b>	03904-RP-006
	PHMSA	Rev A
	Final Report	Page 140 of 213

## 7 Conclusions and Summary Recommendations

The scope of this project was to evaluate how “nil wind” conditions may affect vapor cloud explosion (VCE) hazards in LNG facilities and to present the findings so that PHMSA staff can make an informed decision regarding possible changes to regulatory requirements. This report summarized the work performed during the project.

The following definitions of wind speed categories were proposed, based on the lower bound of wind speeds that can be used by integral models:

- Nil wind = wind speed less than 1 m/s, measured at a height of 10 m above grade.
- Low wind = wind speed equal to or greater than 1 m/s and less than or equal to 2 m/s, measured at a height of 10 m above grade.

A statistical analysis of wind speeds, based on historical weather data for over 3,000 weather stations across the United States over a 10-year period, found nil winds to occur approximately 20.1% of the time and low winds approximately 11.4% of the time. However, these figures are affected by how wind speeds below 1.5 m/s are measured and reported, therefore they likely overestimate the frequency of occurrence of “nil wind” conditions. For accuracy, any siting study would have to be based on data from the nearest (or most relevant) weather station.

A critical review of the 2017 HSE report titled “Review of Vapour Cloud Explosion Incidents” (RR1113) was performed, leading to the following observations:

- The majority of the accidents reviewed in RR1113 occurred at night or during the early morning hours, which is when nil/low wind conditions tend to be prevalent. However, that is also when staffing is reduced, and darkness affects the operators’ ability to detect a release. These factors cannot be discounted when assessing the relative frequency of accidents and appear more reasonable than the unsubstantiated allegation that “a wider range of smaller losses of containment (with much higher frequency) have the potential to cause a large cloud in [nil/low wind] conditions”.
- The concept of episodic deflagration, which RR1113 claims to be responsible for several large vapor cloud explosion accidents, has been sharply criticized and rebuked by several groups of explosion experts, both on the physical basis of the phenomenon and on the evaluation of forensic evidence. Based on the review of available literature on the topic, the current understanding of VCEs appears adequate to explain those accidents, and the hypothesis that episodic deflagration led to those events cannot be supported.
- Only one of the 24 accidents reviewed occurred at an LNG facility (Skikda) and the severe consequences of that accident are attributable to the confined area in which ignition occurred and the high congestion present outside, therefore, wind conditions likely played a minimal role in the accident. In all other cases, the

	<b>Vapor Cloud Explosions at Nil Wind</b>	03904-RP-006
	PHMSA	Rev A
	Final Report	Page 141 of 213

HSE report discussed the causes but did not address the different regulatory requirements between those facilities and PHMSA-jurisdictional LNG facilities, nor their effect on the likelihood of similar accidents occurring at LNG facilities.

The effect of nil wind conditions on flammable releases was evaluated on a prescriptive basis, according to current PHMSA requirements for LNG facility siting and on a risk basis, according to the quantitative risk assessment procedure outlined in NFPA 59A, 2019 edition. In both cases, a generic LNG export facility was specified, at early-design stage, for the purpose of defining realistic scenarios to be evaluated.

For the prescriptive case study, flammable dispersion and vapor cloud explosion hazards were modeled using a CFD tool (FLACS) which has been validated and approved by PHMSA for LNG dispersion modeling. A total of 15 release scenarios were modeled, each under four different wind conditions (no wind; 0.5 m/s; 1 m/s; and 2 m/s) and three wind directions. The modeling results showed that:

- Equivalent stoichiometric cloud (ESC) volumes tend to be higher in low winds than nil winds, for pressurized releases (without rainout). In these cases, the wind direction (relative to the direction of the release) has a stronger effect on ESC volumes than wind speed; the effect of wind direction is reduced for clouds that enter congested areas.
- ESC volumes tend to be higher in nil winds for evaporating liquid spills. This behavior is consistent with a highly stratified cloud, which is progressively diluted at the air/cloud interface by wind-induced turbulence and molecular diffusion.
- It should be noted that liquid spill scenarios, or pressurized jet releases scenarios with rainout, are typically not the bounding cases for LNG facility siting due to the liquid being collected and conveyed into an impoundment to minimize its vaporization rate.

For the risk-based case study, over 120 different release scenarios were evaluated, each modeled under four wind conditions (nil wind, low wind, and higher wind speeds); FLACS was used to determine flammable dispersion distances and ESC volumes. The individual risk was then calculated under two sets of assumptions:

3. The “traditional” approach, where nil-wind conditions are combined with low-wind conditions, so that the frequencies are added together and the consequences are calculated at the representative, low wind speed.
4. The “nil-wind” approach, where nil-wind is considered as its own wind category and the consequences are calculated in zero wind.

The overall risk from a QRA performed while explicitly accounting for nil-wind conditions was found to be slightly smaller than from a “traditional” QRA, meaning that QRAs conducted according to the “traditional” approach tend to be slightly conservative. This outcome was explained by observing that nil wind conditions tend to increase hazards

	<b>Vapor Cloud Explosions at Nil Wind</b>	03904-RP-006
	PHMSA	Rev A
	Final Report	Page 142 of 213

for large-bore releases (particularly with rainout), which are less frequent, but they tend to reduce the same hazards for small-bore and high-pressure releases, which are more frequent.

The project team therefore does not recommend any changes to the regulatory requirements regarding wind speeds to be included in an LNG facility siting study, as currently specified in 49 CFR 193.2059.

	<b>Vapor Cloud Explosions at Nil Wind</b>	03904-RP-006
	PHMSA	Rev A
	Final Report	Page 143 of 213

## 8 Impact from the Research Results

The results of this research are expected to:

- Provide information to PHMSA and other regulatory agencies regarding potential changes to current regulations or regulatory guidance.
- Support public input as well as consensus discussions by the NFPA 59A Technical Committee and others regarding potential updates to future editions of NFPA 59A (e.g., the prescriptive approach in Chapter 5 or the risk-based approach in Chapter 19 of the current 2019 edition).
- Increase understanding of the effect of weather conditions on flammable hazards for regulators, operators, and the public.
- Highlight the difference in the nature of explosion hazards, safety system design requirements, and maintenance procedures for PHMSA-regulated LNG facilities in comparison to historical instances of VCEs in hydrocarbon processing and storage facilities worldwide.

	<b>Vapor Cloud Explosions at Nil Wind</b>	03904-RP-006
	PHMSA	Rev A
	Final Report	Page 144 of 213

## 9 Final Financial Section

The cost of this fixed-price project was 80% funded by the Government, and the project team provided the required 20% cost share.

Project expenses and billing aligned with the associated contract #693JK32010004POTA. There were no discrepancies or variances in contributions that needed to be reconciled.

## 10 Acronyms

API	American Petroleum Institute
BLEVE	Boiling Liquid Expanding Vapor Explosion
BLUE	Blue Engineering and Consulting Company
BOG	Boil-Off Gas
BUT	Butane
CFD	Computational Fluid Dynamics
CFR	Code of Federal Regulations
DDT	Deflagration-to-Detonation Transition
DOT	U.S. Department of Transportation
D8	High wind category (8 m/s, D stability)
ESC	Equivalent Stoichiometric Cloud
ETH	Ethylene
E4	Medium wind category (4 m/s, E stability)
FAQ	Frequently Asked Question
FRED	Failure Rate and Event Data
FV	Flammable Volume
F2	Low wind category (2 m/s, F stability)
H&MB	Heat and Material Balance
HEA	Heavies (heavy condensate)
HSE	Health and Safety Executive
LFL	Lower Flammable Limit
LNG	Liquefied Natural Gas
LPG	Liquefied Petroleum Gas
MR	Mixed Refrigerant
MTPA	Million Tonnes Per Annum
NCEI	National Centers for Environmental Information
NFPA	National Fire Protection Association
NG	Natural Gas
NOAA	National Oceanographic and Atmospheric Administration
OGP	Oil & Gas Producers

	<b>Vapor Cloud Explosions at Nil Wind</b>	03904-RP-006
	PHMSA	Rev A
	Final Report	Page 146 of 213

P&ID	Piping and Instrumentation Diagram
PES	Potential Explosion Site
PFD	Process Flow Diagram
PHMSA	Pipeline and Hazardous Materials Safety Administration
PRO	Propane
QRA	Quantitative Risk Assessment
Q8	A type of ESC volume
Q9	A type of ESC volume
Ri	Richardson number
RP	Recommended Practice
UFL	Upper Flammable Limit
UKOAA	United Kingdom Offshore Operators Association
VCE	Vapor Cloud Explosion
X0	Nil wind category (0 wind speed)

	<b>Vapor Cloud Explosions at Nil Wind</b>	03904-RP-006
	PHMSA	Rev A
	Final Report	Page 147 of 213

## 11 Bibliography

- [1] G. Atkinson, J. Hall, and A. McGillivray, "Review of Vapour Cloud Incidents," Health and Safety Executive, RR1113, 2017.
- [2] National Fire Protection Association, "Standard for the Production, Storage, and Handling of Liquefied Natural Gas (LNG)," National Fire Protection Association, Standards NFPA 59A, 2001.
- [3] A. A. Grachev, E. L. Andreas, C. W. Fairall, P. S. Guest, and P. O. G. Persson, "The Critical Richardson Number and Limits of Applicability of Local Similarity Theory in the Stable Boundary Layer," *Boundary-Layer Meteorol*, vol. 147, no. 1, pp. 51–82, Apr. 2013, doi: 10.1007/s10546-012-9771-0.
- [4] G. A. Briggs, R. S. Thompson, and W. H. Snyder, "Dense gas removal from a valley by crosswinds," *Journal of Hazardous Materials*, vol. 24, no. 1, pp. 1–38, Dec. 1990, doi: 10.1016/0304-3894(90)80001-K.
- [5] H. W. M. Witlox, "Unified Dispersion Model," DNV Software, Sep. 2017.
- [6] J. S. Touma, "Dependence of the Wind Profile Power Law on Stability for Various Locations," *Journal of the Air Pollution Control Association*, vol. 27, no. 9, pp. 863–866, Sep. 1977, doi: 10.1080/00022470.1977.10470503.
- [7] "Large-loss fires in the United States." <https://www.nfpa.org/News-and-Research/Data-research-and-tools/US-Fire-Problem/Large-loss-fires-in-the-United-States> (accessed Mar. 16, 2021).
- [8] Steel Construction Institute, "Buncefield Explosion Mechanism Phase 1. Volume 1 and 2," Health and Safety Executive, RR718, 2009.
- [9] G. Atkinson and L. Cusco, "Buncefield: A violent, episodic vapour cloud explosion," *Process Safety and Environmental Protection*, vol. 89, no. 6, pp. 360–370, Nov. 2011, doi: 10.1016/j.psep.2011.06.019.
- [10] M. A. Hadjipanayis, F. Beyrau, R. P. Lindstedt, G. Atkinson, and L. Cusco, "Thermal radiation from vapour cloud explosions," *Process Safety and Environmental Protection*, vol. 94, pp. 517–527, Mar. 2015, doi: 10.1016/j.psep.2014.11.004.
- [11] J. R. Bakke, K. van Wingerden, P. Hoorelbeke, and B. Brewerton, "A study on the effect of trees on gas explosions," *Journal of Loss Prevention in the Process Industries*, vol. 23, no. 6, pp. 878–884, Nov. 2010, doi: 10.1016/j.jlp.2010.08.007.

	<b>Vapor Cloud Explosions at Nil Wind</b>	03904-RP-006
	PHMSA	Rev A
	Final Report	Page 148 of 213

- [12] S. G. Davis, P. Hinze, O. R. Hansen, and K. van Wingerden, "Investigation techniques used to determine the massive vapor cloud explosion at the Buncefield fuel depot," 2010, p. 12.
- [13] M. Abdel-jawad and F. Gavelli, "The myth of episodic deflagration in large, unconfined vapor clouds," *Proc Safety Prog*, vol. e12162, 2020, [Online]. Available: <https://doi.org/10.1002/prs.12162>
- [14] D. M. Johnson and V. H. Y. Tam, "Why DDT is the only way to explain some vapor cloud explosions," *Proc. Safety Prog.*, vol. 36, no. 3, pp. 292–300, Sep. 2017, doi: 10.1002/prs.11874.
- [15] G. Chamberlain, E. Oran, and A. Pekalski, "An Analysis of Severe Vapour Cloud Explosions and Detonations in the Process Industries," *Chemical Engineering Transactions*, vol. 77, pp. 853–858, Sep. 2019, doi: 10.3303/CET1977143.
- [16] S. Davis *et al.*, "Do not believe the hype: Using case studies and experimental evidence to show why the HSE is wrong about excluding deflagration-to-detonation transitions," *Proc. Safety Prog.*, vol. 38, no. 2, p. e11998, Jun. 2019, doi: 10.1002/prs.11998.
- [17] American Petroleum Institute, *API 2350: Overfill Protection for Storage Tanks in Petroleum Facilities*, vol. 49 CFR 195.428(c).
- [18] National Fire Protection Association, "Standard for the Production, Storage, and Handling of Liquefied Natural Gas (LNG)," National Fire Protection Association, Standards NFPA 59A, 2019.
- [19] F. Gavelli and S. Davis, "The mitigation conundrum: when reducing one hazard may increase another," presented at the 2013 AIChE Spring Meeting, San Antonio, TX, 2013.
- [20] Pipeline and Hazardous Materials Safety Administration, *Final Decision on petition for approval of FLACS (version 9.1 release 2)*. 2011.
- [21] D. A. Crowl, *Understanding explosions*. New York: Center for Chemical Process Safety of the American Institute of Chemical Engineers, 2003.
- [22] R. Pitblado, J. Alderman, and J. K. Thomas, "Facilitating consistent siting hazard distance predictions using the TNO Multi-Energy Model," *Journal of Loss Prevention in the Process Industries*, vol. 30, pp. 287–295, Jul. 2014, doi: 10.1016/j.jlp.2014.04.010.

	<b>Vapor Cloud Explosions at Nil Wind</b>	03904-RP-006
	PHMSA	Rev A
	Final Report	Page 149 of 213

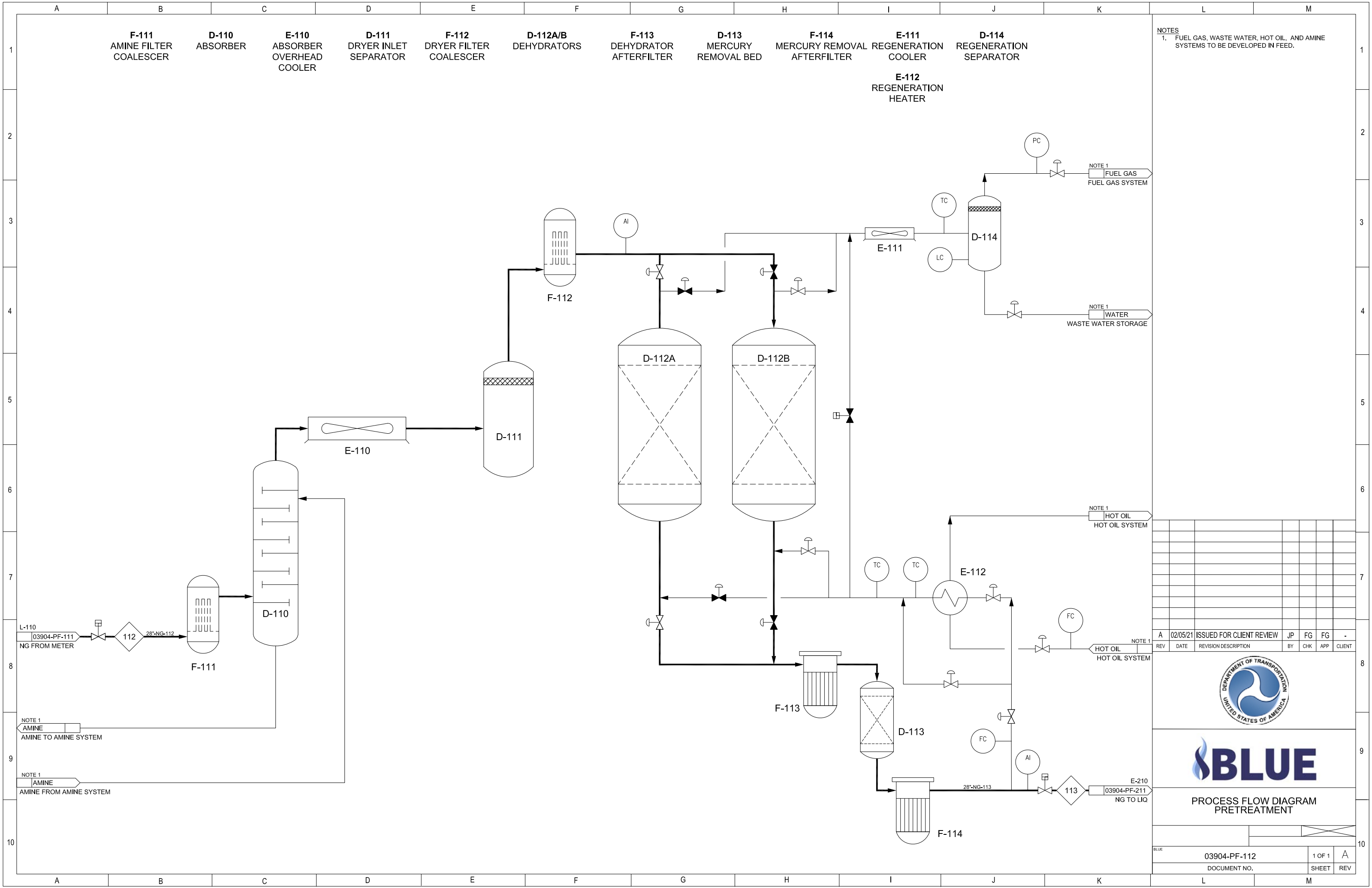
- [23] J. Alderman, R. Pitblado, and J. K. Thomas, "Facilitating consistent siting hazard distance predictions using the TNO Multi-Energy Model," 2012.
- [24] O. R. Hansen, F. Gavelli, S. G. Davis, and P. Middha, "Equivalent cloud methods used for explosion risk and consequence studies," *Journal of Loss Prevention in the Process Industries*, vol. 26, no. 3, pp. 511–527, May 2013, doi: 10.1016/j.jlp.2012.07.006.
- [25] V. Tam, F. Tan, and C. Savvides, "A Critical Review of the Equivalent Stoichiometric Cloud Model Q9 in Gas Explosion Modelling," *Eng*, vol. 2, no. 2, pp. 156–180, Apr. 2021, doi: 10.3390/eng2020011.
- [26] Gas Technology Institute, "Consistency Review of Methodologies for Quantitative Risk Assessment," Final Report 22418, Oct. 2020.
- [27] International Association of Oil & Gas Producers, "Process Release Frequencies," 434–01, Sep. 2019.
- [28] International Association of Oil & Gas Producers, "Ignition Probabilities," 434–06, Sep. 2019.

	<b>Vapor Cloud Explosions at Nil Wind</b>	03904-RP-006
	PHMSA	Rev A
	Final Report	Page 150 of 213

## Appendix A – Facility Design Drawings







NOTES  
 1. FUEL GAS, WASTE WATER, HOT OIL, AND AMINE SYSTEMS TO BE DEVELOPED IN FEED.

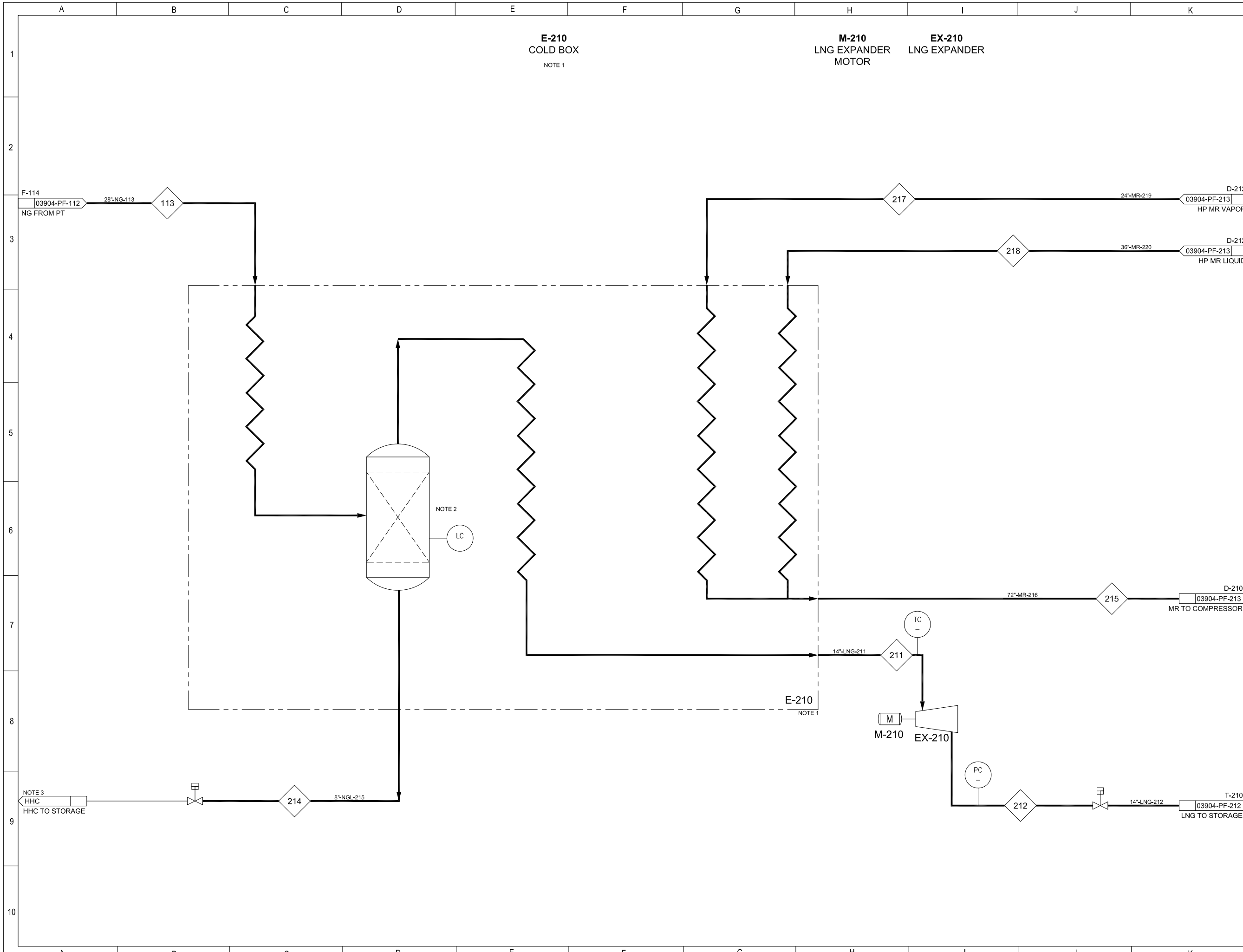
REV	DATE	REVISION DESCRIPTION	BY	CHK	APP	CLIENT
A	02/05/21	ISSUED FOR CLIENT REVIEW	JP	FG	FG	-



**BLUE**

PROCESS FLOW DIAGRAM  
 PRETREATMENT

03904-PF-112	1 OF 1	A
DOCUMENT NO.	SHEET	REV



**E-210**  
COLD BOX  
NOTE 1

**M-210**  
LNG EXPANDER  
MOTOR

**EX-210**  
LNG EXPANDER

- NOTES**
1. COLD BOX TO CONSIST OF SEVERAL EXCHANGERS AND KNOCK OUT DRUMS. THESE ARE NOT SHOWN IN THIS DESIGN.
  2. KNOCKOUT DRUM(S) WILL BE PRESENT INSIDE OF THE COLD BOX TO REMOVE HEAVY HYDROCARBONS FROM THE NATURAL GAS STREAM.
  3. HEAVY HYDROCARBON PROCESSING AND STORAGE SYSTEMS NOT INCLUDED IN THE DESIGN.

NOTE 2  
LC

E-210  
NOTE 1

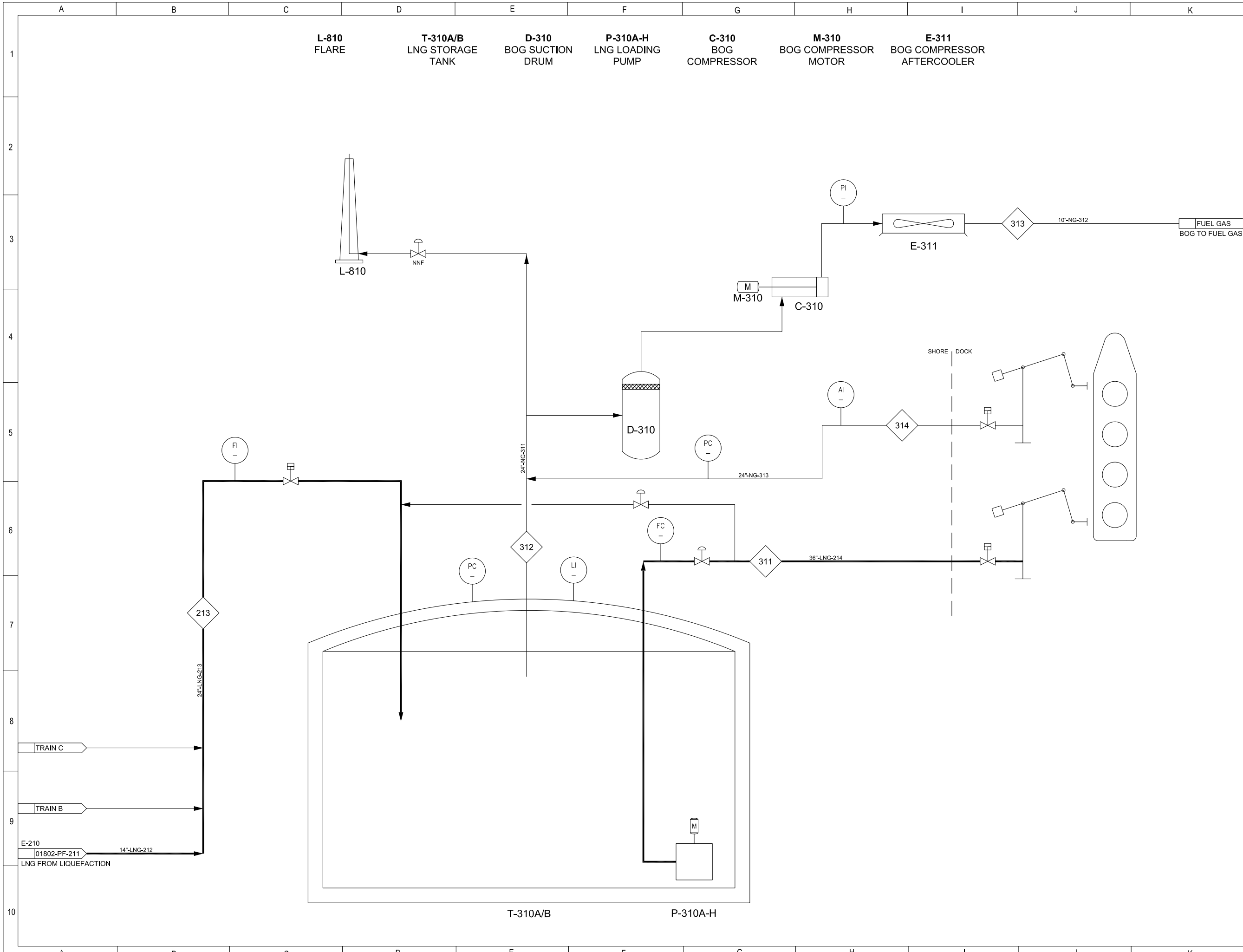
NOTE 3  
HHC  
HHC TO STORAGE

REV	DATE	REVISION DESCRIPTION	BY	CHK	APP	CLIENT
A	02/05/21	ISSUED FOR CLIENT REVIEW	JP	PS	FG	-



PROCESS FLOW DIAGRAM  
LIQUEFACTION

BLUE	03904-PF-211	1 OF 1	A
	DOCUMENT NO.	SHEET	REV



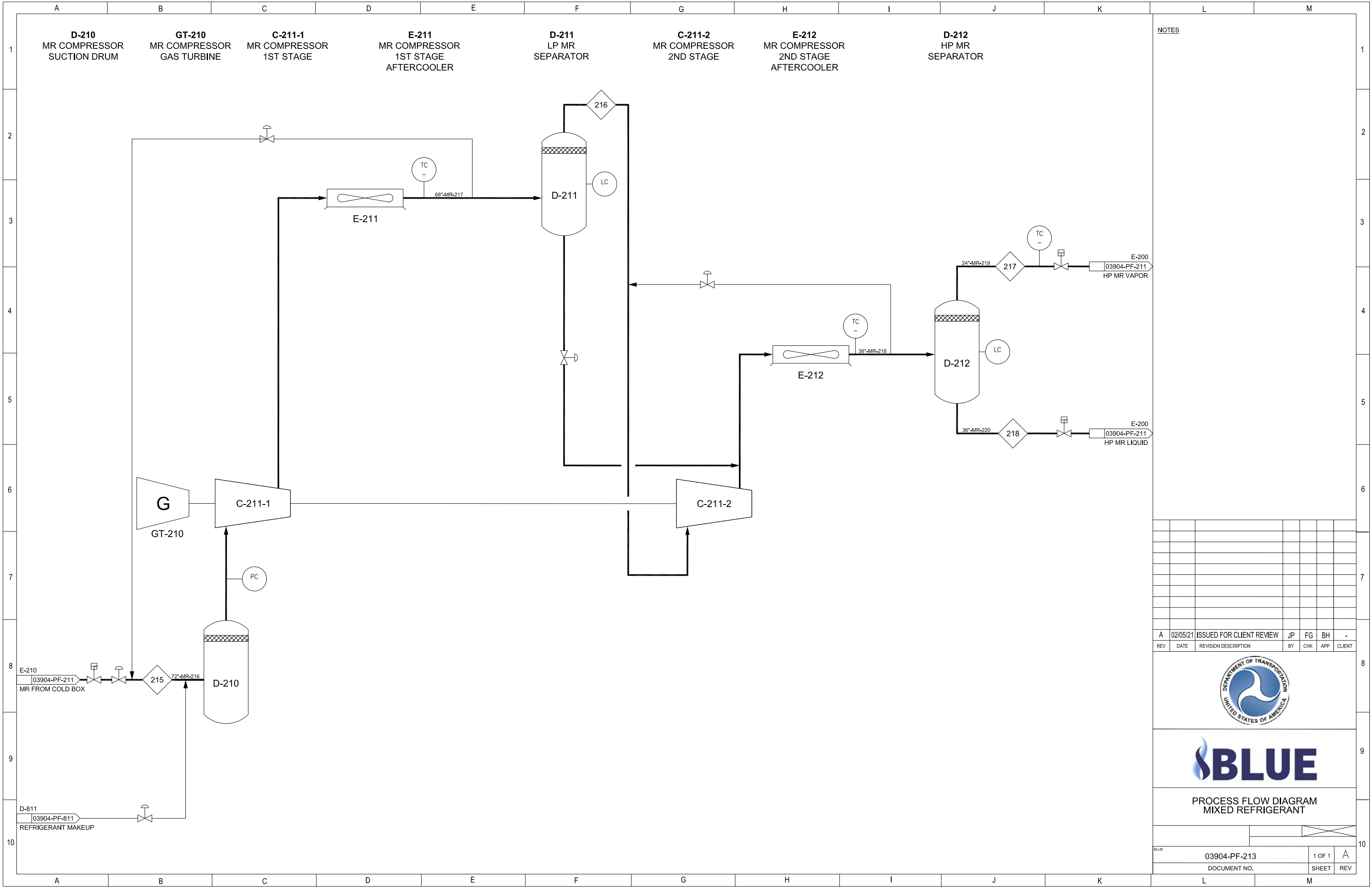
**NOTES**  
 1. FUEL GAS SYSTEM NOT INCLUDED IN THE DESIGN.

REV	DATE	REVISION DESCRIPTION	BY	CHK	APP	CLIENT
A	02/05/21	ISSUED FOR CLIENT REVIEW	JP	PS	FG	-



**PROCESS FLOW DIAGRAM  
 BALANCE OF PLANT**

BLUE	03904-PF-212	1 OF 1	A
	DOCUMENT NO.	SHEET	REV



NOTES

REV	DATE	REVISION DESCRIPTION	BY	CHK	APP	CLIENT
A	02/05/21	ISSUED FOR CLIENT REVIEW	JP	FG	BH	-



**BLUE**

PROCESS FLOW DIAGRAM  
MIXED REFRIGERANT

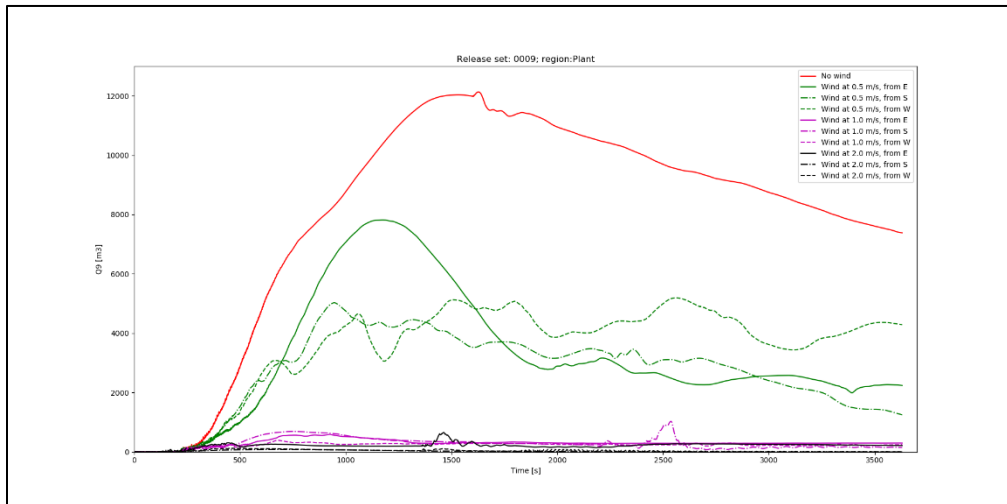
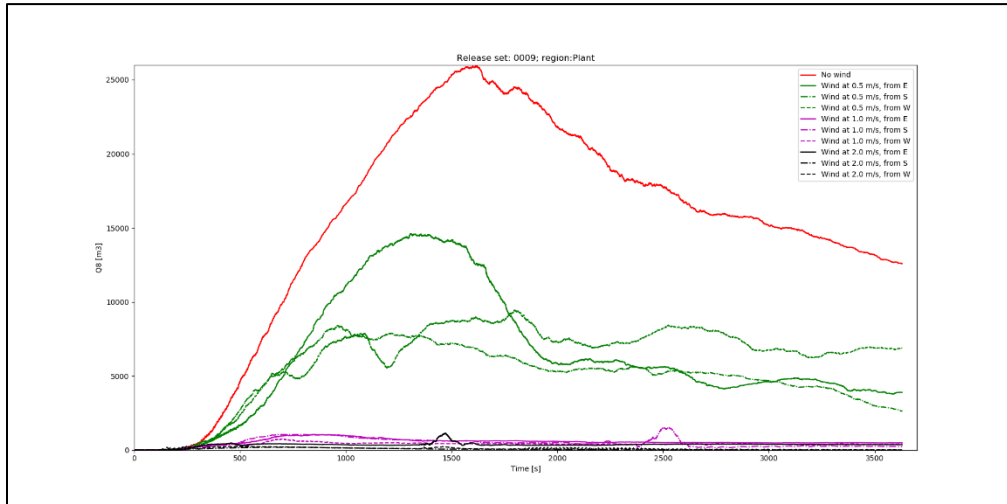
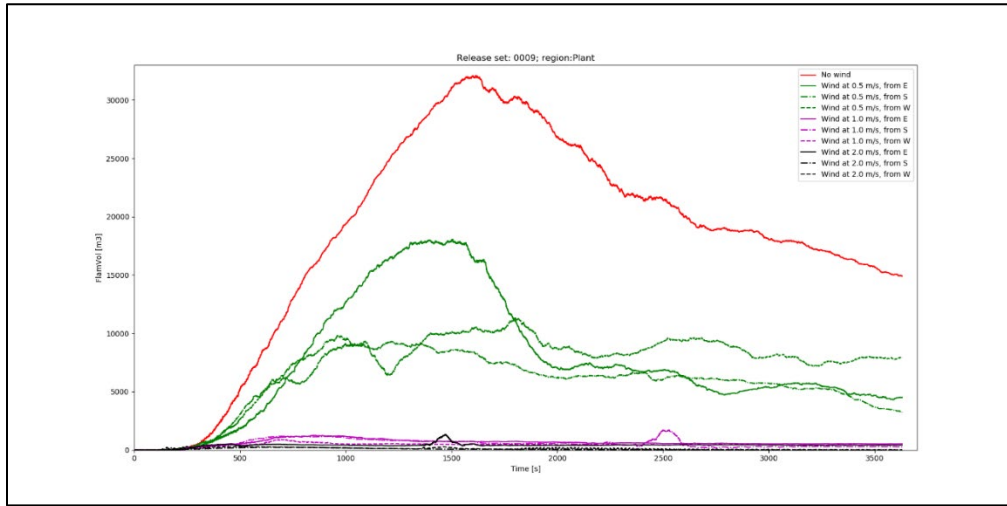
BLUE	03904-PF-213	1 OF 1	A
	DOCUMENT NO.	SHEET	REV



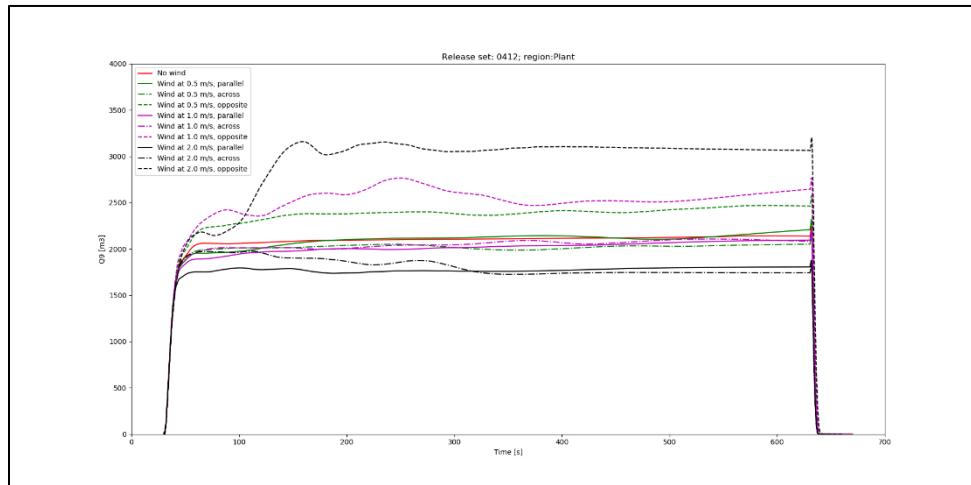
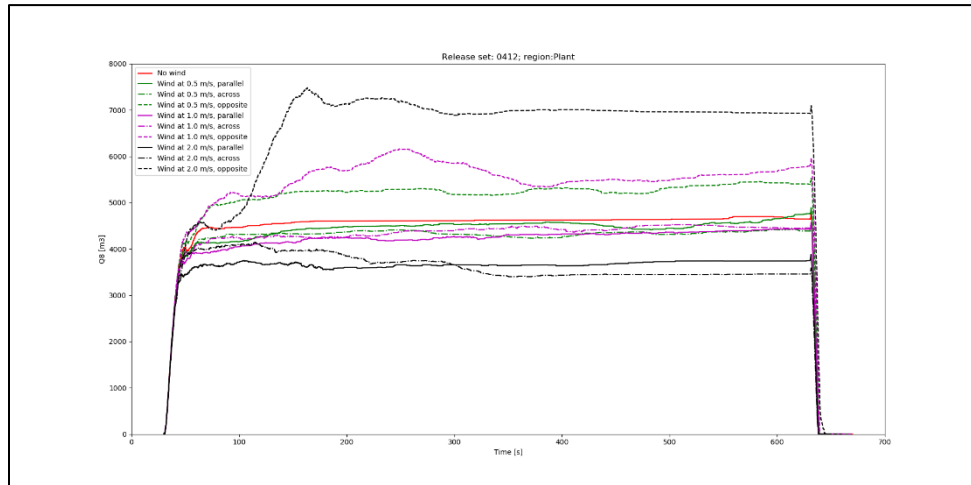
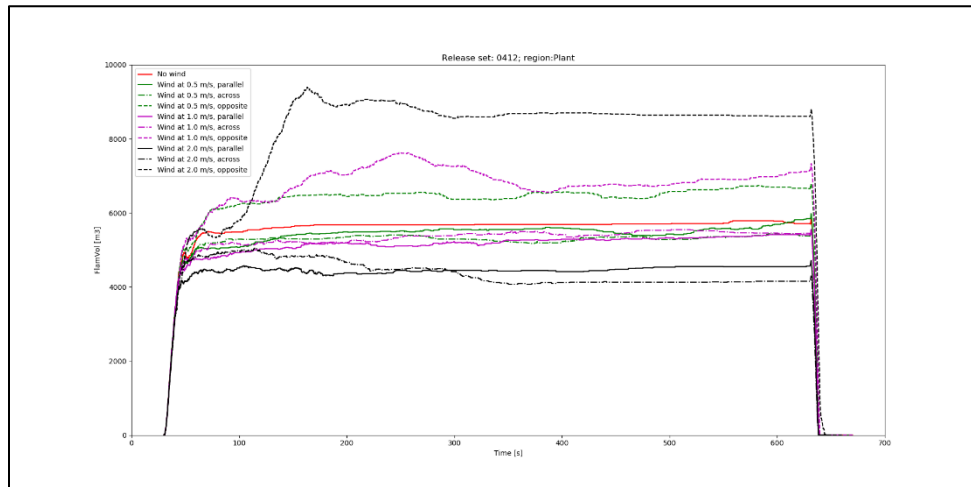


	<b>Vapor Cloud Explosions at Nil Wind</b>	03904-RP-006
	PHMSA	Rev A
	Final Report	Page 159 of 213

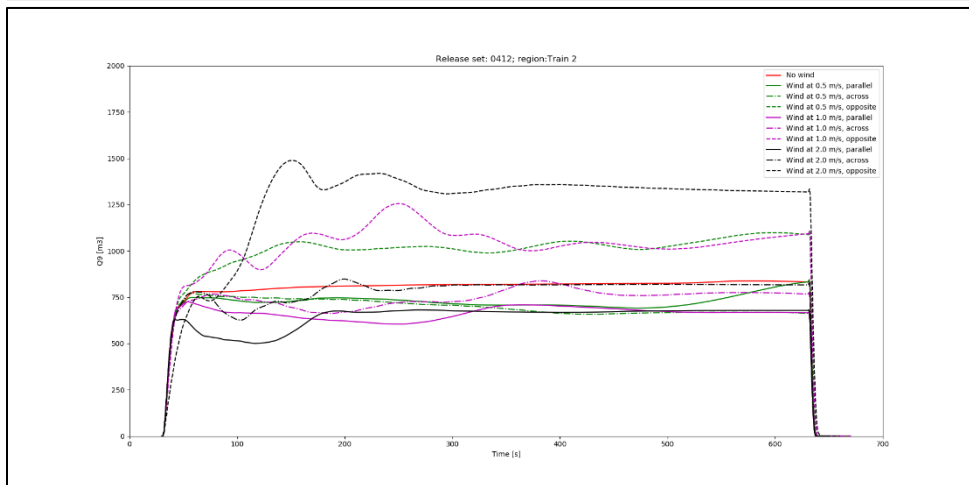
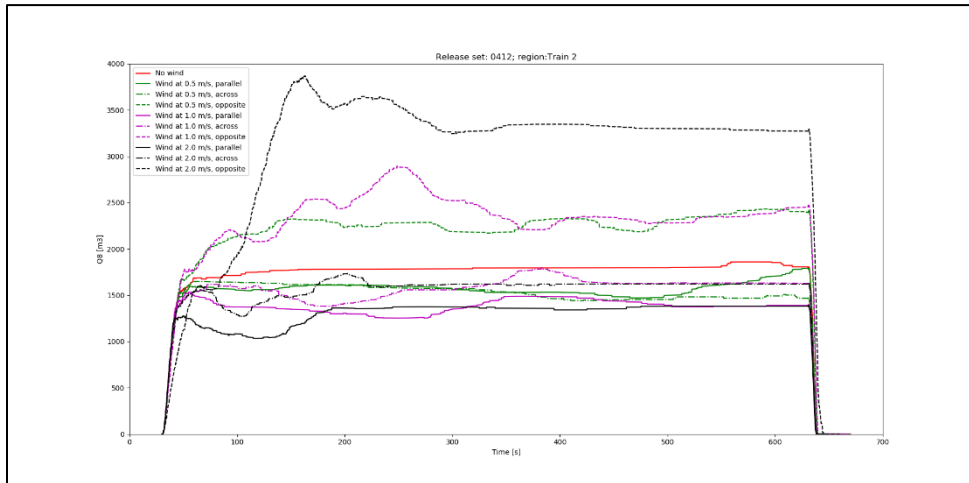
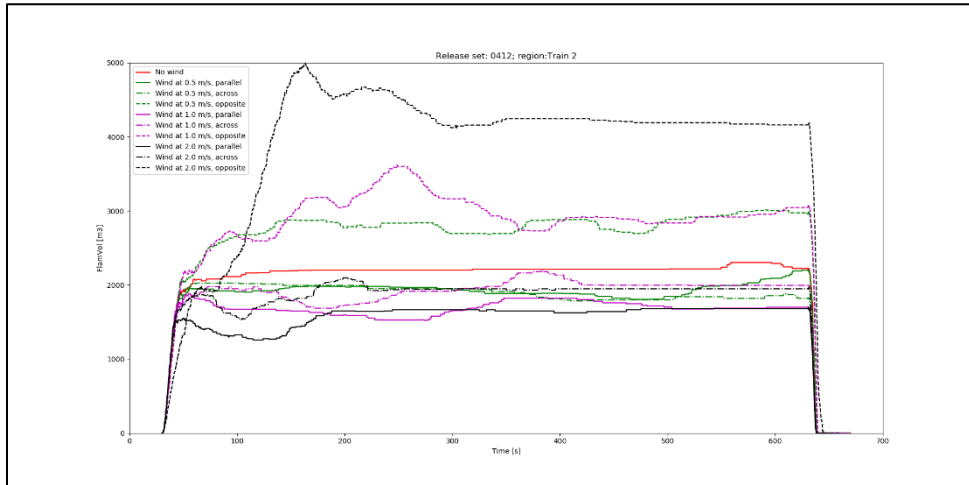
## Appendix B – Equivalent Stoichiometric Cloud Volumes



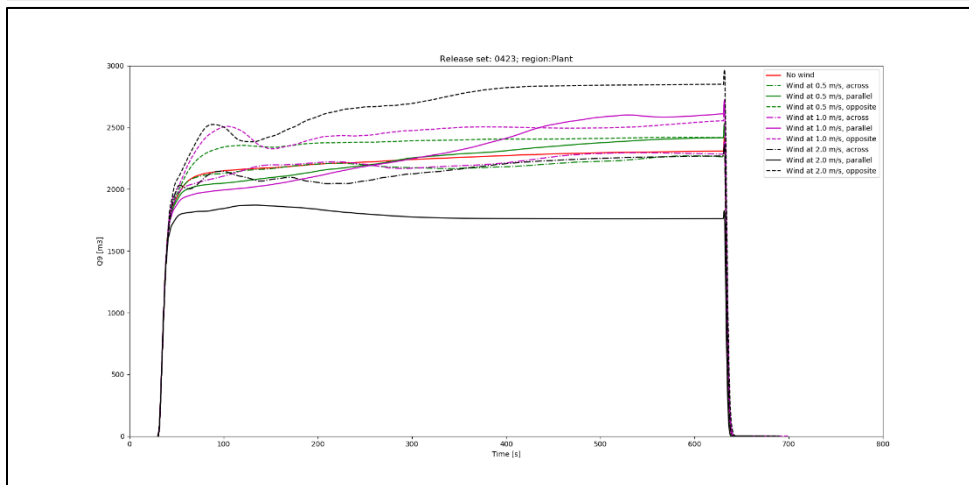
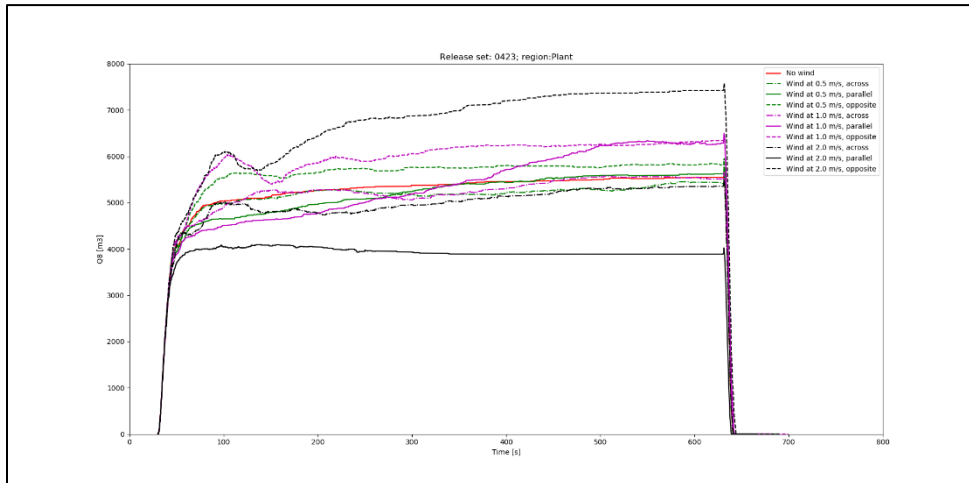
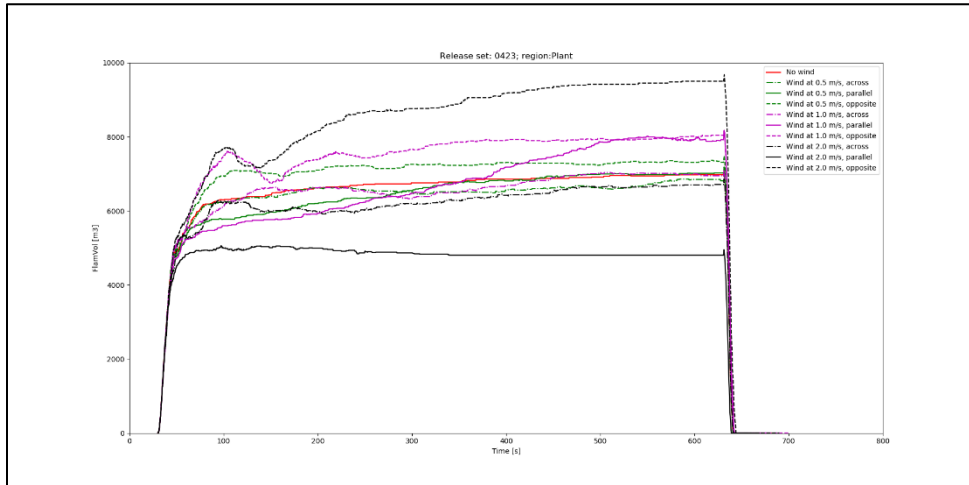
LNG spill (scenario 00): FV (top), Q8 (middle), and Q9 (bottom) ESC for entire Plant area.



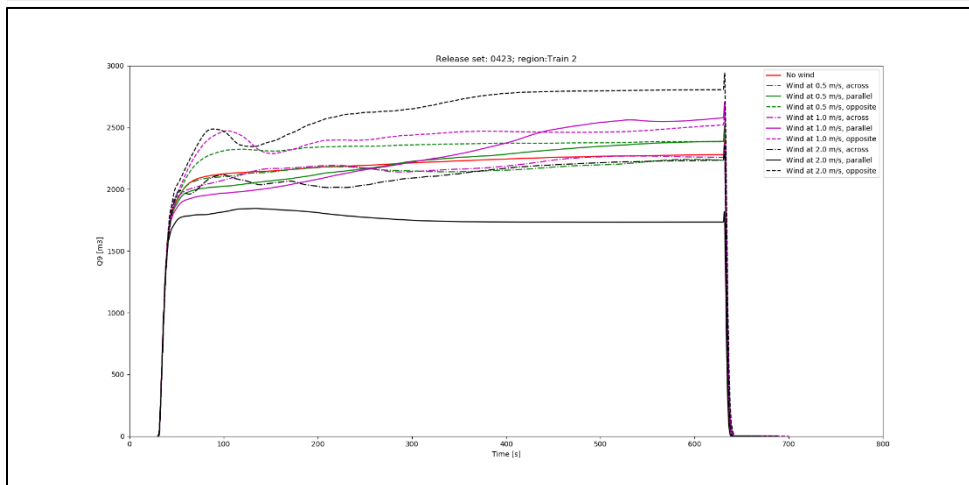
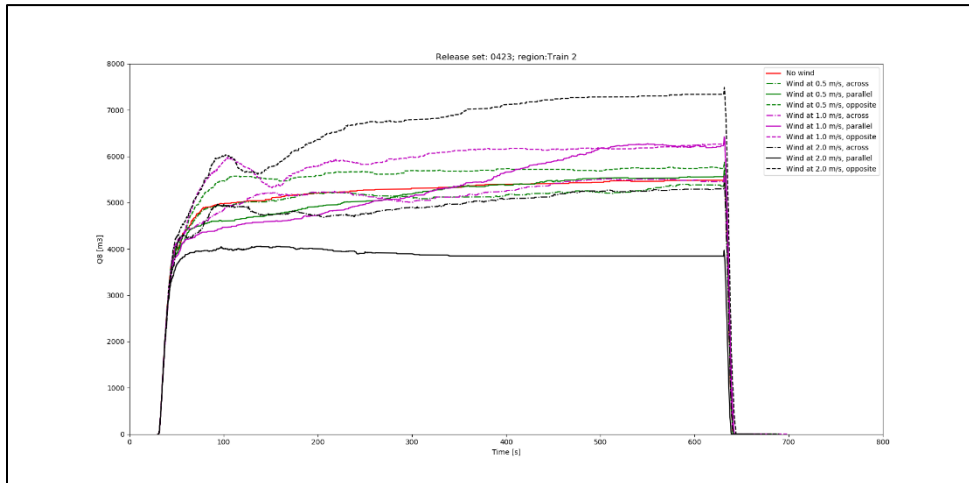
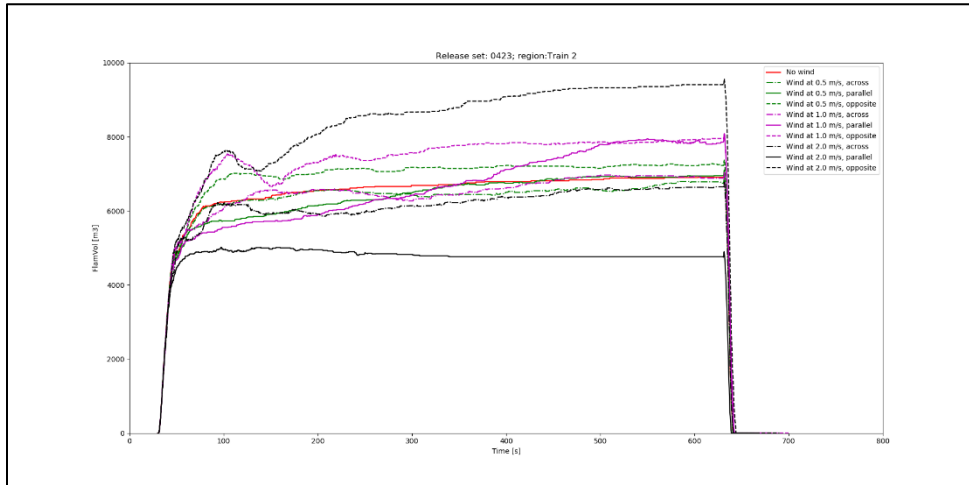
2" LNG release to the West (scenario 04): FV (top), Q8 (mid), and Q9 (bot.) ESC for Plant area.



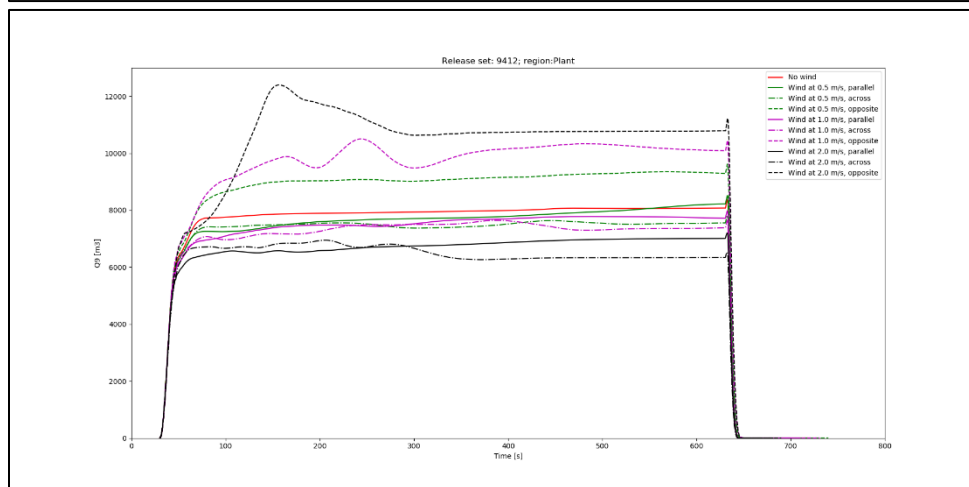
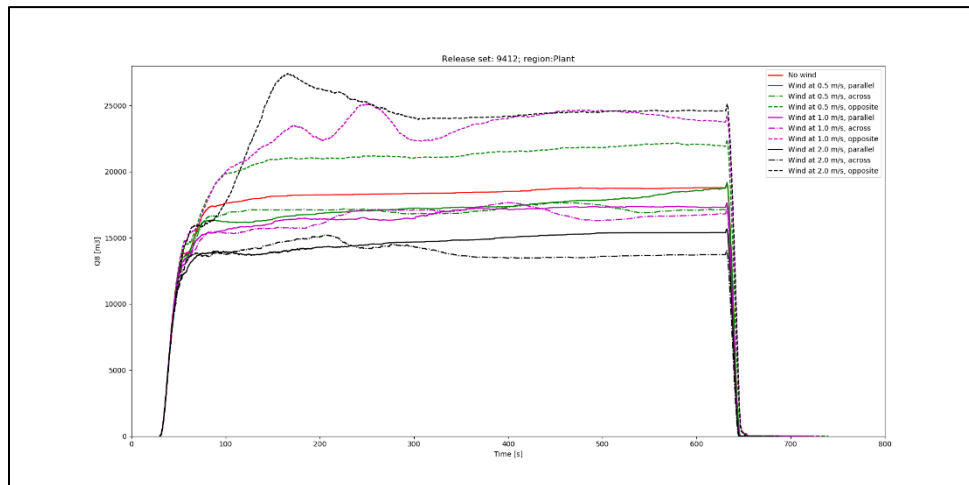
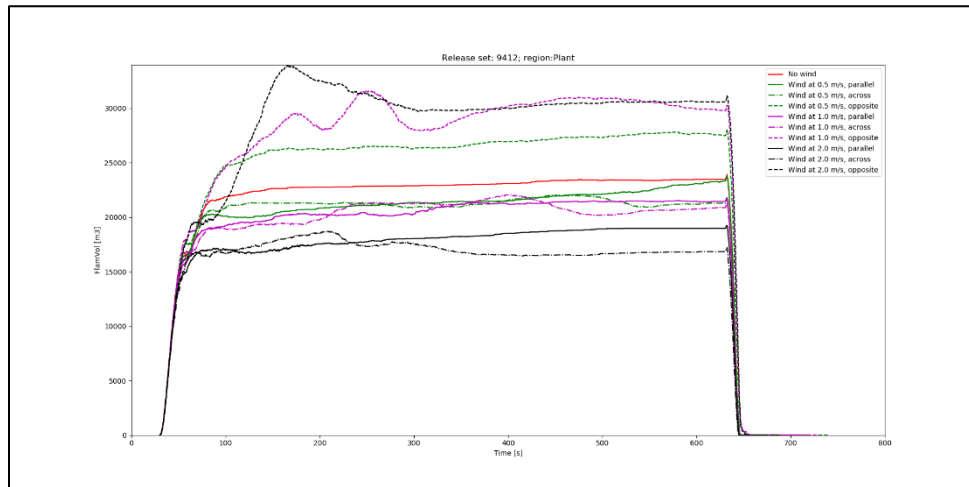
2" LNG release to the West (scenario 04): FV (top), Q8 (mid), and Q9 (bot.) ESC for Train 2 area.



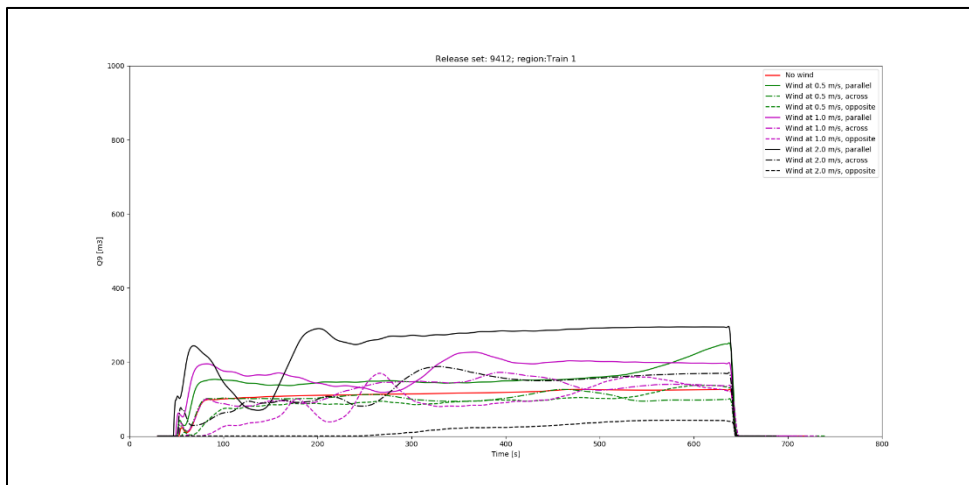
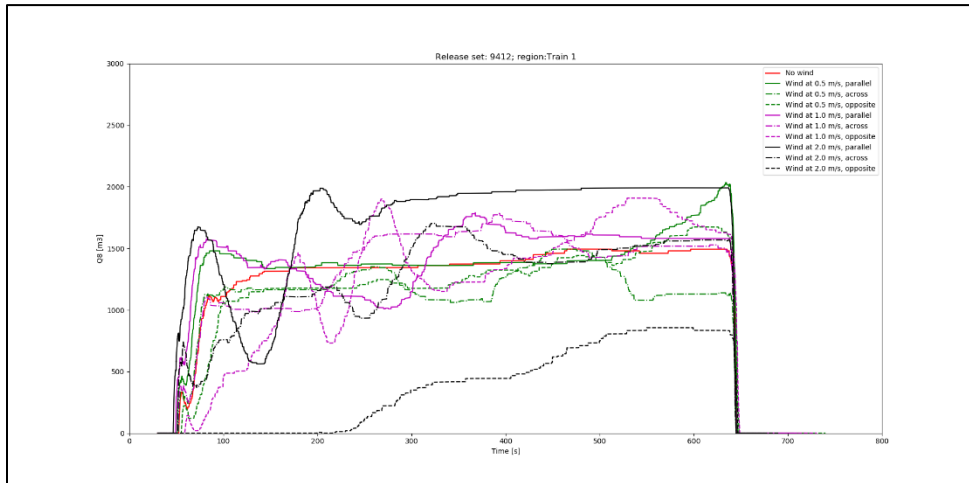
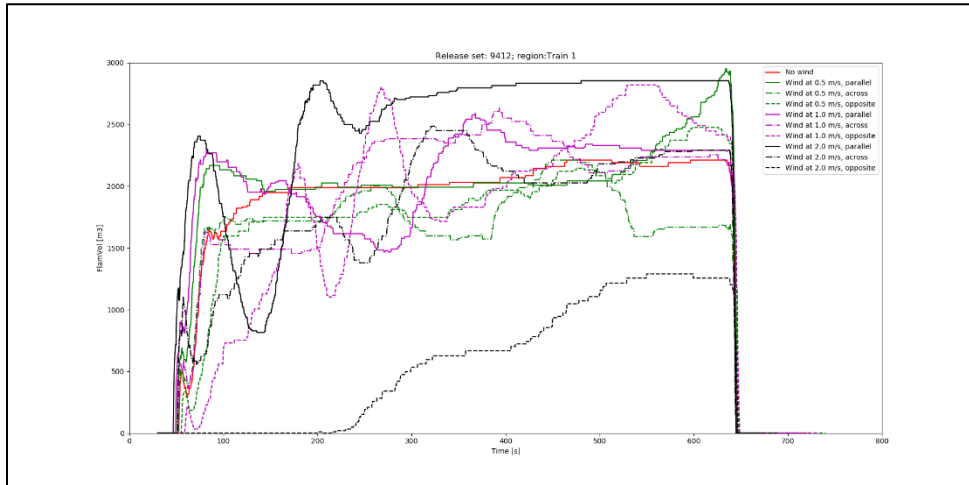
2" LNG release to the North (scenario 04): FV (top), Q8 (mid), and Q9 (bot.) ESC for Plant area.



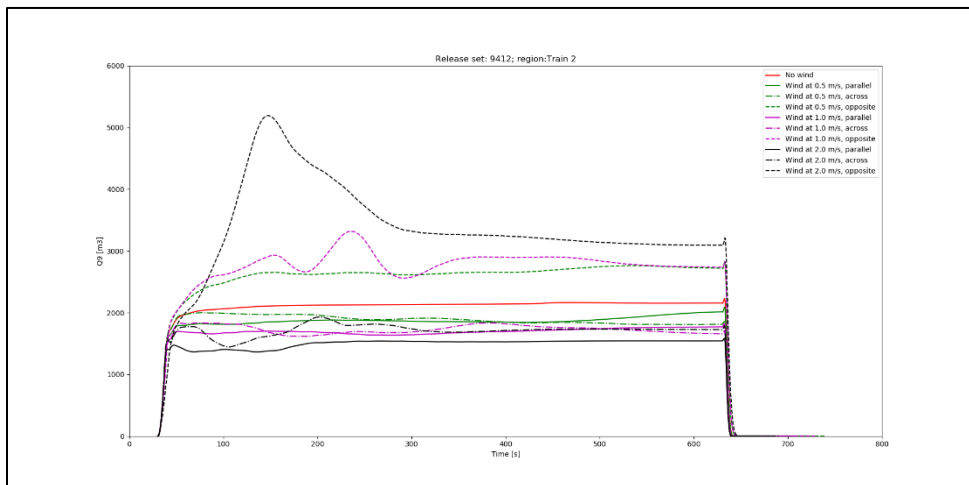
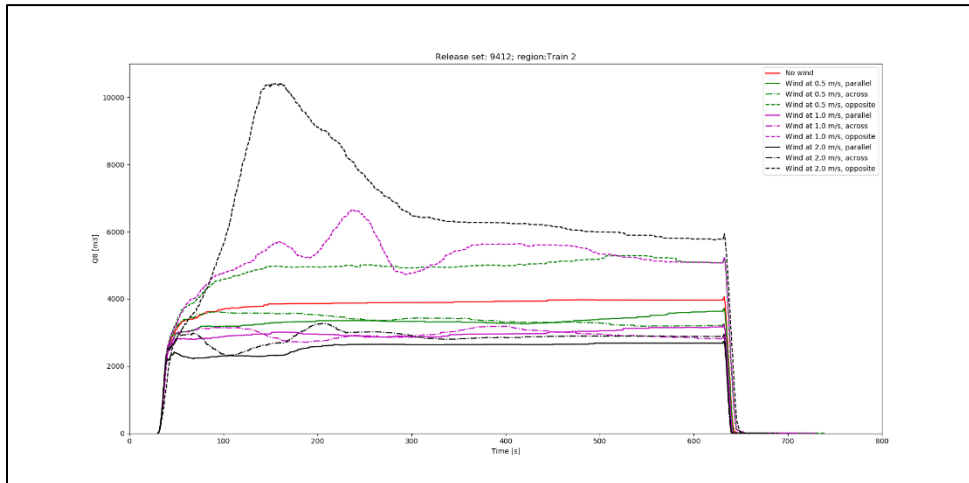
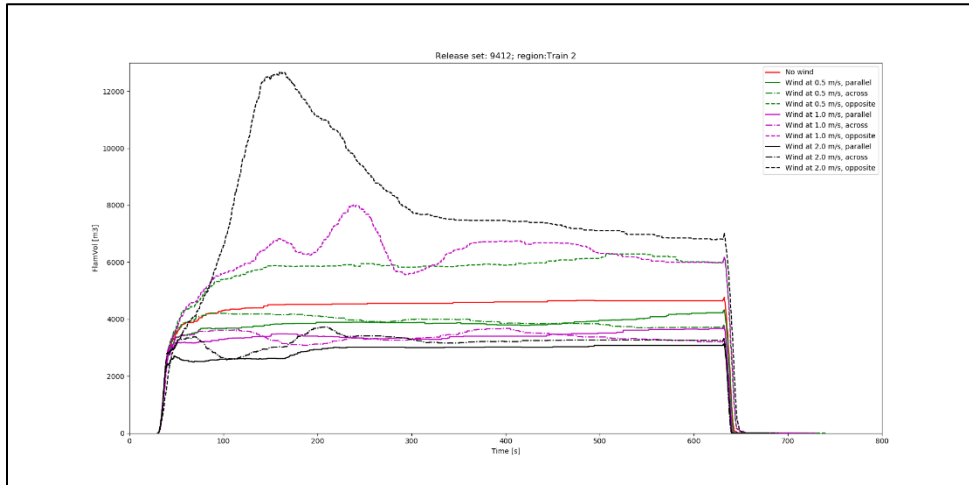
2" LNG release to the North (scenario 04): FV (top), Q8 (mid), and Q9 (bot.) ESC for Train 2 area.



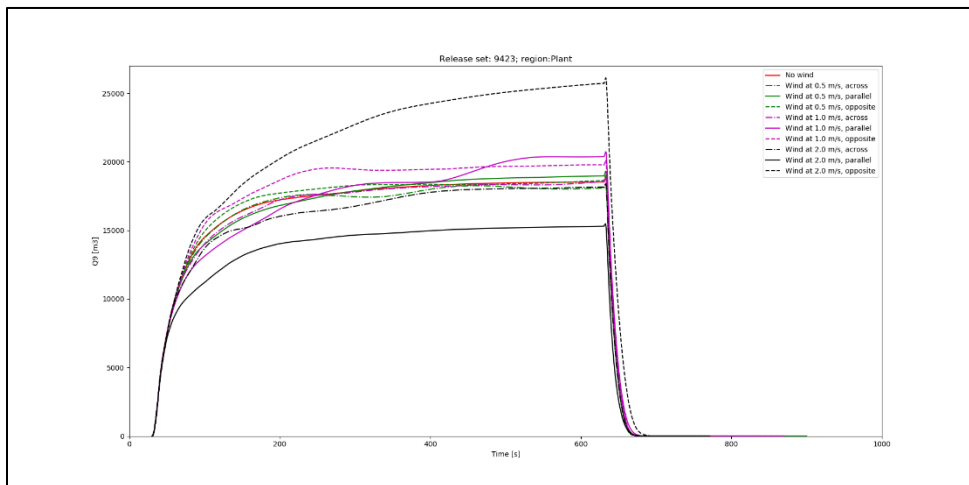
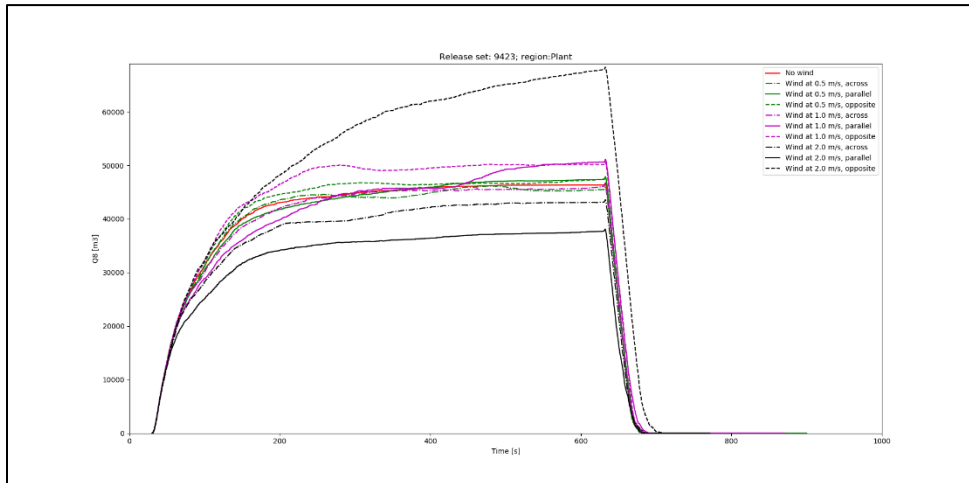
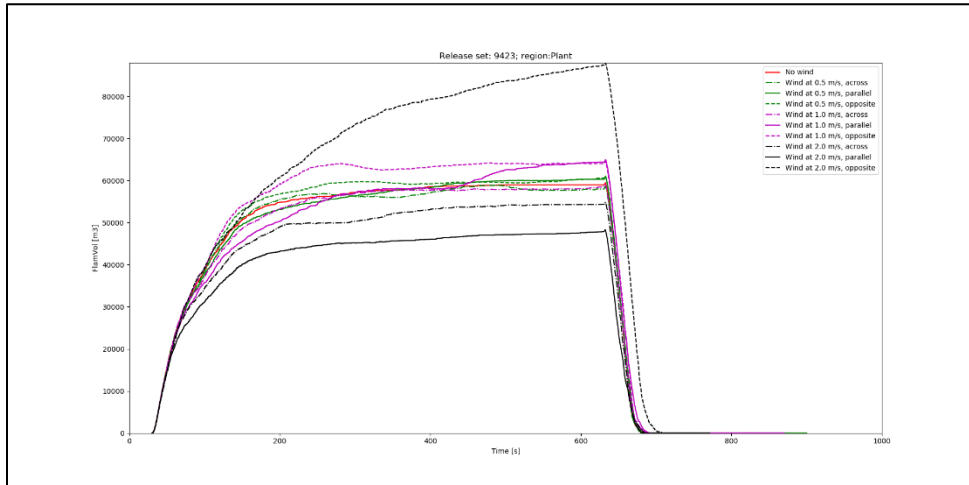
3" LNG release to the West (scenario 04): FV (top), Q8 (mid), and Q9 (bot.) ESC for Plant area.



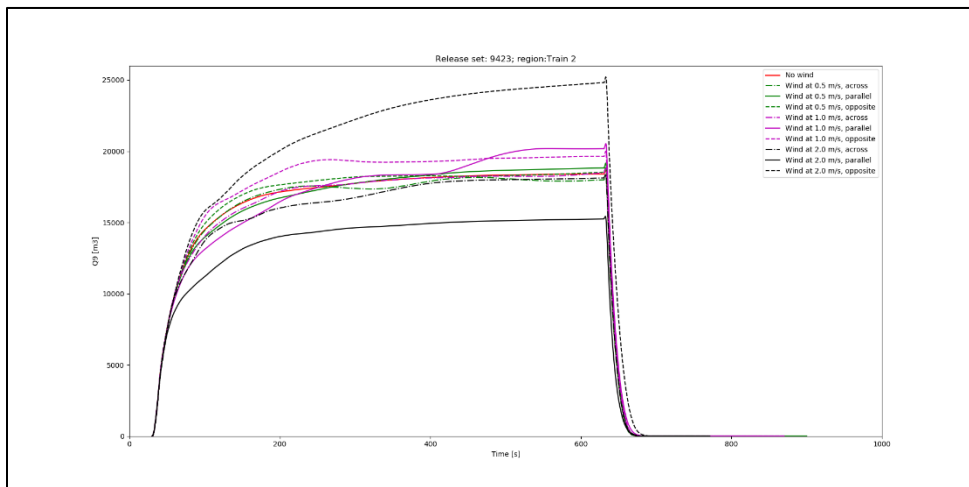
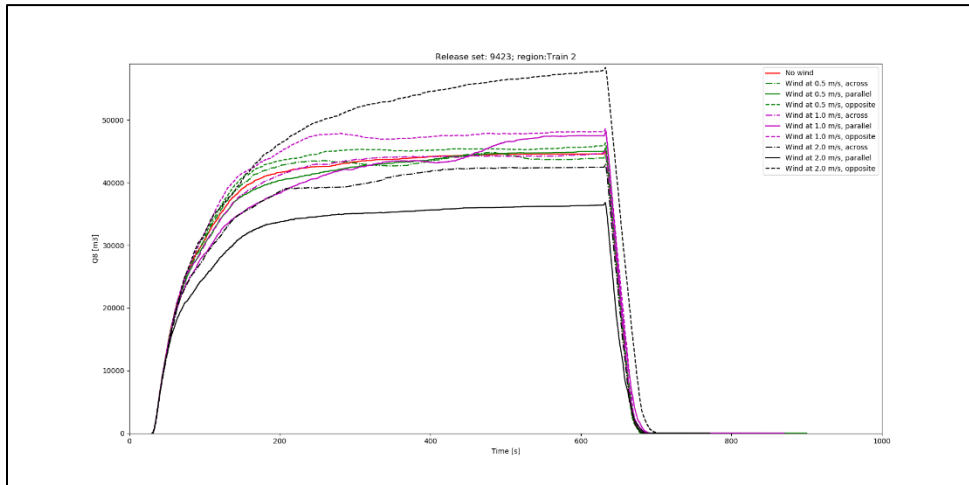
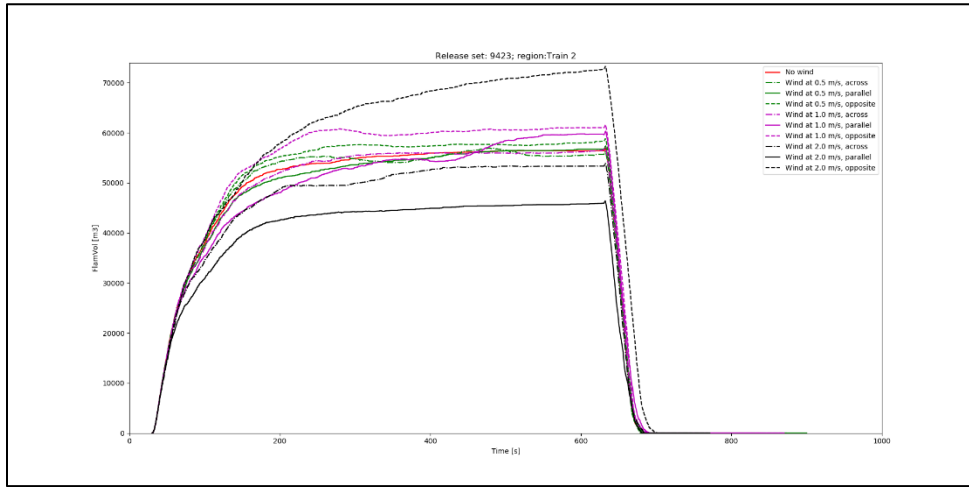
3" LNG release to the West (scenario 04): FV (top), Q8 (mid), and Q9 (bot.) ESC for Train 1 area.



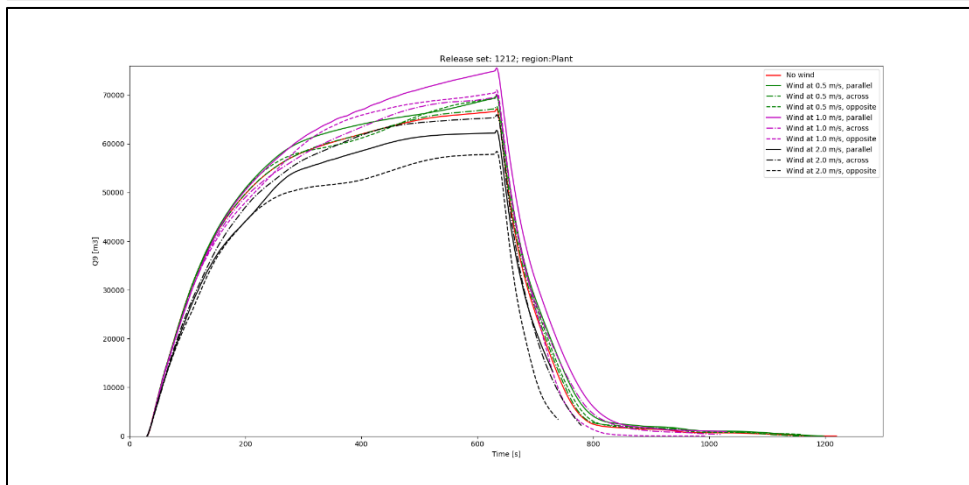
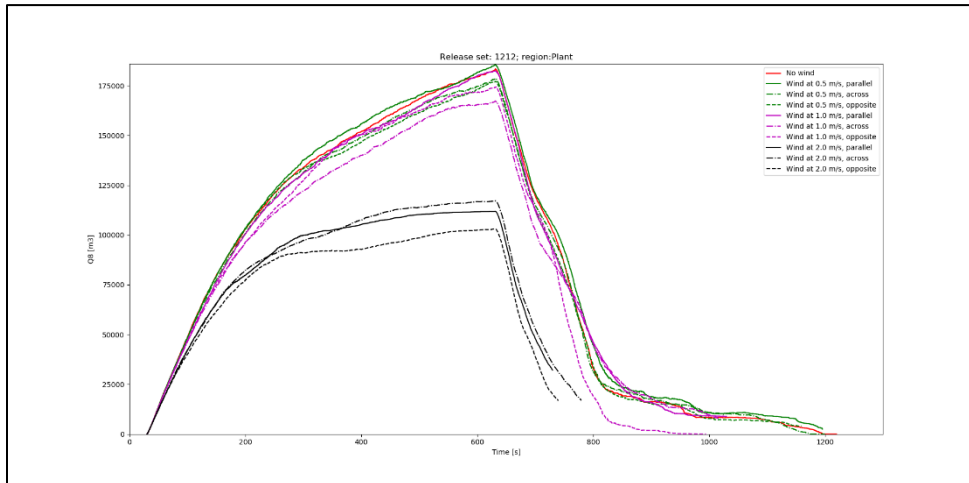
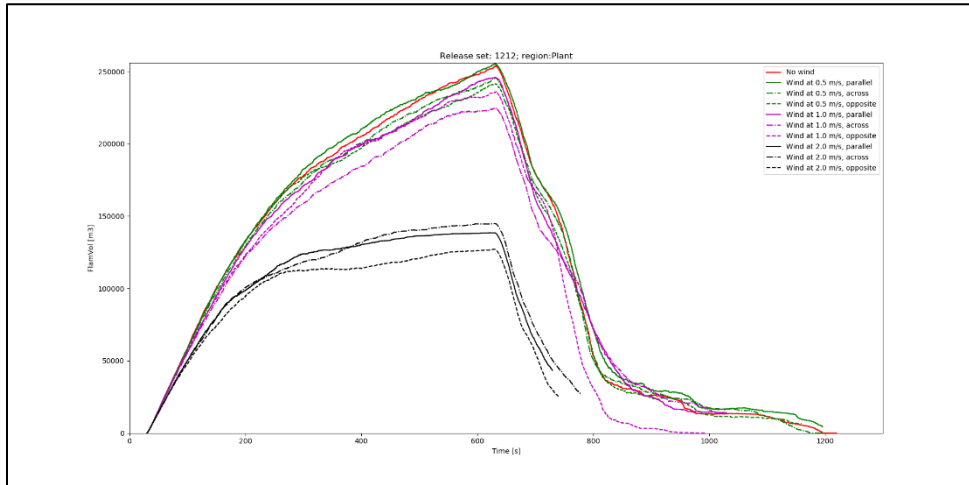
3" LNG release to the West (scenario 04): FV (top), Q8 (mid), and Q9 (bot.) ESC for Train 2 area.



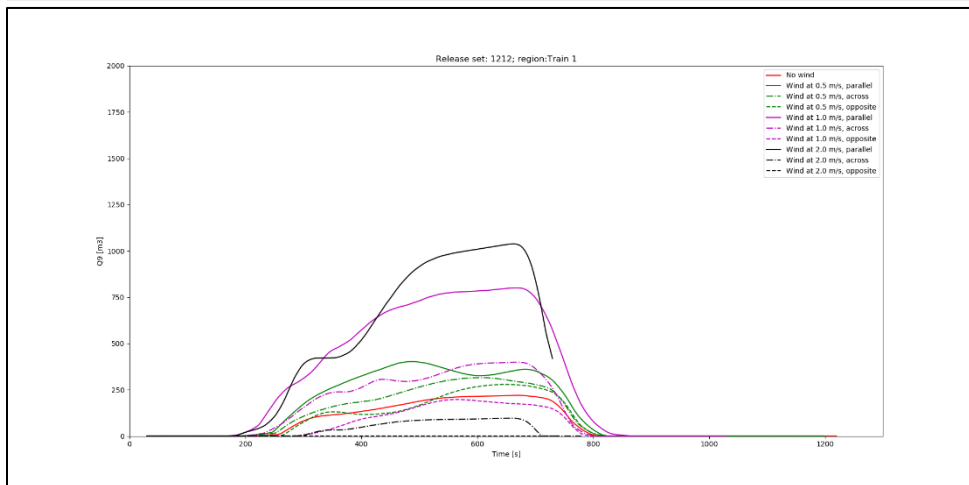
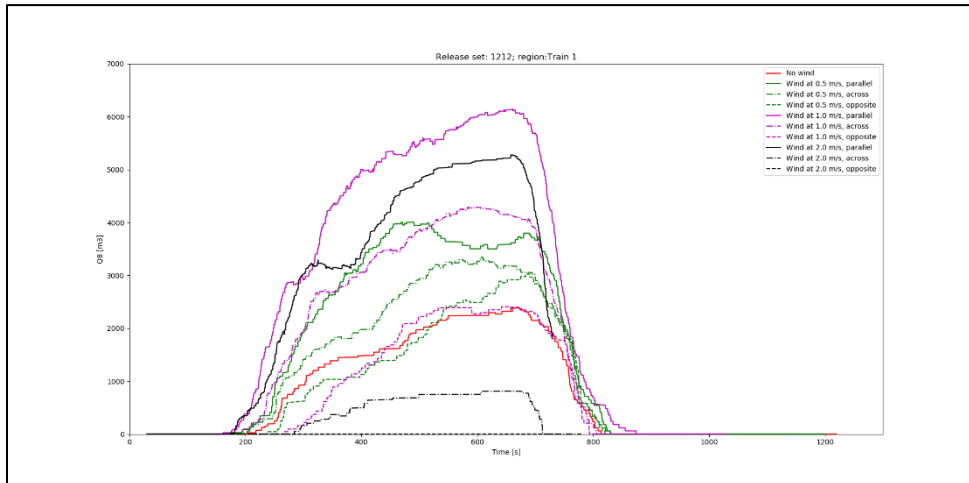
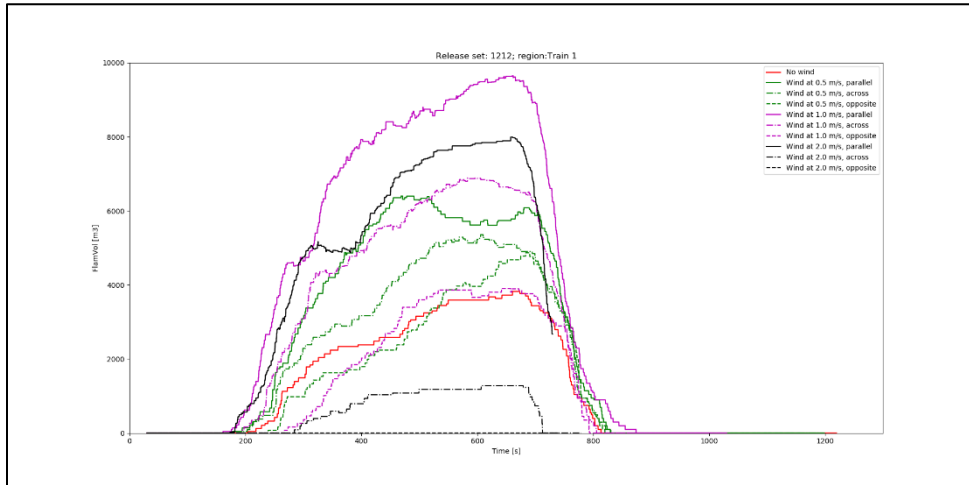
3" LNG release to the North (scenario 04): FV (top), Q8 (mid), and Q9 (bot.) ESC for Plant area.



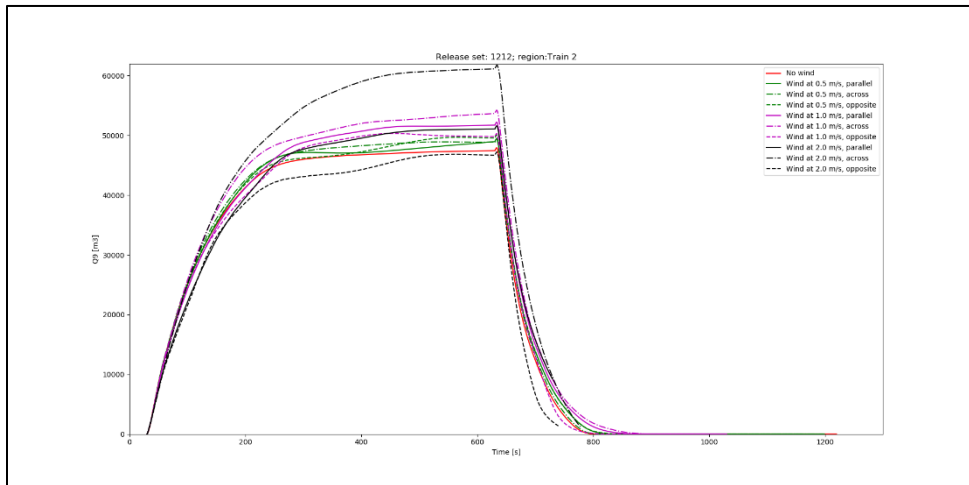
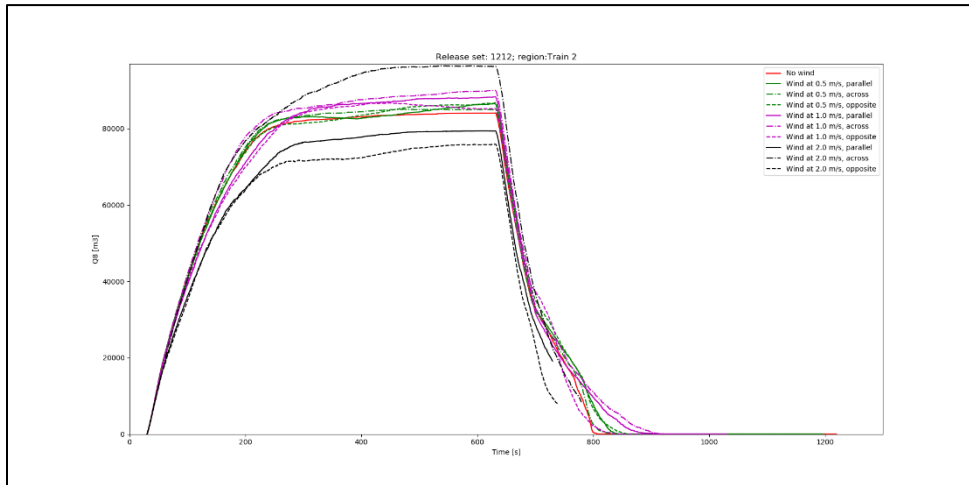
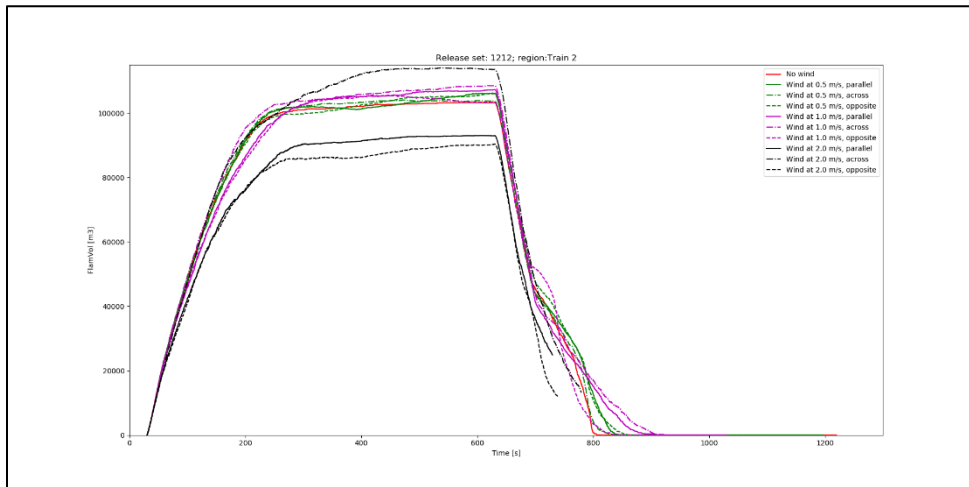
3" LNG release to the North (scenario 04): FV (top), Q8 (mid), and Q9 (bot.) ESC for Train 2 area.



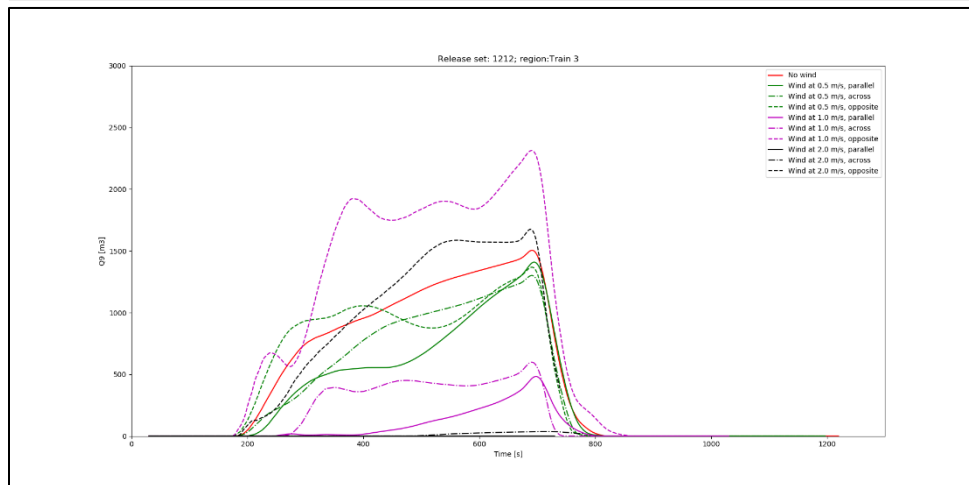
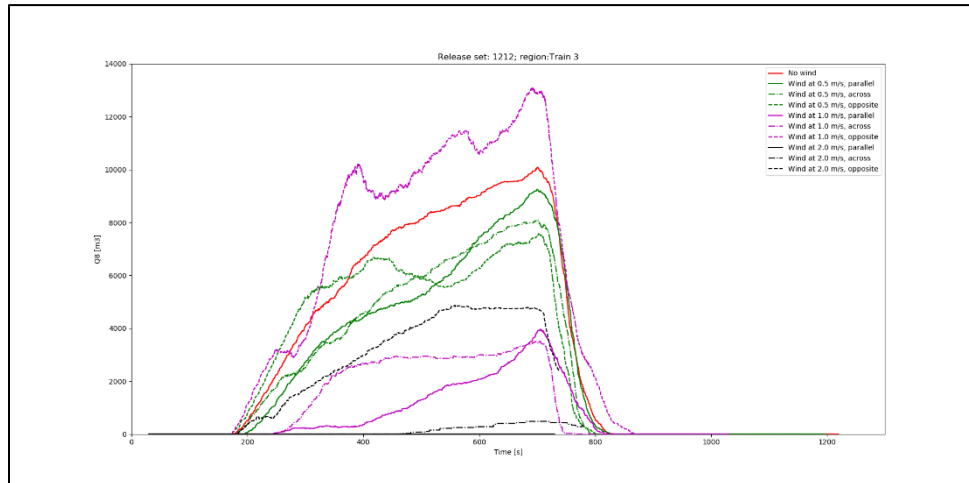
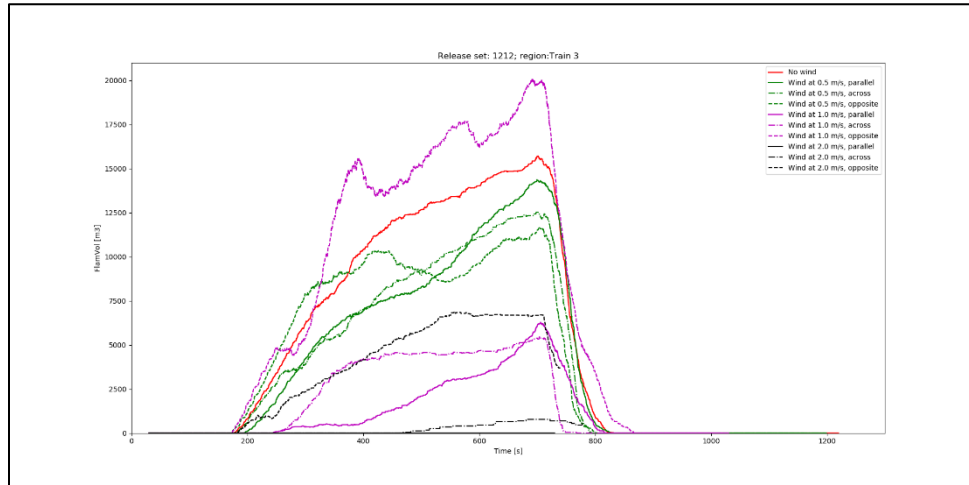
2" MR release to the West (scenario 12): FV (top), Q8 (mid), and Q9 (bot.) ESC for Plant area.



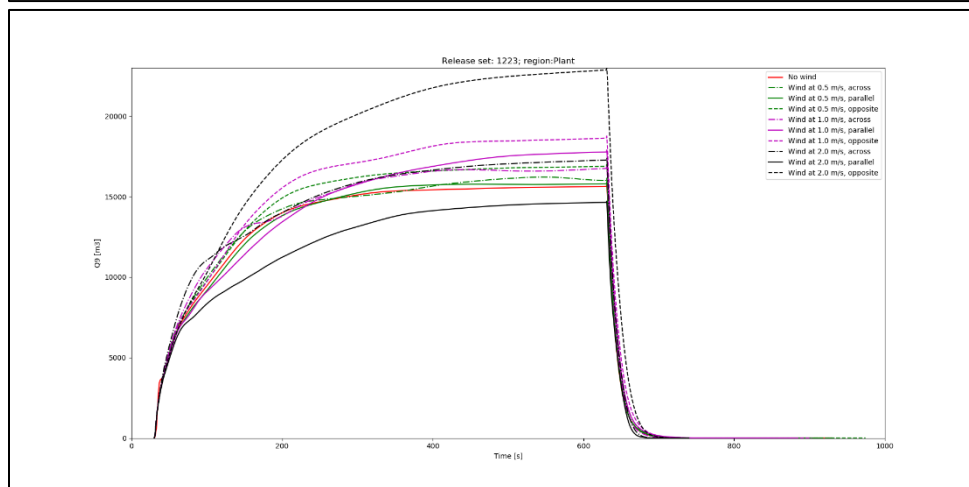
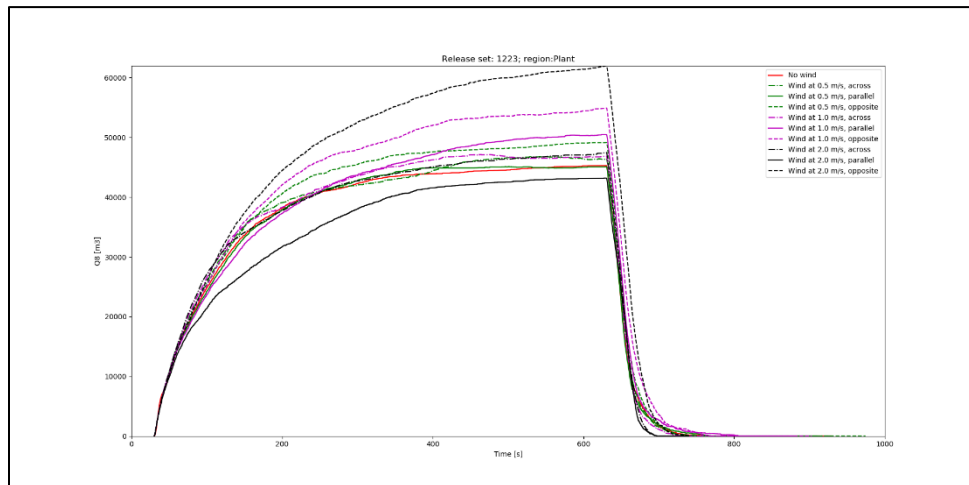
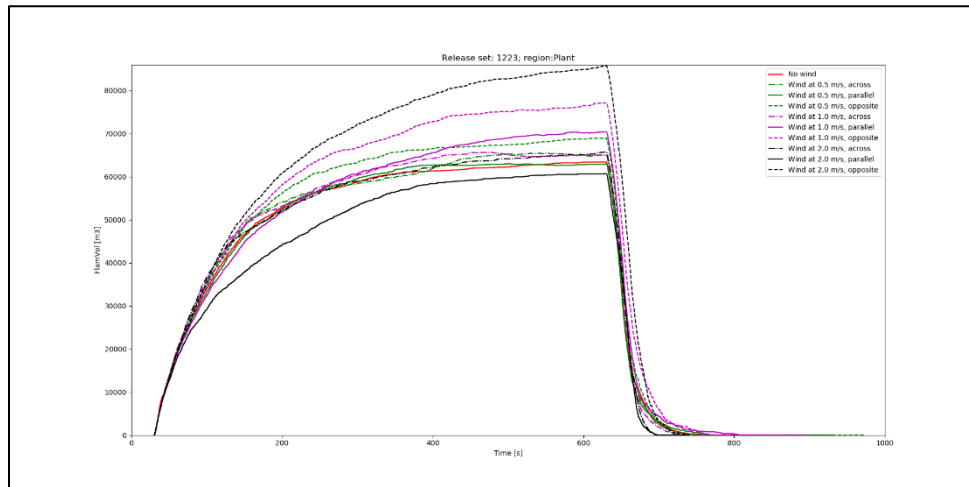
2" MR release to the West (scenario 12): FV (top), Q8 (mid), and Q9 (bot.) ESC for Train 1 area.



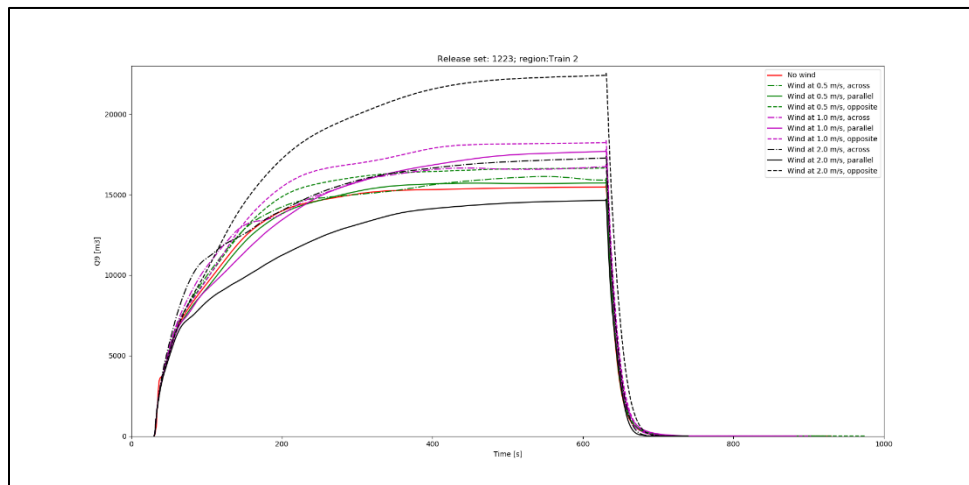
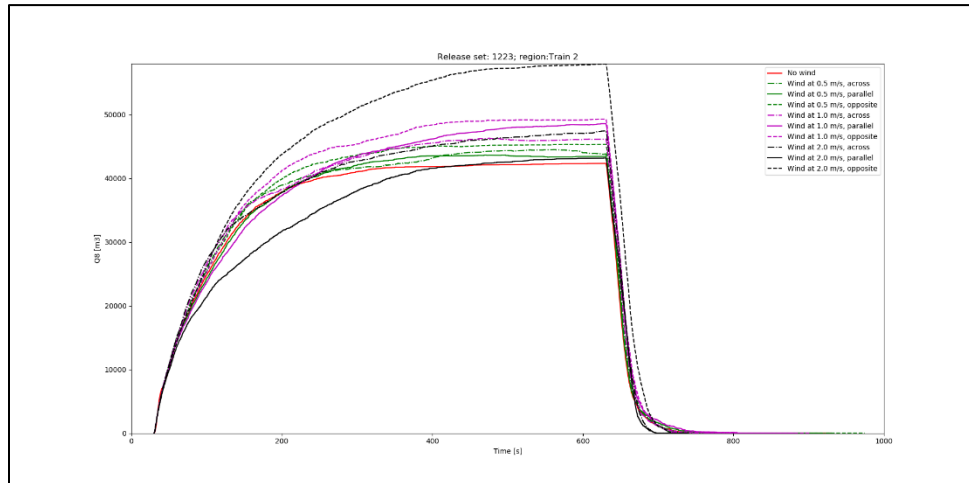
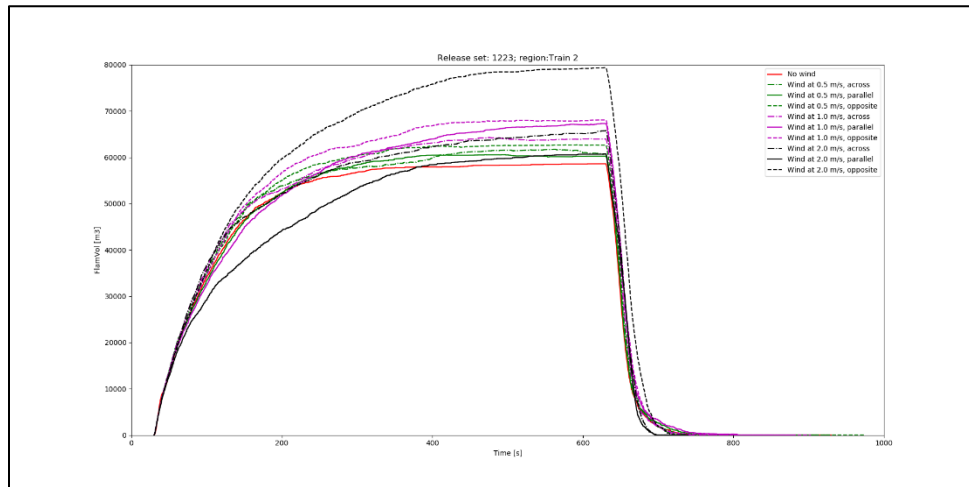
2" MR release to the West (scenario 12): FV (top), Q8 (mid), and Q9 (bot.) ESC for Train 2 area.



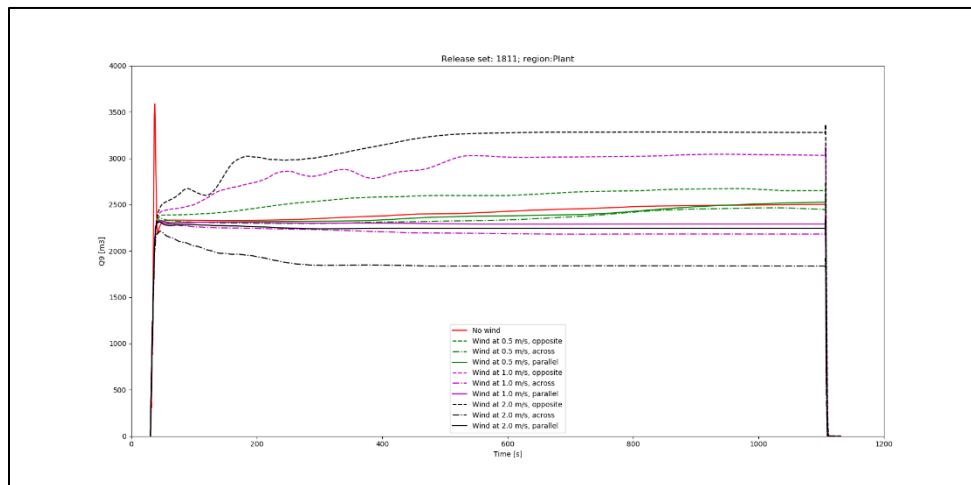
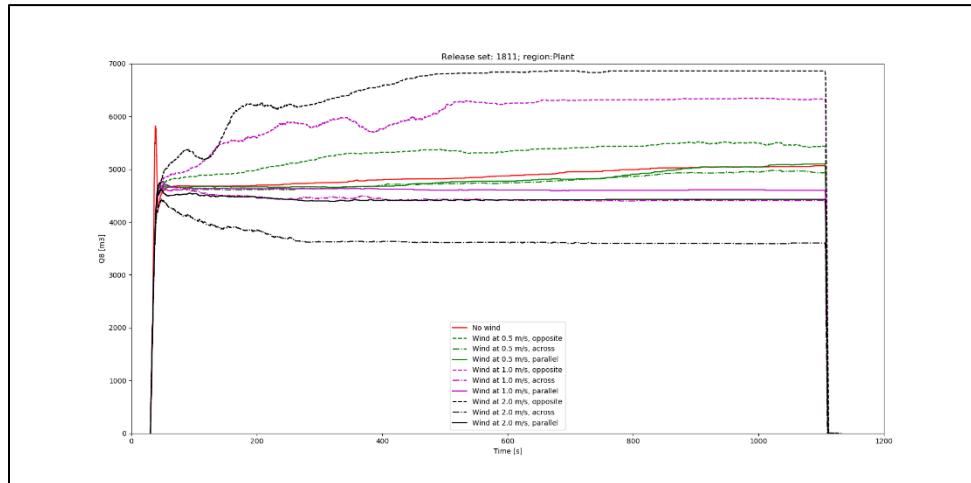
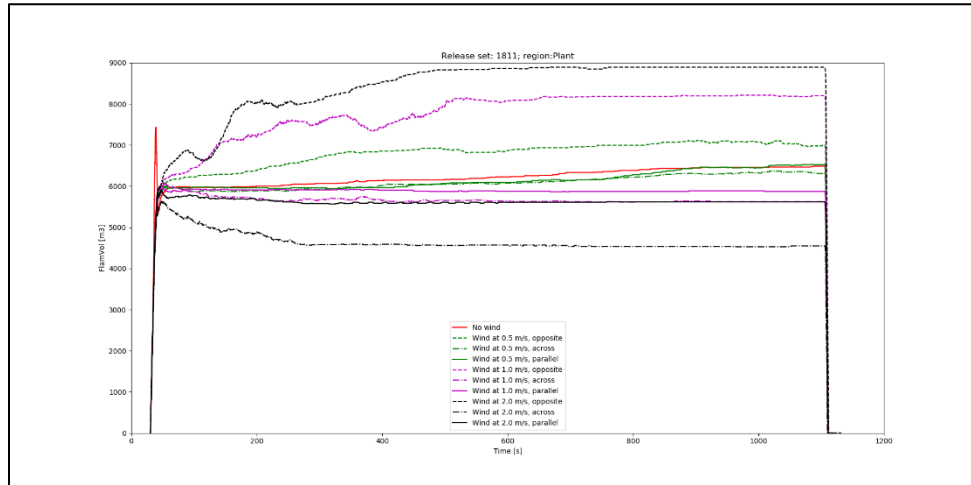
2" MR release to the West (scenario 12): FV (top), Q8 (mid), and Q9 (bot.) ESC for Train 3 area.



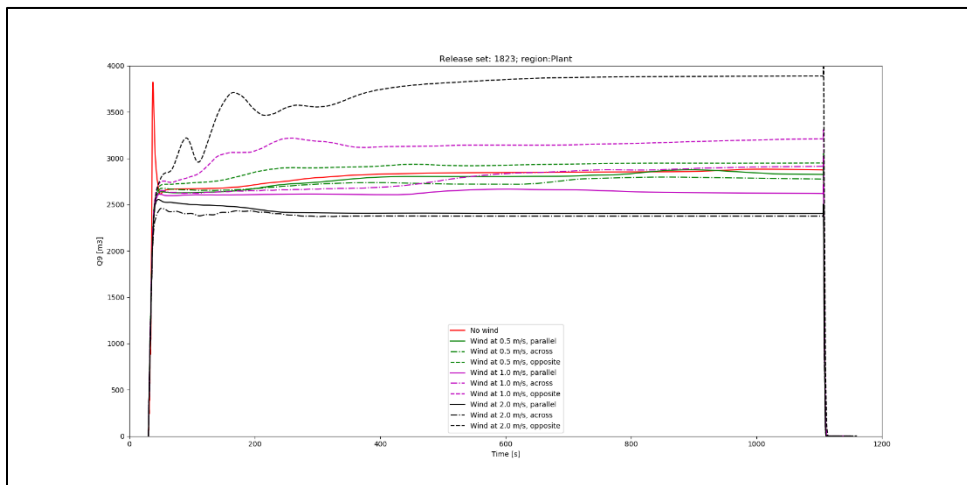
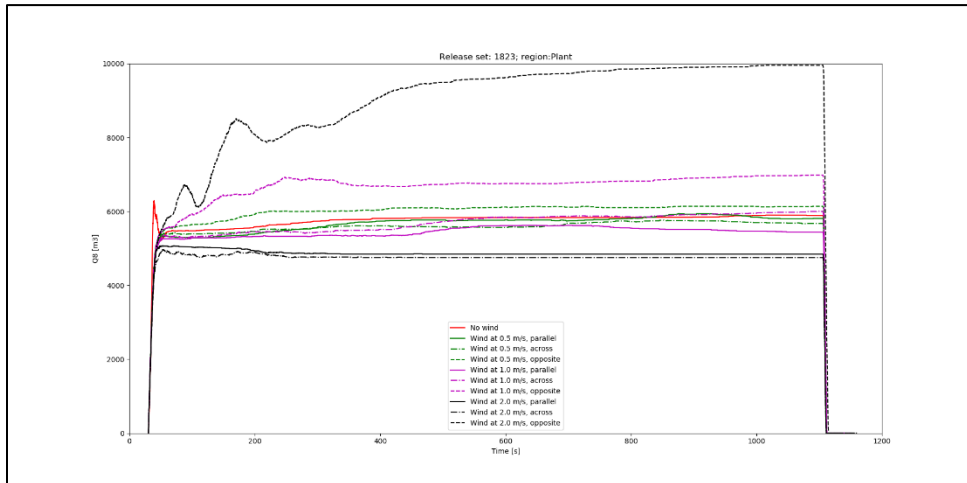
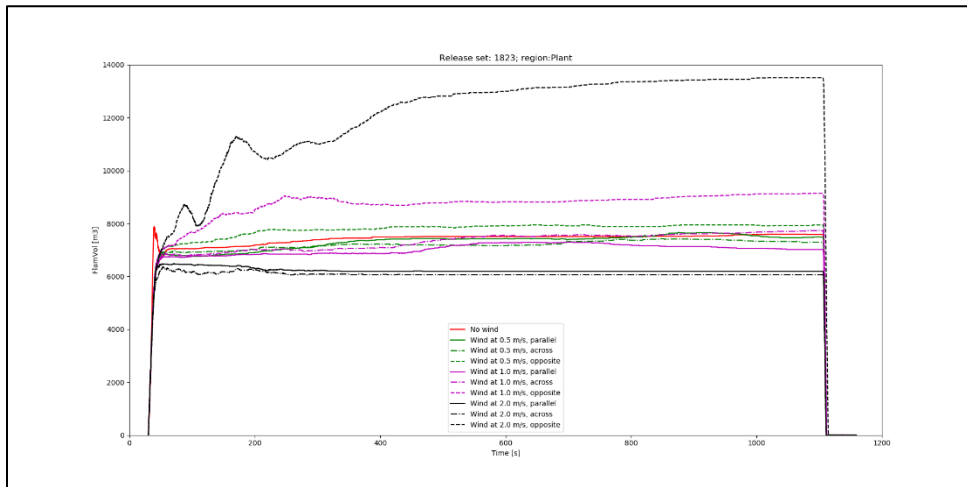
2" MR release to the North (scenario 12): FV (top), Q8 (mid), and Q9 (bot.) ESC for Plant area.



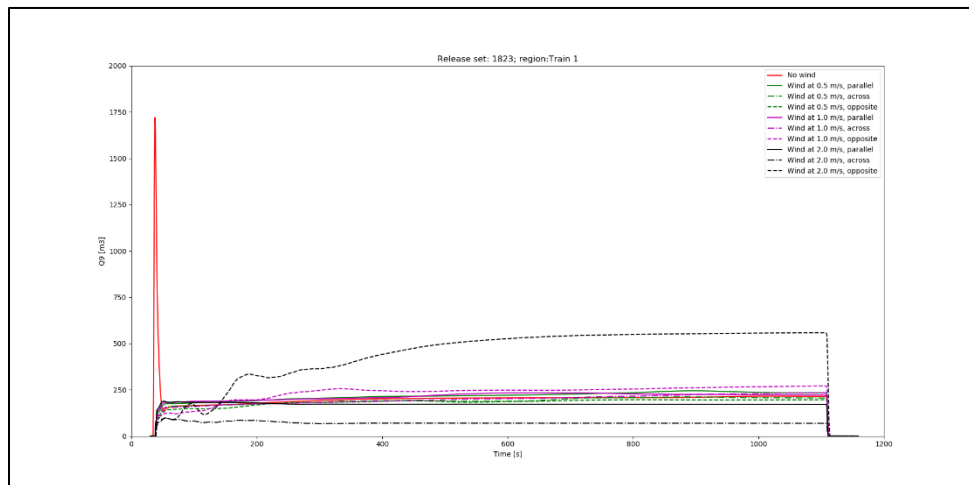
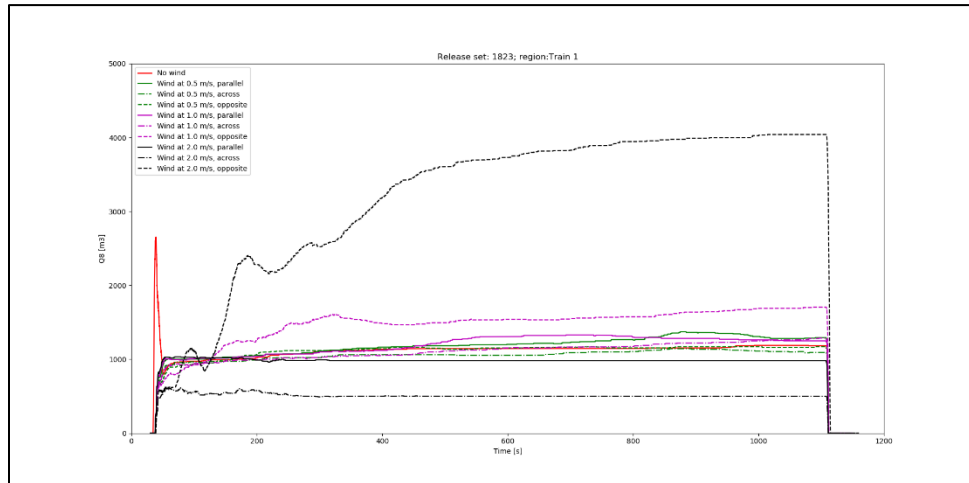
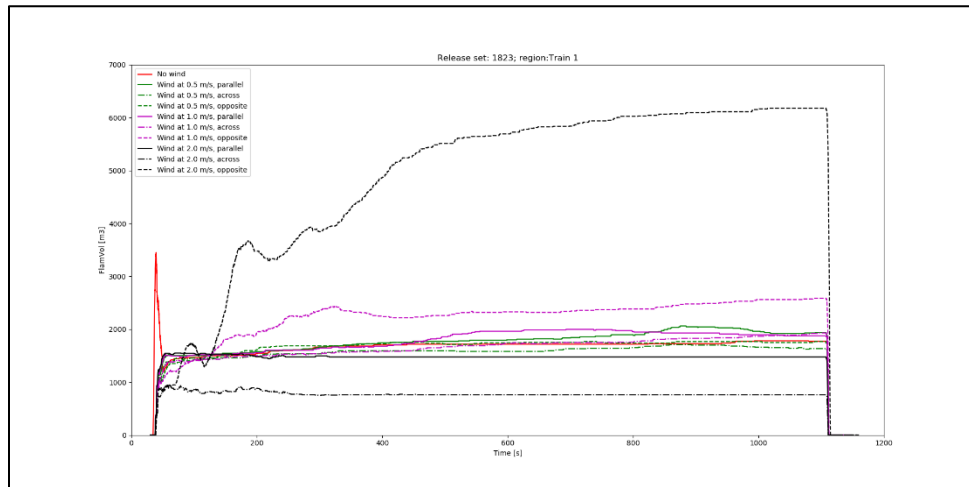
2" MR release to the North (scenario 12): FV (top), Q8 (mid), and Q9 (bot.) ESC for Train 2 area.



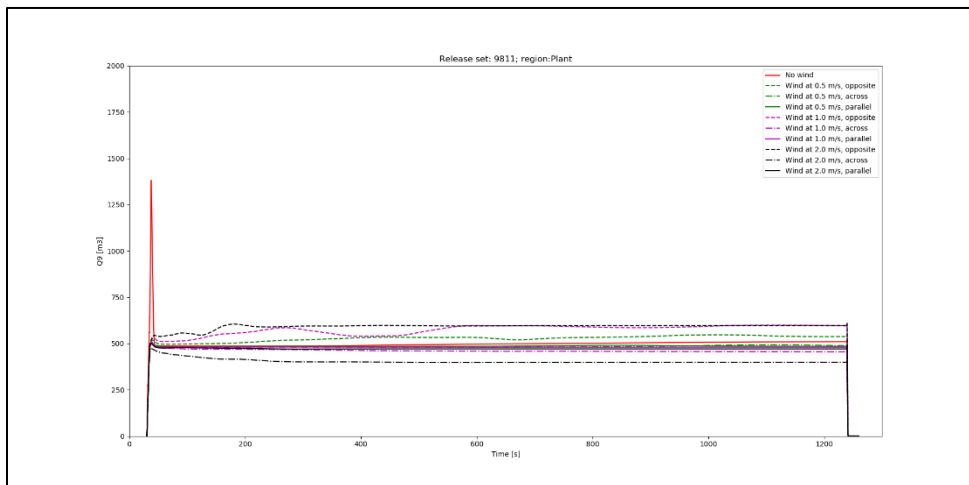
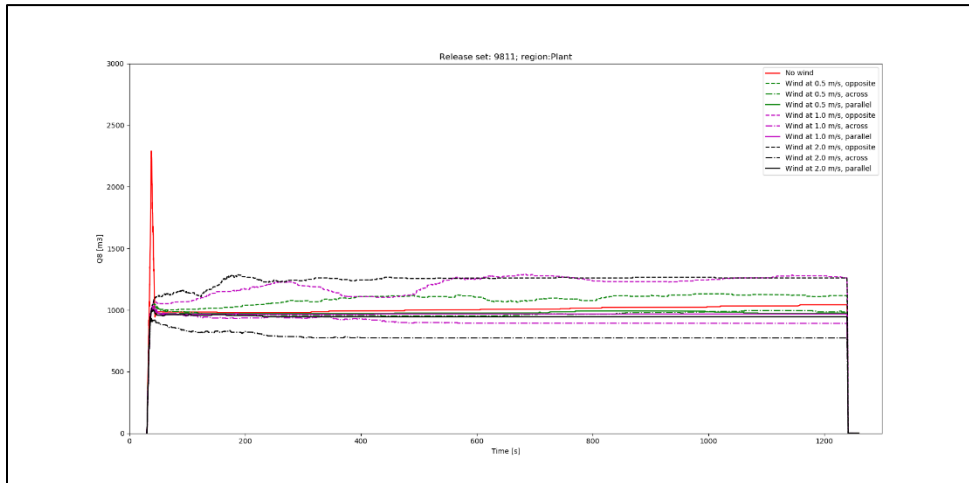
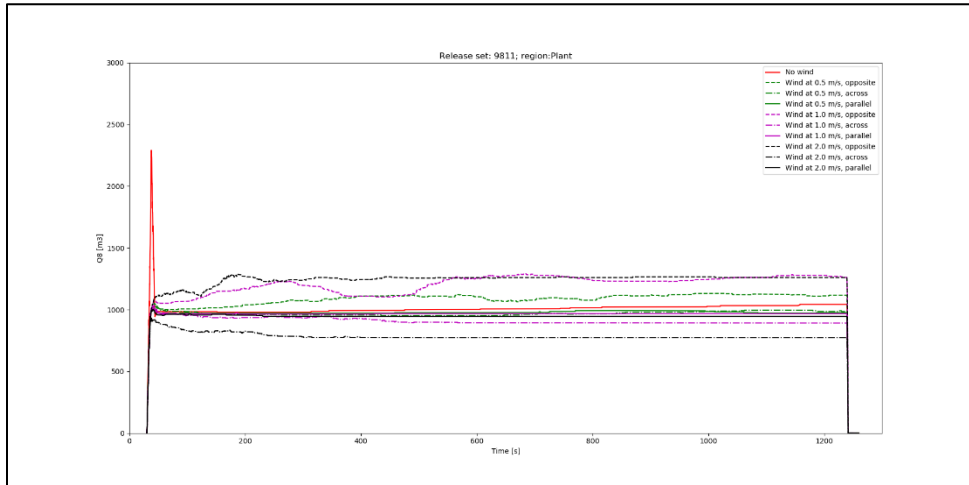
3" PRO release to the East (scenario 18): FV (top), Q8 (mid), and Q9 (bot.) ESC for Plant area.



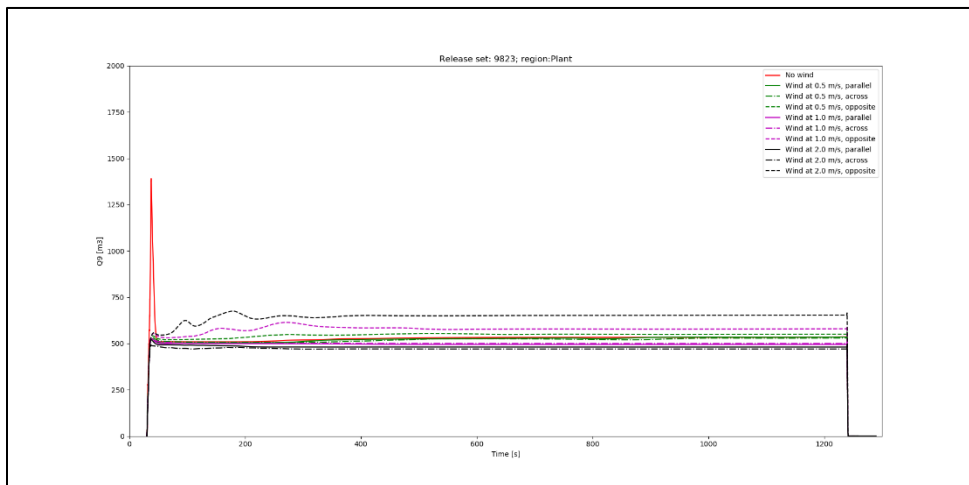
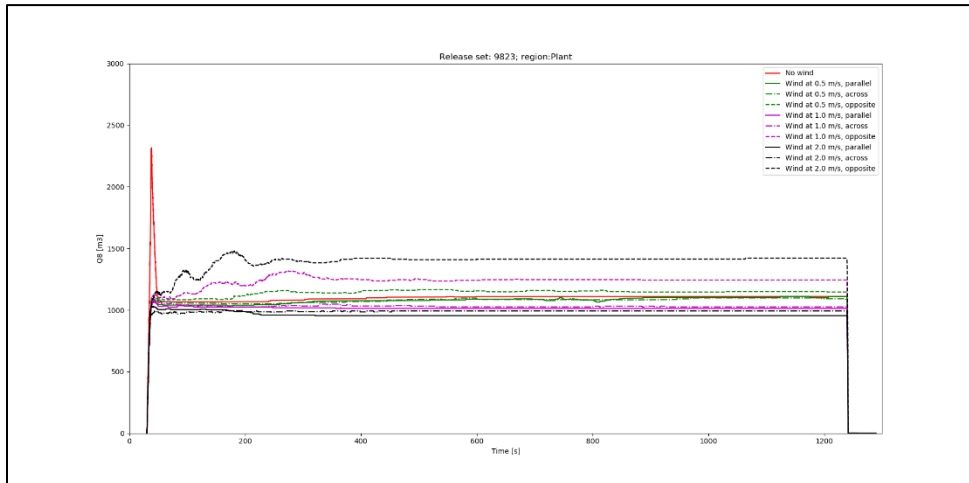
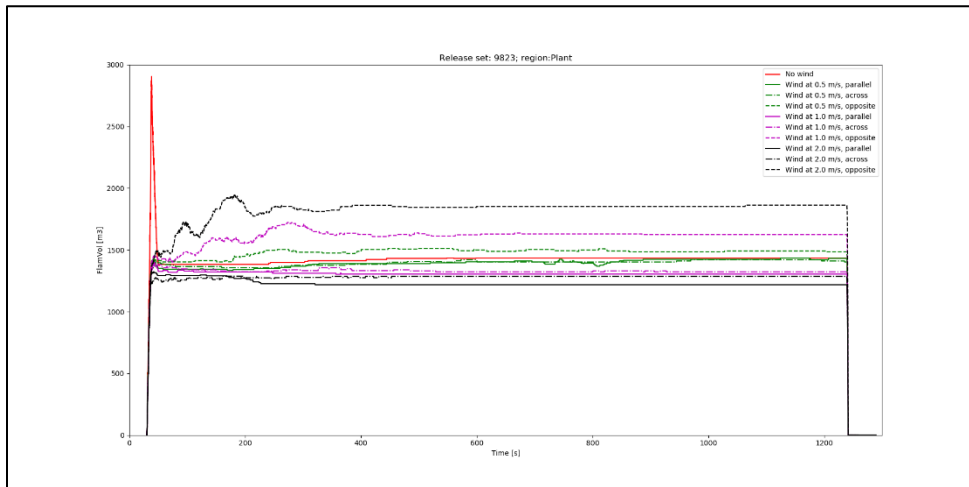
3" PRO release to the North (scenario 18): FV (top), Q8 (mid), and Q9 (bot.) ESC for Plant area.



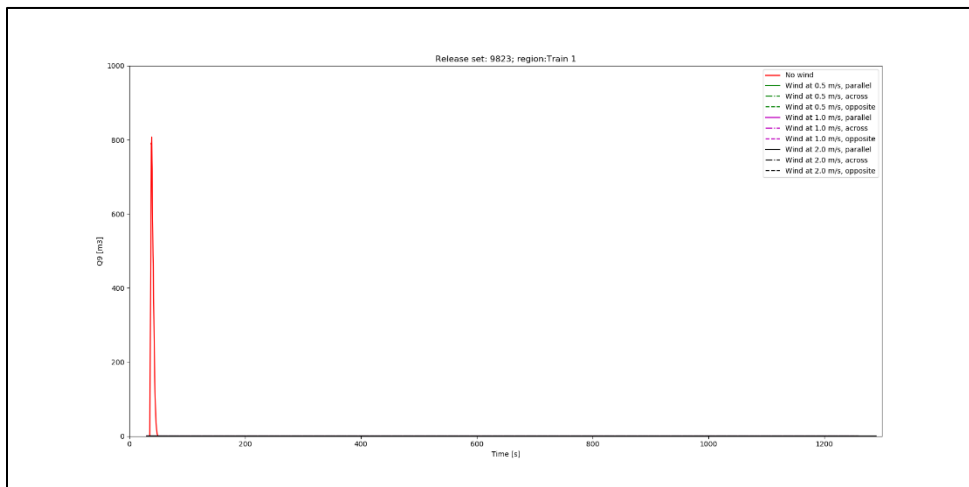
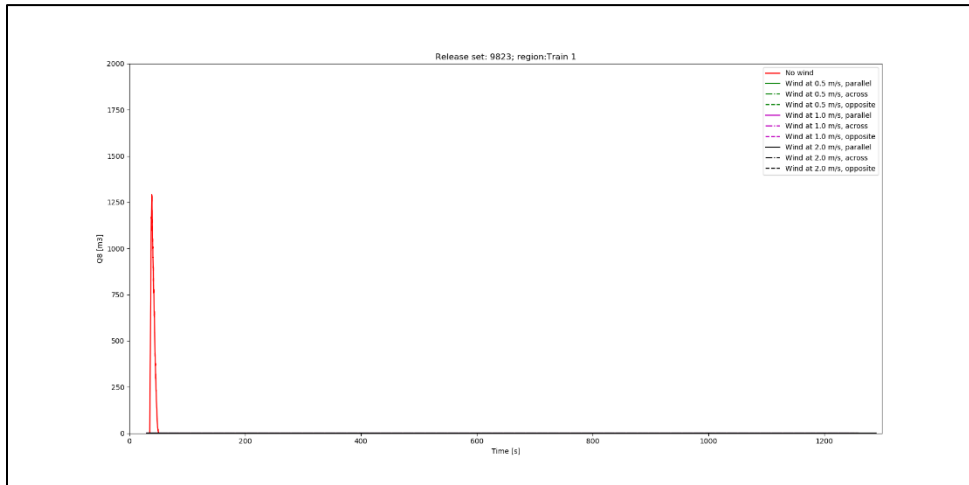
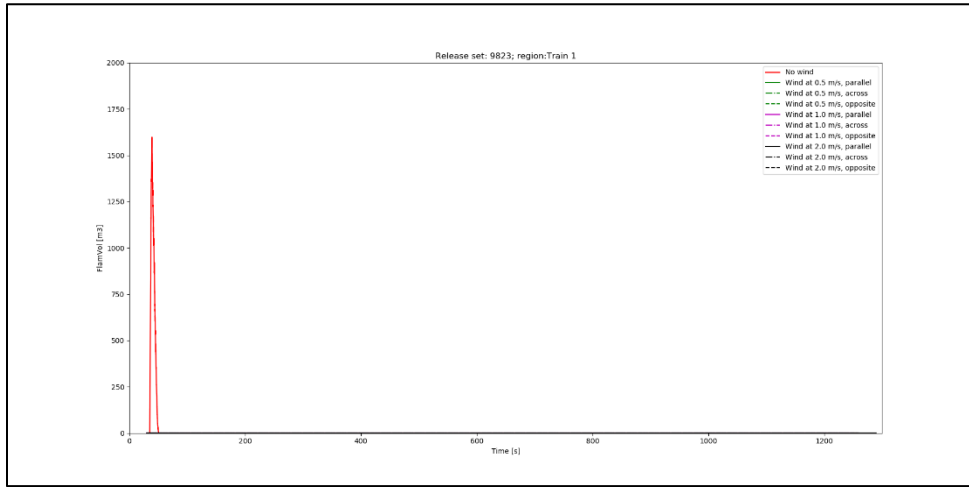
3" PRO release to the North (scenario 18): FV (top), Q8 (mid), and Q9 (bot.) ESC for Train 1 area.



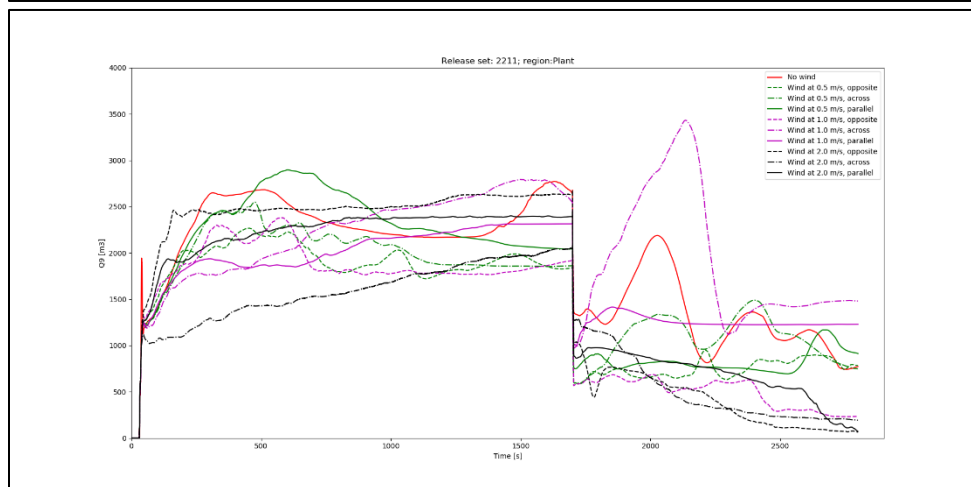
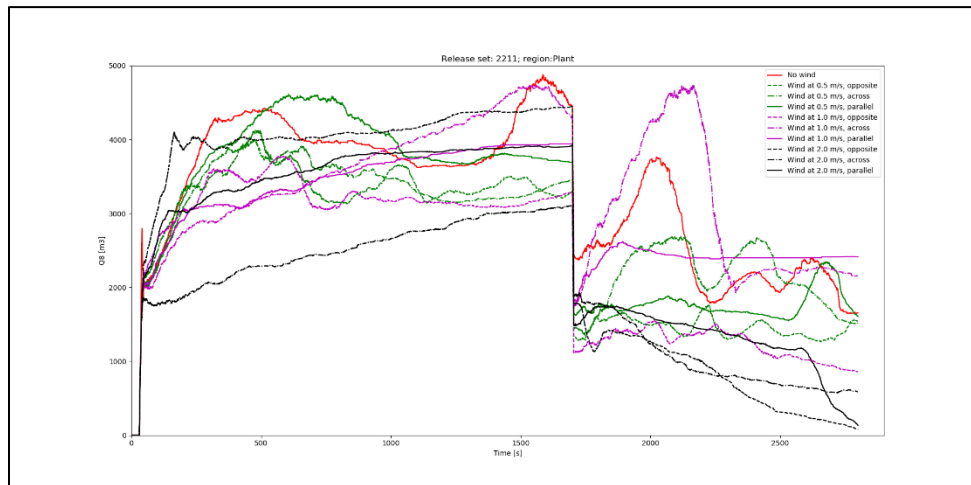
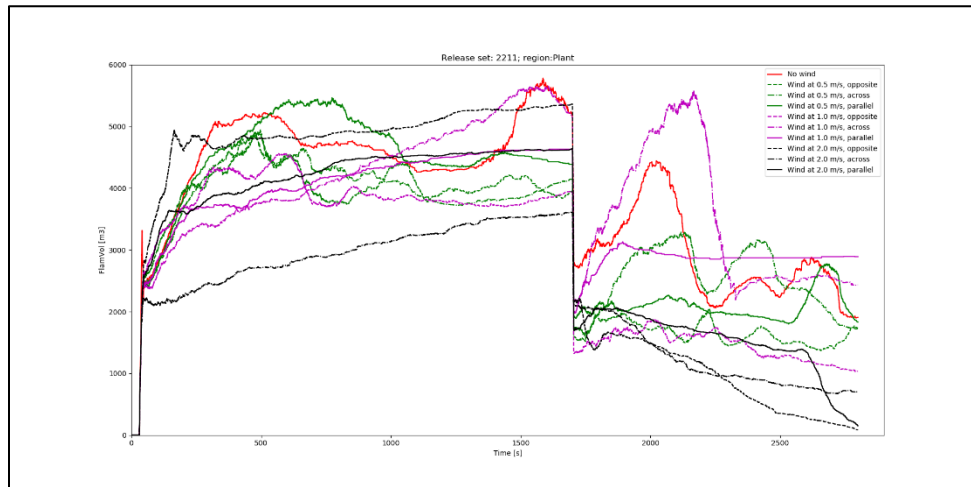
2" PRO release to the East (scenario 18): FV (top), Q8 (mid), and Q9 (bot.) ESC for Plant area.



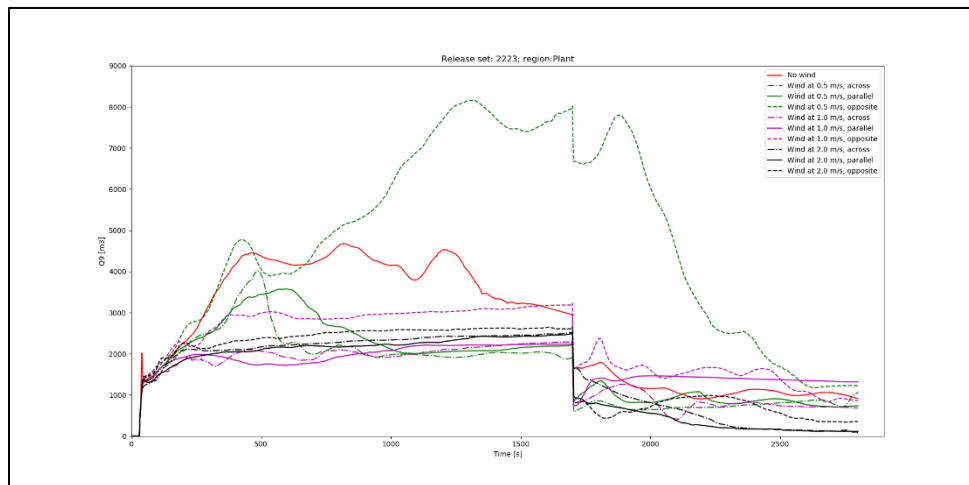
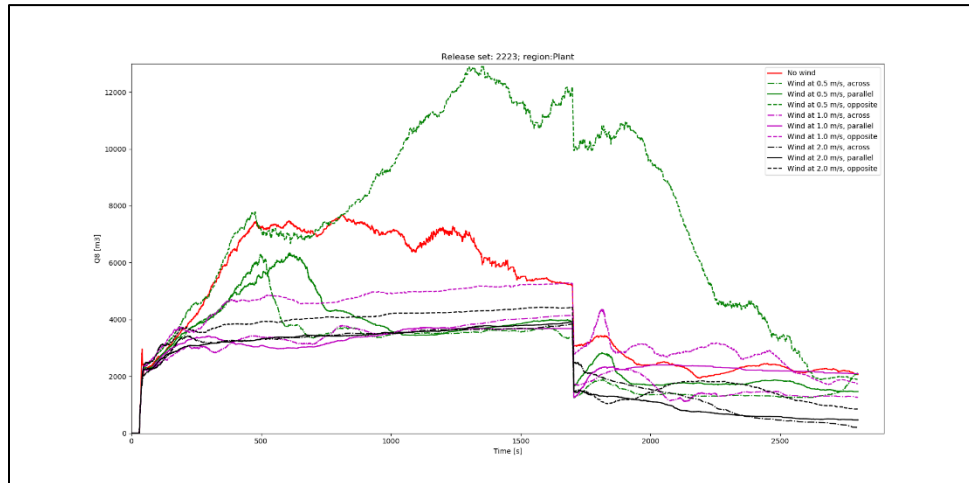
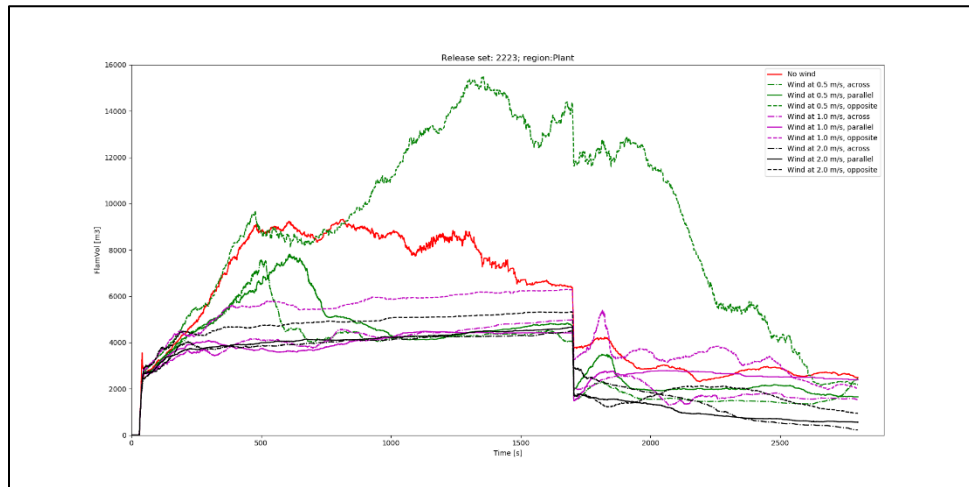
2" PRO release to the North (scenario 18): FV (top), Q8 (mid), and Q9 (bot.) ESC for Plant area.



2" PRO release to the North (scenario 18): FV (top), Q8 (mid), and Q9 (bot.) ESC for Train 1 area.



3" BUT release to the East (scenario 22): FV (top), Q8 (mid), and Q9 (bot.) ESC for Plant area.

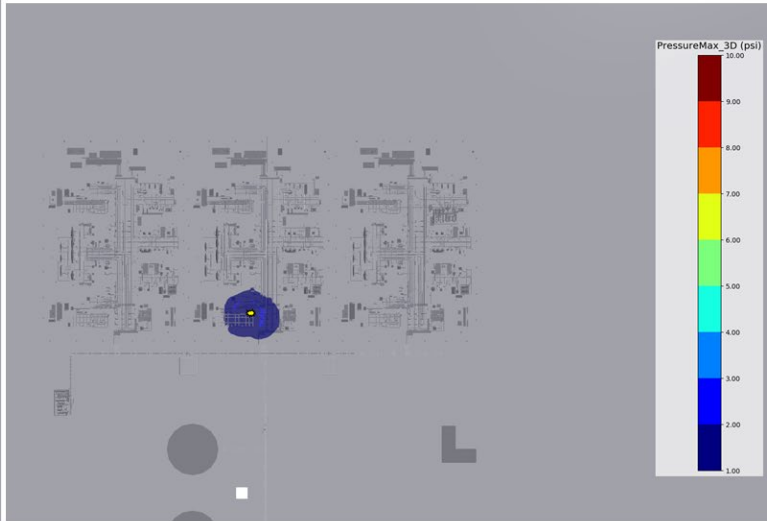


3" BUT release to the North (scenario 22): FV (top), Q8 (mid), and Q9 (bot.) ESC for Plant area.

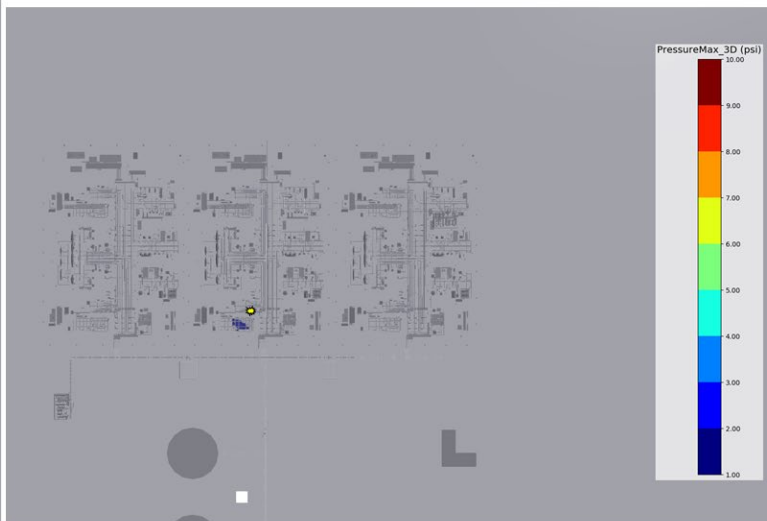
	<b>Vapor Cloud Explosions at Nil Wind</b>	03904-RP-006
	PHMSA	Rev A
	Final Report	Page 184 of 213

## Appendix C – Vapor Cloud Explosion Results

	Vapor Cloud Explosions at Nil Wind	03904-RP-006
	PHMSA	Rev A
	Final Report	Page 185 of 213

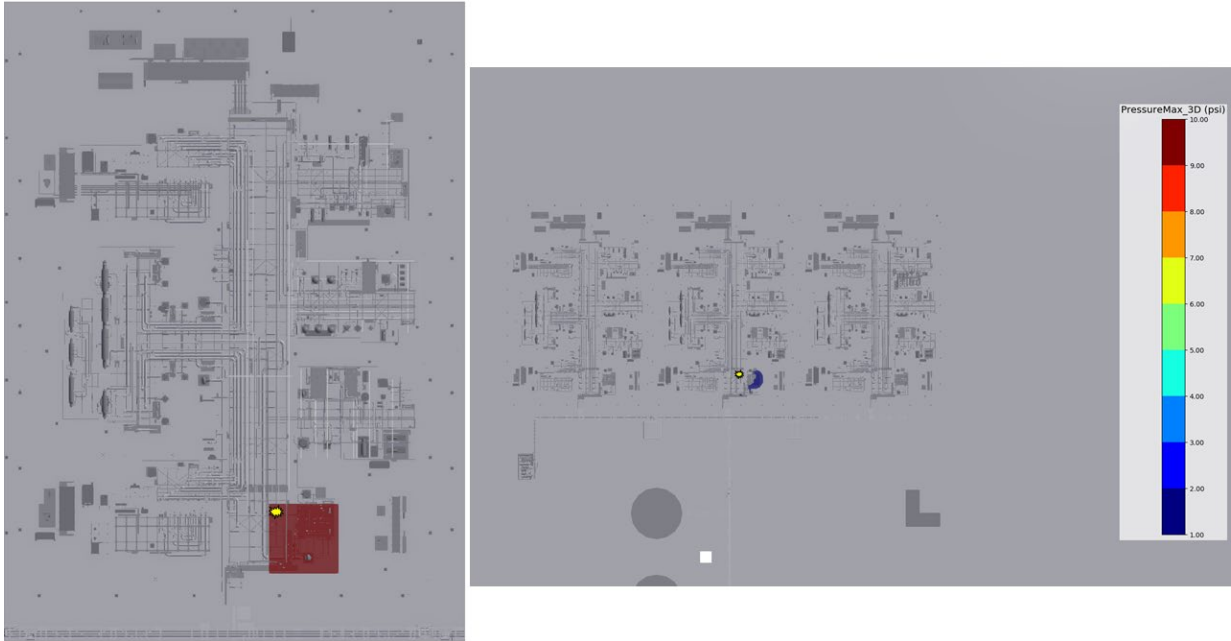


LNG cloud (scenario 00, nil wind): VCE from Q9 in lower left corner, with ignition in center: (left) cloud footprint; (right) peak overpressures  $\geq 1$  psig.

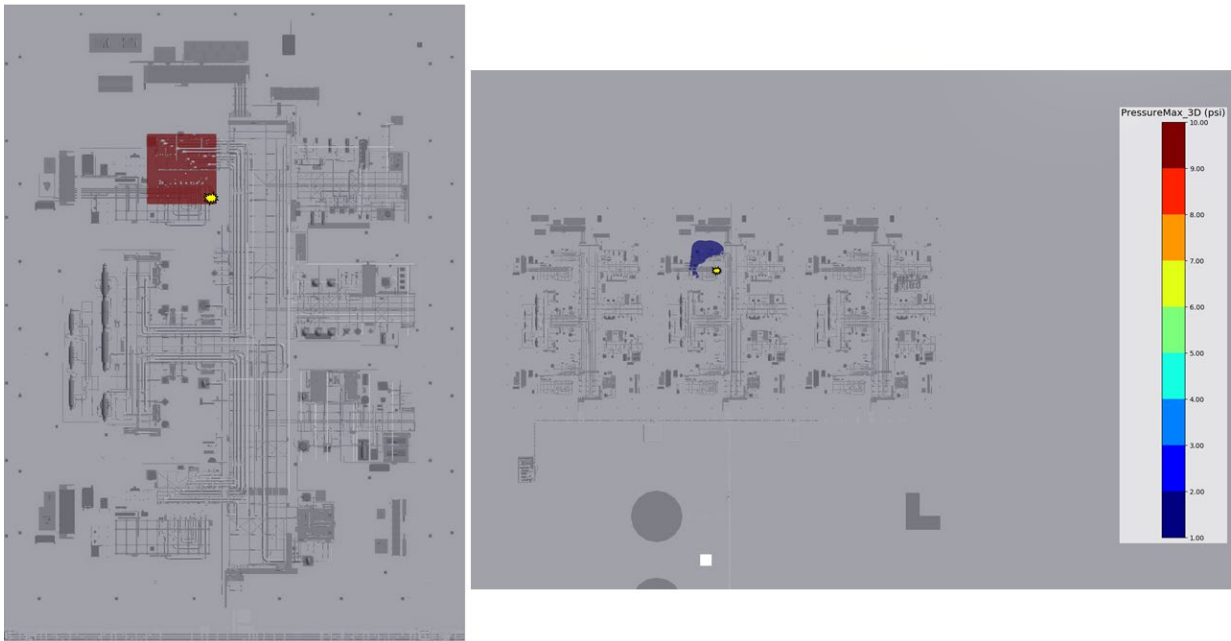


LNG cloud (scenario 00, nil wind): VCE from Q9 in lower left corner, with ignition in upper right corner: (left) cloud footprint; (right) peak overpressures  $\geq 1$  psig.

	Vapor Cloud Explosions at Nil Wind	03904-RP-006
	PHMSA	Rev A
	Final Report	Page 186 of 213

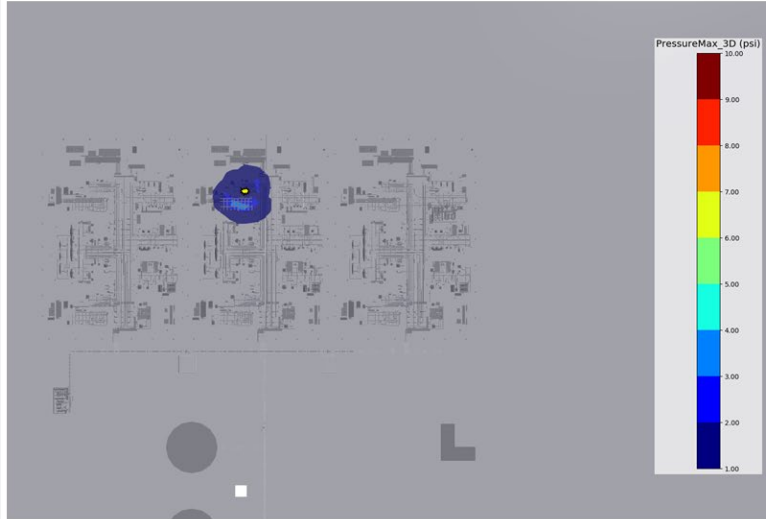


LNG cloud (scenario 00, nil wind): VCE from Q9 in lower right corner, with ignition in upper left corner: (left) cloud footprint; (right) peak overpressures  $\geq 1$  psig.

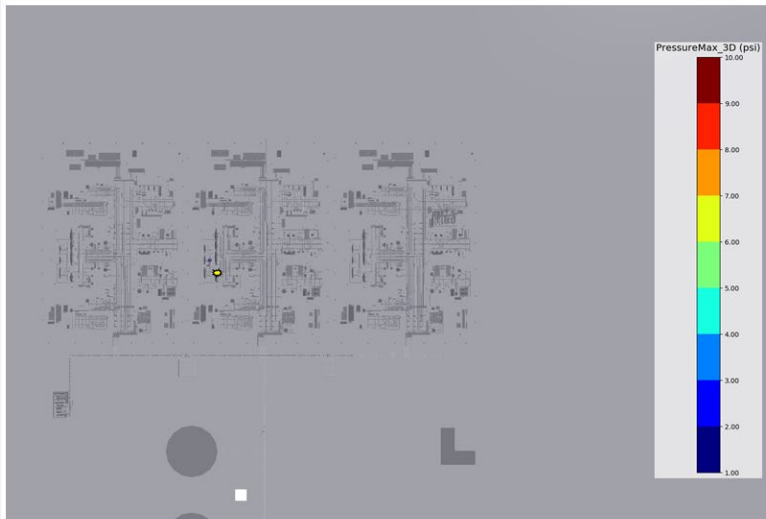
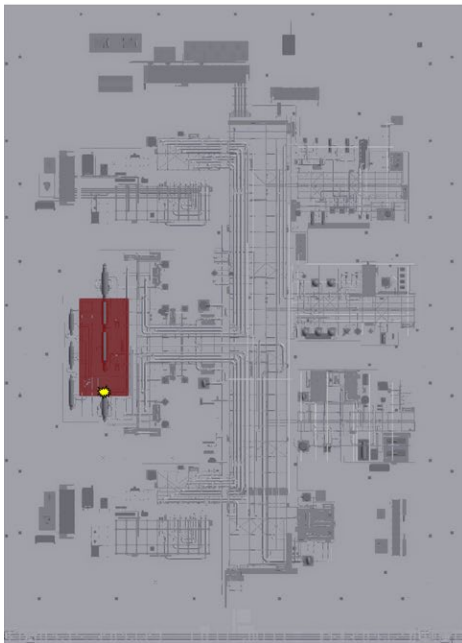


LNG cloud (scenario 00, nil wind): VCE from Q9 in upper left corner, with ignition in lower right corner: (left) cloud footprint; (right) peak overpressures  $\geq 1$  psig.

	Vapor Cloud Explosions at Nil Wind	03904-RP-006
	PHMSA	Rev A
	Final Report	Page 187 of 213

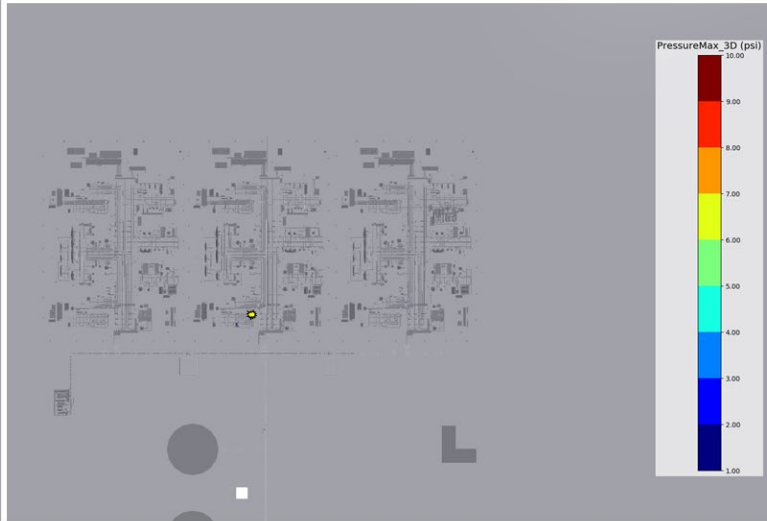
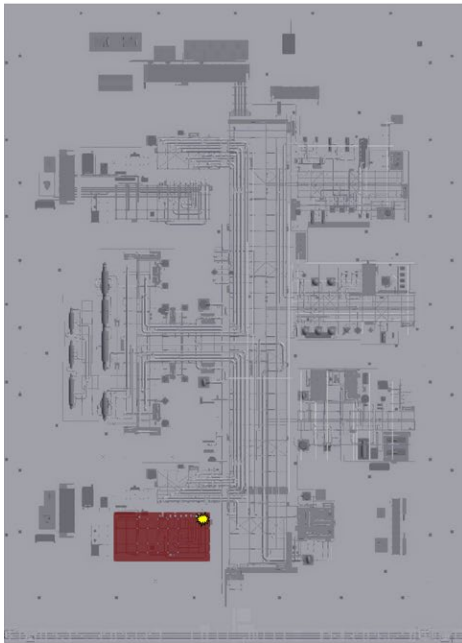


LNG cloud (scenario 00, nil wind): VCE from Q9 in upper left corner, with ignition in center: (left) cloud footprint; (right) peak overpressures  $\geq 1$  psig.

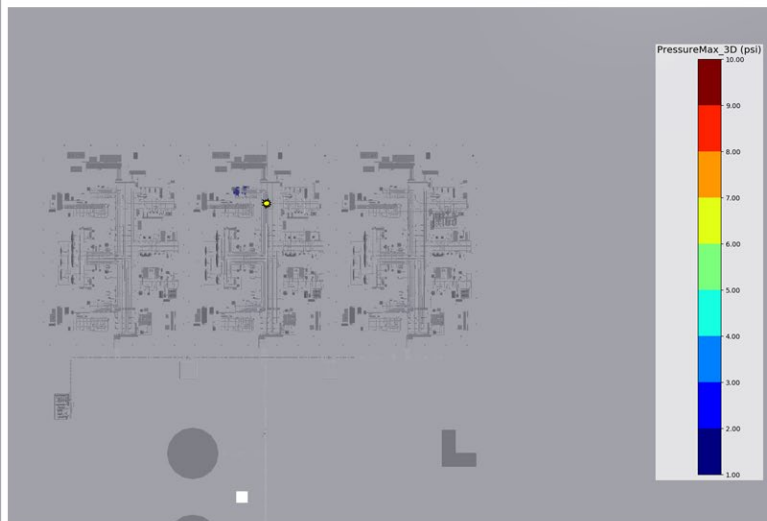


LNG cloud (scenario 00, nil wind): VCE from Q9 near middle left edge, with ignition in center of lower edge: (left) cloud footprint; (right) peak overpressures  $\geq 1$  psig.

	Vapor Cloud Explosions at Nil Wind	03904-RP-006
	PHMSA	Rev A
	Final Report	Page 188 of 213

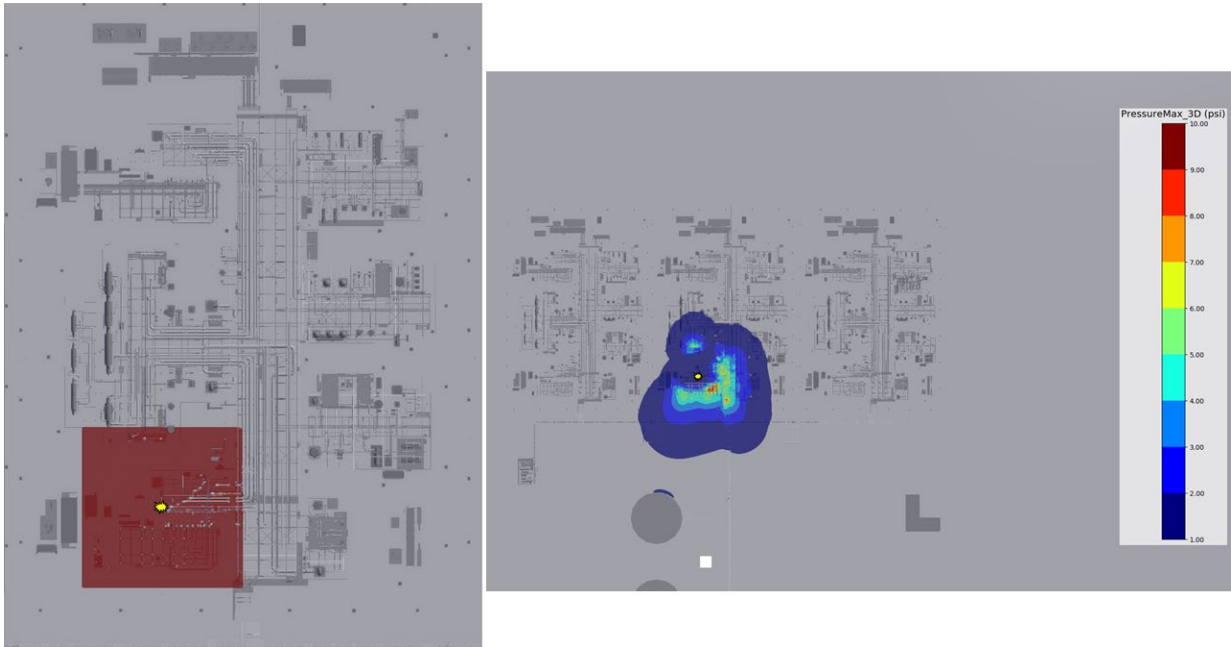


LNG cloud (scenario 00, nil wind): VCE from Q9 in lower left corner, with ignition in upper right corner: (left) cloud footprint; (right) peak overpressures  $\geq 1$  psig.

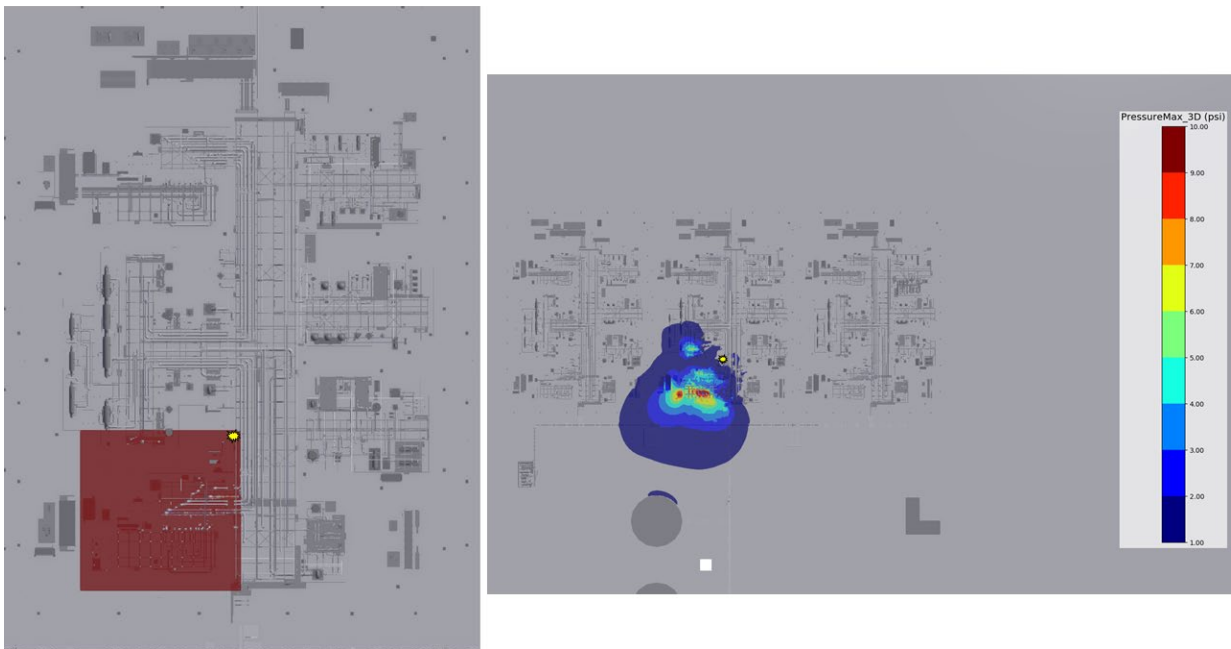


LNG cloud (scenario 00, nil wind): VCE from Q9 in upper left corner, with ignition in lower right corner: (left) cloud footprint; (right) peak overpressures  $\geq 1$  psig.

	Vapor Cloud Explosions at Nil Wind	03904-RP-006
	PHMSA	Rev A
	Final Report	Page 189 of 213

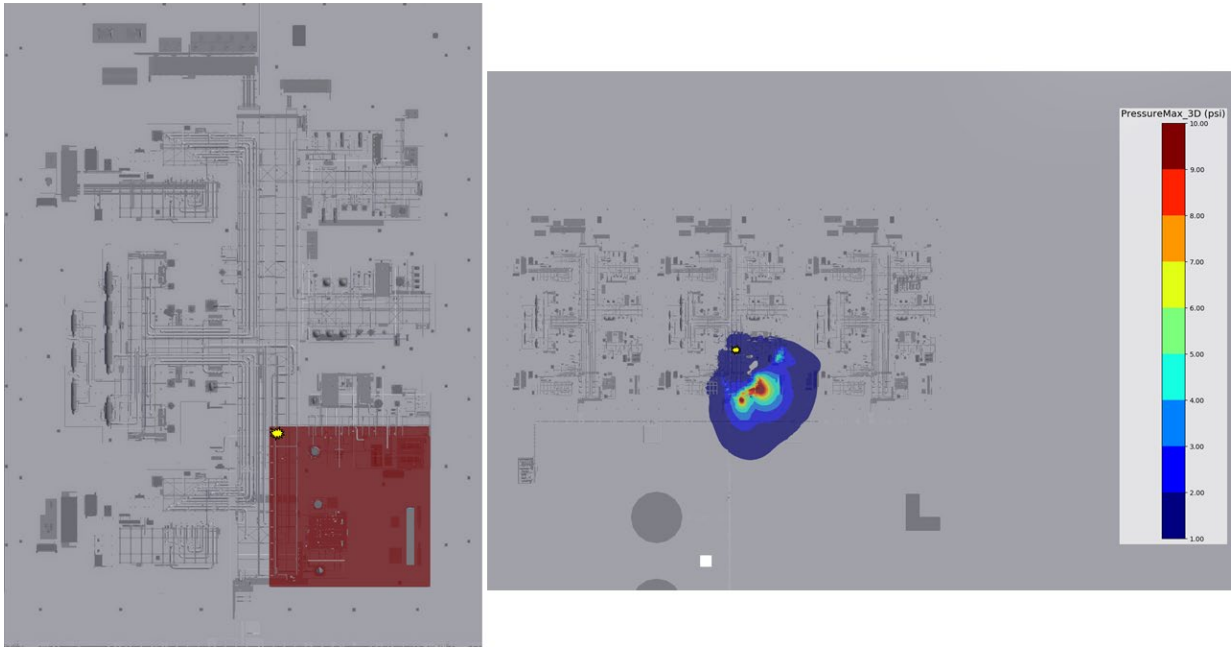


MR cloud (scenario 12, low wind): VCE from Q9 in lower left corner, with ignition in center: (left) cloud footprint; (right) peak overpressures  $\geq 1$  psig.

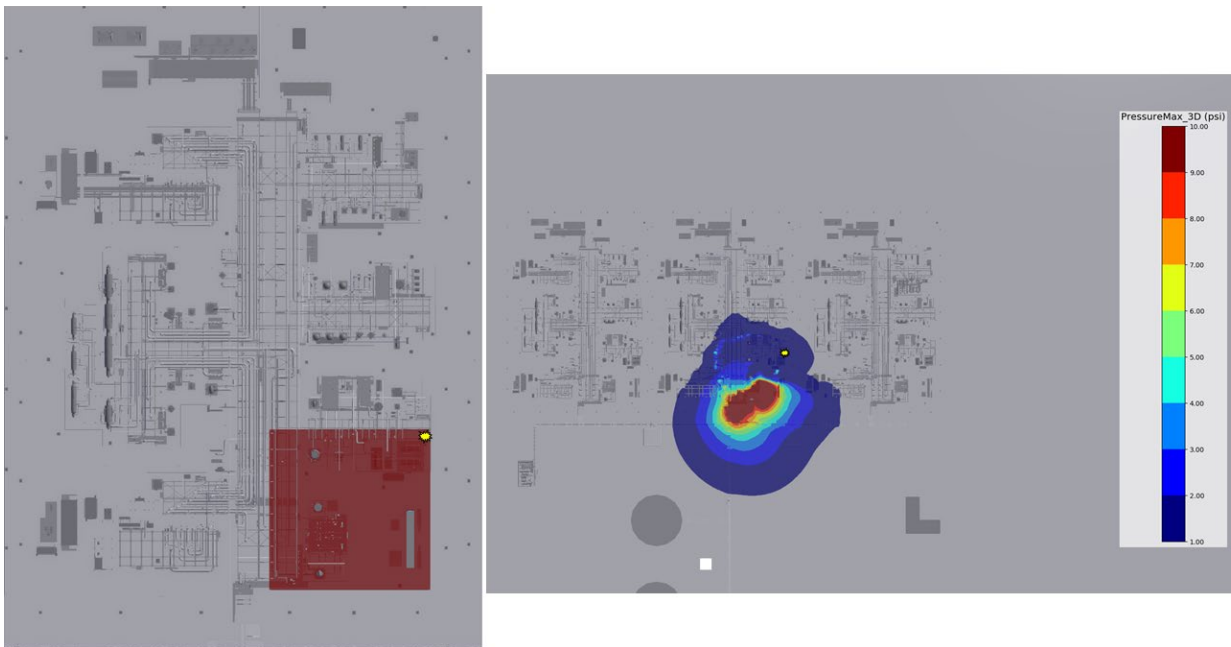


MR cloud (scenario 12, low wind): VCE from Q9 in lower left corner, with ignition in upper right corner: (left) cloud footprint; (right) peak overpressures  $\geq 1$  psig.

	Vapor Cloud Explosions at Nil Wind	03904-RP-006
	PHMSA	Rev A
	Final Report	Page 190 of 213

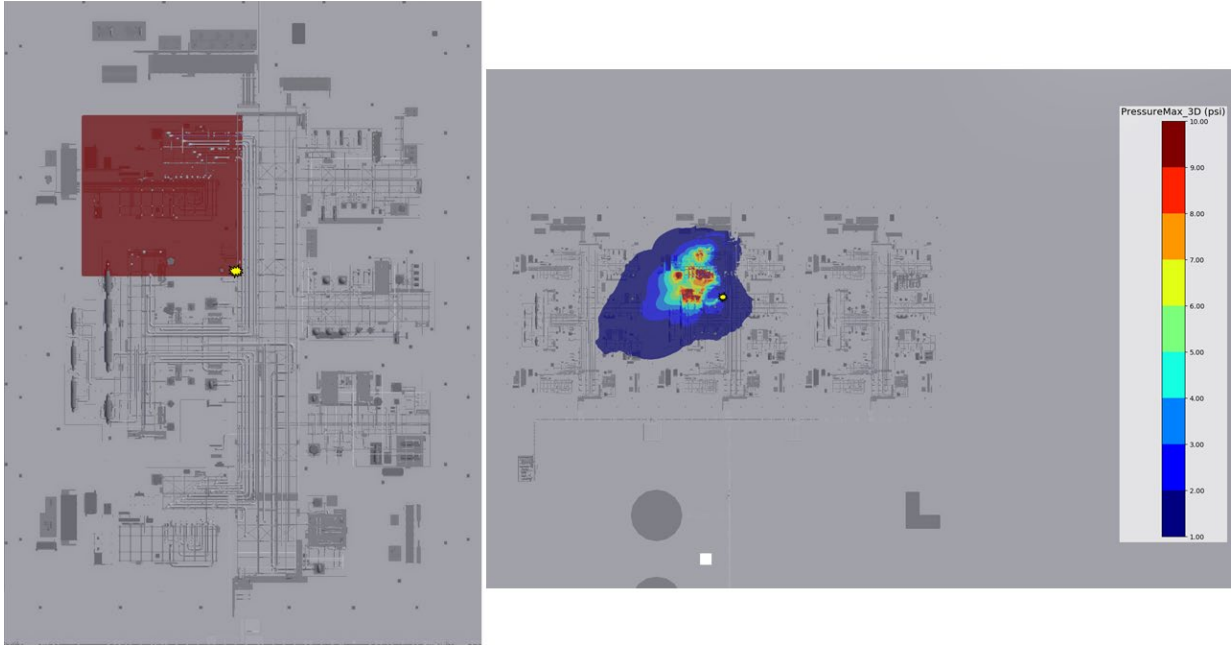


MR cloud (scenario 12, low wind): VCE from Q9 in lower right corner, with ignition in upper left corner: (left) cloud footprint; (right) peak overpressures  $\geq 1$  psig.

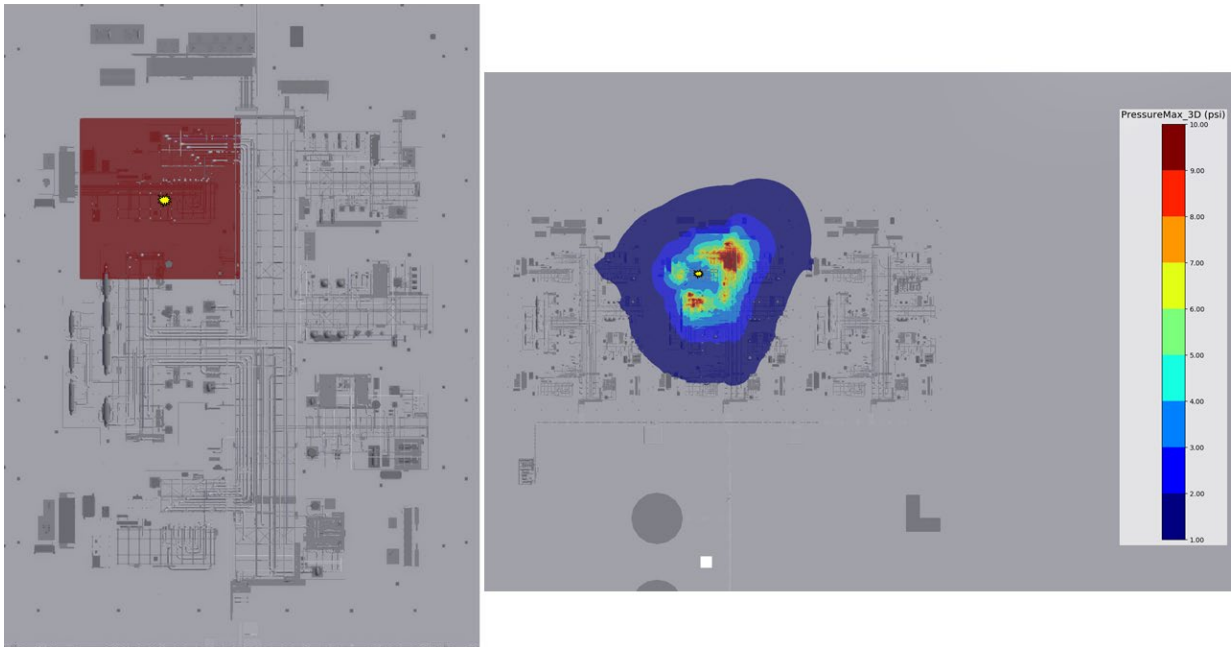


MR cloud (scenario 12, low wind): VCE from Q9 in lower right corner, with ignition in upper right corner: (left) cloud footprint; (right) peak overpressures  $\geq 1$  psig.

	Vapor Cloud Explosions at Nil Wind	03904-RP-006
	PHMSA	Rev A
	Final Report	Page 191 of 213

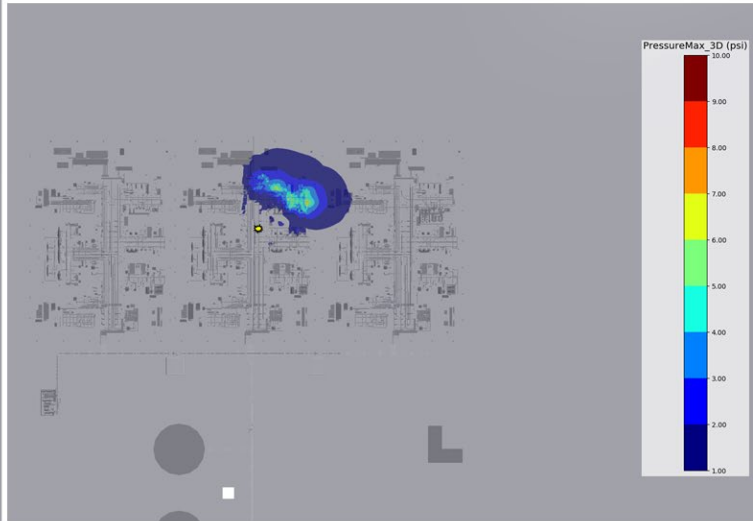
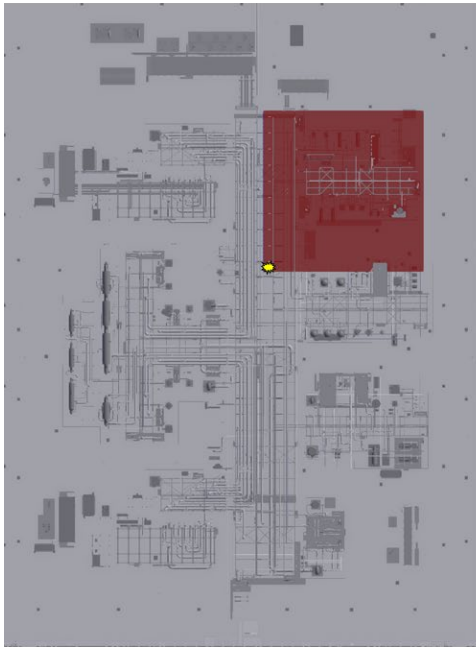


MR cloud (scenario 12, low wind): VCE from Q9 in upper left corner, with ignition in lower right corner: (left) cloud footprint; (right) peak overpressures  $\geq 1$  psig.

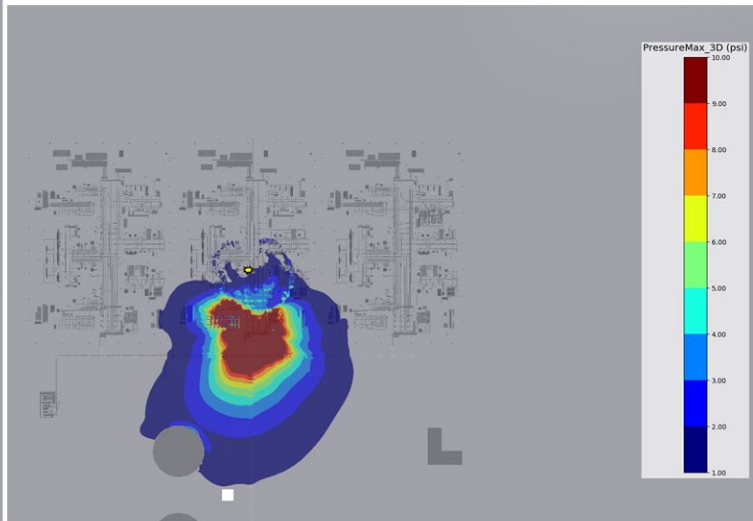
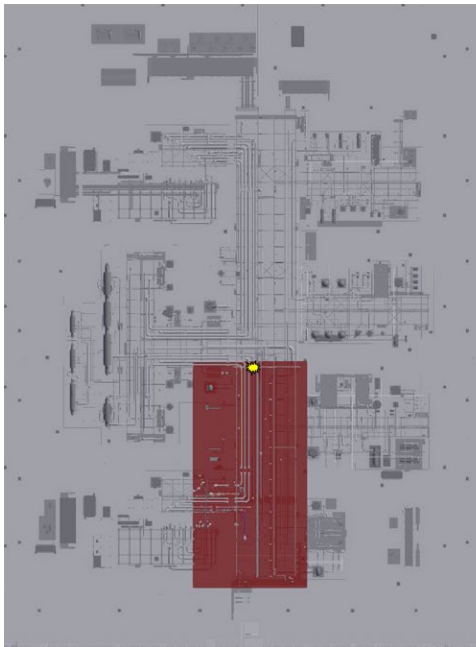


MR cloud (scenario 12, low wind): VCE from Q9 in upper left corner, with ignition in center: (left) cloud footprint; (right) peak overpressures  $\geq 1$  psig.

	Vapor Cloud Explosions at Nil Wind	03904-RP-006
	PHMSA	Rev A
	Final Report	Page 192 of 213

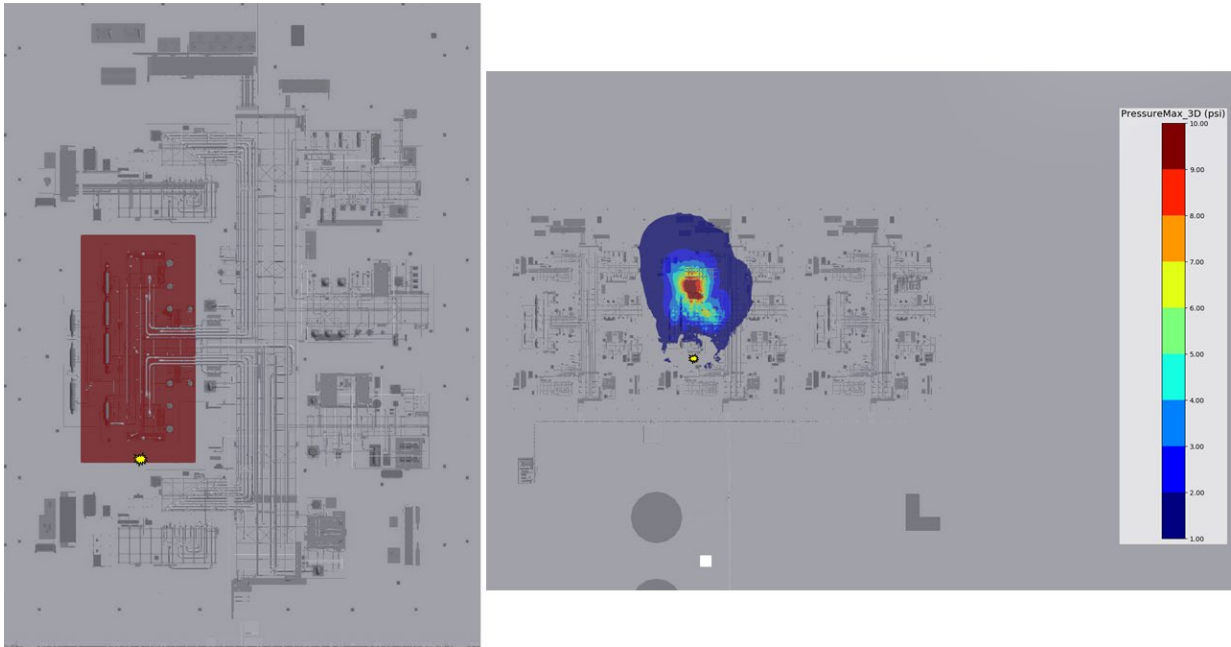


MR cloud (scenario 12, low wind): VCE from Q9 in upper right corner, with ignition in lower left corner: (left) cloud footprint; (right) peak overpressures  $\geq 1$  psig.

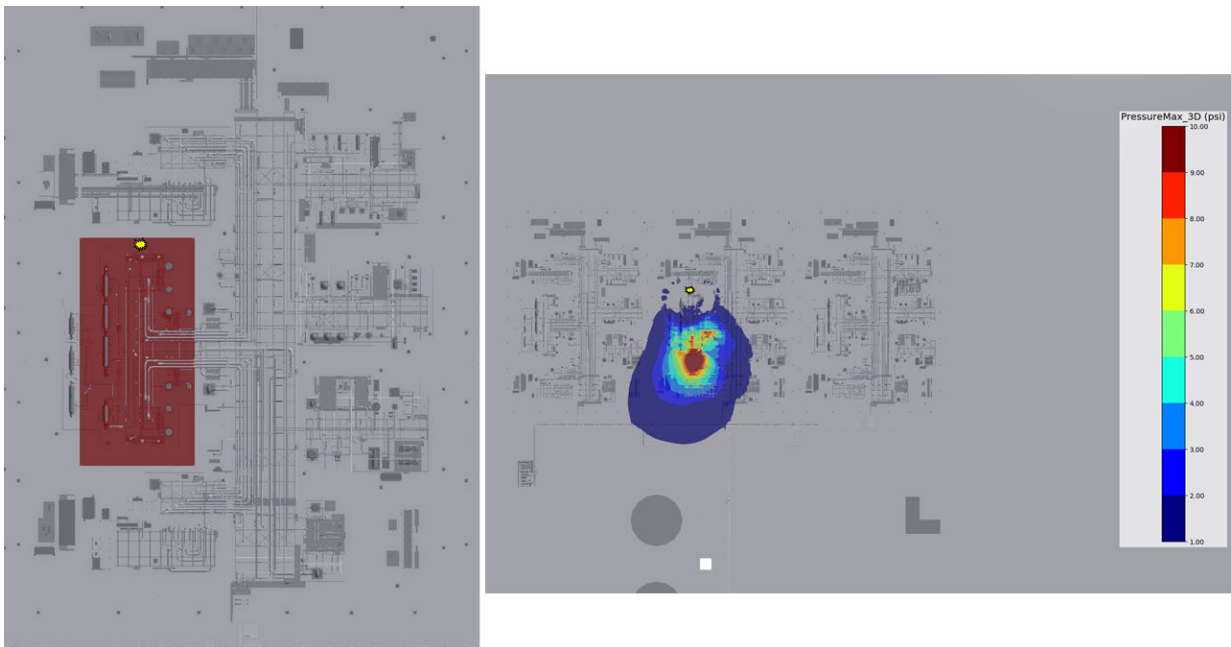


MR cloud (scenario 12, low wind): VCE from Q9 in middle lower edge, with ignition in middle upper edge: (left) cloud footprint; (right) peak overpressures  $\geq 1$  psig.

	Vapor Cloud Explosions at Nil Wind	03904-RP-006
	PHMSA	Rev A
	Final Report	Page 193 of 213

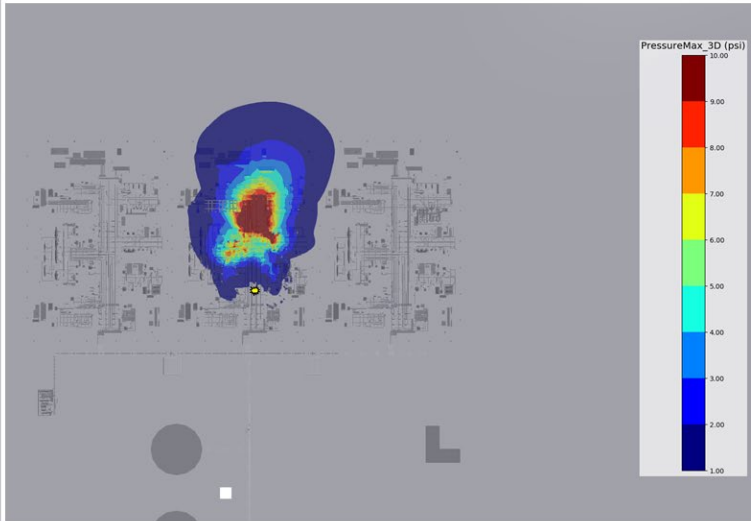
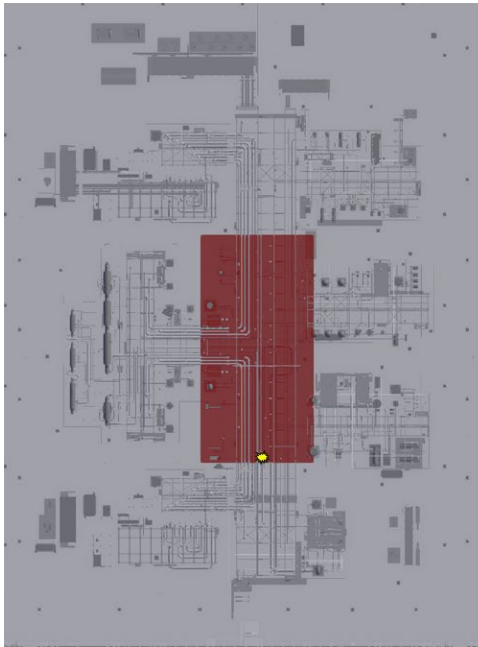


MR cloud (scenario 12, low wind): VCE from Q9 in middle left edge, with ignition in middle lower edge: (left) cloud footprint; (right) peak overpressures  $\geq 1$  psig.

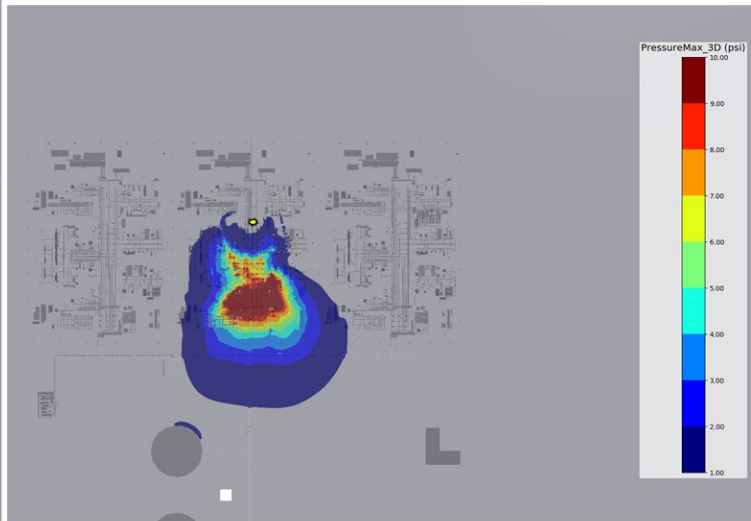
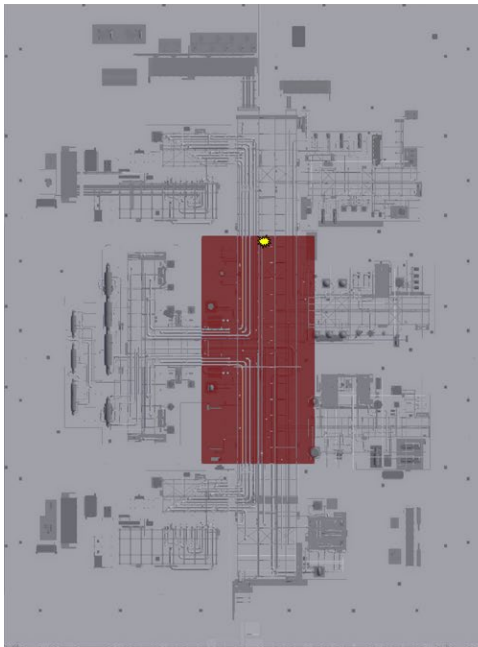


MR cloud (scenario 12, low wind): VCE from Q9 in middle left edge, with ignition in middle upper edge: (left) cloud footprint; (right) peak overpressures  $\geq 1$  psig.

	Vapor Cloud Explosions at Nil Wind	03904-RP-006
	PHMSA	Rev A
	Final Report	Page 194 of 213

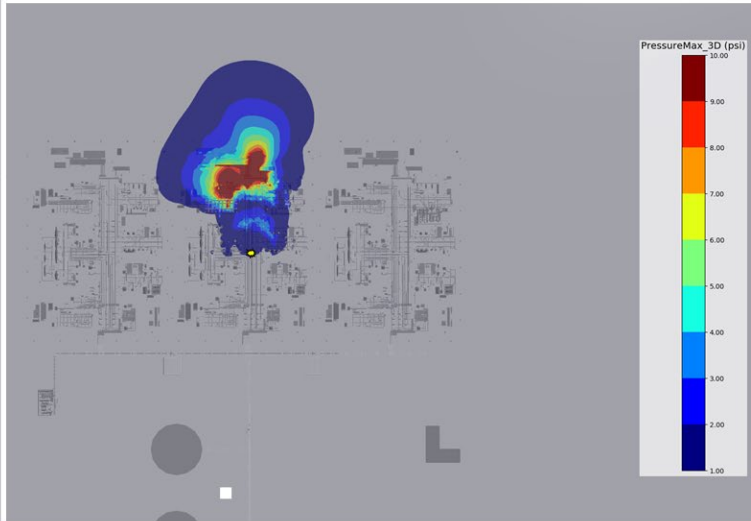
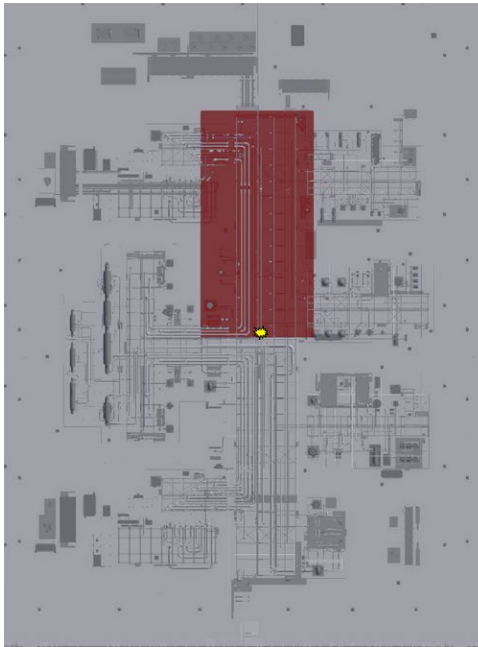


MR cloud (scenario 12, low wind): VCE from Q9 in center, with ignition in middle lower edge: (left) cloud footprint; (right) peak overpressures  $\geq 1$  psig.

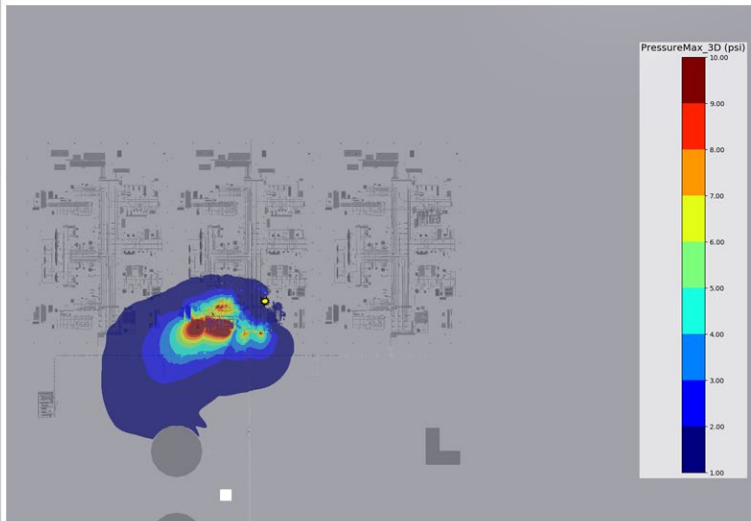
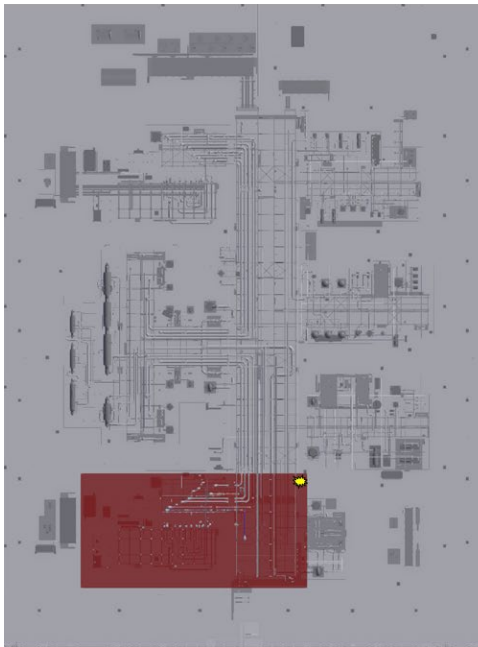


MR cloud (scenario 12, low wind): VCE from Q9 in center, with ignition in middle upper edge: (left) cloud footprint; (right) peak overpressures  $\geq 1$  psig.

	Vapor Cloud Explosions at Nil Wind	03904-RP-006
	PHMSA	Rev A
	Final Report	Page 195 of 213

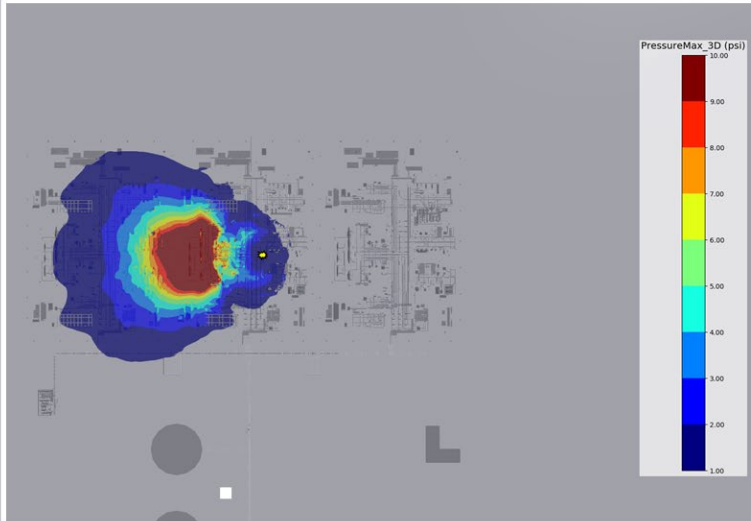
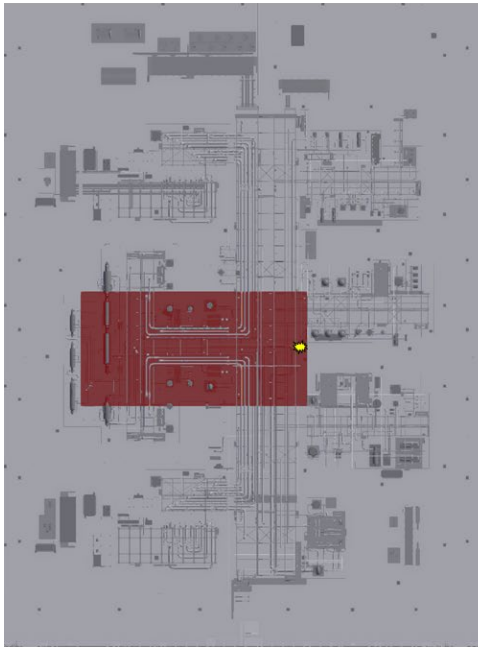


MR cloud (scenario 12, low wind): VCE from Q9 in middle upper edge, with ignition in middle lower edge: (left) cloud footprint; (right) peak overpressures  $\geq 1$  psig.

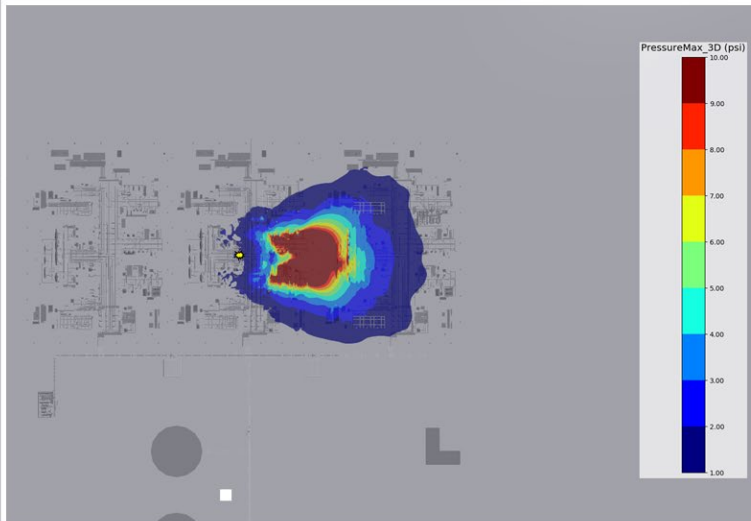
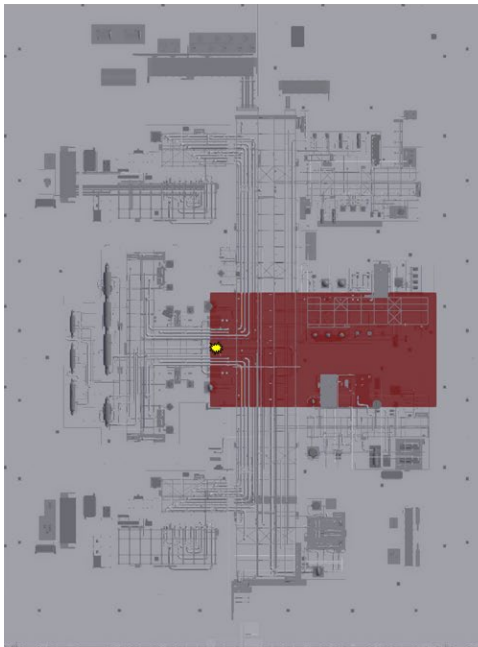


MR cloud (scenario 12, low wind): VCE from Q9 in lower left corner, with ignition in upper right corner: (left) cloud footprint; (right) peak overpressures  $\geq 1$  psig.

	Vapor Cloud Explosions at Nil Wind	03904-RP-006
	PHMSA	Rev A
	Final Report	Page 196 of 213

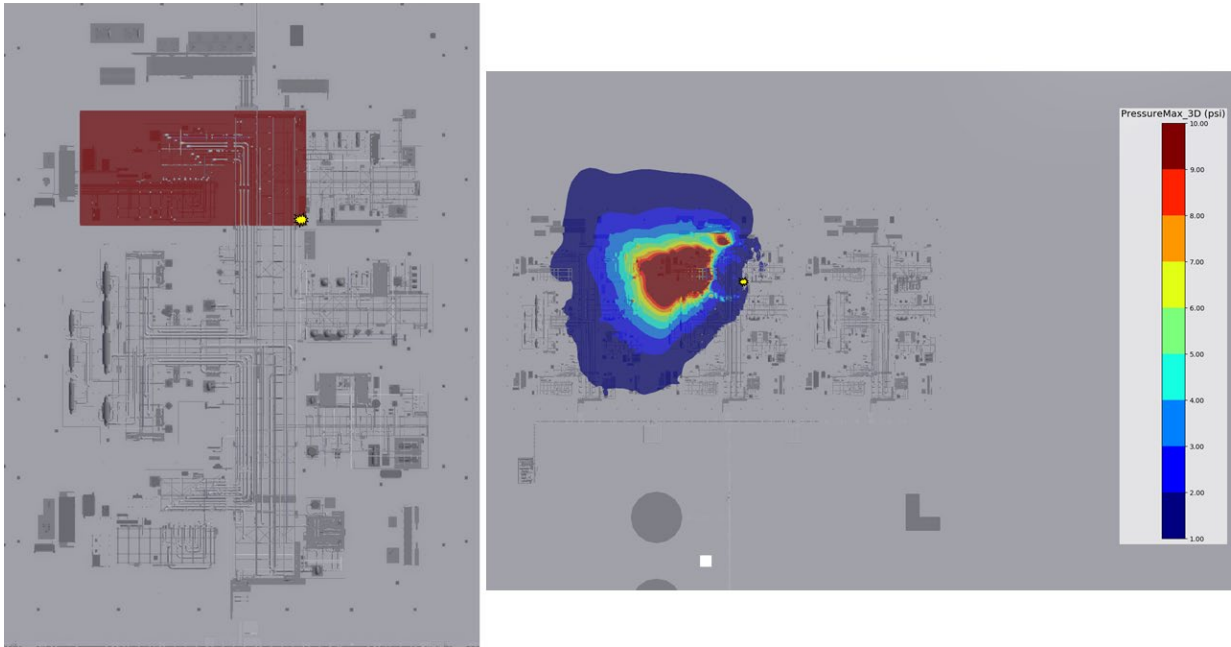


MR cloud (scenario 12, low wind): VCE from Q9 in middle left edge, with ignition in middle right edge: (left) cloud footprint; (right) peak overpressures  $\geq 1$  psig.

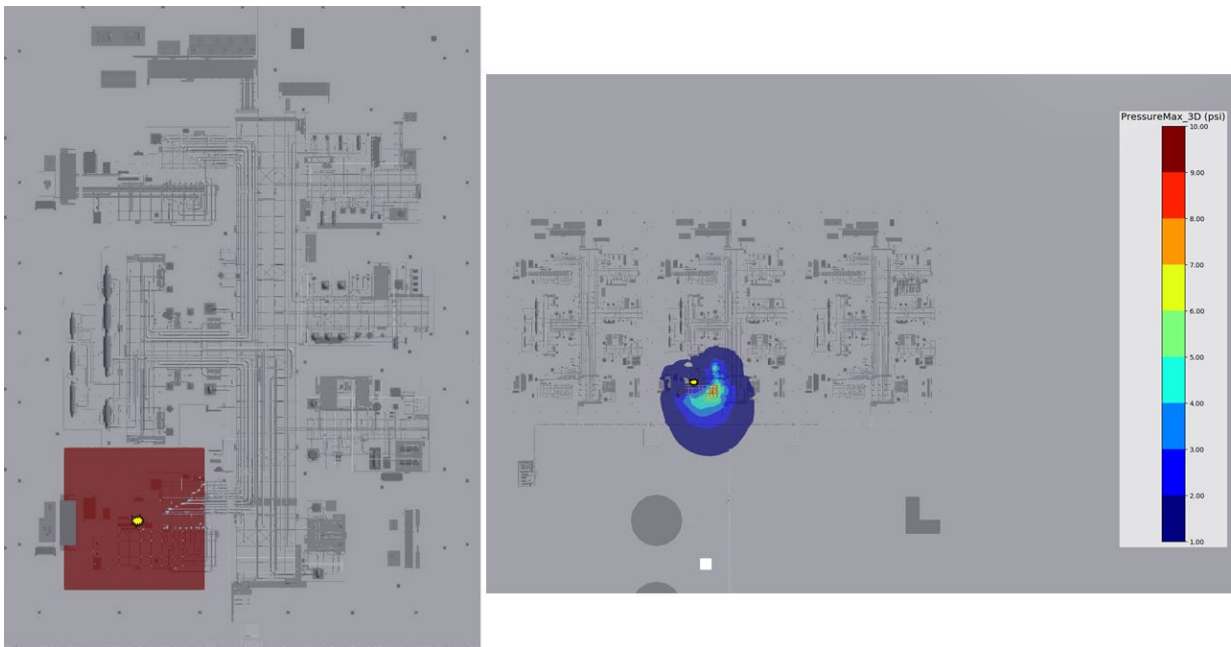


MR cloud (scenario 12, low wind): VCE from Q9 in middle right edge, with ignition in middle left edge: (left) cloud footprint; (right) peak overpressures  $\geq 1$  psig.

	Vapor Cloud Explosions at Nil Wind	03904-RP-006
	PHMSA	Rev A
	Final Report	Page 197 of 213

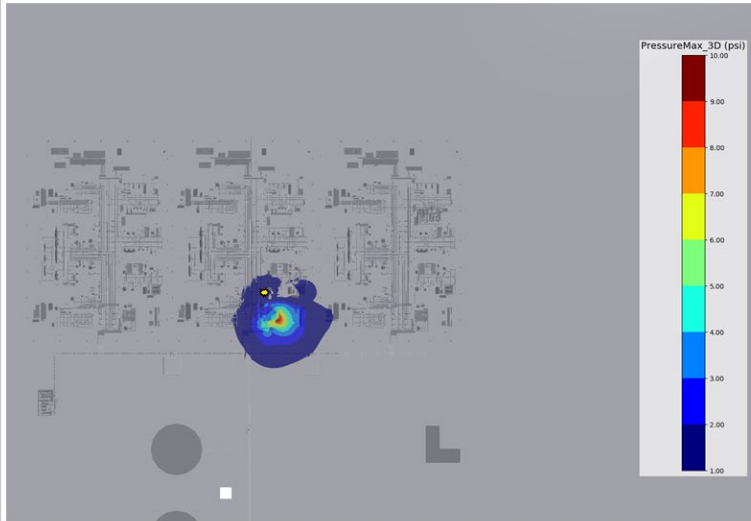
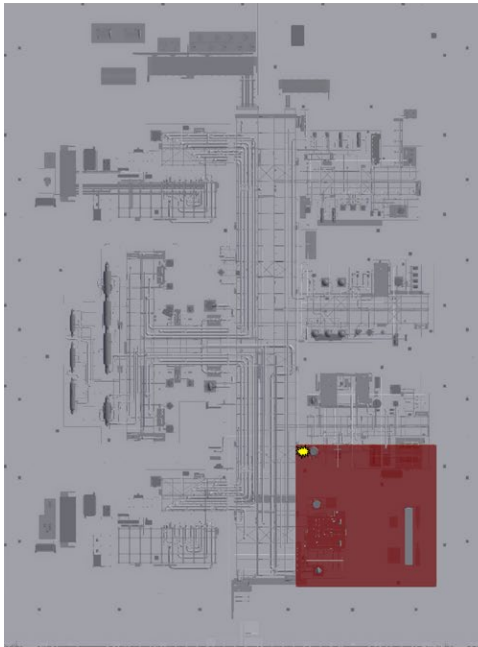


MR cloud (scenario 12, low wind): VCE from Q9 in upper left corner, with ignition in lower right corner: (left) cloud footprint; (right) peak overpressures  $\geq 1$  psig.

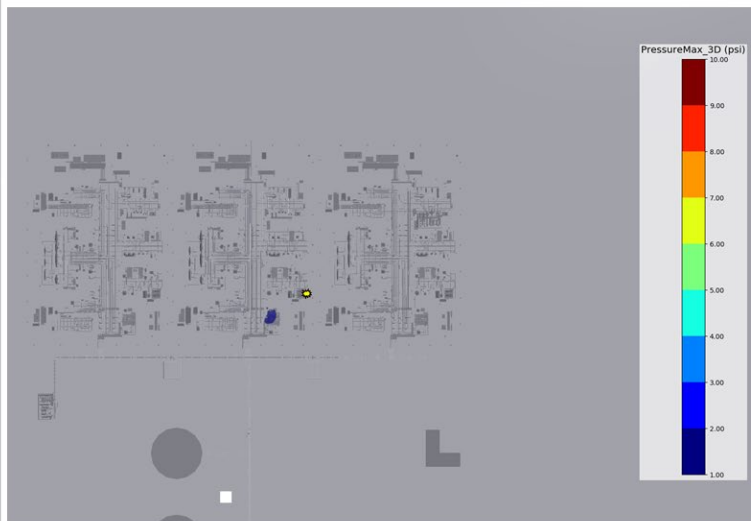
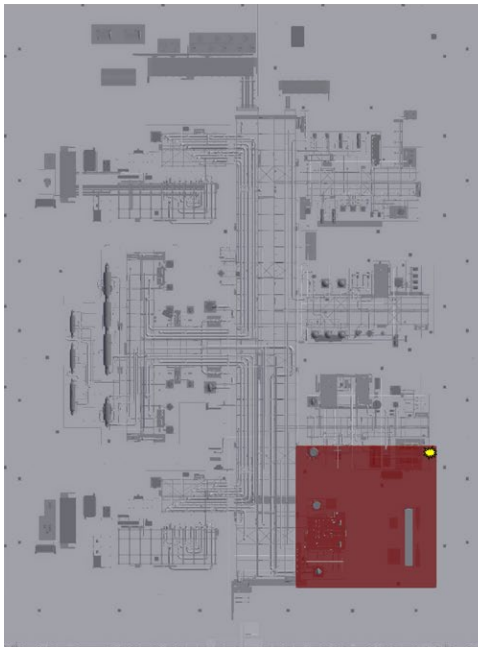


MR cloud (scenario 12, nil wind): VCE from Q9 in lower left corner, with ignition in center: (left) cloud footprint; (right) peak overpressures  $\geq 1$  psig.

	Vapor Cloud Explosions at Nil Wind	03904-RP-006
	PHMSA	Rev A
	Final Report	Page 198 of 213

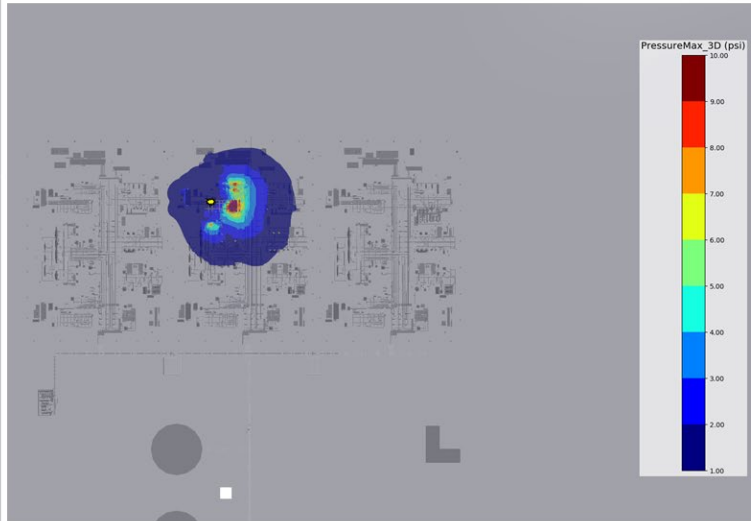
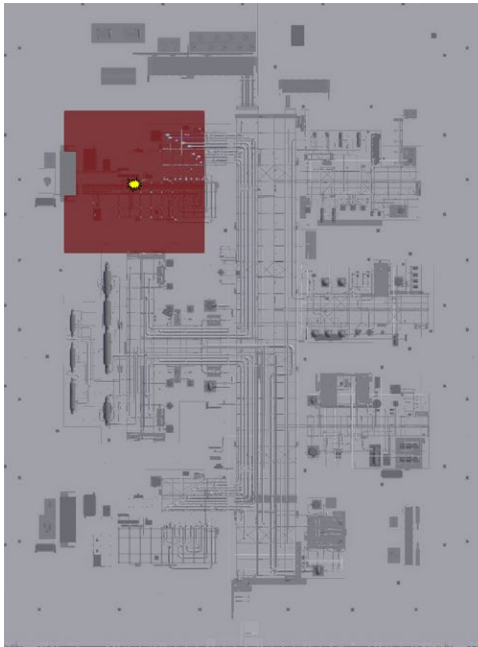


MR cloud (scenario 12, nil wind): VCE from Q9 in lower right corner, with ignition in upper left corner: (left) cloud footprint; (right) peak overpressures  $\geq 1$  psig.

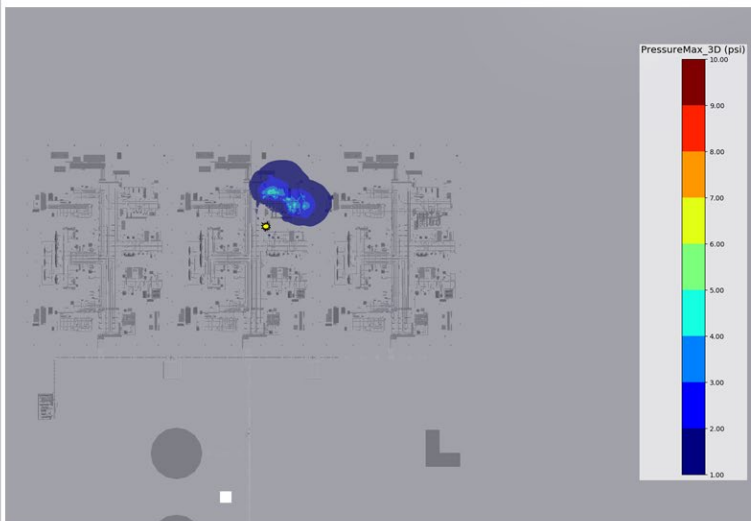
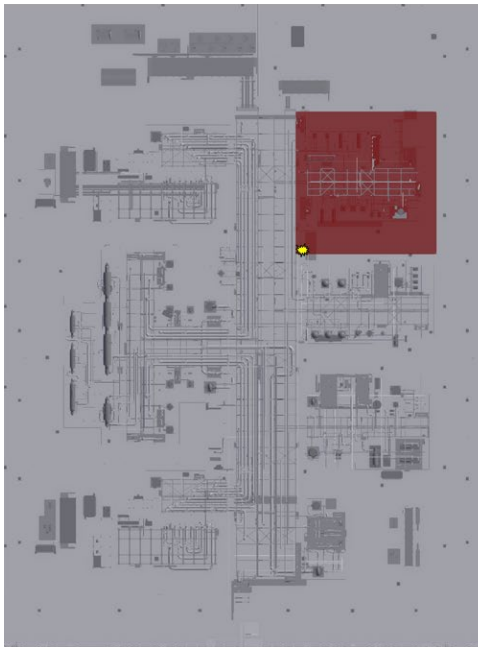


MR cloud (scenario 12, nil wind): VCE from Q9 in lower right corner, with ignition in upper right corner: (left) cloud footprint; (right) peak overpressures  $\geq 1$  psig.

	Vapor Cloud Explosions at Nil Wind	03904-RP-006
	PHMSA	Rev A
	Final Report	Page 199 of 213

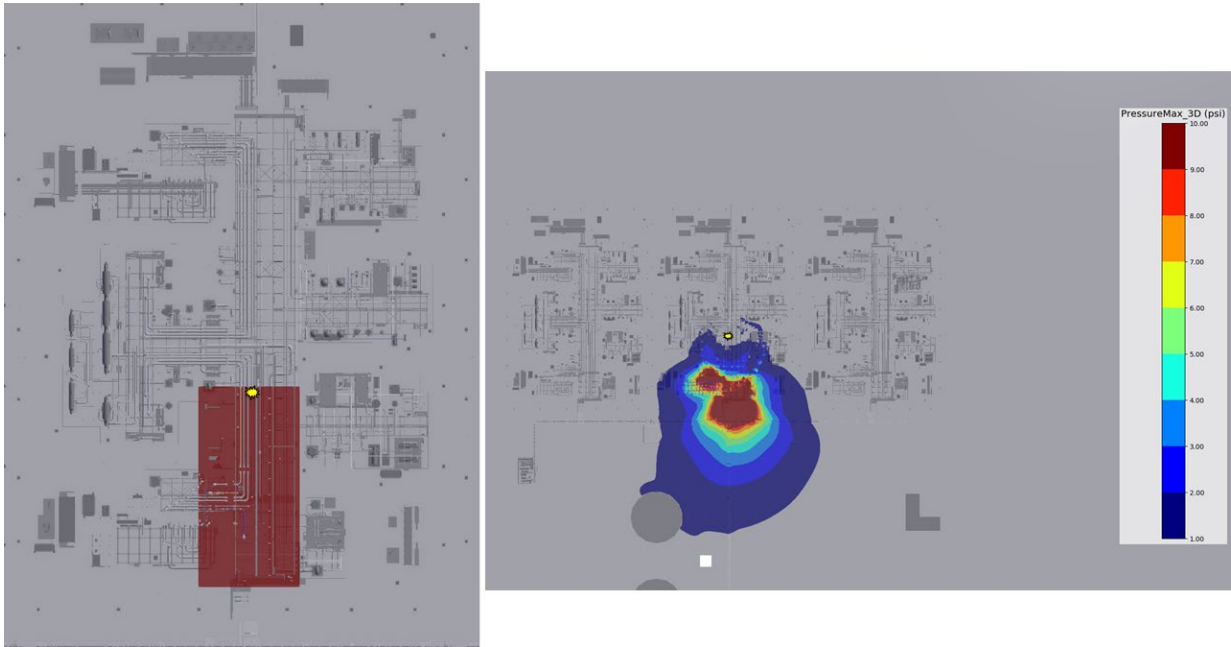


MR cloud (scenario 12, nil wind): VCE from Q9 in upper left corner, with ignition in center: (left) cloud footprint; (right) peak overpressures  $\geq 1$  psig.

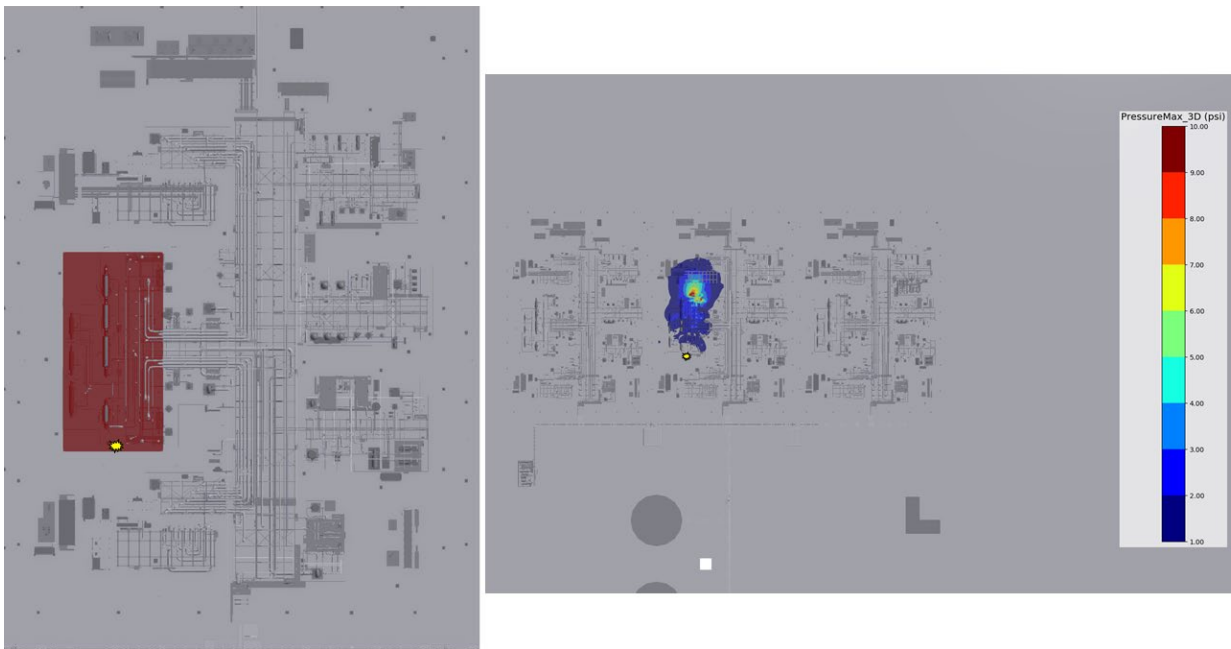


MR cloud (scenario 12, nil wind): VCE from Q9 in upper right corner, with ignition in lower left corner: (left) cloud footprint; (right) peak overpressures  $\geq 1$  psig.

	Vapor Cloud Explosions at Nil Wind	03904-RP-006
	PHMSA	Rev A
	Final Report	Page 200 of 213

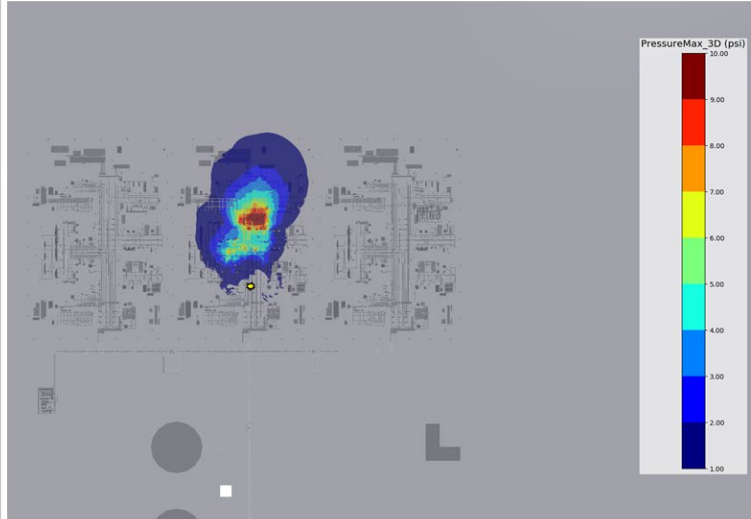
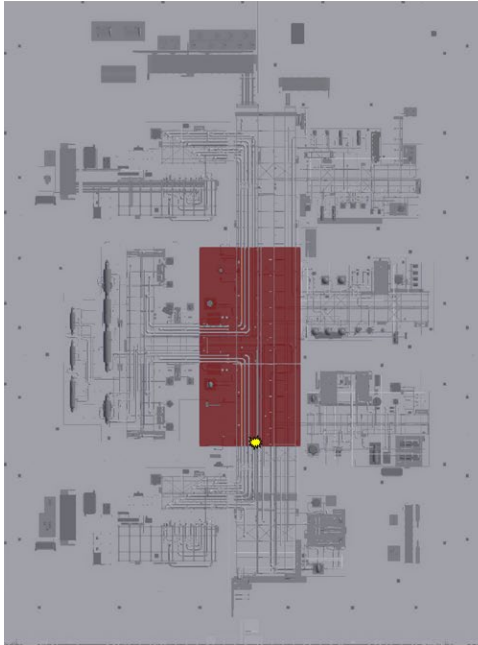


MR cloud (scenario 12, nil wind): VCE from Q9 in middle lower edge, with ignition in middle upper edge: (left) cloud footprint; (right) peak overpressures  $\geq 1$  psig.

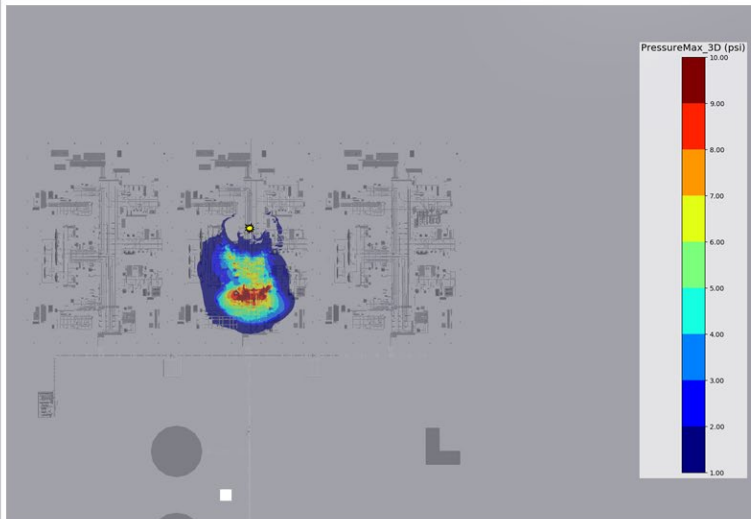
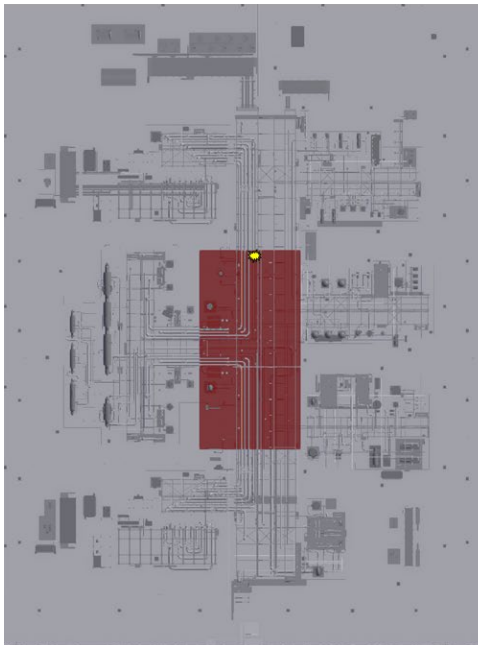


MR cloud (scenario 12, nil wind): VCE from Q9 in middle left edge, with ignition in middle lower edge: (left) cloud footprint; (right) peak overpressures  $\geq 1$  psig.

	Vapor Cloud Explosions at Nil Wind	03904-RP-006
	PHMSA	Rev A
	Final Report	Page 201 of 213

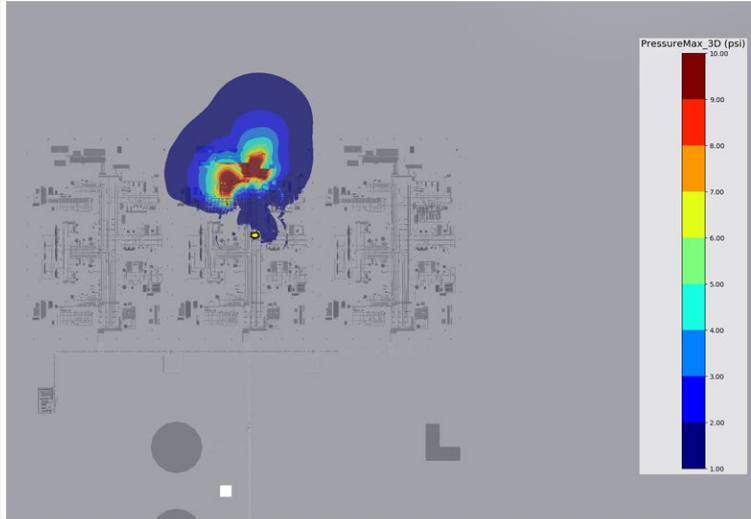
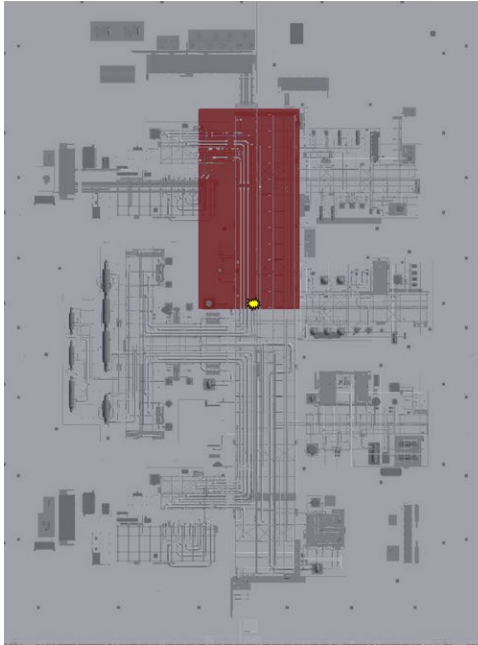


MR cloud (scenario 12, nil wind): VCE from Q9 in center, with ignition in middle lower edge: (left) cloud footprint; (right) peak overpressures  $\geq 1$  psig.

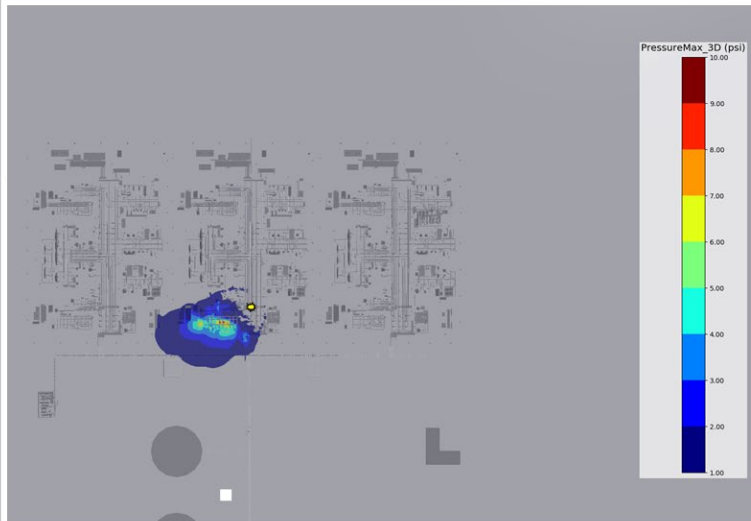
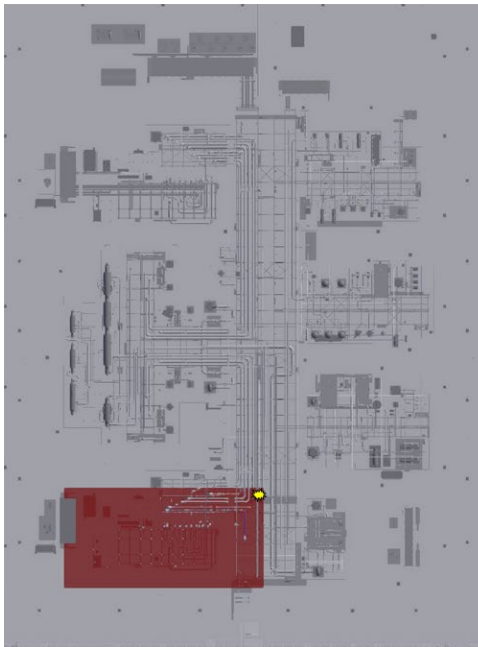


MR cloud (scenario 12, nil wind): VCE from Q9 in center, with ignition in middle upper edge: (left) cloud footprint; (right) peak overpressures  $\geq 1$  psig.

	Vapor Cloud Explosions at Nil Wind	03904-RP-006
	PHMSA	Rev A
	Final Report	Page 202 of 213

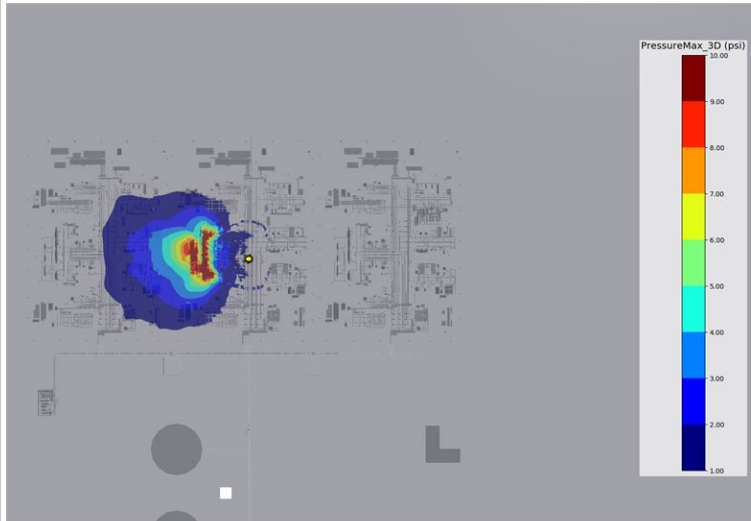
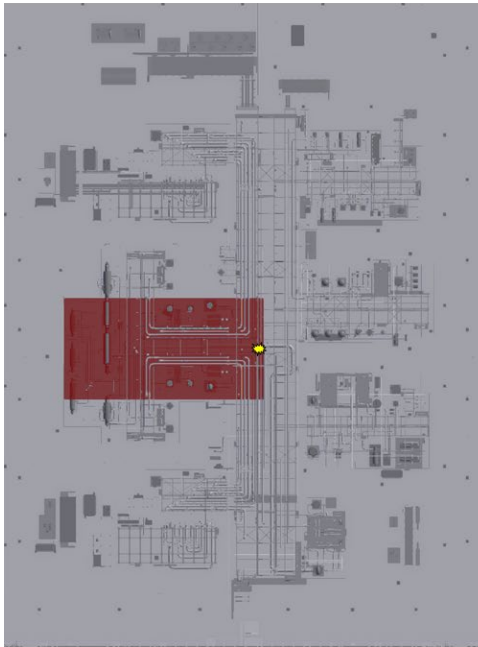


MR cloud (scenario 12, nil wind): VCE from Q9 in middle upper edge, with ignition in middle lower edge: (left) cloud footprint; (right) peak overpressures  $\geq 1$  psig.

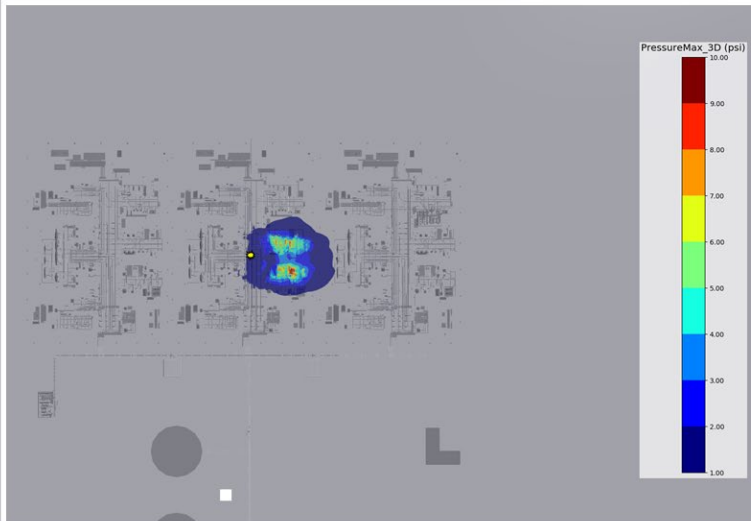
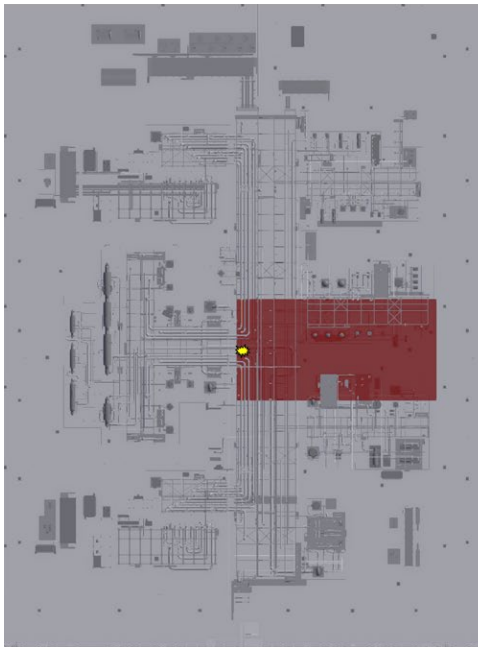


MR cloud (scenario 12, nil wind): VCE from Q9 in lower left corner, with ignition in upper right corner: (left) cloud footprint; (right) peak overpressures  $\geq 1$  psig.

	Vapor Cloud Explosions at Nil Wind	03904-RP-006
	PHMSA	Rev A
	Final Report	Page 203 of 213

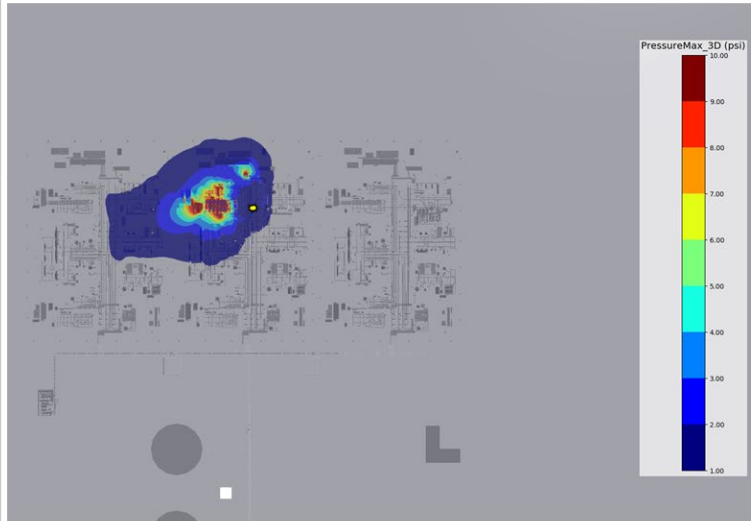
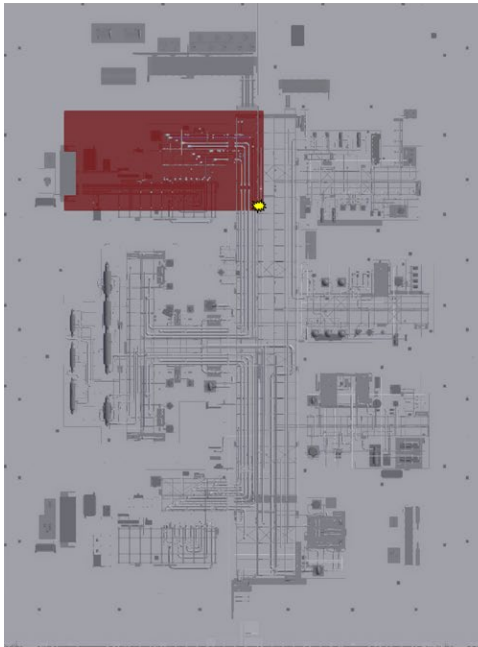


MR cloud (scenario 12, nil wind): VCE from Q9 in middle left edge, with ignition in middle right edge: (left) cloud footprint; (right) peak overpressures  $\geq 1$  psig.

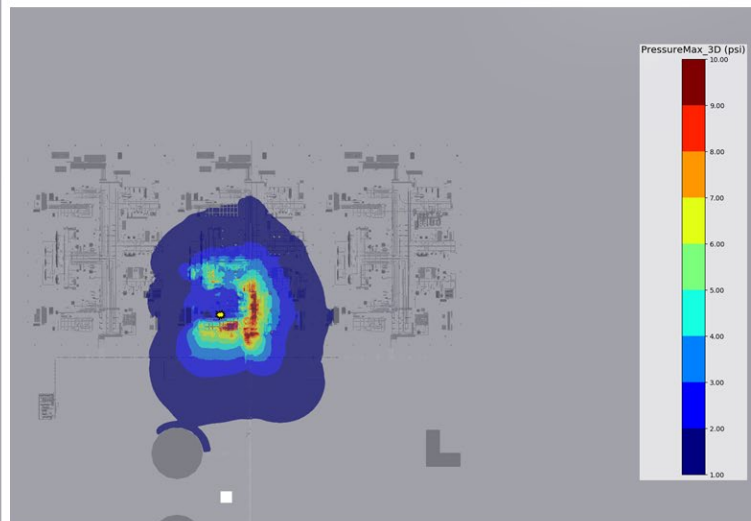
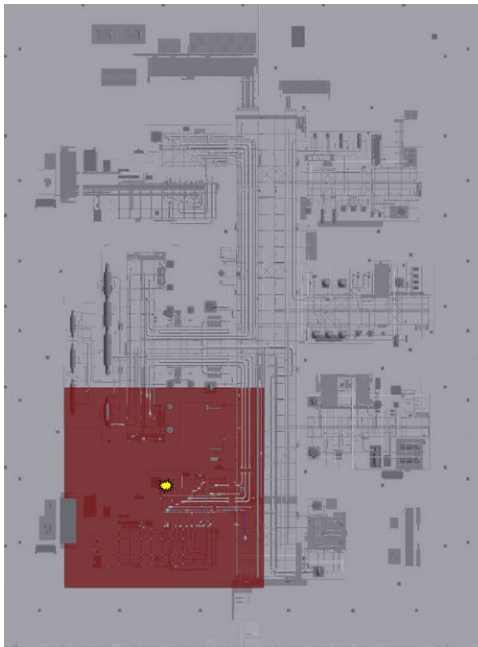


MR cloud (scenario 12, nil wind): VCE from Q9 in middle right edge, with ignition in middle left edge: (left) cloud footprint; (right) peak overpressures  $\geq 1$  psig.

	Vapor Cloud Explosions at Nil Wind	03904-RP-006
	PHMSA	Rev A
	Final Report	Page 204 of 213

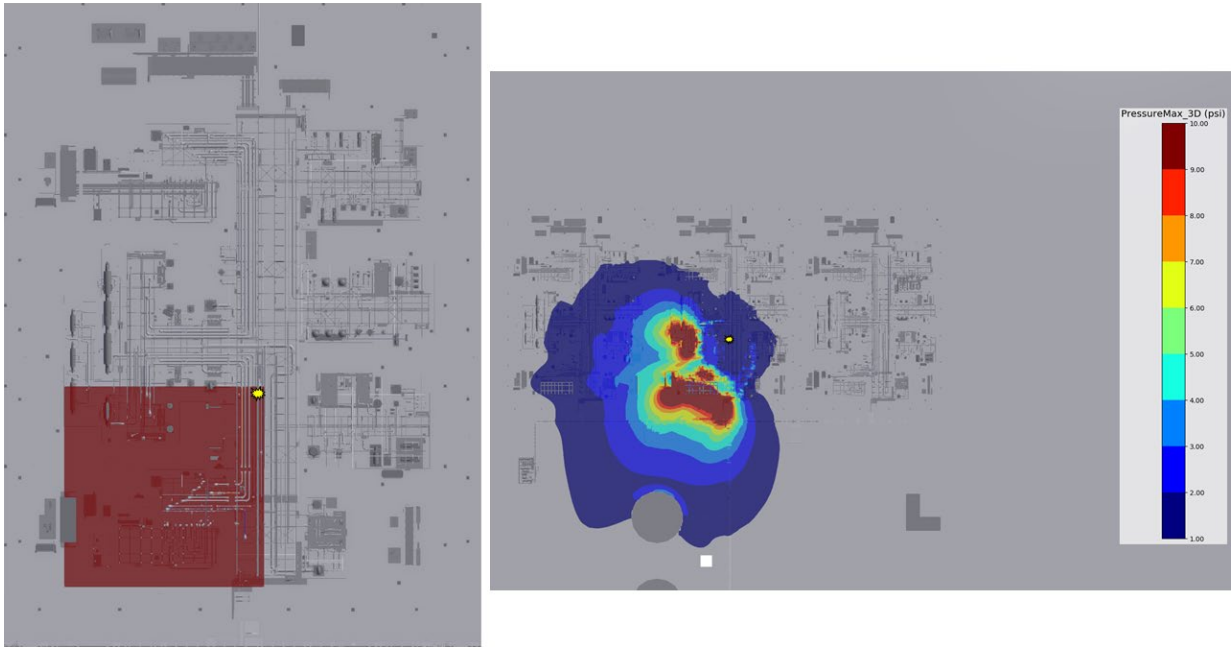


MR cloud (scenario 12, nil wind): VCE from Q9 in upper left corner, with ignition in lower right corner: (left) cloud footprint; (right) peak overpressures  $\geq 1$  psig.

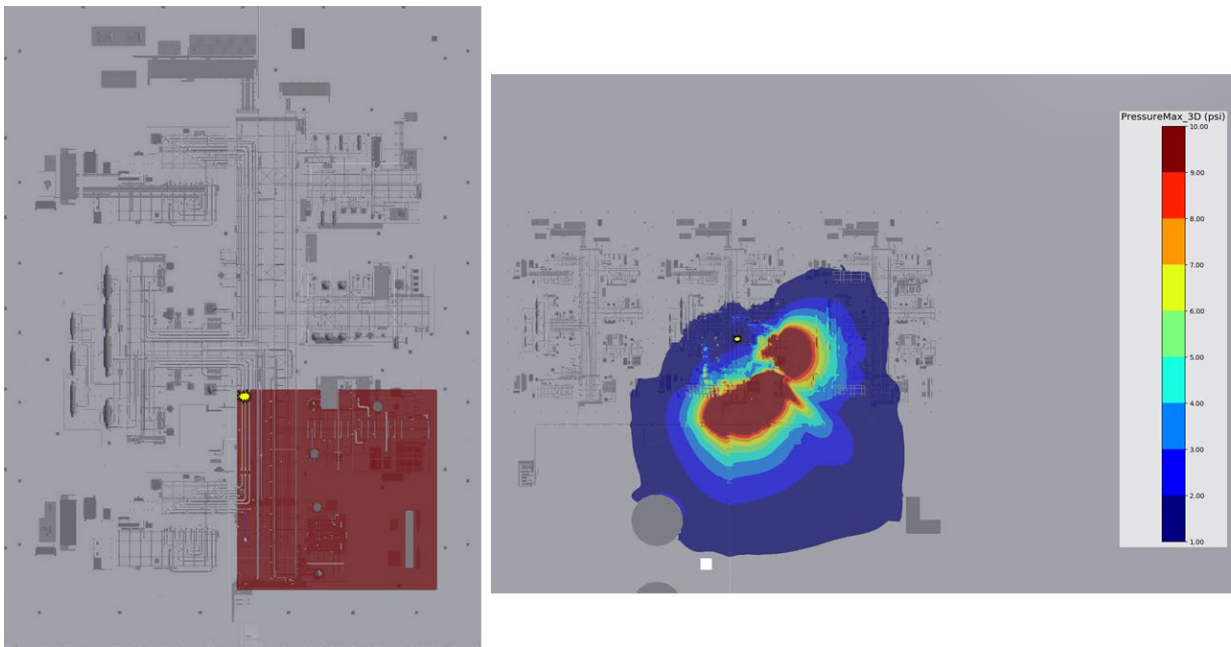


MR cloud (scenario 12, low wind): VCE from Q8 in lower left corner, with ignition in center: (left) cloud footprint; (right) peak overpressures  $\geq 1$  psig.

	Vapor Cloud Explosions at Nil Wind	03904-RP-006
	PHMSA	Rev A
	Final Report	Page 205 of 213

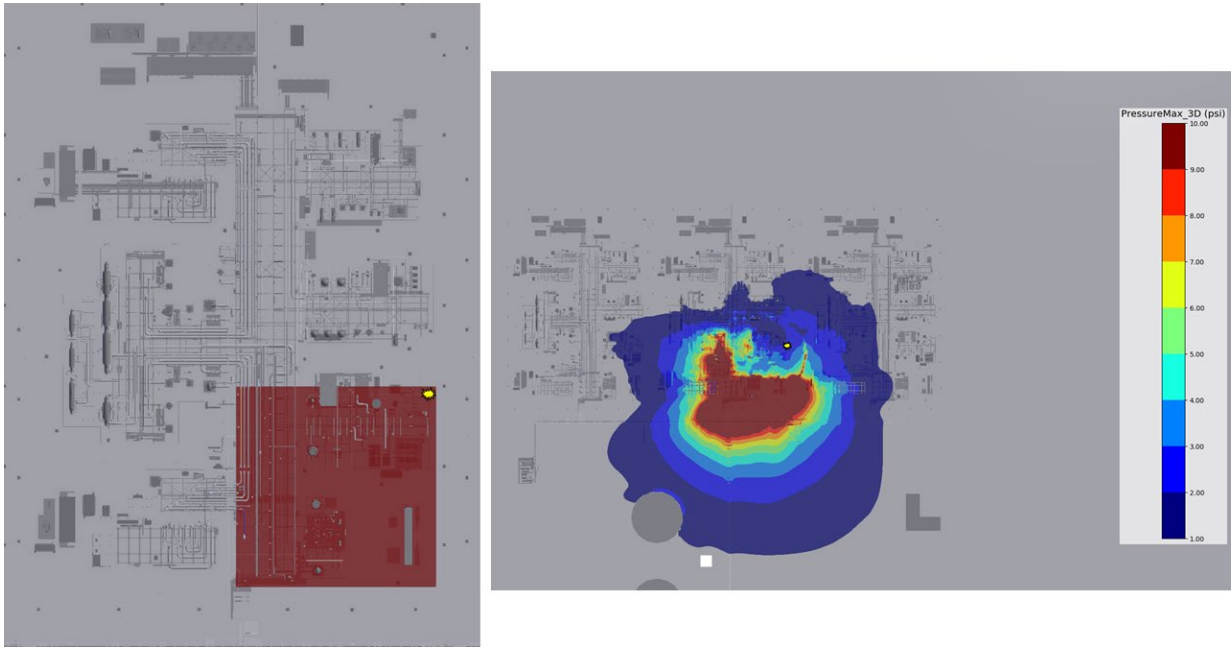


MR cloud (scenario 12, low wind): VCE from Q8 in lower left corner, with ignition in upper right corner: (left) cloud footprint; (right) peak overpressures  $\geq 1$  psig.

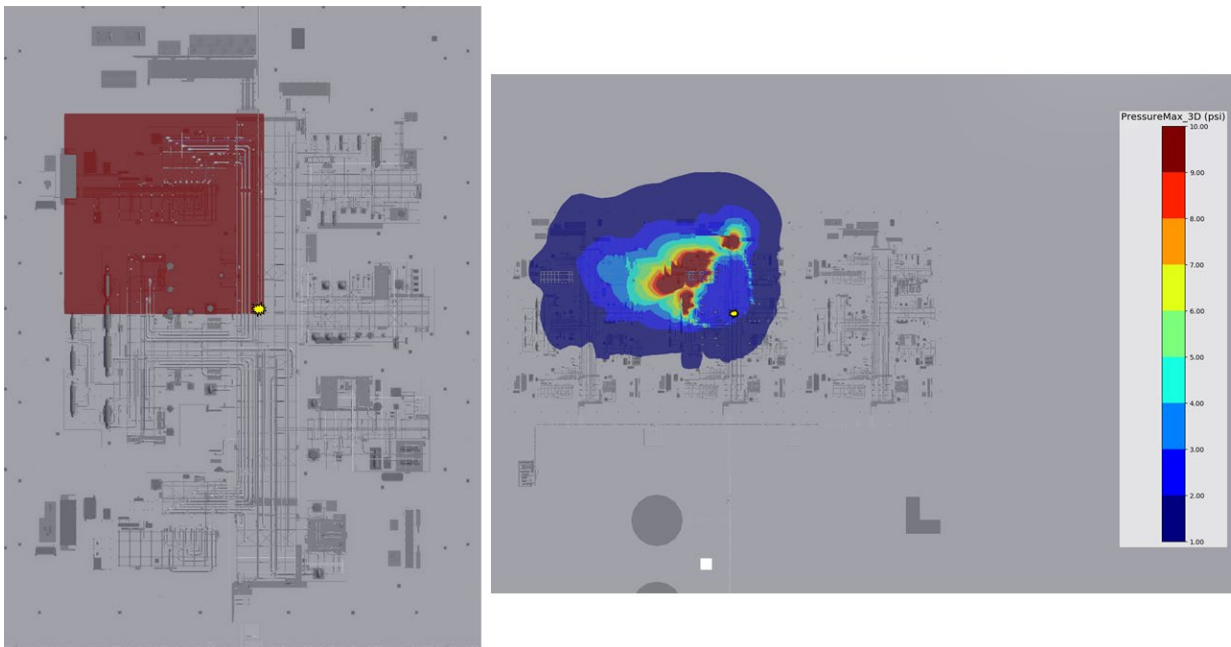


MR cloud (scenario 12, low wind): VCE from Q8 in lower right corner, with ignition in upper left corner: (left) cloud footprint; (right) peak overpressures  $\geq 1$  psig.

	Vapor Cloud Explosions at Nil Wind	03904-RP-006
	PHMSA	Rev A
	Final Report	Page 206 of 213

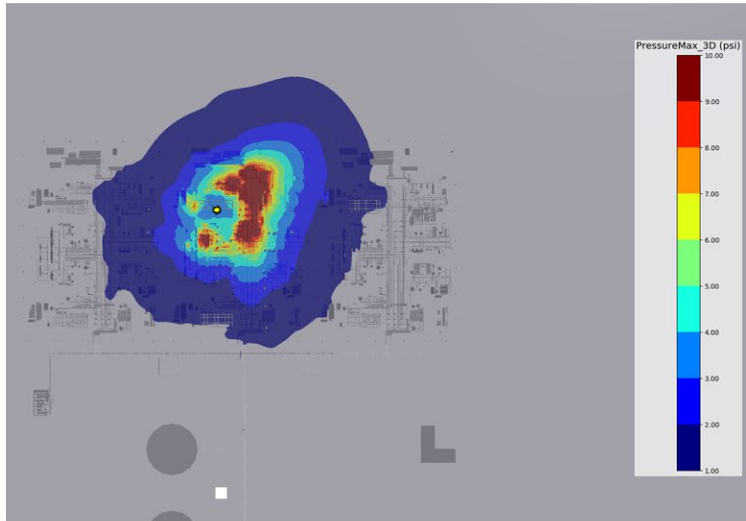
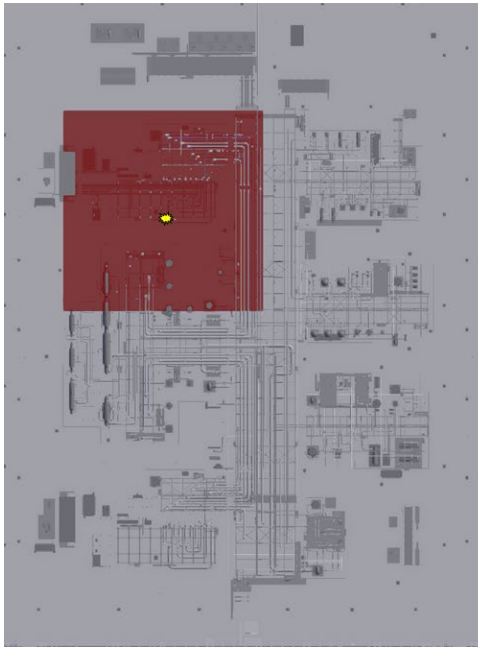


MR cloud (scenario 12, low wind): VCE from Q8 in lower right corner, with ignition in upper right corner: (left) cloud footprint; (right) peak overpressures  $\geq 1$  psig.

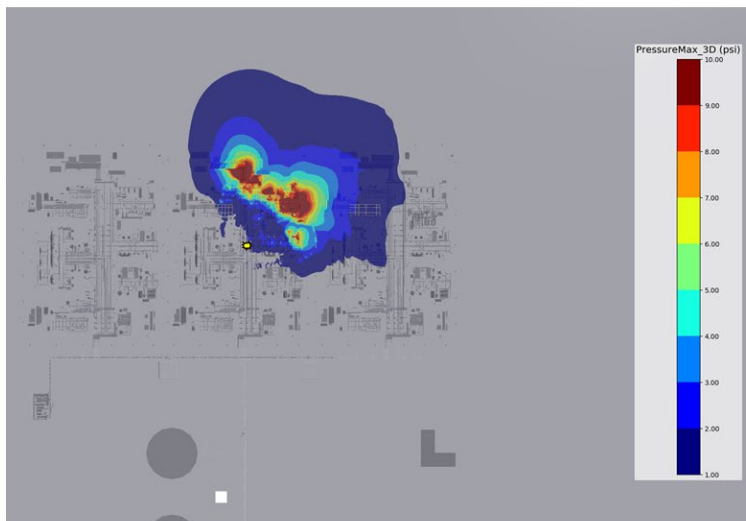
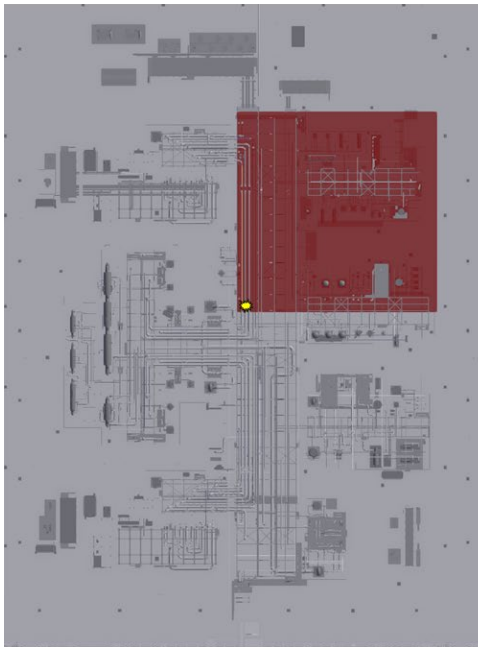


MR cloud (scenario 12, low wind): VCE from Q8 in upper left corner, with ignition in lower right corner: (left) cloud footprint; (right) peak overpressures  $\geq 1$  psig.

	Vapor Cloud Explosions at Nil Wind	03904-RP-006
	PHMSA	Rev A
	Final Report	Page 207 of 213

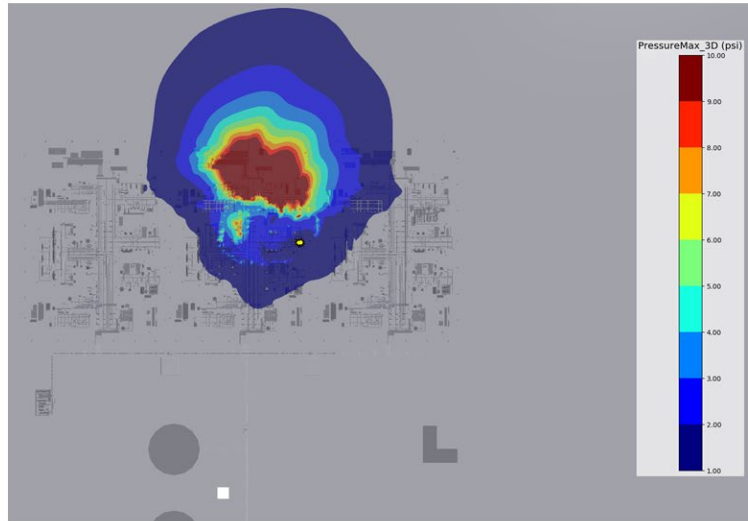
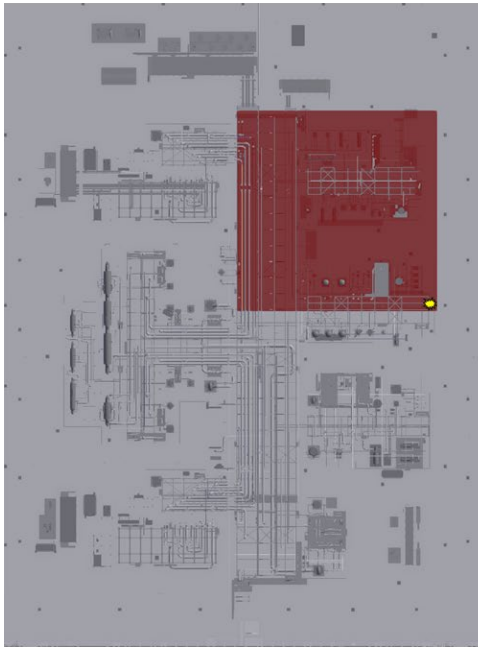


MR cloud (scenario 12, low wind): VCE from Q8 in upper left corner, with ignition in center: (left) cloud footprint; (right) peak overpressures  $\geq 1$  psig.

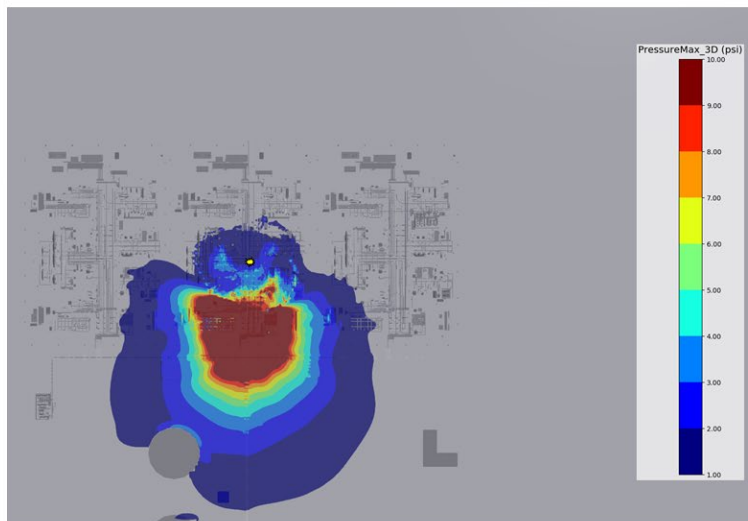
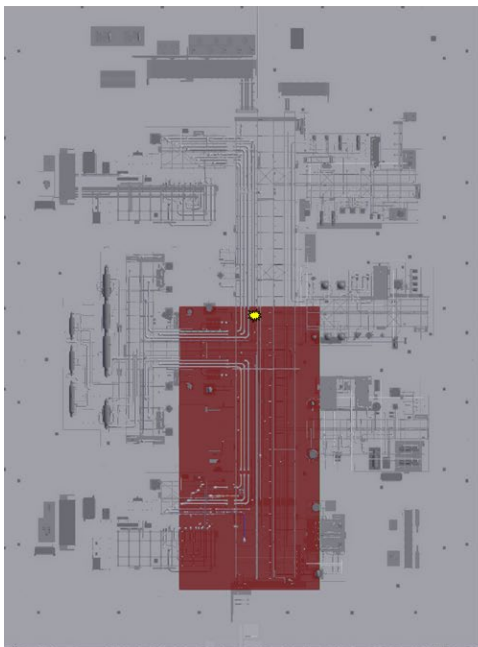


MR cloud (scenario 12, low wind): VCE from Q8 in upper right corner, with ignition in lower left corner: (left) cloud footprint; (right) peak overpressures  $\geq 1$  psig.

	Vapor Cloud Explosions at Nil Wind	03904-RP-006
	PHMSA	Rev A
	Final Report	Page 208 of 213

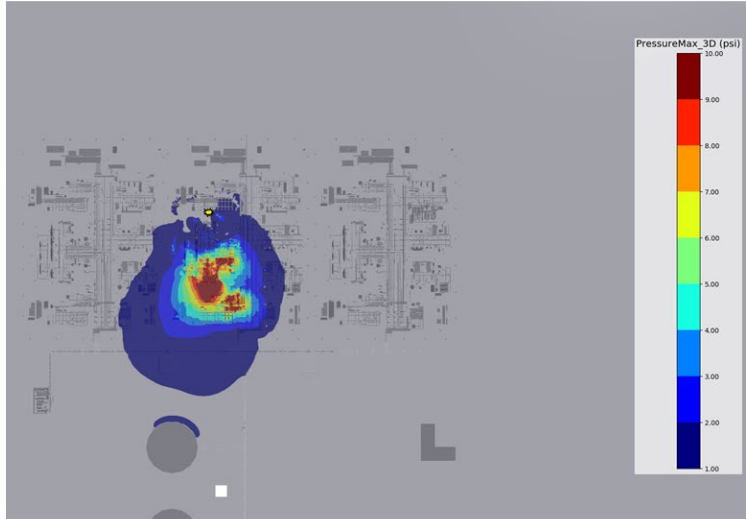
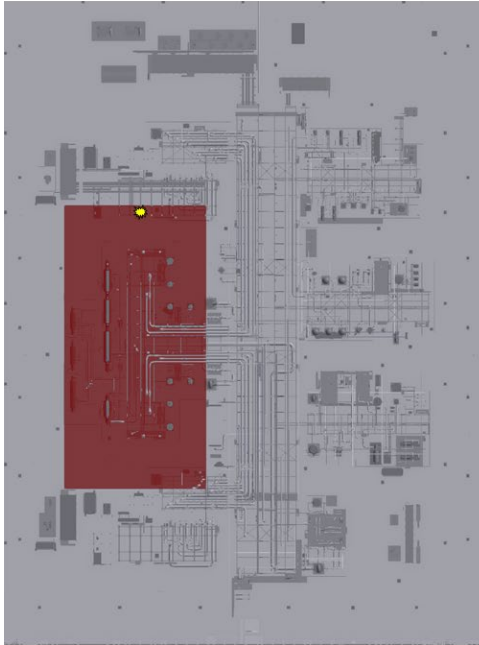


MR cloud (scenario 12, low wind): VCE from Q8 in upper right corner, with ignition in lower right corner: (left) cloud footprint; (right) peak overpressures  $\geq 1$  psig.

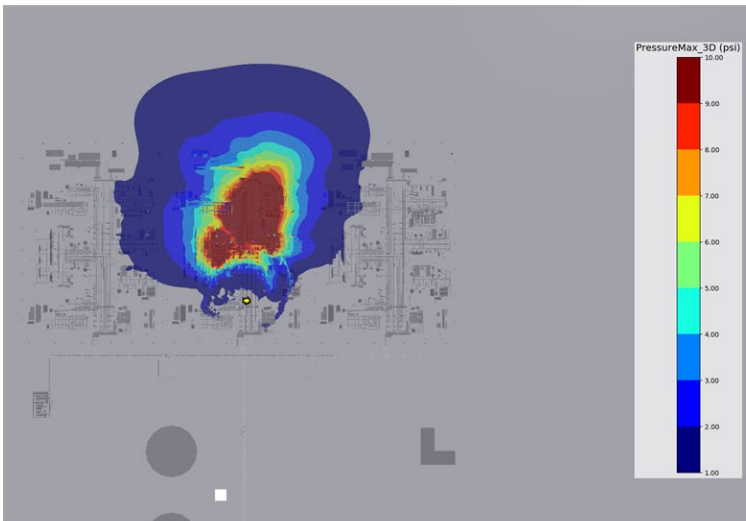
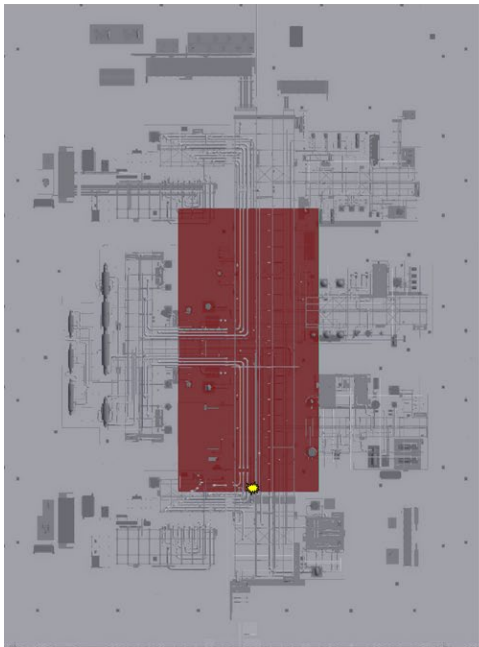


MR cloud (scenario 12, low wind): VCE from Q8 in middle lower edge, with ignition in middle upper edge: (left) cloud footprint; (right) peak overpressures  $\geq 1$  psig.

	Vapor Cloud Explosions at Nil Wind	03904-RP-006
	PHMSA	Rev A
	Final Report	Page 209 of 213

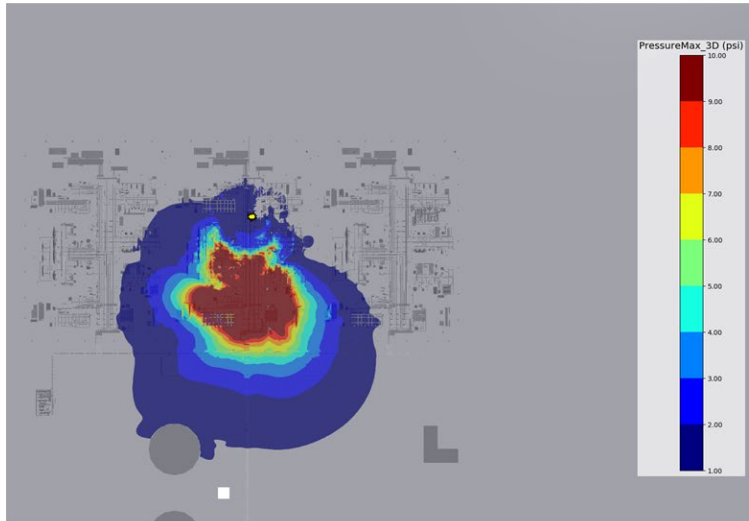
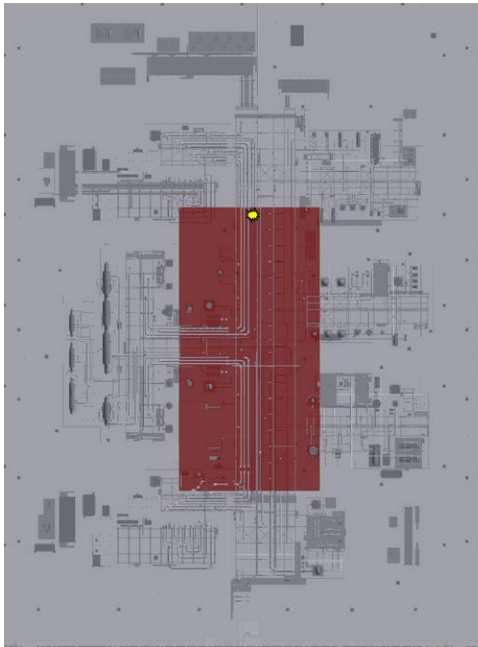


MR cloud (scenario 12, low wind): VCE from Q8 in middle left edge, with ignition in middle upper edge: (left) cloud footprint; (right) peak overpressures  $\geq 1$  psig.

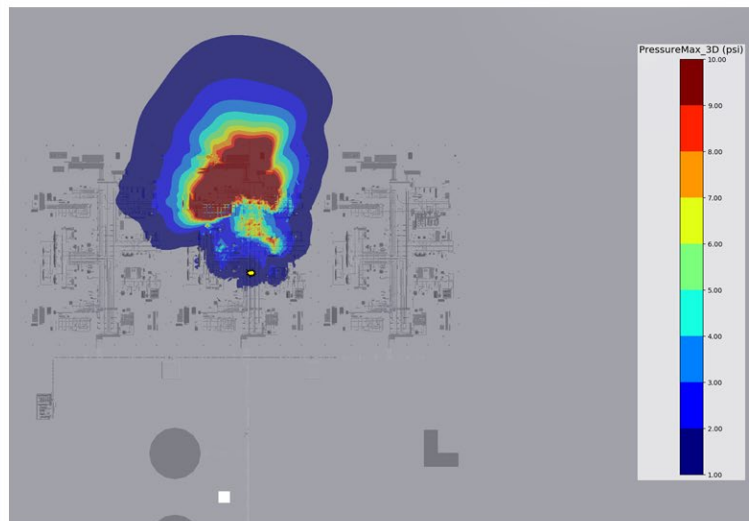
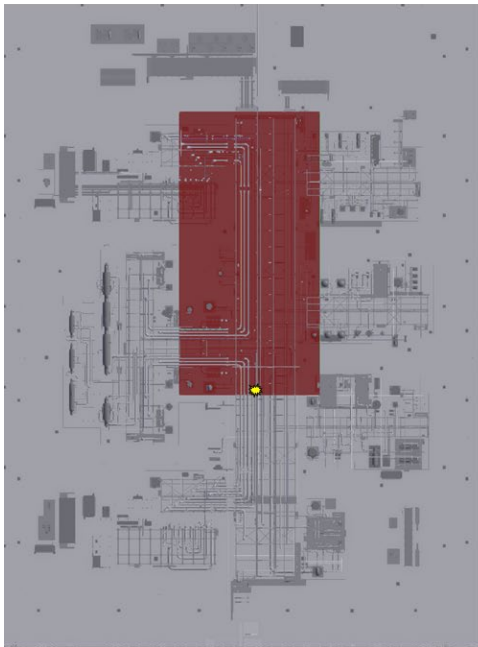


MR cloud (scenario 12, low wind): VCE from Q8 in center, with ignition in middle lower edge: (left) cloud footprint; (right) peak overpressures  $\geq 1$  psig.

	Vapor Cloud Explosions at Nil Wind	03904-RP-006
	PHMSA	Rev A
	Final Report	Page 210 of 213

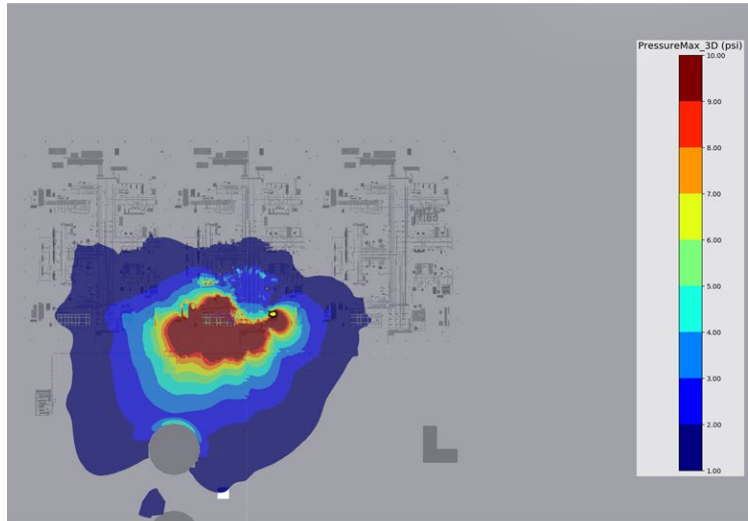
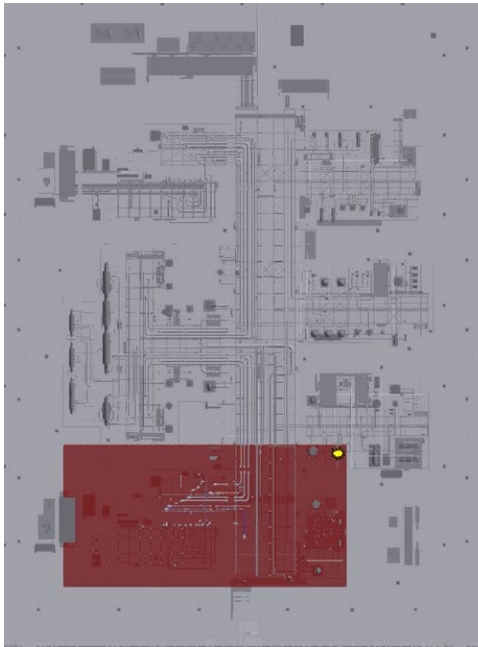


MR cloud (scenario 12, low wind): VCE from Q8 in center, with ignition in middle upper edge: (left) cloud footprint; (right) peak overpressures  $\geq 1$  psig.

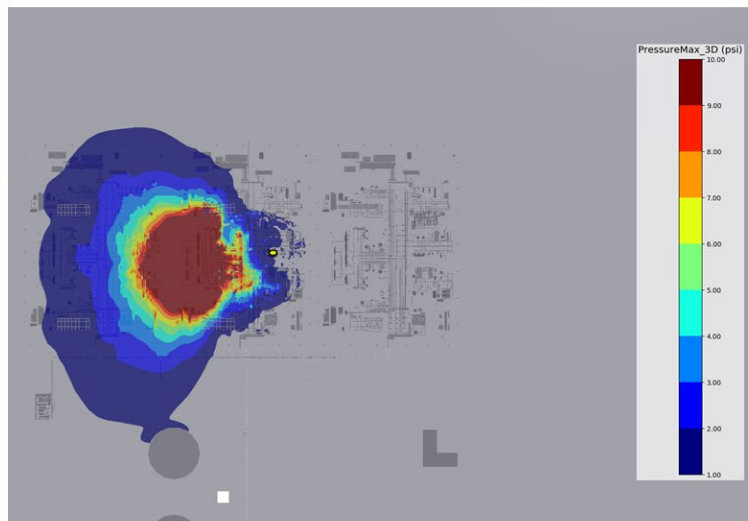
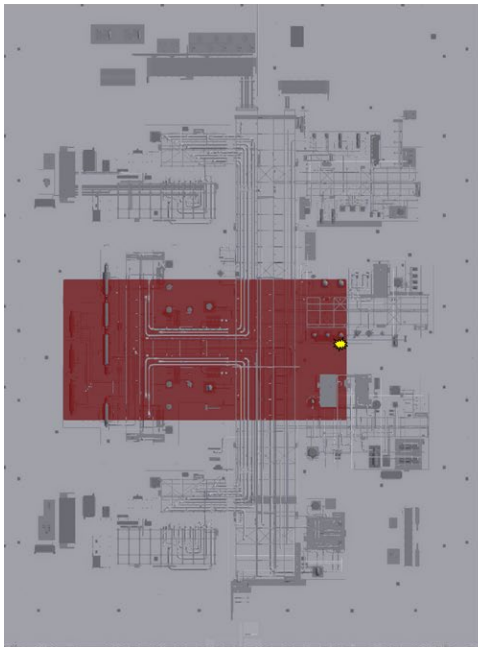


MR cloud (scenario 12, low wind): VCE from Q8 in middle upper edge, with ignition in middle lower edge: (left) cloud footprint; (right) peak overpressures  $\geq 1$  psig.

	Vapor Cloud Explosions at Nil Wind	03904-RP-006
	PHMSA	Rev A
	Final Report	Page 211 of 213

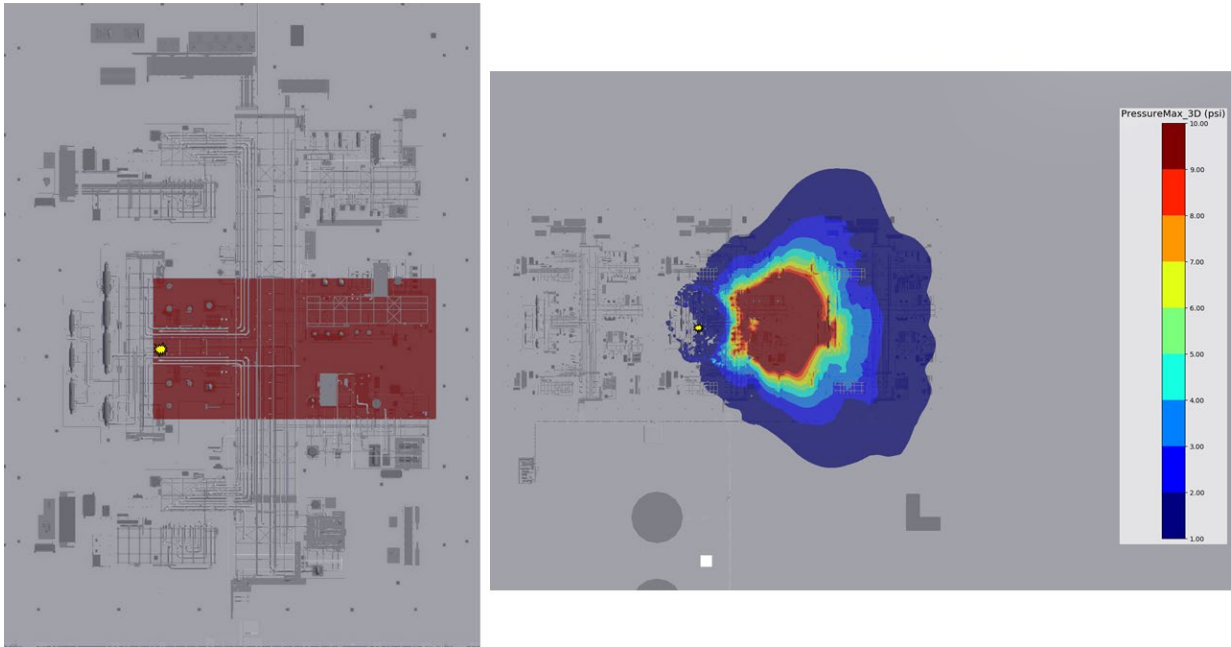


MR cloud (scenario 12, low wind): VCE from Q8 in lower left corner, with ignition in upper right corner: (left) cloud footprint; (right) peak overpressures  $\geq 1$  psig.

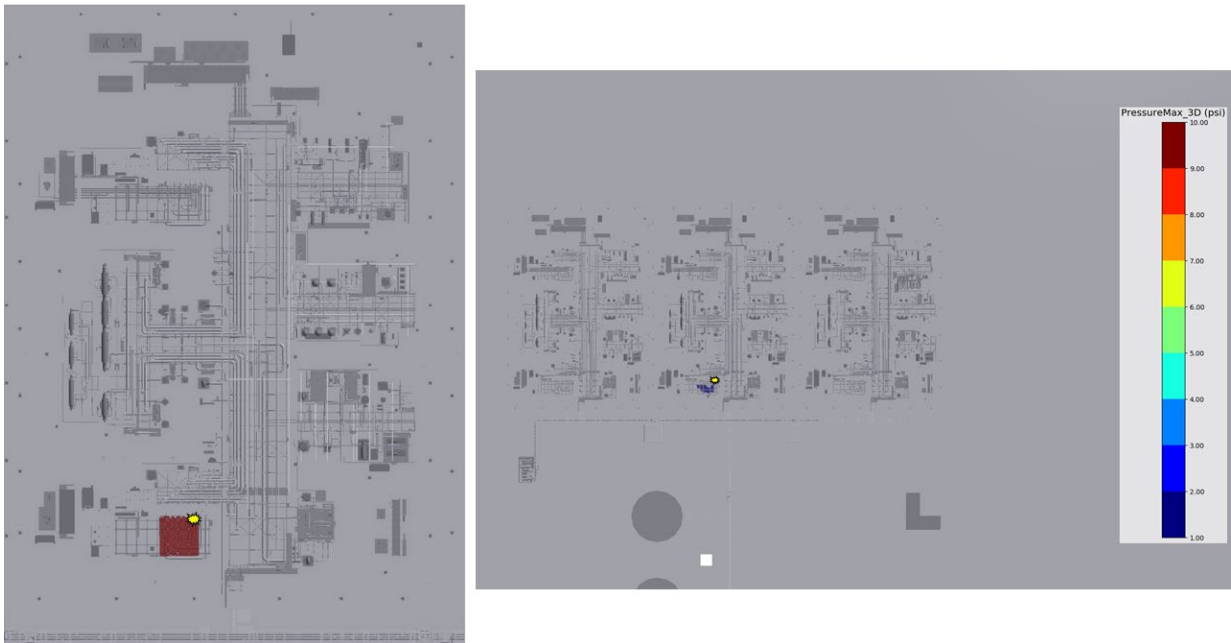


MR cloud (scenario 12, low wind): VCE from Q8 in middle left edge, with ignition in middle right edge: (left) cloud footprint; (right) peak overpressures  $\geq 1$  psig.

	Vapor Cloud Explosions at Nil Wind	03904-RP-006
	PHMSA	Rev A
	Final Report	Page 212 of 213

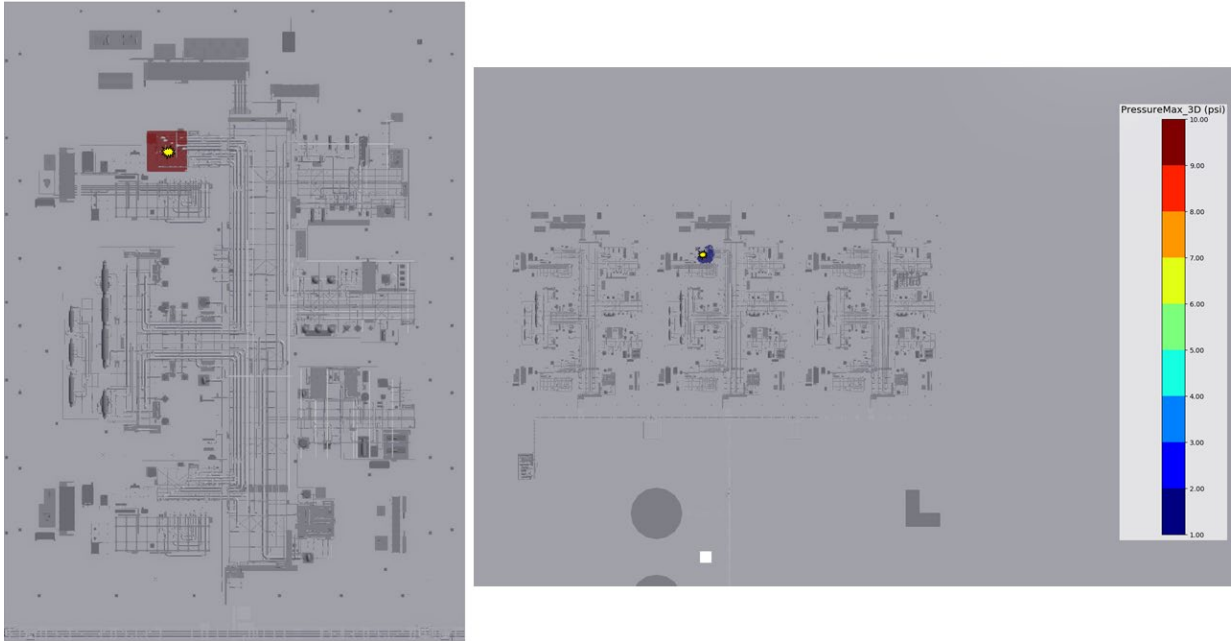


MR cloud (scenario 12, low wind): VCE from Q8 in middle right edge, with ignition in middle left edge: (left) cloud footprint; (right) peak overpressures  $\geq 1$  psig.



Propane cloud (scenario 12, low wind): VCE from Q9 in lower left corner, with ignition in upper right corner: (left) cloud footprint; (right) peak overpressures  $\geq 1$  psig.

	Vapor Cloud Explosions at Nil Wind	03904-RP-006
	PHMSA	Rev A
	Final Report	Page 213 of 213



Propane cloud (scenario 12, low wind): VCE from Q9 in upper left corner, with ignition in center: (left) cloud footprint; (right) peak overpressures  $\geq 1$  psig.